

**Development of Quantitative Structure-Property Relationships for Predicting Mutual Trans Influence and Ligand Bond Dissociation Energies in Pd(II), Pt(II) and Hypervalent Iodine Complexes**

Thesis submitted to the  
**UNIVERSITY OF KERALA**  
for the award of Degree of

**DOCTOR OF PHILOSOPHY**  
in Chemistry under the Faculty of Science

*By*

**SAJITH P. K.**



**Computational Modeling and Simulation Section  
Process Engineering and Environmental Technology Division  
National Institute for Interdisciplinary Science and Technology (CSIR-NIIST)  
Thiruvananthapuram – 695 019  
Kerala, India**

**2012**

## DECLARATION

I hereby declare that the Ph.D. thesis entitled “**Development of Quantitative Structure-Property Relationships for Predicting Mutual Trans Influence and Ligand Bond Dissociation Energies in Pd(II), Pt(II) and Hypervalent Iodine Complexes**” is an independent work carried out by me at the Computational Modeling and Simulation Section, Process Engineering and Environmental Technology Division, National Institute for Interdisciplinary Science and Technology (CSIR-NIIST), Trivandrum, under the supervision of Dr. C. H. Suresh and it has not been submitted elsewhere for any other degree, diploma or title.

**Sajith P. K.**



**CSIR-National Institute for Interdisciplinary  
Science & Technology**

*(Formerly Regional Research Laboratory)*  
(Council of Scientific & Industrial Research) India

Industrial Estate P.O., Pappanamcode, Trivandrum – 695 019

**Dr. Cherumuttathu H. Suresh**  
Scientist

E-Mail: sureshch@gmail.com  
Phone: 0471 – 2535506, 9446552294

---

July 22, 2012

**CERTIFICATE**

This is to certify that the work embodied in the thesis entitled “**Development of Quantitative Structure-Property Relationships for Predicting Mutual Trans Influence and Ligand Bond Dissociation Energies in Pd(II), Pt(II) and Hypervalent Iodine Complexes**” has been carried out by Mr. Sajith P. K. under my supervision and guidance at the Computational Modeling and Simulation Section, Process Engineering and Environmental Technology Division, National Institute for Interdisciplinary Science and Technology (CSIR-NIIST), Trivandrum and this work has not been submitted elsewhere for a degree.

Dr. C. H. Suresh  
(Thesis Supervisor)

## ACKNOWLEDGEMENT

First and foremost I would like to thank God for reasons too numerous to mention. No words can express my gratitude to my God, the Almighty.

I take immense pleasure to thank my research supervisor Dr. C. H. Suresh, Senior Scientist, Chemical Sciences and Technology Division, CSIR-National Institute for Interdisciplinary Science and Technology (CSIR-NIIST), Trivandrum for suggesting the research problem and also for his encouragement, inspiring guidance and timely advice throughout the course of this work.

I owe my sincere thanks to Dr. Suresh Das, Director, CSIR-NIIST and former directors, Prof. T. K. Chandrashekar and Dr. B. C. Pai for having given me an opportunity to carry out my doctoral work in this institution.

I extend my gratitude to Dr. Roschen Sasikumar, Dr. Elizabeth Jacob and Dr. S. Savithri for their constant encouragement and support that have been valuable throughout the research. I express my heartfelt thanks to Dr. K. P. Vijayalakshmi for her valuable encouragement.

I shall always cherish the golden moments I spent with my friends at Computational Modeling and Simulation Section Dr. Jomon Mathew, Fareed Bhasha Sayyed, Manoj M., Sudeep P. M., Alex Andrews, Dr. Jijoy Joseph, Dr. Panneer Selvam, Hareesh R. S, Adarsh V. K., Anish S., Dr. Manju M. S., Rejitha John, Neetha Mohan, Sandhya K. S, Shaija P. B., Ajitha M. J., Remya K., and Rakhi R.

I wish to thank my friends Dr. S. Ramakrishnan, Jatishkumar, Kiran Kumar, Baiju T. V., Manu Jose, and Sujith S.

Dr. Saleesh Kumar and Dr. C. N. Ramachandran are immensely acknowledged for their constant encouragement.

I am obliged to all my teachers for their help and encouragement at different stages of my life.

Council of Scientific and Industrial Research (CSIR) is highly acknowledged for their support through a net work project NWP-53. I also thank CSIR centre for Mathematical Modelling and Computer Simulation(C-MMACS), National Chemical Laboratory (CSIR-NCL), and Centre for Modelling Simulation and Design (CMSD), University of Hyderabad for providing computational facilities.

I wholeheartedly extend my thanks to all my friends at NIIST.

I am deeply grateful to my family for their constant love and care.

Last but not least, I thank the funding agency University Grants Commission (UGC), Government of India for the research fellowship.

Sajith P. K.

**CONTENTS**

	<b>Page</b>
<b>Declaration</b>	<b>i</b>
<b>Certificate</b>	<b>ii</b>
<b>Acknowledgements</b>	<b>iii</b>
<b>List of Tables</b>	<b>ix</b>
<b>List of Figures</b>	<b>xii</b>
<b>List of Schemes</b>	<b>xviii</b>
<b>List of Abbreviations</b>	<b>xix</b>
<b>Preface</b>	<b>xx</b>
<b>Chapter 1: Introduction</b>	
<b>Part A - Trans Influence &amp; Part B - Computational Chemistry</b>	
<b>1.1 Trans Influence</b>	<b>2</b>
<b>1.1.1 Mutual Influence of Ligands</b>	<b>2</b>
<b>1.1.2 Trans Effect and Trans Influence</b>	<b>3</b>
<b>1.1.3 Origin of Trans Influence</b>	<b>5</b>
<b>1.1.4 Various Classes of Ligands</b>	<b>6</b>
<b>1.1.5 Trans Influence in Square Planar Complexes</b>	<b>8</b>
<b>1.1.5.1 Trans Influence of Various Ligands</b>	<b>9</b>
<b>1.1.5.2 Trans Influence and Anti-cancer Ability of Transplatin</b>	<b>16</b>
<b>1.1.5.3 Trans Influence in Transition Metal Catalysed Reactions</b>	<b>17</b>
<b>1.1.6 Trans Influence in Octahedral Transition Metal Complexes</b>	<b>21</b>
<b>1.1.7 Trans Influence in Other Transition Metal Complexes</b>	<b>24</b>
<b>1.1.8 Trans Influence in Main Group Elements and Lanthanides</b>	<b>25</b>

<b>1.2</b>	<b>Computational Chemistry</b>	<b>28</b>
1.2.1	Molecular Mechanics Methods	28
1.2.2	Quantum Mechanical Methods	31
1.2.2.1	Ab initio Molecular Orbital Theory	31
1.2.2.2	Hartree-Fock Method	32
1.2.2.3	Post Hartree-Fock Methods	34
1.2.2.4	Basis Sets	34
1.2.3	Semi-empirical Quantum Chemical Methods	36
1.2.4	Density Functional Theory (DFT)	37
1.2.5	Molecular dynamics and Monte Carlo simulations	40
1.2.6	Hybrid Quantum Mechanics/Molecular Mechanics (QM/MM) Methods	41
1.2.7	Quantum Theory of Atoms in Molecule Analysis (QTAIM)	42
1.2.8	Molecular Electrostatic Potential (MESP)	45
1.2.9	Quantitative Structure Activity/Property Relationships (QSAR/QSPR)	48
1.3	Conclusion	50

## **Chapter 2: Quantification of the Trans Influence in Pd(II) and Pt(II) Complexes**

2.1	Abstract	52
2.2	Introduction	53
2.3	Computational Details	54
2.4	Results and Discussion	
2.4.1	Analysis of trans Pd <sup>II</sup> -Cl and Pt <sup>II</sup> -Cl Bond Lengths	55

2.4.2	Trans Influence from Trans Bond Length	57
2.4.3	Trans Influence from Isodesmic Reactions	59
2.4.4	AIM Analysis	64
2.4.5	Comparison of Mutual Trans Influence of Different Ligands in Pd(II) and Pt(II) Complexes	68
2.4.6	Mutual Trans Influence of Two Trans Ligands X and Y	69
2.4.7	Prediction of $E_{XY}$ Values	72
2.4.8	Electrons Density Values as a Measure of Trans Influence	76
2.4.9	Bond Dissociation Energies in $[M^{II}X(Y)Cl_2]$ Complexes	77
2.4.10	Bond dissociation energies in $[M^{II}X(Y)X'(Y')]$ Complexes	79
2.4.11	Comparison of Different DFT Methods for the Calculation of BDEs	85
2.4.12	Significance of MLR Equations for Predicting BDEs	87
2.5	Conclusion	88

### **Chapter 3: Mechanisms of Reductive Eliminations in Square Planar Pd(II) Complexes: Nature of Eliminated Bonds and Role of Trans Influence**

3.1	Abstract	91
3.2	Introduction	92
3.3	Computational Methods	95
3.4	Results and Discussion	96
3.4.1	Reductive Elimination of $CH_3CH_3$ and $CH_3Cl$	96
3.4.2	Trans influence from Isodesmic Reactions	102
3.4.3	Molecular Electrostatic Potential Minimum ( $V_{min}$ ) of Free Phosphine Ligands	104

3.4.4	AIM Analysis	107
3.5	Conclusion	116

## Chapter 4: Quantification of the Trans Influence in Hypervalent Iodine Complexes

4.1	Abstract	119
4.2	Introduction	120
4.3	Computational Methods	123
4.4	Results and Discussion	124
4.4.1	Trans Influence from Trans Bond Length	124
4.4.2	Quantification of Trans Influence Using $\rho(\mathbf{r})$ Values	125
4.4.3	Trans Influence and Covalent Nature of the Hypervalent Bonds	128
4.4.4	MESP minimum as a Measure of Trans Influence	130
4.4.5	Trans influence in Other $\lambda^3$ -iodanes	134
4.4.6	Trans influence in Iodine(V) Compounds	136
4.4.7	Isodesmic reactions to Study Mutual Trans Influence of Two Ligands X and Y	138
4.4.8	Bond Dissociation Energy and Trans Influence	144
4.5	Conclusions	151
	List of Publications	153
	References	154

## List of Tables

			<b>Page</b>
1.	Table 2.1	Comparison of experimental and calculated trans M–Cl bond lengths (in Å) in complexes of the type $[M^{II}Cl_3X]^{n-}$ (where M is Pd, Pt and X is H <sub>2</sub> O, CO, Cl <sup>-</sup> , NH <sub>3</sub> , C <sub>2</sub> H <sub>4</sub> , PEt <sub>3</sub> , NO <sub>2</sub> and PPh <sub>3</sub> ).	<b>56</b>
2.	Table 2.2	Values of the trans M–Cl (where M = Pd, Pt) bond length for the complexes of the type $[M^{II}Cl_3X]^{n-}$ .	<b>58</b>
3.	Table 2.3	The isodesmic reaction energies ( $E_X$ ) in kcal/mol for the reaction $M^{II}Cl_2X + M^{II}Cl_3 \longrightarrow M^{II}Cl_2 + M^{II}Cl_3X$ .	<b>63</b>
4.	Table 2.4	M–Cl bond critical point trans to X for the complexes of the type $[M^{II}Cl_3X]^{n-}$ .	<b>67</b>
5.	Table 2.5	The isodesmic reaction energy ( $E_{XY}$ ) for $M^{II}Cl_2X + M^{II}Cl_2Y \longrightarrow M^{II}Cl_2 + M^{II}Cl_2XY$ .	<b>71</b>
6.	Table 2.6	Isodesmic reactions used for the training set and predicted $E_{XY}$ values.	<b>75</b>
7.	Table 2.7	Isodesmic reactions used for the test set and predicted $E_{XY}$ values.	<b>76</b>
8.	Table 2.8	Dissociation energy $D_{IX}$ for M–X bond in $[MCl_3X]^{n-}$ complexes.	<b>80</b>
9.	Table 2.9	Calculated and predicted bond dissociation energies of the ligands (using Eq. 2.7) in complexes of the type $[Pd^{II}X(Y)X'(Y')]$ .	<b>82</b>

10.	Table 2.10	Calculated and predicted bond dissociation energies of the ligands (using Eq. 2.8) in complexes of the type $[\text{Pt}^{\text{II}}\text{X}(\text{Y})\text{X}'(\text{Y}')].$	<b>82</b>
11.	Table 2.11	The bond dissociation energies of various ligands in $[\text{M}^{\text{II}}\text{X}(\text{Y})\text{X}'(\text{Y}')].$ complexes predicted using $D_{\text{IX}}$ and $\rho(\mathbf{r})$ values.	<b>83</b>
12.	Table 2.12	BDEs of various ligands in $[\text{Pd}^{\text{II}}\text{X}(\text{Y})\text{X}'(\text{Y}')].$ , calculated at different levels of theory. (X, Y) and (X', Y') are trans combinations.	<b>86</b>
13.	Table 2.13	Correlation Matrix of 7 DFT functionals.	<b>87</b>
14.	Table 3.1	$E_{act}$ values for the reductive elimination of $\text{CH}_3\text{CH}_3$ and $\text{CH}_3\text{Cl}$ via direct and dissociative mechanisms.	<b>99</b>
15.	Table 3.2	Calculated trans Pd–C bond length in $\text{Pd}(\text{CH}_3)_2\text{L}_2,$ $\text{Pd}(\text{CH}_3)_2\text{L}$ and $\text{Pd}(\text{CH}_3)(\text{Cl})\text{L}_2$ complexes along with Pd–Cl bond length in $\text{Pd}(\text{CH}_3)(\text{Cl})\text{L}_2$ and $\text{Pd}(\text{CH}_3)(\text{Cl})\text{L}$ complexes.	<b>100</b>
16.	Table 3.3	AIM parameters at the bcp of Pd–C <sub>methyl</sub> bond in $\text{Pd}(\text{CH}_3)_2\text{L}_2$ complexes.	<b>109</b>
17.	Table 3.4	AIM parameters at the bcp of trans Pd–C <sub>methyl</sub> and cis Pd–C <sub>methyl</sub> bonds in $\text{Pd}(\text{CH}_3)_2\text{L}$ complexes.	<b>110</b>
18.	Table 3.5	AIM parameters at the bcp of Pd–C <sub>methyl</sub> and Pd–Cl bonds in $\text{Pd}(\text{CH}_3)(\text{Cl})\text{L}_2$ complexes.	<b>110</b>
19.	Table 3.6	AIM parameters at the bcp of Pd–C <sub>methyl</sub> and Pd–Cl bonds in $\text{Pd}(\text{CH}_3)(\text{Cl})\text{L}$ complexes.	<b>111</b>

20.	Table 4.1	QTAIM parameters at the (3,-1) bond critical points of Trans I-Cl bond in $\text{CF}_3[\text{I}(\text{X})\text{Cl}]$ complexes along with the trans I-Cl bond length.	<b>127</b>
21.	Table 4.2	$V_{\text{min}}$ values of $\text{CF}_3[\text{I}(\text{X})\text{Cl}]$ complexes.	<b>133</b>
22.	Table 4.3	Trans influence parameters of $\lambda^3$ -aryl iodanes.	<b>135</b>
23.	Table 4.4	Trans influence parameters of $\lambda^5$ -aryl iodanes.	<b>138</b>
24.	Table 4.5	Calculated and predicted $E_{\text{XY}}$ .	<b>140</b>
25.	Table 4.6	Isodesmic reactions used for the test set. Calculated and predicted $E_{\text{XY}}$ are given.	<b>142</b>
26.	Table 4.7	The BDE of X in the $\text{CF}_3[\text{I}(\text{X})(\text{Cl})]$ complexes ( $D_{\text{IX}}$ ).	<b>145</b>
27.	Table 4.8	Calculated and bond dissociation energy values of the X and Y in $\text{CF}_3[\text{I}(\text{X})(\text{Y})]$ complexes.	<b>146</b>
28.	Table 4.9	Predicted bond dissociation energy values of the X and Y for $\text{CF}_3[\text{I}(\text{X})(\text{Y})]$ complexes used for the training set.	<b>147</b>
29.	Table 4.10	The Predicted bond dissociation energy values of the X and Y for $\text{CF}_3[\text{I}(\text{X})(\text{Y})]$ complexes used for the test set.	<b>150</b>

## List of Figures

			<b>Page</b>
1.	Figure 1.1	Grinberg's polarization theory.	<b>5</b>
2.	Figure 1.2	(a) Formation of <i>sd</i> hybrid orbitals.  (b) MO diagram formed by the interaction of metal <i>sd</i> orbital and ligand $\sigma$ -orbitals.	<b>6</b>
3.	Figure 1.3	$\sigma$ -donor ligand.	<b>7</b>
4.	Figure 1.4	$\sigma$ -donor- $\pi$ -acceptor ligand.	<b>7</b>
5.	Figure 1.5	$\sigma$ -donor- $\pi$ -donor ligand.	<b>8</b>
6.	Figure 1.6	Dinuclear complexes of Pt and Pd with sulfite coordinated bridging ligand.	<b>10</b>
7.	Figure 1.7	Trans influence in homobimetallic compound.	<b>13</b>
8.	Figure 1.8	Structure of PSiT derivatives.	<b>13</b>
9.	Figure 1.9	Interconversion of dimer and monomer of a chelate complex.	<b>19</b>
10.	Figure 1.10	Regioisomeric arylpalladium amido complexes.	<b>20</b>
11.	Figure 1.11	Trans influence in Co(III) complexes with trans ligands OH and SO <sub>3</sub> .	<b>22</b>
12.	Figure 1.12	Cobaloxime derivatives, where X = Me, Et, iPr.	<b>22</b>
13.	Figure 1.13	Bimetallic complex of Pt, where Pt–Pt bond is affected by trans ligand X (X = ONO <sub>2</sub> <sup>-</sup> , Cl <sup>-</sup> , NO <sub>2</sub> <sup>-</sup> and Br <sup>-</sup> ).	<b>23</b>
14.	Figure 1.14	(a) Grubbs first generation catalyst.  (b) Grubbs second generation catalyst.	<b>25</b>

15. Figure 1.15 Molecular graph of cubane (B3LYP/6-311++G(d,p)) showing the bond paths (lines) and different critical points: nuclear (colour-coded by element C = black, H = grey), red for (3, -1) or bond CP, yellow for (3, +1) or ring CP, and green for (3, +3) or cage CP. **43**
16. Figure 1.16 Electrostatic potential on molecular surface of N-heterocyclic carbenes molecule, computed at B3LYP/6-311++G(d,p) level of theory. **48**
17. Figure 2.1 Optimised structures of  $[M^{II}Cl_3X]^{n-}$  complexes (where M = Pd, Pt and X = H<sub>2</sub>O, PH<sub>3</sub>) at MPWB1K-COSMO/BS1 level of theory. Trans bond length in Å are also shown. **57**
18. Figure 2.2 Correlation between  $E_X$  and trans Pd–Cl bond length in complexes of the type  $[Pd^{II}Cl_3X]^{n-}$  (blue diamond is for neutral ligands and red circle is for negatively charged ligands). **61**
19. Figure 2.3 Correlation between  $E_X$  and trans Pt–Cl bond length for  $[Pt^{II}Cl_3X]^{n-}$  complexes (blue diamonds show neutral ligands and red circles show anionic ligands). **64**
20. Figure 2.4 AIM topological plot of  $[Pd^{II}Cl_3X]^{n-}$  and  $[Pt^{II}Cl_3X]^{n-}$  complexes with X = H<sub>2</sub>O and PH<sub>3</sub>. Big circles correspond to attractors (atomic nuclei) and small red circles indicate bond critical points. The  $\rho(\mathbf{r})$  in au at bond critical point of Pd–Cl and Pt–Cl bonds are also shown. **65**

21. Figure 2.5 Correlation between (a)  $E_X$  and  $\rho(\mathbf{r})$  at the bond critical point of Pd-Cl bond trans to X for the complexes of the type of  $[\text{Pd}^{\text{II}}\text{Cl}_3\text{X}]^{n-}$  (b)  $E_X$  and  $\rho(\mathbf{r})$  at the bond critical point of Pt-Cl bond trans to X for complexes of the type of  $[\text{Pt}^{\text{II}}\text{Cl}_3\text{X}]^{n-}$ . **66**
22. Figure 2.6 Correlation between  $E_{XY}$  and predicted  $E_{XY}$  values in Pd(II) complexes. **74**
23. Figure 2.7 Correlation between  $E_{XY}$  and predicted  $E_{XY}$  values in Pt(II) complexes. **74**
24. Figure 2.8 Correlation between  $E_{XY}$  and predicted  $E_{XY}$  (using  $\rho(\mathbf{r})$  values) in Pd(II) complexes. **78**
25. Figure 2.9 Correlation between  $E_{XY}$  and predicted  $E_{XY}$  (using  $\rho(\mathbf{r})$  values) in Pt(II) complexes. **78**
26. Figure 2.10 Agreement between  $D_{3X}$  and predicted  $D_{3X}$  values in Pd(II) complexes. **81**
27. Figure 2.11 Agreement between  $D_{3X}$  and predicted  $D_{3X}$  values in Pt(II) complexes. **81**
28. Figure 3.1 Structures of reactants and transition states involved in the reductive elimination of  $\text{CH}_3\text{CH}_3$  and  $\text{CH}_3\text{Cl}$  through direct mechanism with  $\text{PMe}_3$  as ancillary ligands. Selected bond distances (in Å) are given. **97**
29. Figure 3.2 Structures of reactants and transition states involved in the reductive elimination of  $\text{CH}_3\text{CH}_3$  and  $\text{CH}_3\text{Cl}$  through dissociative mechanism with  $\text{PMe}_3$  as ancillary ligands. Selected bond distances (in Å) are given. **98**

30. Figure 3.3 Correlation between and trans Pd–C bond length and  $E_{act}$  for the reductive elimination of  $\text{CH}_3\text{CH}_3$  as well as correlation between trans Pd–Cl bond length and  $E_{act}$  for the reductive elimination of  $\text{CH}_3\text{Cl}$  (◆  $\text{CH}_3\text{Cl}$  direct, ■  $\text{CH}_3\text{CH}_3$  direct, ▲  $\text{CH}_3\text{Cl}$  dissociative, ●  $\text{CH}_3\text{CH}_3$  dissociative mechanisms). **101**
31. Figure 3.4 Correlation between  $E_L$  and  $E_{act}$  values for the reductive elimination of  $\text{CH}_3\text{CH}_3$  and  $\text{CH}_3\text{Cl}$  via direct and dissociative mechanisms. **104**
32. Figure 3.5 MESP isosurface at -9.0 kcal/mol for various phosphine ligands. The  $V_{min}$  in kcal/mol is also depicted. **106**
33. Figure 3.6 Correlations between  $V_{min}$  and  $E_L$  values. **106**
34. Figure 3.7 AIM features of representative (a)  $\text{Pd}(\text{CH}_3)(\text{Cl})\text{L}_2$  and (b)  $\text{Pd}(\text{CH}_3)(\text{Cl})\text{L}$  systems, where  $\text{L} = \text{PH}_3$ . The (3,-1) bond critical points are marked by small red circles. The  $\rho(\mathbf{r})$ ,  $\nabla^2\rho(\mathbf{r})$ ,  $H(\mathbf{r})$  (all values are in au) and  $k(\mathbf{r})$  at the bcp of the bonds that are cleaved during reductive elimination is marked along with the definitions of  $\rho(\mathbf{r})_s$ ,  $\nabla^2\rho(\mathbf{r})_s$ ,  $H(\mathbf{r})_s$  and  $k(\mathbf{r})_s$ . **108**
35. Figure 3.8 Correlation between  $\rho(\mathbf{r})_s$  and  $E_{act}$  values. **114**
36. Figure 3.9 Correlation between  $H(\mathbf{r})_s$  and  $E_{act}$  values. **114**
37. Figure 3.10 Correlation between  $\nabla^2\rho(\mathbf{r})_s$  and  $E_{act}$  values. **115**
38. Figure 3.11 Correlation between  $k(\mathbf{r})_s$  and  $E_{act}$  values. **115**
39. Figure 4.1 Examples of  $\lambda^3$ -iodanes and  $\lambda^5$ -iodanes **121**
40. Figure 4.2 MOs of the 3c-4e bond formed in the hypervalent iodine (III) complexes **122**

41. Figure 4.3 Structures of  $\text{CF}_3[\text{I}(\text{X})\text{Cl}]$  complexes ( $\text{X} = \text{OOtBu}, \text{C}_6\text{F}_5, \text{OMe}, \text{Ph}$ ). Trans bond length in  $\text{\AA}$  are also. **125**
42. Figure 4.4 AIM topological plot of  $\text{CF}_3[\text{I}(\text{X})\text{Cl}]$  complexes with  $\text{X} = \text{OOtBu}, \text{C}_6\text{F}_5, \text{OMe}$  and  $\text{Ph}$ . Big circles correspond to attractors (atomic nuclei) and small red circles indicate bond critical points. The  $\rho(\mathbf{r})$  in au at bond critical point of I-Cl bond is also shown. **126**
43. Figure 4.5 Correlation between electron density at the bond critical point of trans I-Cl bond and trans I-Cl distance in  $\text{CF}_3[\text{I}(\text{X})\text{Cl}]$  complexes. **128**
44. Figure 4.6 Correlation between total electron energy density and trans I-Cl bond length in  $\text{CF}_3[\text{I}(\text{X})\text{Cl}]$  complexes. **129**
45. Figure 4.7 Correlation between  $k(\mathbf{r})$  and trans I-Cl bond length in  $\text{CF}_3[\text{I}(\text{X})\text{Cl}]$  complexes **130**
46. Figure 4.8 Representation of MESP isosurface in  $\text{CF}_3[\text{I}(\text{X})\text{Cl}]$  complexes at -23 kcal/mol along with  $V_{\min}$  in kcal/mol. The ligand X are (a)  $\text{OOtBu}$  (b)  $\text{C}_6\text{F}_5$  (c)  $\text{OMe}$  and (d)  $\text{Ph}$  **132**
47. Figure 4.9 Correlation between  $V_{\min}$  and trans I-Cl bond length in  $\text{CF}_3[\text{I}(\text{X})\text{Cl}]$  complexes. **134**
48. Figure 4.10 (top) AIM topological plot of  $\lambda^3$ -aryl iodanes with  $\text{X} = \text{OMe}$  and  $\text{Ph}$ . Big circles corresponds to attractors (atomic nuclei) and small red circles indicate bond critical points. (bottom) The representation of MESP isosurface at -46 kcal/mol along with  $V_{\min}$  value in kcal/mol. **135**

49. Figure 4.11 System considered for the study of trans influence in iodine (V) compounds, where X indicates the trans ligand. **136**
50. Figure 4.12 (a) AIM topological plot of  $\lambda^5$ -aryl iodane with X = OMe. The  $\rho(r)$  value in au is shown. Big circles corresponds to attractors (atomic nuclei) and small red circles indicate bond critical points. The  $\rho(\mathbf{r})$  in au at bond critical point of I–O bond is shown.  
(b) Representation of MESP isosurface at -37 kcal/mol when X = OMe. The corresponding  $V_{min}$  in kcal/mol is also given. **137**
51. Figure 4.13 Correlation between calculated and predicted  $E_{XY}$  values. The Eq. 4.3 is used for the prediction of  $E_{XY}$ . **143**
52. Figure 4.14 Agreement between calculated and predicted bond dissociation energy values. **151**

## List of Schemes

1. Scheme 1.1 Preparation of cis and trans isomers of  $[\text{PtCl}_2(\text{NH}_3)_2]$  **4**
2. Scheme 2.1 Isodesmic reaction in which the reactant side is free from mutual trans influence between X and  $\text{Cl}^-$ . Oxidation state +2 of the metal is also shown. The total charge of the system depends on the type of ligand X. **60**
3. Scheme 2.2 Isodesmic reaction in which the reactant side is free from Mutual trans influence between X and Y. Oxidation state +2 of the metal is also shown. The total charge of the system depends on the type of ligands X and Y. **69**
4. Scheme 3.1 Formation of R–R' through direct and dissociative mechanisms, where L is ancillary phosphine ligands. **94**
5. Scheme 3.2 Isodesmic reactions modeled to quantify the trans influence of the ligand L in Pd(II) complexes. **103**
6. Scheme 4.1 Isodesmic reactions used to study the mutual trans ligand influence due to X and Y **139**

## List of Abbreviations

BCP	: Bond Critical Point
BDE	: Bond Dissociation Energy
CC	: Coupled Cluster
CCSD	: Coupled Cluster Single and Double
CI	: Configuration Interaction
CP	: Critical Point
DFT	: Density Functional Theory
ECP	: Effective Core Potential
Et	: Ethyl
G03	: Gaussian 03
GGA	: Generalized Gradient Approximation
GTO	: Gaussian Type Orbitals
HF	: Hartree-Fock
HK	: Hohenberg-Kohn
LDA	: Local Density Approximation
MD	: Molecular Dynamics
MESP	: Molecular Electrostatic Potential
MM	: Molecular Mechanics
MO	: Molecular Orbital
MP	: Moller-Plesset Perturbation Theory
NHC	: N-Heterocyclic Carbene
ONIOM	: Our N-layered Integrated Molecular Orbital + Molecular Mechanics
Ph	: Phenyl
Py	: Pyridine
QM	: Quantum Mechanics
QSAR	: Quantitative Structure Activity Relationship
QSPR	: Quantitative Structure Property Relationship
QTAIM	: Quantum Theory of Atoms in Molecule Analysis
R	: Alkyl
STO	: Slater Type Orbitals
TS	: Transition State

## Preface

Quantification of various factors contributing to the bond dissociation energies of a metal-ligand bond is one of the main objectives of an inorganic chemist. A coordinated ligand X can exert an intense effect on the strength of the metal ligand bond (M–Y), where X and Y are trans ligands, and this thermodynamic effect is known as trans influence. Trans influence is well-known in transition metal complexes and even extended to the main group elements and lanthanides. The overall objective of the thesis is to quantify the trans influence in square planar Pd(II) and Pt(II) complexes as well as in hypervalent iodine complexes and hence to study the contribution of trans influence in ligand bond dissociation energies.

A detailed literature review of trans influence and its importance is illustrated in the first part of Chapter 1. Nowadays, computational chemistry has made a rapid advance in understanding and predicting chemical phenomena. This area is very broad and variety of computational methods is available now and the second part of the chapter 1 describes various computational methods and their theoretical basis.

The second chapter deals with the quantification of trans influence in Pd(II) and Pt(II) complexes using a combined approach of isodesmic reactions and quantum theory of atoms in molecules analysis. Using trans influence parameters such as trans bond length, electron density values and isodesmic reaction energy values, a quantitative structure-property relationship is derived to predict the mutual trans influence of the ligands X and Y. We also find that the contribution of trans influence to the bond dissociation energy of ligands X or Y in complexes of the type  $[M^{II}Cl_2XY]^{n-}$  (where M = Pd, Pt) can be quantified in terms of trans influence parameters. Further, we extended this approach to the complexes of the type  $[M^{II}X(Y)X'(Y')]$ , the X and Y as well as X' and Y' are trans to each other wherein two different mutual trans influences will operate

in the system at the same time. Using multiple linear regression approach involving trans influence parameters, a very good prediction of the bond dissociation energies can be achieved for  $[M^{II}X(Y)X'(Y')]$  complexes.

The trans influence of various phosphine ligands (L) in direct as well as dissociative reductive elimination pathways yielding  $CH_3CH_3$  from  $Pd(CH_3)_2L_2$  and  $CH_3Cl$  from  $Pd(CH_3)(Cl)L_2$  is described in the third chapter. Our analysis showed that in the absence of large steric effect, trans influence parameters correlated linearly with the activation barrier ( $E_{act}$ ) of both direct and dissociation pathways. Further, the nature of bonds which are eliminated during the reductive elimination have been analysed in terms of atoms in molecules (AIM) parameters. AIM analysis of the reactant complexes suggests that when the covalent nature of the Pd–leaving group/atom bond increases, the energy of activation for the reductive elimination decreases and vice versa.

The fourth chapter deals with the quantification of trans influence in hypervalent iodine complexes. Trans I–Cl bond length, electron density at the (3,-1) bond critical point at the trans I–Cl bond and the molecular electrostatic minimum ( $V_{min}$ ) at the chloro ligand in  $CF_3[I(X)(Cl)]$  complexes have been proposed as parameters for the quantification of trans influence of various ligands in hypervalent complexes. Simple isodesmic reaction of the type  $CF_3[I(X)Cl] + CF_3[I(Y)Cl] \rightarrow CF_3[I(Cl)Cl] + CF_3[I(X)Y]$  are useful for understanding the preferred trans combination of a variety of X and Y ligands. The isodesmic reaction energy,  $E_{XY}$  indicates the mutual trans influence between X and Y ligands. The mutual trans influence of a large number of (X, Y) combination is predicted with good accuracy using the trans influence parameters of X and Y ligands. Empirical equations using trans influence and mutual trans influence parameters have been derived for predicting the bond dissociation energy of either X or Y ligand in  $CF_3[I(X)Y]$  complexes.

# **Introduction**

**Part A - Trans Influence  
&**

**Part B - Computational Chemistry**

---

# Part A - Trans Influence

---

## 1.1 Trans Influence

### 1.1.1 Mutual Influence of Ligands

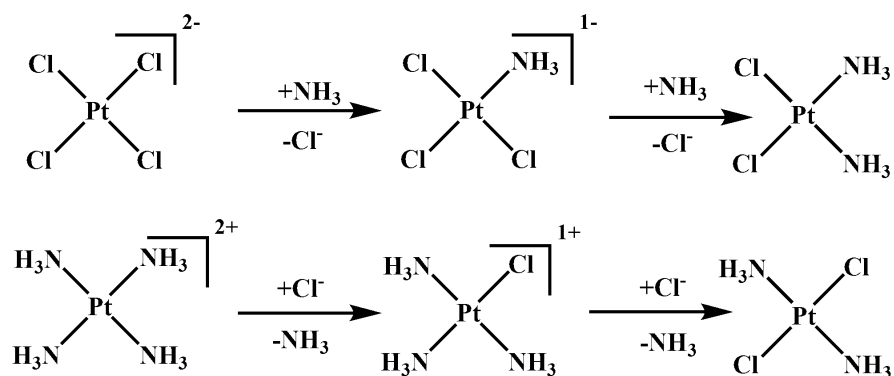
Understanding the mutual influence of ligands in a metal complex is one of the fundamental aspects of coordination chemistry. The coordination of a ligand X to a metal ion (M) influences all the other metal ligand bonds present in that complex [Pidcock *et al.* 1966; Hartley 1973; Crabtree 2001]. These types of directive influences are common in square planar and octahedral transition metal complexes and are generally classified into two, cis influence and trans influence [Chernyaev 1926; Pidcock *et al.* 1966; Mason and Towl 1970; Honeychuck and Hersh 1987]. The cis influence is defined as the ability of a ligand X' to weaken the metal-ligand bond M–X, where X' is cis to the ligand X. Similarly, the trans influence is defined as the ability of a ligand (Y) to weaken the metal-ligand bond (M–X) trans to it, where the X and Y are trans ligands [Chernyaev 1926; Basolo and Pearson 1962; Chermette *et al.* 2006]. The cis as well as trans influence of ligands is widely studied both theoretically and experimentally in square planar complexes of Pt(II) [Manojlovic-Muir *et al.* 1977; Anastasi and Deeth 2009].

The cis and trans influences of a ligand are generally evident in changes in the metal-ligand bond length, IR frequencies, and NMR chemical shifts [Hartley 1973; Coe and Glenwright 2000; Rigamonti *et al.* 2011]. Thus X-ray crystallography or spectroscopic techniques are frequently used to monitor these influences, though these investigations have some limitations [Roecker *et al.* 1983; Nakajima *et al.* 1985; Kukushkin *et al.* 1991; Kapoor *et al.* 1998]. The metal-ligand bond length obtained from X-ray crystallography may be influenced by packing interactions in the crystal structure as well as conformational

effects [Kapoor and Kakkar 2004]. The metal-ligand frequencies are also a good measure of strength of that bond while considerable interactions of M–X vibrations with others make this technique difficult to use for the study of cis and trans influence for a variety of ligands [Hartley 1973; Coe and Glenwright 2000]. The NMR investigations can also be used only if both M and X are NMR active such as  $^{195}\text{Pt}$ – $^{31}\text{P}$  and  $^{103}\text{Rh}$ – $^{31}\text{P}$  [Michelin and Ros 1989; Rigamonti *et al.* 2009, <sup>a</sup>Rigamonti *et al.* 2010, Rigamonti *et al.* 2011]. The experimental parameters to measure the cis and trans influences are not very sensitive to subtle electronic variations and theoretically derived molecular properties have been used as a powerful descriptors to quantify these effects [Landis *et al.* 1998; Kapoor and Kakkar 2004]. It is generally observed that the mutual influence of trans ligands are significantly higher than the mutual influence between cis ligands [Hartley 1973; Tau and Meek 1979; Muenzenberg *et al.* 1998 ; <sup>b</sup>Rigamonti *et al.* 2010].

### 1.1.2 Trans Effect and Trans Influence

In 1893, Werner introduced the principle of “trans elimination” on the basis of the observation that certain ligands can affect the reactions of other ligand which is present trans to it [Werner 1893]. Later in 1926, Chernyaev discovered that in square planar Pt(II) complexes, some ligands facilitates the departure of its trans ligand and this labilisation is generally known as trans effect [Chernyaev 1926]. The trans effect has been defined as the effect of a ligand over the rate of substitution of another ligand which is present trans to it [Huheey *et al.* 1993]. This is illustrated in Scheme 1.1 wherein the preparation of cis and trans isomers of  $[\text{PtCl}_2(\text{NH}_3)_2]$  is shown.



**Scheme 1.1** Preparation of cis and trans isomers of  $[\text{PtCl}_2(\text{NH}_3)_2]$ .

In the first reaction, two  $\text{Cl}^-$  are substituted by the ligand  $\text{NH}_3$ , and the product formed is a cis-isomer. In the first step of this reaction, one  $\text{Cl}^-$  is substituted by  $\text{NH}_3$  and in the second step, the  $\text{Cl}^-$  trans to another  $\text{Cl}^-$  is substituted. This is due to the fact that  $\text{Cl}^-$  has higher trans effect than  $\text{NH}_3$ . The formation of trans-isomer can also be explained on the basis of this. The trans effect of various ligands increases in the order:  $\text{F}^- \sim \text{H}_2\text{O} \sim \text{OH}^- < \text{NH}_3 < \text{Py} < \text{Cl}^- < \text{Br}^- < \text{I}^- < \text{SCN}^- \sim \text{NO}_2^- \sim \text{Ph}^- < \text{PR}_3 \sim \text{AsR}_3 < \text{CH}_3^- < \text{H}^- < \text{CO} < \text{CN}^-$  [Venanzi 1968; Huheey *et al.* 1993; Chval *et al.* 2008].

The trans effect originates mainly because of reactant state destabilization or/and transition state stabilization by the trans ligand. The first effect is the ground state phenomenon called trans influence (or, structural trans effect) and the second one is the kinetic factor, known as kinetic trans effect [Elder and Trkula 1974; Elder and Trkula 1977; Kastner *et al.* 1989; Atwood 1997; Coe and Glenwright 2000]. Thus it is clear that the trans influence and trans effects are interrelated and their separation is seldom achieved. It may be noted that a ligand exhibiting high trans effect does not necessarily show high trans influence. However, a high trans influencing ligand weakens the trans bond and thereby enhance the rate of substitution of the trans ligand [Venanzi 1968; Stein *et al.* 1976; Arnold and Bennett 1984].

### 1.1.3 Origin of Trans Influence

The first proposed theory of trans influence was the ‘polarization theory’ [Grinberg 1932]. This is an electrostatic theory in which the dipole induced in Y by the metal ion M induces a dipole in M, this tend to repel the negative charges in the trans ligand X [Grinberg 1932; Nekrasov 1937] (Figure 1.1). This theory cannot explain the observation that the ligands show largest trans influence are those which form the most covalent metal-ligand bonds [Appleton *et al.* 1973].

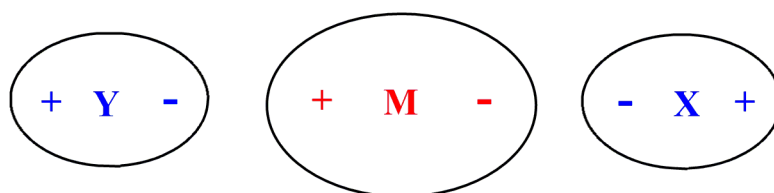


**Figure 1.1** Grinberg’s polarization theory.

Syrkin described trans influence in terms of hybridisation at the metal ion, the X and Y ligands will compete for the available hybrid orbital with strength proportional to their covalent bond character [Syrkin 1948]. According to MO theory, trans influence is described as the competition between two trans ligands X and Y for a single, metal based orbital. In square planar Pt(II) complexes, metal hybrid orbital is formed by the combination of  $5d_{x^2-y^2}$ , 6s, and 6p orbitals [Appleton *et al.* 1973; Harvey *et al.* 2003]. The hybrid orbital used by the metal ion for the interaction of  $\sigma$ - orbitals of two trans ligands X and Y contains higher proportion of  $5d_{x^2-y^2}$  and 6s orbitals and less 6p orbital since the orbital energies follows the order  $5d \sim 6s < 6p$ , and the resultant orbital usually regarded as *sd* hybrid orbital (Fig 1.2(a)). The interaction of ligand  $\sigma$ - orbital with the metal *sd* orbital results in the formation of 3 MOs, in which one very stable bonding orbital, one mostly non-bonding one and one anti-bonding orbital (Figure 1.2(b) ). If the trans ligands X and Y

are not identical, they compete to donate into the  $sd$  hybrid and if Y is donating strongly into the empty metal based orbital ( $sd$ ), there will be a differential weakening of the M–X bond.

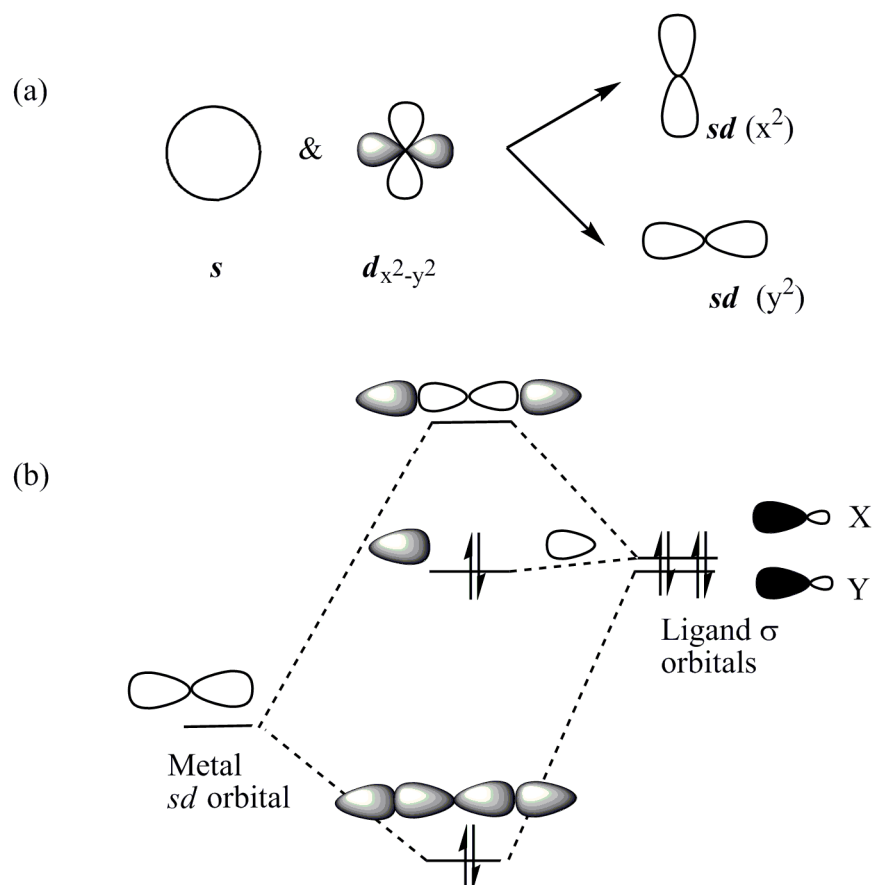


**Figure 1.2** (a) Formation of  $sd$  hybrid orbitals. (b) MO diagram formed by the interaction of metal  $sd$  orbital and ligand  $\sigma$ -orbitals.

### 1.1.4 Various Classes of Ligands

Ligands are generally classified into 3 classes, *viz.*  $\sigma$ -donor ligands,  $\sigma$ -donor- $\pi$ -acceptor ligands, and  $\sigma$ -donor- $\pi$  donor ligands [Coe and Glenwright 2000].

The elementary feature of a coordination complex is the donation of electron pair by the ligand to the metal ion results in the formation of a coordinate covalent bond and the ligands are generally known as  $\sigma$ -donor ligands. A  $\sigma$ -donor ligand donates electrons from

lone pairs to the metal orbital typically from either 's' or 'p' orbitals (Figure 1.3). The ligands such as water, ammonia, amines, alkyl, phenyl, hydrides, silyl ligands are examples for this. The alkyl, phenyl, silyl and hydride behaves as a strong  $\sigma$ -donating ligands and intense trans influence due to polarization effects while water, ammonia, and amines are weak  $\sigma$ -donor ligands and are weak trans influencing.

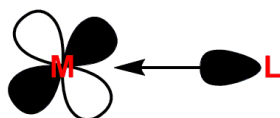


**Figure 1.3**  $\sigma$ -donor ligand.

Certain ligands are capable of  $\pi$  bonding interactions with metal ion by acting as a  $\pi$ -acceptor (Figure 1.4). The ligands included in this group are CO, olefin, carbenes,  $\text{NO}^+$ ,  $\text{CN}^-$ ,  $\text{CNR}$  and  $\text{PR}_3$ . Carbon monoxide and olefins act as weak  $\sigma$ -donors but a strong  $\pi$ -acceptor [Zobi 2009]. Cyanide and isocyanides are strong  $\sigma$ -donor ligands shows high trans influence but a relatively weak  $\pi$ -accepting ability. Carbenes are comparatively good  $\sigma$ -donor ligands but compared to CO, these species are weaker  $\pi$ -acceptors [Gusev 2009]. The linearly bonded  $\text{NO}^+$  ligand is a poor  $\sigma$ -donor while exhibit a very strong  $\pi$ -accepting behavior.  $\text{PR}_3$  ligands possess a wide range of  $\sigma$ -donor and  $\pi$ -acceptor properties depending on the R group present in it [Tolman 1970; Tolman 1977]. Generally,  $\text{PR}_3$  ligands are considered as moderate trans influencing ligands.

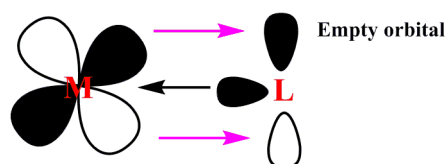


**Figure 1.4**  $\sigma$ -donor- $\pi$ -acceptor ligand.

Certain ligands are capable of donating a pair of electrons to form a  $\pi$  bond with metal ion (Figure 1.5). Though many types of ligand such as halides and pseudo halides are capable of acting as  $\pi$ -donors, strong trans influence are caused only by species which

form double or triple bonds to transition metals, e.g. oxo, nitride and imido ligands [Coe and Glenwright 2000].

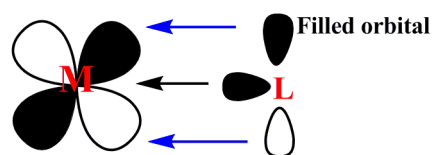


Figure 1.5  $\sigma$ -donor- $\pi$ -donor ligand.

### 1.1.5 Trans Influence in Square Planar Complexes

Trans influence in square planar complexes particularly in Pt(II) complexes are extensively studied from the early observation itself, and this phenomenon has been used to assess the bond strengths and reactivity [Belluco *et al.* 1966; Watt and Cude 1968; Al-Najjar *et al.* 1970; Hope *et al.* 1986; Atwood 1997]. Mason and coworkers explained trans influence on the basis of  $S^2/\Delta E$  values, where  $S$  is the overlap integral between the ligand orbital and the appropriate metal orbital, and  $\Delta E$  is the energy difference between these orbitals [McWeeny *et al.* 1969]. Molecular orbital calculations on a series of trans-[PtCl<sub>2</sub>(L)(NH<sub>3</sub>)], (where L = H<sub>2</sub>O, NH<sub>3</sub>, Cl<sup>-</sup>, H<sub>2</sub>S, PH<sub>3</sub>, H<sup>-</sup>, and CH<sub>3</sub><sup>-</sup>) were carried out by Zumdahl and Drago [Zumdahl and Drago 1968]. The main conclusion was that the order of trans influence showed a parallel behavior to the order of trans effect for the selected ligands. Also, the cis-influence, though smaller in magnitude was comparable to trans influence. In 1973, Pearson, explained trans influence in terms of “antisymbiosis” [Pearson 1973]. Soft ligands coordinated to a soft metal at trans positions will have a destabilizing effect and this can explain the observation that most of the dialkyls of square planar Pd(II) and Pt(II) are cis to each other [Jorgensen 1964].

### 1.1.5.1 Trans Influence of Various Ligands

Classification of different ligands on the basis of their relative trans influence has been the subject of extensive experimental studies over the past 50 years [Wendt and Elding 1997; Roodt *et al.* 2003; Zhu *et al.* 2005]. Hartley used the trans Pt–Cl bond length as a structural descriptor to classify the ligands into three broad groups of trans influence [Hartley 1973]. The modest  $\sigma$ -donor ligands with coordinating atoms such as oxygen, nitrogen, sulphur, chlorine and  $\pi$ -acceptors such as CO, C<sub>2</sub>H<sub>4</sub>, SCN<sup>−</sup> fall in the first group in which the trans Pt–Cl bond length is below 2.33 Å. Ligands showing strong  $\sigma$ -donating and modest  $\pi$ -accepting abilities (tertiary phosphine, and carbenes) fall in the second group in which the Pt–Cl trans bond length is between 2.36 and 2.39 Å. The third group includes those having powerful  $\sigma$ -donor capabilities but no  $\pi$ -acceptor abilities which include alkyl, aryl, hydride, and silyl ligands where the trans Pt–Cl bond lengths are higher than 2.40 Å. The general observation is that the trans Pt–Cl bond lengths increases with decreasing electronegativity of the influencing ligand.

The oxygen and sulphur coordinated ligands act as weak  $\sigma$ -donating ligands and hence weak trans influence is expected. Darensbourg *et al.* reported the order of trans influence of various X donor ligands by analyzing the spectroscopic properties of the Ni–H bond in trans-[NiH(X)(PCy<sub>3</sub>)<sub>2</sub>] complexes [Darensbourg *et al.* 1989]. The following trend in trans influence is obtained for X ligands: Ph<sup>−</sup> (1805) ~ Me<sup>−</sup> (1807) > CN<sup>−</sup> (1870) > SH<sup>−</sup> (1904) > S(p-tol)<sup>−</sup> (1932) ~ SPh<sup>−</sup> (1929) ~ SCN<sup>−</sup> (1928) ~ O<sub>2</sub>CCH<sub>3</sub><sup>−</sup> (1925) ~ O<sub>2</sub>CH<sup>−</sup> (1931) > OPh<sup>−</sup> (1946) ~ O<sub>2</sub>CCF<sub>3</sub><sup>−</sup> (1944) > O<sub>2</sub>CPh<sup>−</sup> (1960), where values in parenthesis are Ni–H stretching frequencies. When more covalently bonded ligands such as methyl or phenyl are trans ligands, a decrease in the stretching frequency of Ni–H bond and smaller upfield chemical shifts for nickel hydride <sup>1</sup>H NMR values were noted compared to more electronegative anionic ligands such as O coordinated ligands. Breitingner and co-workers

synthesized dinuclear complexes of Pt and Pd with two parallel sulfite bridges (Figure 1.6) [Krieglstein *et al.* 2001]. The molecular structures clearly reveal the higher trans influence of S-coordinated sulfite on M–N bond length compared to O-coordinated sulfite. The Pt(1)–N<sub>average</sub> bonds (2.091 Å) which is trans to S coordinated sulfite are significantly longer than the Pt(2)–N<sub>average</sub> bond (2.021 Å), wherein O is the trans ligand. These type of observations were also noted in Pd dinuclear complexes where Pd–N<sub>average</sub> bond trans to O atom (2.014 Å) is shorter than Pd–N<sub>average</sub> bond trans to S (2.074 Å) atom of sulfite ligand.

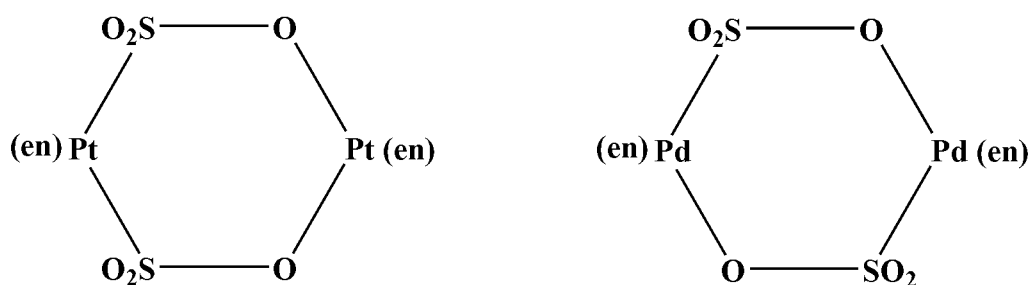


**Figure 1.6** Dinuclear complexes of Pt and Pd with sulfite coordinated bridging ligand.

Several structural studies were carried out to understand the trans influence of halide ions. Howard and Woodward analysed the X-ray structure of *cis*-[(Ph<sub>3</sub>P)<sub>2</sub>Pd(F)(CH(CF<sub>3</sub>)<sub>2</sub>)] complex and found that the Pd–P distance trans to F<sup>–</sup> ligand was too short (2.22 Å), suggesting very weak trans influence of F<sup>–</sup> [Howard and Woodward 1973]. The X-ray structural study of [(C<sub>6</sub>F<sub>5</sub>)<sub>4</sub>Ni<sub>2</sub>(μ-X)<sub>2</sub>]<sup>2–</sup> complexes (where, X = Cl<sup>–</sup> or F<sup>–</sup>), showed that the trans influence of F<sup>–</sup> is less compared to Cl<sup>–</sup> ligands [Brezinski *et al.* 1989]. Flemming *et al.* investigated various crystal structures of *trans*-[(Ph<sub>3</sub>P)<sub>2</sub>Pd(Ph)X] and on the basis of *trans* Pd–C bond length, *trans* influence of various halide ligands follows the order; I<sup>–</sup> > Br<sup>–</sup> > Cl<sup>–</sup> > F<sup>–</sup> [Flemming *et al.* 1998]. Moigno *et al.* compared *trans* influence of various halide ligands to CPh<sup>–</sup> and CH<sub>3</sub><sup>–</sup> using FT-Raman spectroscopy in *trans*-[Rh(X)(=C=CHPh)(P*i*Pr<sub>3</sub>)<sub>2</sub>] complexes [Moigno *et al.* 2001]. On the basis of Rh=C

stretching mode, the sequence of trans influence obtained is  $\text{CCPh}^- > \text{CH}_3^- > \text{I}^- > \text{Br}^- > \text{Cl}^- > \text{F}^-$  [Moigno *et al.* 2001].

A number of studies were also undertaken to understand the trans influence of N coordinated ligands [Hartley 1973]. Of particular interest in this regard are pyridine and related ligands. For example, the cis and trans influence of substituted pyridine ligands  $\text{NC}_5\text{H}_4\text{X}$ , where  $\text{X} = \text{CN}, \text{CO}_2\text{Me}, \text{H}, \text{Ph}, \text{Me}, t\text{-Bu}$  and  $\text{NMe}_2$ , in cycloplatinated species of cis- and trans- $[\text{Pt}(\text{Pmes}_2\text{C}_6\text{H}_2\text{Me}_2\text{CH}_2)\text{Cl}(\text{NC}_5\text{H}_4\text{X})]$  complexes were studied by comparing the  $^1J(^{195}\text{Pt}-^{31}\text{P})$  coupling constants [Malito and Alyea 1992]. An inverse correlation is obtained between cis and trans influence of  $\text{NC}_5\text{H}_4\text{X}$  ligands. Further, high basicity of  $\text{NC}_5\text{H}_4\text{X}$  indicates strong trans-influence while a weak cis-influence and vice versa. In a computational study at B3LYP level, Stromberg and co-workers analysed the binding energies of ethylene to Ni(II), Pd(II), and Pt(II) complexes and found that  $\text{Cl}^-$  exerts more trans influence on ethylene than  $\text{NH}_3$  [Stromberg *et al.* 1997]. They also noticed that trans influence is not sensitive to the nature of metal atom present and hence it can be assumed that trans influence does not depend on the amount of  $\pi$ -back donation. Tessier and Roshon compared the trans influence of pyridine and its derivatives (YPy) with  $\text{Cl}^-$  and  $\text{I}^-$  ligands (X) by analyzing X-ray crystals of various complexes of the types cis- and trans- $\text{Pt}(\text{YPy})_2\text{X}_2$  [Tessier and Roshon 1999] and the following order of trans influence was obtained:  $\text{I}^- > \text{Cl}^- > \text{YPy}$ . Prenzler and co-workers investigated the trans influence of imino ether ( $\text{NH}=\text{C}(\text{OR}')\text{R}$ ) ligands [Prenzler *et al.* 1997]. They observed that the  $^2J(\text{Pt}-\text{CF}_3)$  coupling constant in trans- $[\text{Pt}(\text{CF}_3)\text{Cl}(\text{PMe}_2\text{Ph})_2]$  is 757 Hz, while for a series of trans- $[\text{Pt}(\text{CF}_3)\text{L}(\text{PMe}_2\text{Ph})_2]^+$  complexes (where  $\text{L} = \text{ArCN}, \text{HN}=\text{C}(\text{OMe})\text{C}_6\text{F}_5, \text{pyridine}, \text{EtNC}$ ) the corresponding  $^2J(\text{Pt}-\text{CF}_3)$  coupling constant obtained is 778, 724, 702, and 662 Hz, respectively. This indicates that the trans influence of imino ligand is similar to that of chloride and pyridine. A theoretical analysis was carried out to understand the bonding interaction of  $\text{Pd}^{\text{II}}$ -Phosphine and trans influence of  $\text{NMe}_3$  ligand [Yamanaka and Mikami

2005]. The model system used was  $\text{PR}_3\text{Pd}^{\text{II}}$  and  $\text{PR}_3\text{Pd}^{\text{II}}\text{NMe}_3$  ( $\text{R} = \text{H}, \text{Ph}$ ) and paired interacting orbital (PIO) analysis was carried out. The results showed that after coordinating  $\text{NMe}_3$  ligand,  $\sigma$ -donation to the vacant 4d orbital of palladium in  $\text{PPh}_3\text{Pd}^{\text{II}}$  is increased while keeping the  $\pi$ -back-donation to the  $\text{P}-\text{C}$   $\sigma^*$ -orbital. A similar observation also noted for  $\text{BIPEHP}-\text{Pd}^{\text{II}}$  by the coordination of strongly donating amine ligand such as DPEN (where, BIPEHP = biphenyl phosphine, DPEN = diphenylethylenediamine).

Phosphine ligands possess a wide range of trans influence depending upon the substituent on P atom [Cooney *et al.* 2003]. Some of the recent studies regarding trans influence of P coordinated ligands and its comparison with other ligands are summarised here. Wendt and Elding synthesized various  $[\text{PtI}_3\text{L}]^-$  complexes and based on Pt-I bond length they observed that the trans influence of these ligands decreases in the order:  $\text{PPh}_3$  (2.662 Å) >  $\text{AsPh}_3$  (2.658 Å) >  $\text{SbPh}_3$  (2.637 Å), the values in the parenthesis are the trans Pt-I trans bond length [Wendt and Elding 1997]. The higher trans influence of P coordinated ligand is evident from  $[\text{Pd}(\text{PTA})_3\text{Cl}]^+$  complex, where PTA is 1,3,5-triaza-7-phosphaadamantane [Darensbourg *et al.* 1999]. Crystal structure of this complex showed that the Pd-P average bond distance cis to chloride ligand is 2.334 Å while the Pd-P bond trans to  $\text{Cl}^-$  is only 2.238 Å, which is significantly shorter than the cis bond Pd-P. This is due to the higher mutual trans influence between two P coordinated ligands. Otto and Johansson reported trans influence of various L ligands in the series of complexes of the type  $\text{cis}-[\text{PtCl}_2(\text{L})_2]$  and on the basis of Pt-Cl trans bond length, trans influence follows the order:  $\text{PMe}_2\text{Ph} > \text{PPh}_3 > \text{AsPh}_3 \sim \text{SbPh}_3 > \text{Me}_2\text{SO} > \text{SMe}_2 > \text{SPh}_2 > \text{NH}_3 > \text{olefin} > \text{Cl}^- > \text{MeCN}$  [Otto and Johansson 2002]. Salcedo *et al.* also reported higher trans influence of  $\text{PPh}_3$  over  $\text{SbPh}_3$  on the basis of bond order values obtained from NBO calculation [Salcedo *et al.* 2002]. Trans influence of  $\text{PPh}_3$  ligand was compared to carbon coordinated  $\text{C}_6\text{H}_4\text{PPh}_3$  ligand in a palladium bimetallic complex [Lang *et al.* 2006]. Crystallographic data of the structure shown in the Figure 1.7 shows two  $\mu$ -bridging iodides with different Pd-I

separations suggesting higher trans influence of  $C_6H_4PPh_3$  compared to  $PPh_3$ . Tsuji and co-workers synthesized a variety of PSiT ligands (where PSiT = 9-phospha-10-silatriptycenes and its derivatives, shown in Figure 1.8) [Tsuji *et al.* 2006]. They compared the trans influence of PSiT ligands with  $PPh_3$  and  $PMe_2Ph$  from  $cis-[PtMe_2(PSiT)_2]$ ,  $cis-[PtMe_2(PPh_3)_2]$  and  $cis-[PtMe_2(PMe_2Ph)_2]$  complexes by measuring  $^1J(Pt-C)$  coupling constant. The trans influence of PSiT ligands is found greater than  $PPh_3$  while it is less than that of  $PMe_2Ph$ .

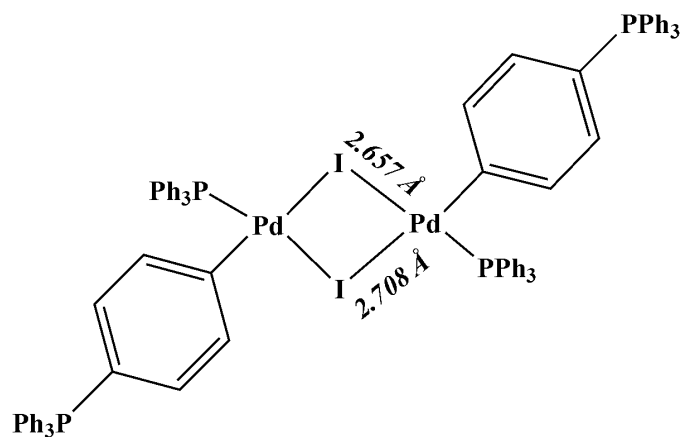


**Figure 1.7** Trans influence in homobimetallic compound

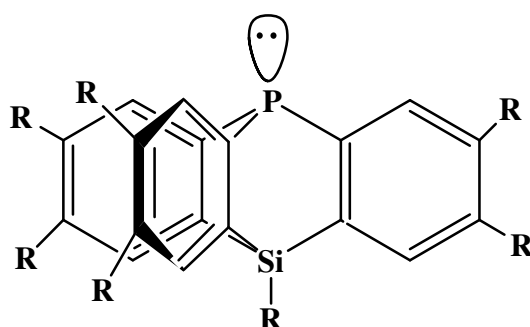


**Figure 1.8** Structure of PSiT derivatives.

Appleton and Bennett presented the order of trans influence of various  $\sigma$ -donating carbon ligands on the basis of platinum-phosphorus coupling constants in the derivatives of

hydroxo(methyl)-1,2-bis(diphenylphosphino)ethaneplatinum(II) complexes [Appleton and Bennett 1978]. The decreasing order of trans influence of various carbon ligands obtained was  $C_6H_9^- \sim C_2H_5^- > C_6H_5^- > CH_2Ph^- \sim CH_3^- > CF_3^- > CH_2COCH_3^- > CH_2CN^- > C_2Ph^- \sim CH_2NO_2^- > C_3H_5^- > CN^- \sim ONO^- > CH(COCH_3)_2^- > CH(CN)_2^- > CO > C(COCH_3)_3^-$ . They noted that on the basis of  $J(Pt-P)$  values, the  $CF_3^-$  ligand shows slightly less trans influence than that of  $CH_3^-$ . On the other hand, Pt-Cl bond length and Pt-Cl stretching frequency in trans-PtClCH<sub>3</sub>(PMePh<sub>2</sub>)<sub>2</sub> and trans-PtClCF<sub>3</sub>(PMePh<sub>2</sub>)<sub>2</sub> complexes show that the trans influence of  $CF_3^-$  to be considerably lower than that of  $CH_3^-$ . These differences may be due to the fact that  $J(Pt-P)$  values reflect mainly the changes in the hybridisation while the electrostatic effects induced by the electronegative fluorine atoms influences the Pt-Cl bond length. Suzuki and Yamamoto investigated trans influence of various carbon ligands of the type CH<sub>2</sub>COR in Pd complexes by comparing Pd-Cl stretching frequencies and the trans influence follows the order :  $CH_2COCH_3 > CH_2COC_6H_5 > CH_2COCH_2Cl \sim CH_2CN$  [Suzuki and Yamamoto 1993]. Strong trans influence of phenyl group was reported in square planar Au(III) complexes [Parish *et al.* 1996] while a comparison of trans influence among three different aryl groups was done by Wendt and co-workers [Wendt *et al.* 1997]. They observed that in Pt(II) complexes mesityl group shows higher trans influence than phenyl group while phenyl and p-anisyl groups show very similar trans influence. In all the three cases, the trans Pt-Cl bond was found between 2.40 and 2.44 Å, showing higher trans influence of the aryl group. Hughes and co-workers investigated the impact of three α-fluorinated ligands (*viz.*  $CF_2CF_3^-$ ,  $CFHCF_3^-$ ,  $CH_2CF_3^-$ ) on the trans Pd-N bond length and observed there is no significant variation of the trans Pd-N distance suggesting that trans influence of these three fluorinated alkyl ligands are almost same [Hughes *et al.* 2004]. Netland *et al.* reported the strong trans influence of N-heterocyclic carbene group compared to the imine group [Netland *et al.* 2010].

The very high trans influence of silyl ligands was originally established by IR spectroscopic studies [Chatt *et al.* 1966] and further confirmed by crystallographic studies in Pt(II) complexes [Yamashita *et al.* 1988]. In square planar  $[(\kappa^2\text{-P,N})\text{-Me}_2\text{NCH}_2\text{CH}_2\text{PPh}_2]\text{Pt MeSi(OMe)}_3$  complexes, the ligand  $\text{Si(OMe)}_3^-$  is found trans to nitrogen atom while the ligand  $\text{CH}_3^-$ , which is having lower trans influence compared to  $\text{Si(OMe)}_3^-$  is found trans to P atom [Pfeiffer and Schubert 1999]. Even though silyl ligands are high trans influencing ligands, the influence of silyl ligands on the reactivity of transition-metal complexes are little known due to the facile cleavage of metal-silicon bond [Tilley *et al.* 1989]. Hence chelate type (phosphinoalkyl)silyl ligands have been developed to suppress the elimination of silyl groups from the metal center [Okazaki 2002]. These types of metal complexes show some unusual reactivities which results from the strong trans influence of silyl ligands. For instance dehydrogenative coupling of monohydrosilanes can be mediated by the (phosphinoethyl)silyl rhodium complexes [Okazaki 2002]. Kapoor and Kakkar modeled the trans influence of various X ligands in  $\text{PtClX(dms)}_2$  complexes (where, dms = dimethyl sulfoxide) [Kapoor and Kakkar 2004]. They found that highly trans influencing ligands such as  $\text{SiH}_3^-$ ,  $\text{CH}_3^-$ ,  $\text{H}^-$ ,  $\text{C}_6\text{H}_5^-$  have properties different from the moderate and weak trans influencing ligands. On the basis of trans Pt–Cl bond length, the trans influence of X ligands increases in the order,  $\text{H}_2\text{O} < \text{NH}_3 < \text{AsH}_3 < \text{H}_2\text{S} < \text{F}^- < \text{PH}_3 < \text{Cl}^- < \text{Br}^- < \text{I}^- < \text{C}_6\text{H}_5^- < \text{H}^- < \text{CH}_3^- < \text{SiH}_3^-$ . Furthermore, they noted that a linear relationship exist between the trans Pt–Cl bond lengths with hardness of the ligands, and with population of platinum and chlorine orbitals.

Zhu *et al.* analysed the trans influence of different boryl ligands in Pt(II) complexes by using natural bond orbital analysis and the order of trans influence of different boryl ligands are explained in terms of the Pt–B  $\sigma$ -bonding interaction [Zhu *et al.* 2005; Zeng and Sakaki 2012]. They compared the trans influence of alkyl, aryl, hydride and silyl ligands with boryl ligands and the following order of trans influence has been obtained:

$\text{BMe}_2^- > \text{SiMe}_3^- > \text{BH}_2^- > \text{SnMe}_3^- > \text{BCl}_2^- \sim \text{BBr}_2^- \sim \text{SiH}_3^- > \text{CH}_2\text{CH}_3^- > \text{CH}=\text{CH}_2^- > \text{H}^- > \text{Me}^- > \text{C}_6\text{H}_5^- > \text{SiCl}_3^- > \text{SnCl}_3^- > \text{CCH}^-$ . Very recently, Braunschweig *et al.* synthesized platinum(II) complexes of general formula  $\text{trans}-(\text{PCy}_3)_2\text{PtBr}(\text{BX}_2)$  and found that experimental trans influence order of various  $\text{BX}_2^-$  ligands is correlating with the computed trans influence order obtained by Lin and Marder [Braunschweig *et al.* 2007].

### 1.1.5.2 Trans influence and Anti-cancer Ability of Transplatin

Many studies have been devoted to the cisplatin and its derivatives due to the potential importance of these complexes as anti-cancer drug [Rosenberg *et al.* 1969; Giandomenico 1991; Melnik and Holloway 2006]. The transition state for the chloride ligand replacement with water and guanine in cisplatin derivatives was studied by Chval *et al.* [Chval *et al.* 2000]. Wysokinski and Michalska compared the vibrational spectra of cisplatin and carboplatin at different DFT methods and compared the results with experimental measurements [Wysokinski and Michalska 2001]. The affinity of cisplatin to the amino acids and DNA bases were computationally studied by Deubel [Deubel 2004]. The interaction of cisplatin with DNA has been theoretically studied during recent years [Chval and Sip 2006]. The first step involves the hydrolysis of cisplatin which is followed by the interaction of N (or S) sites in the peptide or the bases present in the DNA/RNA.

In contrast, the transplatin ( $\text{trans-PtCl}_2(\text{NH}_3)_2$ ) is more unstable compared to the cisplatin [Knipp *et al.* 2007]. Zakovska *et al.* proposed that by using sterically hindering carrier ligands, the antitumor properties of transplatin can be increased [Zakovska *et al.* 1998]. It is also reported that by modifying  $\text{trans-Pt}^{\text{II}}\text{Cl}_2$  complexes with aliphatic amine, iminoether, planar amine, carboxylate, piperidine, phosphine or pyridine like carrier ligands can make these complexes anticancer-active [Kasparkova *et al.* 2003]. The weakly coordinating ligands present in the trans positions (weak mutual trans influence) gives

remarkable chemical stability on the transplatin structure [Bulluss *et al.* 2007]. The trans influence of N and S containing ligands in transplatin complex were computationally investigated by Manalastas and coworkers [Manalastas *et al.* 2009]. They noticed that though small in magnitude, the neutral sulfur ligands exert slightly greater trans-influence than neutral nitrogen ligands. They also predicted that for the development of trans-Pt(NR)(NR')Cl(X) anticancer agent, the adenine is most suitable candidate among naturally occurring organic ligands (X).

### 1.1.5.3 Trans Influence in Transition Metal Catalysed Reactions

Very often the trans influence has been invoked in coordination and organometallic chemistry to explain several reaction pathways [Kapadia *et al.* 1997; Thomson and Hal 2001; Owen *et al.* 2004; Zhu and Ziegler 2006; Mathew *et al.* 2007; Canovese *et al.* 2009; Das *et al.* 2009; Hopmann and Conradie 2009; Hruszkewycz *et al.* 2012]. Lin and Hall presented a detailed mechanism of substitution reactions of square-planar transition metal complexes and noticed that  $\sigma$ - and  $\pi$ - effects of trans ligand determines the stability of the pseudo-trigonal-bipyramidal transition state [Lin and Hall 1991]. Strong  $\sigma$ -donor ligands such as hydride and alkyl ligand weaken the trans bonds between metal and entering/leaving ligands in the pseudo-transition state and hence reduces the electron repulsion between lone pairs on the central metal and the lone pairs on the entering/leaving ligands. Ligands such as CO and C<sub>2</sub>H<sub>4</sub> are considered as  $\pi$ -acceptor which stabilizes the transition state through the  $\pi$ -back bond. Thus a unified picture of trans effect in terms of  $\sigma$ -donors and  $\pi$ -acceptor ability of the trans ligands was obtained from these results.

The feasibility of ethylene insertion in Pt–H and Pt–SiH<sub>3</sub> bonds in [PtH(SiH<sub>3</sub>)PH<sub>3</sub>C<sub>2</sub>H<sub>4</sub>] complex was investigated by Sakaki and coworkers and found that ethylene insertion preferentially occurs Pt–H bond than Pt–SiH<sub>3</sub> bond due to the hardness

of the latter bond [Sakaki *et al.* 1994]. The barrier height for the insertion of  $C_2H_4$  can be controlled by the proper choice of trans ligand. For example, when  $SiH_3$  is trans to H ligand, the barrier height to Pd–H insertion is only 4.4 kcal/mol while when  $PH_3$  is trans to H, the barrier rises to 20.6 kcal/mol at the MP4SDQ level. Similar features have also found for  $[Pt(H)(PH_3)_2(X)(C_2H_4)]$  system, where X (either  $Cl^-$  or  $SnCl_3^-$ ) is trans to migrating hydrogen atom [Rocha and deAlmeida 1998]. For the lowest trans influencing  $Cl^-$  ligand, the computed activation energy is 33.9 kcal mol<sup>-1</sup> while for stronger trans influencing ligand  $SnCl_3$ , barrier height is 11.8 kcal mol<sup>-1</sup> only at MP4SDQ//MP2 level of theory. Sakaki and coworkers investigated the insertion of acetylene molecule into Pt–H and Pt– $SiH_3$  bond in complexes of the type  $[PtH(SiH_3)PH_3C_2H_2]$  at MP2 method [Sugimoto *et al.* 1999]. They noted quite long Pd–C bond (2.52 Å) when  $SiH_3$  is trans to  $C_2H_2$  compared to the Pd–C bond trans to H (2.40 Å), indicates the higher trans influence of  $SiH_3$  ligand. Here also Pt–H insertion is more facile compared to Pt– $SiH_3$  insertion.

Sargent and Hall carried out a detailed theoretical study of the oxidative addition of dihydrogen to Vaska-type complexes, trans- $[IrX(CO)(PR_3)_2]$  [Sargent and Hall 1992]. They reported that the strong trans influencing ligands such as  $H^-$  and  $PR_3$  destabilize the five coordinate transition state while weak trans influencing ligands such as  $OH^-$  and  $Cl^-$  stabilize the transition state. Gupta *et al.* reported the dynamic behavior of square planar Pd complexes containing 2-pyridinethiolate (pyS) in solution (Figure 1.9) [Gupta *et al.* 1995]. The rate of formation of dimers depends on the order of trans influence of  $PR_3$ , which follows the order:  $PMe_3 > PMe_2Ph > PMePh_2 > PPh_3$ . When  $PR_3$  is  $PPh_3$ , stable monomers are found in solution while for  $PMe_3$ , the dimer formation is more favored.

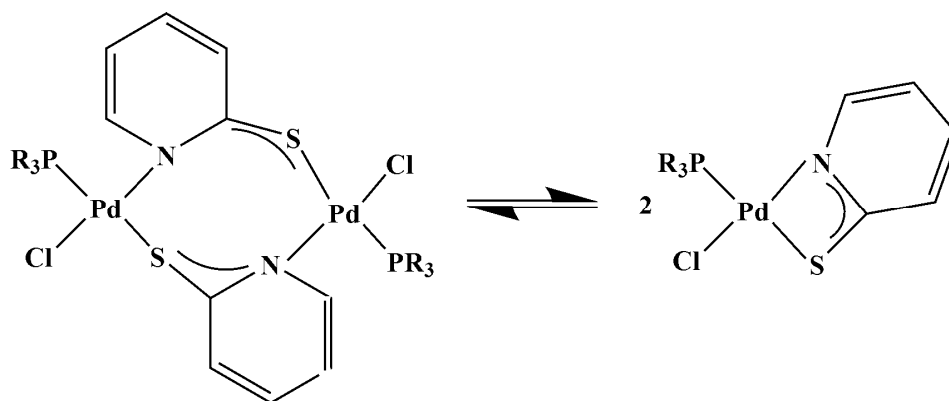


**Figure 1.9** Interconversion of dimer and monomer of a chelate complex.

von Schenck presented a detailed computational study of energetics of propene insertion into the Pd–phenyl bond of a set of Pd(II) complexes with N–N, P–O, and N–O chelating ligands at B3LYP level [von Schenck *et al.* 2003]. The neutral Pd(II) complexes favors 2,1-insertion in contrast to cationic palladium(II)-diamine complexes which favours 1,2-insertion. They identified that the insertion barrier is primarily affected by the trans influence in the unsymmetrical ligand systems. Hartwig and co-workers investigated the rate of C–N reductive elimination reactions from arylpalladium amido complexes bearing symmetrical and unsymmetrical DPPF (bis(diphenylphosphino)ferrocene) derivatives [Hartwig *et al.* 2003]. They noticed that the rate of reductive elimination reaction is controlled more by substituent effects on ground state stability than on transition state energies. This is illustrated using two regioisomers shown in the Figure 1.10 wherein isomer **a** is the minor isomer. The minor regioisomer underwent reductive elimination faster than the major regioisomer in all reactions of regioisomeric arylpalladium amido complexes. This faster reductive elimination of the minor regioisomers can be explained by ground-state destability due to trans influence.

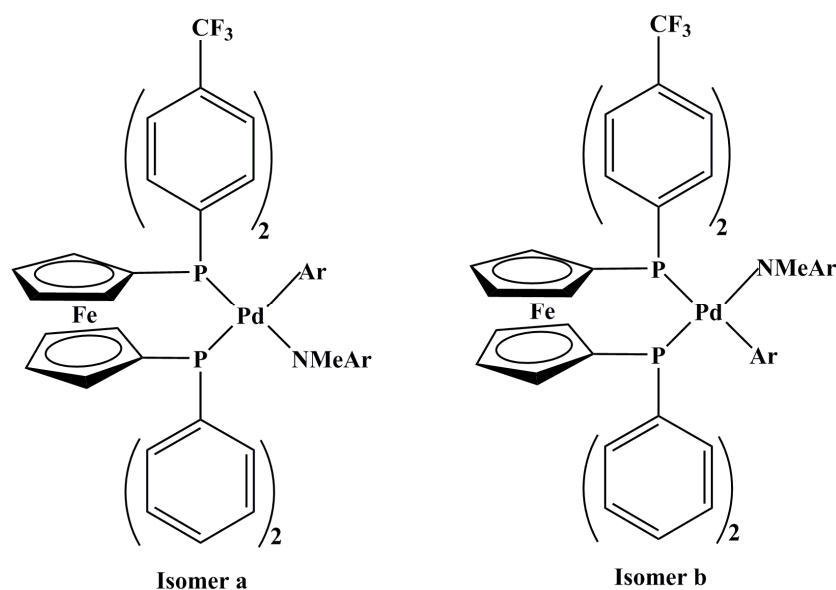


**Figure 1.10** Regioisomeric arylpalladium amido complexes.

A computational study at MP4(SDQ) method on the mechanism of hydrogenation of carbon dioxide to formic acid catalyzed by *cis*-[Ru(H<sub>2</sub>)(PMe<sub>3</sub>)<sub>3</sub>] and *cis*-[Ru(H<sub>2</sub>)(PH<sub>3</sub>)<sub>3</sub>] suggested that due to the higher trans influence of PMe<sub>3</sub> compared with the PH<sub>3</sub>, the reaction occurs more easily in *cis*-[Ru(H<sub>2</sub>)(PMe<sub>3</sub>)<sub>3</sub>] systems [Ohnishi *et al.* 2005]. Chval and co-workers investigated the mechanism of substitution of water exchange reactions in complexes of the type *trans*-Pt[(NH<sub>3</sub>)<sub>2</sub>T(H<sub>2</sub>O)]<sup>n+</sup> (where T = H<sub>2</sub>O, NH<sub>3</sub>, OH<sup>-</sup>, F<sup>-</sup>, Cl<sup>-</sup>, Br<sup>-</sup>, H<sub>2</sub>S, CH<sub>3</sub>S<sup>-</sup>, SCN<sup>-</sup>, CN<sup>-</sup>, PH<sub>3</sub>, CO, CH<sub>3</sub><sup>-</sup>, H<sup>-</sup>, C<sub>2</sub>H<sub>4</sub>) [Chval *et al.* 2008]. They found that the trans effect is directly controlled by trans influence except for the ligands with the strongest π-donation ability such as CO and C<sub>2</sub>H<sub>4</sub>. They concluded that the trans influence can be understood as a competition between trans ligands for their ability to donate the electron density to the centre Pt(II) atom. Zhu and Ziegler investigated the influence of different X ligands (X = F<sup>-</sup>, Cl<sup>-</sup>, Br<sup>-</sup>, I<sup>-</sup>, NO<sub>2</sub><sup>-</sup>, and CN<sup>-</sup>) on the C–H bond activation of CH<sub>4</sub> in complexes of the type *trans*-[PtCl<sub>2</sub>X(CH<sub>4</sub>)]<sup>-</sup> wherein X is trans to CH<sub>4</sub> [Zhu and Ziegler 2008; Zhu and Ziegler 2009]. They found that the Pt–CH<sub>4</sub> bond energy and C–H

bond activation energy barrier increases along the series  $F^- < Cl^- < Br^- < I^- < NO_2^- < CN^-$ , which is in agreement with the trans influence of these ligands.

### 1.1.6 Trans Influence in Octahedral Transition Metal Complexes

The phenomenon trans influence is well established in octahedral transition metal complexes also [Anastasi *et al.* 2007; Tubert *et al.* 2009; Farrer *et al.* 2011]. Unlike square planar complexes, the trans effect and trans influence series in octahedral complexes often correlates since ligand substitutions in octahedral complexes are generally follow dissociative mechanism [Huheey *et al.* 1993]. Five coordinate intermediate formed during the substitution reaction can be stabilized by the highly  $\sigma$ -donating ligand. Thus the highly trans influencing ligands show high trans effect. On the other hand,  $\pi$ -accepting ligands such as CO and  $C_2H_4$  show weak trans effect due to the fact that these ligands further deplete the electron density at the metal centre in the electron deficient transition state [Wilkins 1991].

Coe and Glenwright reviewed the trans influence in octahedral complexes and concluded that a general trans influence series for ligands in octahedral complexes is not possible due to the mutual influencing nature of trans ligands [Coe and Glenwright 2000]. Also, trans influence of a ligand depend on the electronic properties of the complexed metal centre. They classified majority of ligands into three classes on the basis of differences between cis and trans metal ligand bond length. Ligand showing very large trans influence fall in the first group in which the ligands are very strong  $\sigma$  donors and in most cases  $\pi$ -electron donating abilities also. Examples are  $SiR_3^-$ , NO,  $N^{3-}$ ,  $O^{2-}$ ,  $S^{2-}$ , and  $RC^{3-}$ . Some ligands can form metal ligand multiple bonds also. Second group includes those ligands having strong  $\sigma$ -donating abilities hence show large trans influence and the ligands are  $H^-$ ,  $R^-$ ,  $Ph^-$ ,  $RCO^-$ , and  $RN_2^-$ . The moderate trans influencing ligands such as CO,  $CN^-$ , CNR,

$R_2C$ ,  $NO_2^-$ ,  $NS^+$ ,  $RN_2^+$ ,  $PR_3$ ,  $P(OR)_3$ ,  $RNH^-$ ,  $RS^-$  are included in the third category. In the following section, some examples showing the importance of trans influence in ligand substitution kinetics have been described.

The release of  $H_2O$  from Co(III) complex **a** is about 3700 times faster than Co(III) complex **b** (Figure 1.11) due to higher trans influence of sulfito ligand compared to  $OH^-$  [Stranks and Yandell 1970].

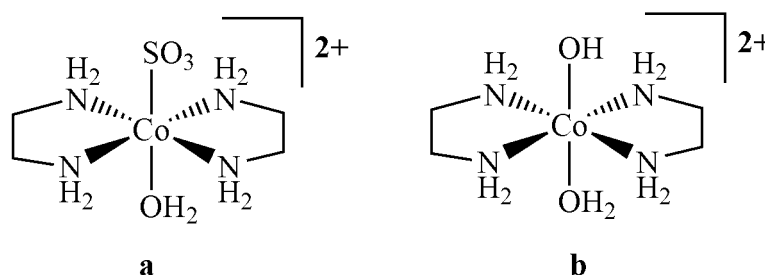


**Figure 1.11** Trans influence in Co(III) complexes with trans ligands OH and  $SO_3$ .

In alkyl cobaloxime shown in the Figure 1.12, the substitution of  $H_2O$  by  $N_3^-$  or  $NCS^-$  follows in the order of its trans influence,  $Me^- < Et^- < iPr^-$  [Crumbliss and Wilmarth 1970]. Several attempts have been made to examine the trans influence of various ligands in organo cobaloxime and hence to understand various factors contributing to the strength of Co–C bond [Randaccio *et al.* 2000; Madhuri and Satyanarayana 2005; Dutta *et al.* 2009; Kumar and Gupta 2011].

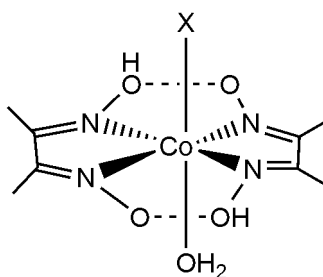


**Figure 1.12** Cobaloxime derivatives, where X = Me, Et, *iPr*.

In  $[\text{Co}^{\text{III}}(\text{dmgH})_2(\text{PR}_3)(\text{H}_2\text{O})]^+$  complexes, the rate of water substitution by  $\text{SO}_3^{2-}$  is investigated to assess the trans effect of phosphine ligands and the following series is derived:  $\text{PMePh}_2 < \text{PPh}_3 < \text{PEtPh}_2 < \text{PEt}_2\text{Ph} < \text{PEt}_3 < \text{P}(\text{nBu})_3 < \text{P}(\text{iPr})_3 < \text{PCy}_3$ , which is attributed to increasing  $\sigma$ -donating abilities of phosphine ligands [Dreos-Garlatti and Tazher 1988]. Similarly,  $\text{Cl}^-$  ligand trans to  $\text{PMe}_2\text{Ph}$  in  $\text{trans-}[\text{Rh}(\text{PMe}_2\text{Ph})_3\text{Cl}_2\text{CO}]$  complexes can be replaced more easily than  $\text{Cl}^-$  ligand trans to  $\text{CO}$  [Lupin and Shaw 1968]. This can be exploited for the preparation of disubstituted product [Marchant *et al.* 1977; Tfouni and Ford 1980; Coe and Glenwright 2000].

Trans influence is also evident in the Pt–Pt bond of the complex shown in Figure 1.13 [Hollis *et al.* 1983]. When  $\text{X} = \text{ONO}_2^-$ ,  $\text{Cl}^-$ ,  $\text{NO}_2^-$  and  $\text{Br}^-$  the corresponding Pt–Pt distances are 2.547 Å, 2.568 Å, 2.576 Å, 2.582 Å respectively, which follows the general order of trans influence.

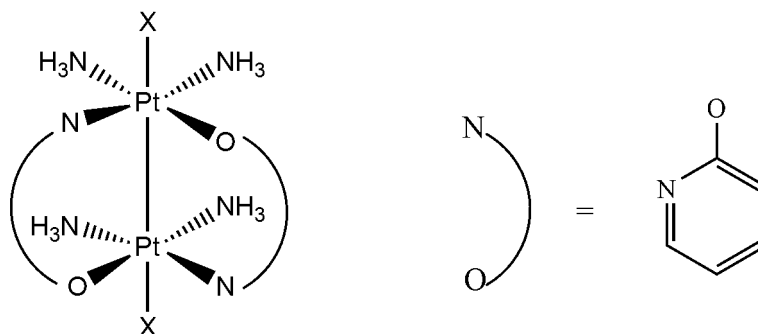


**Figure 1.13** Bimetallic complex of Pt, where Pt–Pt bond is affected by trans ligand X ( $\text{X} = \text{ONO}_2^-$ ,  $\text{Cl}^-$ ,  $\text{NO}_2^-$  and  $\text{Br}^-$ ).

## 1.1.7 Trans Influence in Other Transition Metal Complexes

The impact of trans ligand on the ground state properties of complexes having structures linear, T-shaped, and trigonal bipyramidal metal complexes were also reported. The linear complexes  $[L-M-X]^q$ , where  $M = Ag(I), Au(I)$  complexes are used for the synthesis of variety of organic molecules. Jones and co-workers investigated the trans influence of the various ligands on the Ag-Cl bond by using nuclear quadrupole resonance spectroscopy [<sup>a</sup>Jones and Williams 1977; <sup>b</sup>Jones and Williams 1977]. Palusiak *et al.* carried out detailed theoretical analysis of X-Au-Y complexes using energy decomposition analysis and found that  $\pi$ -electronic communication through the Ag(I) valence shell occurs mainly in complexes that involve a  $\pi$ -donor as well as a  $\pi$ -acceptor ligand [Palusiak *et al.* 2009]. Green and co-workers synthesized neutral metal gallyl complexes of the type  $[(NHC)M\{Ga\{[N(Ar)C(H)]_2\}\}]$  ( $M=Cu, Ag, \text{ or } Au$ ) and characterised the Ga-M bond [Green *et al.* 2007]. On the basis of spectroscopic studies, they noted that trans influence of various heterocyclic gallium are intermediate between cyclic boryl and chloro ligands. Very recent theoretical study on the trans influence of Au(I) complexes suggests that trans influence results from the competition of  $\sigma$ -donor ligands for their electron density transfer to the sd hybrid orbital of gold [Sokolov 2010].

Sturmayr and Schubert studied the geometries of several T-shaped Pt(II) complexes of the type  $(H_3P)PtXY$  ( $X, Y = Cl^-, CH_3^-, SiH_3^-, Si(OH)_3^-$ ) at ab-initio level [Sturmayr and Schubert 2003]. The Pt-P trans bond lengths in these complexes suggest the following order of trans influence;  $Cl^- < CH_3^- < SiH_3^- < Si(OH)_3^-$ . The ligand with smaller trans influence trans to  $PH_3$  ligand is found more stable isomer.

Direct structural evidence of trans influence in trigonal bipyramidal complexes were noted in  $[Fe(CO)_3XY]$  complexes [Hitchcock *et al.* 1986]. Harvey and co-workers reported

the importance of trans influence in Grubbs catalysed olefin metathesis reactions. They suggested that the strong trans influence of NHC ligands in 2<sup>nd</sup> generation catalysts would labilize the metal-phosphine bond (Figure 1.14) [Tsipis *et al.* 2005]. Experimental observations reveal that even though NHC ligands are showing higher trans influence than phosphine ligands, the dissociation of phosphine ligand from the precatalyst take place at higher rate in first generation system compared with the second generation system [Cavallo 2002; Cavallo *et al.* 2005; Correa and Cavallo 2009]. The importance of carbene rotameric state in the phosphine dissociation process is recently demonstrated by Truhlar and co-workers [Yang *et al.* 2011].

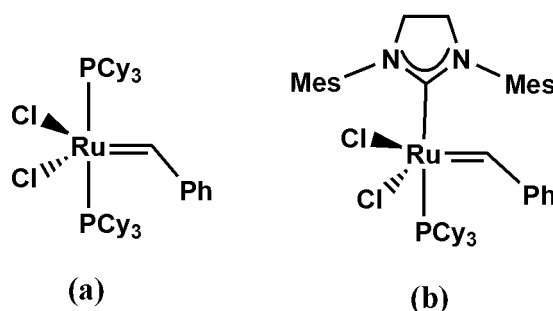


**Figure 1.14** (a) Grubbs first generation catalyst (b) Grubbs second generation catalyst.

### 1.1.8 Trans Influence in Main Group Elements and Lanthanides

The phenomenon trans influence is not only significant in transition metal complexes but also its scope can be extended to main group and lanthanide elements [Shustorovich and Buslaev 1976; Shustorovich 1978; Herrmann *et al.* 1990; Edelman 1995; Domingos *et al.* 2002; Milani *et al.* 2002]. The mutual influence of ligands in main group coordination complexes was theoretically studied by Shustorovich and Buslaev, who found that the trans influence between two ligands X and Y is always present when the central atom retained the ns<sup>2</sup> lone pair [Shustorovich and Buslaev 1976]. Trans influence is noted in complexes of

Sn(II), Sb(III), Te(IV), I(V), and Xe(VI) having the quasi-octahedral structure as well as for quasi square planar complexes of Te(II) complexes [Shustorovich and Buslaev 1976]. The Te–Br bond length in *cis*-Te(tu)<sub>2</sub>Br<sub>2</sub> (tu = thiourea) is longer by 0.27 Å compared to the Te–Br bond in *trans*-Te(tu)<sub>2</sub>Br<sub>2</sub>, shows higher *trans* influence of tu than Br. In *trans*-Te(tu)<sub>2</sub>(C<sub>6</sub>H<sub>5</sub>)Cl complexes, the *trans* Te–Cl bond length is about 0.70 Å higher than compared to Te–Cl bond in *cis*-Te(tu)<sub>2</sub>Cl<sub>2</sub> [Foss 1970]. Lewinski *et al.* reported that the presence of *trans*-influence of axial substituents is a significant factor controlling the structure and stability of five-coordinate aluminium compounds Me<sub>2</sub>Al[OC(Me)C<sub>6</sub>H<sub>4</sub>-2-O]. ( $\gamma$ -picoline) [Lewinski 1999].

*Trans* influence is also present in T-shaped hypervalent complexes of the type Y–M(L)–X, M = I, Se, S, Br and Te complexes, where Y and X are the ligands present in the axial position and L in the equatorial position of the T-shaped structure [Foss *et al.* 1987; Rudd *et al.* 1997; Ochiai *et al.* 2010]. In main group elements, *trans* influence can be taken as a function of polarisability and the electronegativity of the ligands [Foss *et al.* 1987 ; Rudd *et al.* 1997]. Thus the order of *trans* influence among halogens are I > Br > Cl > F. Similarly, the *trans* influence decreases in the order Se > S > O [Rudd *et al.* 1997]. Ochai *et al.* analyzed various crystal structures of iodine (III) complexes, classified various ligands in the order of their *trans* influence and found that *trans* influence order matches the order of inductive effect of various ligands present [Ochiai *et al.* 2006].

*Trans* influence in lanthanide complexes was noted in *mer*-octahedral lanthanide thiolate coordination compound (Py)<sub>3</sub>Yb(SPh)<sub>3</sub>, wherein the Yb–S bond *trans* to pyridine Py is being significantly shorter than the Yb–S bond *trans* to SPh [Lee *et al.* 1995]. These observations are conflicted since it was believed that the bonding in lanthanide (Ln) complexes is purely electrostatic in nature [Raymond 1980]. Later, these types of bond lengthening is noted in *fac*-octahedral halide coordination compounds, chalcogen idobased cluster compounds, in chalcogenolate complexes and in fluorinated phenolate compounds

[Freedman *et al.* 1998; Kornienko *et al.* 2002; Norton *et al.* 2009; Krogh-Jespersen *et al.* 2010]. In all the cases, the assessment of Ln–ligand bond length showed that when an anionic ligand is trans to it, its bond length is significantly longer than the bond trans to a neutral ligand. On the basis of experimental and DFT studies, Krogh-Jespersen *et al.* demonstrated that the partial covalent character is responsible for the trans influence in lanthanide complexes [Krogh-Jespersen *et al.* 2010]. Most recently, by using QTAIM analysis, Gholivand and Mahzouni proved that the partial covalent character of Ln–Cl bond is responsible for its bond lengthening nature [Gholivand and Mahzouni 2012].

# Part B - Computational Chemistry

---

## 1.2 Computational Chemistry

Computational chemistry is a branch of theoretical chemistry in which the applications of chemical, mathematical and computing skills are used for solving chemical problems. There are different methods available in computational chemistry ranges from highly accurate to very approximate to determine the structure and properties of molecular systems. Depending upon formalism, these methods are mainly classified into (i) molecular mechanics (MM) (ii) quantum chemical methods (iii) semi-empirical quantum chemical methods (iv) density functional theory (DFT) methods (v) molecular dynamics and Monte Carlo simulations (vi) hybrid quantum mechanics/molecular mechanics (QM/MM) methods. These methods are briefly discussed in the following sections.

### 1.2.1 Molecular Mechanics Methods

Molecular mechanics (MM) uses Classical/Newtonian Mechanics to describe the structures and properties of a molecule [Weiner and Kollman 1981; Boyd and Lipkowitz 1982]. MM is an attempt to predict the molecular properties assuming that molecules are a set of spheres which are held together by 'springs'. Here the spheres correspond to atoms while spring represents the bonding between atoms. The mathematics corresponds to the deformation of springs is used to describe the capability of bonds to stretch, bend, and twist. The objective of molecular mechanics is to predict the energy associated with a given conformation of a molecule [Bowen and Allinger 1991; Dinur and Hagler 1991]. A simple molecular mechanics energy equation is given by Eq. 1.1, and these types of equations

together with the data (parameters) required to describe the behavior of different kinds of atoms and bonds are generally called a force-field.

$$E = E_{str} + E_{ang} + E_{tor} + E_{nb} + E_{col} \quad \dots \text{(Eq. 1.1)}$$

In the above equation,  $E$  is termed as the steric energy, which is a measure of the intra-molecular strain relative to a hypothetical situation.  $E_{str}$  is the energy for bond stretching,  $E_{ang}$  is the energy for deforming a bond angle from equilibrium,  $E_{tor}$  is the energy results from deforming the torsional angle,  $E_{nb}$  is the energy results from non bonded interactions and  $E_{col}$  is the energy arising from the coulombic forces. Let us consider each of the terms in the above equation,

**Bond stretching:** By applying Hooks law in ball and spring model, we can evaluate the energy needed to stretch and bend from their equilibrium values and the corresponding equation is,

$$E_{str} = \sum \frac{1}{2} k_{str} (b - b_{eq})^2 \quad \dots \text{(Eq. 1.2)}$$

where,  $k_{str}$  is the proportionality constant or force constant of that particular bond,  $b$  and  $b_{eq}$  are the length of the bond when stretched and equilibrium bond length of that bond respectively.

**Bond deformation:** Analogous to the above situation, if the strain free energy of a particular angle is given as  $\beta_{eq}$ , then any deformation from this value will lead to a change in its potential energy and the corresponding expression of this potential energy function describing the deformation is

$$E_{ang} = \sum \frac{1}{2} k_{\beta} (\beta - \beta_{eq})^2 \quad \dots \text{(Eq. 1.3)}$$

where,  $k_{\beta}$  is the force constant of the particular angle (related to the strength of the bonding situation),  $\beta_{eq}$  and  $\beta$  are the equilibrium angle and the deformed angle respectively.

**Torsion:** The intramolecular rotations about bonds do not occur without energy costs. One of the well studied examples is the rotation about a carbon-carbon bond in ethane. These energies are usually expressed in terms of a Fourier series,

$$E_{tor} = \sum \frac{1}{2} V_i (1 + \cos \gamma) \quad \dots \text{(Eq. 1.4)}$$

where  $V_i$  is the Fourier coefficients and  $\gamma$  is the dihedral angle.

**Non Bonded Interactions:** These type of interactions are usually modeled by London dispersive Forces (for attraction) and Van der Waals forces (for the repulsion). A general way to approximate non bonded interactions is using the so-called Lennard-Jones potential.

$$E_{nb} = \sum \left[ \left( \frac{\sigma}{r} \right)^{12} - \left( \frac{\sigma}{r} \right)^6 \right] \quad \dots \text{(Eq. 1.5)}$$

Here ' $r$ ' is the distance between the centre's of the non bonded atoms or groups and ' $\sigma$ ' is the finite distance at which the inter-particle potential is zero.

**Electrostatic Interactions:** The electrostatic interactions can be modeled using Coulombic potential.

$$E_{col} = \sum \frac{q_i q_j}{r_{ij}} \quad \dots \text{(Eq. 1.6)}$$

The electrostatic energy is a function of the charge ( $q$ ) on the non-bonded atoms, their interatomic distance ( $r$ ), and a molecular dielectric expression that accounts for the decrease of electrostatic interaction due to the environment (such as by solvent or the molecule itself).

When all these energy terms are substituted in the Eq. 1.1, a model which is called the functional form of the force field is obtained. The constants ( $k_{str}$ ,  $k_{\beta}$ ,  $V_i$ ) and the equilibrium values ( $b_{eq}$ ,  $\beta_{eq}$ ) are atomic parameters which can be experimentally derived from spectroscopic techniques and theoretically by ab initio calculations on a given class of molecules. The most influential term, the electrostatic term, however is not fully

understood. Hence the variation in results from different force fields can be attributed, to a large extent, to the electrostatic term.

One of the advantages of molecular methods is that it requires less computation time compared to other methods and it is highly useful for large molecules such as proteins. Major disadvantage of using MM method is that it cannot be applied for calculations involving electronic properties. Also, the force field parameters derived for one set of molecules is not likely to perform well for other set of molecules.

## 1.2.2 Quantum Mechanical Methods

### 1.2.2.1 Ab initio Molecular Orbital Theory

Quantum mechanical methods are based on Schrödinger wave equation [Schrödinger 1926].

$$\mathbf{H}\Psi = E\Psi \quad \dots \text{(Eq. 1.7)}$$

where  $\mathbf{H}$  is the Hamiltonian operator comprising of the nuclear and electronic kinetic energy operators and the potential energy operators corresponding to the nuclear-nuclear, nuclear-electron and electron-electron interactions. The many-particle wave function  $\Psi$  describes the system, while  $E$  is the energy eigen value of the system. The Hamiltonian operator for  $N$  electron and  $M$  nucleus can be written as

$$\mathbf{H} = -\sum_{i=1}^N \frac{1}{2} \nabla_i^2 - \sum_{A=1}^M \frac{1}{2M_A} \nabla_A^2 - \sum_{i=1}^N \sum_{A=1}^M \frac{Z_A}{r_{iA}} + \sum_{i=1}^N \sum_{j>i}^N \frac{1}{r_{ij}} + \sum_{A=1}^M \sum_{B>1}^M \frac{Z_A Z_B}{R_{AB}} \quad \dots \text{(Eq. 1.8)}$$

where  $R_A$  and  $r_i$  are the position vectors of nuclei and electrons. The distance between the  $i^{\text{th}}$  electron and  $A^{\text{th}}$  nucleus is  $r_{iA}$ ; the distance between  $i^{\text{th}}$  and  $j^{\text{th}}$  electron is  $r_{ij}$  and the distance between the  $A^{\text{th}}$  nucleus and  $B^{\text{th}}$  nucleus is  $R_{AB}$ .  $M_A$  is the ratio of the mass of the nucleus to the mass of an electron and  $Z_A$  is the atomic number of nucleus  $A$ . The above Hamiltonian is difficult to solve. The problem can be simplified by separating the nuclear and electron

motions. This is called the Born Oppenheimer approximation [Born and Oppenheimer 1927]. The Hamiltonian for a molecule with stationary nuclei is,

$$\mathbf{H}_{elec} = -\sum_{i=1}^N \frac{1}{2} \nabla_i^2 - \sum_{i=1}^N \sum_{A=1}^M \frac{Z_A}{r_{iA}} + \sum_{i=1}^N \sum_{j>i}^N \frac{1}{r_{ij}} \quad \dots \text{(Eq. 1.9)}$$

The first term is the electronic kinetic energy operator summed over the number of electrons,  $N$ . The second term represents Coulombic attraction between electrons  $i$  and  $M$  nuclei  $A$ , while  $Z_A$  are the nuclear charges. The last term attributes to the Coulombic repulsion between electrons.

Once the wavefunction  $\Psi$  is obtained, any property of the individual molecule can be determined. This is done by taking the expectation value of the operator for that property [McQuarrie and Simon 1997]. For example, the energy is the expectation value of the Hamiltonian operator given by,

$$\langle E \rangle = \int \Psi^* \mathbf{H} \Psi \quad \dots \text{(Eq. 1.10)}$$

For an exact solution, this is the same as the energy predicted by the Schrödinger equation. Properties other than the energy are not variational, because only the Hamiltonian is used to obtain the wave function in the widely used computational chemistry methods.

### 1.2.2.2 Hartree-Fock Method

In Hartree-Fock method, the wave function is expressed as an antisymmetrized product of spin orbitals in the form of a Slater determinant [Hartree 1928; Slater 1930; Fock 1930]. Thus, an  $N$ -electron wave function within the HF formulation can be written as

$$\psi(\mathbf{x}_1, \mathbf{x}_2, \dots, \mathbf{x}_N) = \frac{1}{\sqrt{N!}} \begin{vmatrix} \chi_i(\mathbf{x}_1) & \chi_j(\mathbf{x}_1) & \dots & \chi_N(\mathbf{x}_1) \\ \chi_i(\mathbf{x}_2) & \chi_j(\mathbf{x}_2) & \dots & \chi_N(\mathbf{x}_2) \\ \cdot & \cdot & \dots & \cdot \\ \chi_i(\mathbf{x}_N) & \chi_j(\mathbf{x}_N) & \dots & \chi_N(\mathbf{x}_N) \end{vmatrix} \quad \dots \text{(Eq. 1.11)}$$

The factor  $1/\sqrt{N!}$  is a normalization factor. The spin orbitals are denoted as  $\chi$ 's, while  $\mathbf{x}_1$ ,

$\mathbf{x}_2...$ *etc.* represent the combined spatial and spin coordinates of the respective electrons. The normalized Slater determinant can also be represented in a shorter notation as

$$\psi(\mathbf{x}_1, \mathbf{x}_2, \dots, \mathbf{x}_N) = |\chi_i \chi_j \dots \chi_N\rangle \quad \dots \text{(Eq. 1.12)}$$

In this notation it is presumed that the electrons 1, 2...*etc.* sequentially occupy the spin orbitals. The simplest antisymmetric wavefunction which can be used to describe the ground state of an N–electron system is a single Slater determinant,

$$|\psi_0\rangle = |\chi_i \chi_j \dots \chi_N\rangle \quad \dots \text{(Eq. 1.13)}$$

The choice of approximation of wave function guarantees a proper description of the electron which obeys the Pauli exclusion principle. According to variation principle, the best spin orbital of this functional form is one which gives the lowest possible energy,

$$E_0 = \langle \psi_0 | H | \psi_0 \rangle \quad \dots \text{(Eq. 1.14)}$$

where  $H$  is the full electronic Hamiltonian. By minimizing  $E_0$  with respect to the choice of spin orbitals, one can derive an equation called the Hartree–Fock (HF) equation which determines the optimal spin orbitals. Hartree-Fock equation is an eigen value equation of the form

$$f(i)\chi(x_i) = \mathcal{E}\chi(x_i) \quad \dots \text{(Eq. 1.15)}$$

where  $f(i)$  is a one electron operator called the Fock operator of the form

$$f(i) = -\frac{1}{2}\nabla_i^2 - \sum_{A=1}^M \frac{Z_A}{r_{iA}} + V^{HF}(i) \quad \dots \text{(Eq. 1.16)}$$

where  $V^{HF}(i)$  is the Hartree-Fock potential which is the average potential experienced by the  $i^{\text{th}}$  electron due to the presence of other electrons. Thus, the HF approximation replaces the complicated many electron problem by a one electron problem in which electron-electron repulsion is treated in an average way. The procedure of solving the HF equation is called the self–consistent field (SCF) method.

### 1.2.2.3 Post Hartree-Fock Methods

One of the major problems of HF method is that it completely neglects the correlations between electrons with same spin [Szabo and Ostlung 1989]. The energy associated with the electron correlation is given as [Boys 1950]:

$$E_{corr} = E_{exact} - E_{HF} \quad \dots \text{(Eq. 1.17)}$$

where  $E_{exact}$  is the exact energy of the system and  $E_{HF}$  is the HF energy.  $E_{corr}$  is always negative because  $E_{HF}$  is always greater than  $E_{exact}$ .

Post Hartree-Fock methods in quantum mechanics are the set of methods developed to improve the Hartree-Fock method by taking into account of electron correlation. Post Hartree-Fock methods include configuration interaction (CI), Moller-Plesset perturbation, and coupled cluster. The basis for CI method is that the wave function may be written as a linear combination of Slater determinants rather than one single Slater determinant in HF and which is used to approximate the wave function [Pople *et al.* 1976; Foresman *et al.* 1992]. In perturbation theory, a perturbation term is added to involve the electron repulsion and the HF solution is treated as the first term in a Taylor series. Including second order perturbation corrections lead to the method MP2 [Brillouin 1934; Kelly 1969]. Coupled cluster methods are the more mathematically refined technique for estimating the electron correlation energy through the use of a coupled cluster [Čizek 1966; Kümmel 2002]. Post HF methods are computationally too expensive for larger systems [Cramer 2004]. For a system of N atoms, HF calculations scale as  $N^4$  while for MP2 and MP4 scales as  $N^5$  and  $N^7$  respectively.

### 1.2.2.4 Basis Sets

Basis sets are mathematical functions used to represent the size and shape of atomic orbitals. These functions are expanded as a linear combination of atomic orbitals to describe molecular orbitals [Clementi 1964]. The basis functions are classified into two

main types, *viz.* Slater type orbitals (STOs) [Allen and Karo 1960] and Gaussian type orbitals (GTOs) [<sup>a</sup>Boys 1950; Feller and Davidson 1990].

***The expression for STO is given as:***

$$STO = Nr^{n-1}e^{-\zeta r}Y_{lm}(\Theta, \phi) \quad \dots \text{(Eq. 1.18)}$$

Where  $N$  is the normalization constant,  $Y_{lm}$  is the angular momentum part,  $\zeta$  is the exponent,  $r$ ,  $\Theta$  and  $\phi$  are spherical coordinates. The principal, angular momentum and magnetic quantum numbers are represented by the notations  $n$ ,  $l$  and  $m$ .

***The expression for GTO is given as:***

$$GTO = Nx^l y^m z^n e^{-\alpha r^2} \quad \dots \text{(Eq. 1.19)}$$

Here,  $N$  is the normalization constant, and  $x$ ,  $y$ ,  $z$  are cartesian coordinates. GTOs have the exponential dependence of  $e^{-\alpha r^2}$ . Compared to GTOs, STOs are very difficult to handle computationally since the two electron repulsion integrals in the STO are difficult to evaluate and hence GTOs are commonly used [Shavitt 1963; Stewart 1970]. Also, it is proved that a number of GTOs can be combined to approximate a STO and this often more efficient than a STO itself [Huzinaga 1984].

There are varieties of Gaussian basis sets available now, which have been continuously improved over the years [Schlegel 1982]. The single-zeta Gaussian basis sets, also known, as minimal basis set, are the simplest GTOs. In the most popular single-zeta basis set STO-3G each Slater type orbital consists of 3 primitive Gaussian type orbitals (PGTO) [Hehre *et al.* 1969; Ditchfield *et al.* 1971]. Since the inner-shell electrons are not so vital to the calculation, they are described with a single Slater Orbital and usually double-zeta is used only for valence orbitals. This method is called a split-valence basis set. 3-21G and 6-31G are common examples of split-valence basis sets [Hehre *et al.* 1972; Binkley *et al.* 1980]. The notation 3-21G shows that a single basis set consisting of 3 gaussian functions for inner electrons and the valence electrons are represented by two separate basis functions,

one consisting of 2 gaussian functions and the other 1 gaussian function. In 6-31G, the number of gaussian functions is increased. Basis sets can be elaborated using polarization functions and/or diffuse functions. Interaction between atoms induces a deformation of the electronic cloud around each atom and this is called polarisation. This is usually denoted as \* or \*\* describing the use of an extra set of d-orbitals on heavy atoms and p-orbitals on hydrogens. Another way to represent this is to add (d) or (d, p) after the G in the notation of the basis sets. To spread the electron density over the molecule diffuse functions are added, and these are denoted by + or aug in the name of basis set. If the diffuse functions are included on hydrogen atoms it is indicated by ++ signs. For calculations involving transition metals, the inner core of these atoms is very large and a large number of basis functions are required to describe these. Because the valence electrons are involved in bonding, the basis functions corresponding to core electrons can be replaced by an Effective core potential (ECP) [Hay and Wadt 1985; Jensen 1999]. These basis functions are generated from relativistic atomic calculations hence this includes some relativistic effects on the system studied.

### 1.2.3 Semi-empirical Quantum Chemical Methods

The practical applications of ab initio quantum chemical methods are limited particularly for larger systems because of their heavy demands of computational time. The semi-empirical methods are also based on Schrödinger wave equation. In semiempirical calculations extensive use of approximations are made and the core electrons are not included in the calculations [Pople and Beveridge 1970; Stewart 1990]. Certain complicated integrals in the Hartree-Fock calculations are omitted. The approximations are mainly in the construction of Fock matrix. To correct these limitations, this method is parametrized using results of experimental data or ab initio calculations.

In the most popular semi-empirical methods used today (MNDO, AM1 and PM3) are based on the Neglect of Diatomic Differential Overlap (NDDO) method. Here the overlap matrix  $S$  is replaced by the unit matrix. Hence the Hartree-Fock secular equation  $|\mathbf{H} - \mathbf{E}\mathbf{S}| = 0$  can be replaced with a simpler equation  $|\mathbf{H} - \mathbf{E}| = 0$ . The modern semiempirical methods differ by further approximations that are made such as evaluating the one and two-electron integrals and the parameterization technique. RM1 and PM6 are recent extensions of the AM1 and PM3 methods, and these methods gives more accurate results compared to other semiempirical methods.

Semi-empirical methods are excellent computational tools which give fast quantitative estimates for a number of properties and this method is particularly useful for scanning a chemical problem before proceeding with higher-level treatments and for correlating large sets of experimental and theoretical data. Semi-empirical calculations are much faster may be by several orders of magnitude when compared to ab initio method. One of the disadvantage is that semi-empirical methods are less accurate and the errors are less systematic hence difficult to rectify.

## 1.2.4 Density Functional Theory (DFT)

Density functional theory is another approach to the electronic structure calculation of atoms and molecules. DFT is based on determining the electron density  $\rho(\mathbf{r})$ , and not the wave function as in Hartree-Fock method [Thomas 1927; Fermi 1927; Fermi 1928]. Unlike wave function, the electron density is a physically observable quantity. The energy of the system can be completely described on the basis of electron density associated with the Hamiltonian operator. The electron density is related to the component of one electron orthonormal orbitals  $\psi_i$  of a single determinant wave function by,

$$\rho(\mathbf{r}) = \sum_{i=1}^N |\psi_i|^2 \quad \dots \text{(Eq. 1.20)}$$

In 1964, Hohenberg and Kohn established two fundamental theorems, which is regarded as the foundation of the modern DFT [Hohenberg and Kohn 1964]. According to the Hohenberg-Kohn (HK) theorems, (i) the external potential  $V_{ext}(\mathbf{r})$  and hence the total energy  $E$  is a unique functional of electron density  $\rho(\mathbf{r})$  and (ii) the ground state energy can be obtained variationally: the density that minimizes the total energy is the exact ground state density. A straightforward consequence of the first Hohenberg and Kohn theorem is that the ground state energy is also uniquely determined by the ground-state charge density [Kohn and Sham 1965]. The energy functional can be written as,

$$E[\rho(\mathbf{r})] = F[\rho(\mathbf{r})] + \int V_{ext}(\mathbf{r})\rho(\mathbf{r})d\mathbf{r} \quad \dots \text{(Eq. 1.21)}$$

The first term arises from the interaction of electrons with an external potential  $V_{ext}(\mathbf{r})$  and the second term  $F[\rho(\mathbf{r})]$  is the sum of the kinetic energy of the electrons and the contribution from inter electronic interactions. Kohn and Sham found that most of the problems are associated with the way the kinetic energy is described and suggested a suitable method to handle the HK theorem for a set of interacting electrons. They divided the total energy into the following parts:

$$E[\rho(\mathbf{r})] = T_s[\rho(\mathbf{r})] + E_H[\rho(\mathbf{r})] + E_{XC}[\rho(\mathbf{r})] + \int V_{ext}(\mathbf{r})\rho(\mathbf{r})d\mathbf{r} \quad \dots \text{(Eq. 1.22)}$$

where  $T_s[\rho(\mathbf{r})]$  is the kinetic energy  $E_H[\rho(\mathbf{r})]$  is the electron-electron coulombic energy and  $E_{XC}[\rho(\mathbf{r})]$  contains contributions from exchange and correlation. The computation of the kinetic energy can be expressed in terms of one electron function,

$$T_s[\rho(\mathbf{r})] = \sum_{i=1}^N \int \psi_i(\mathbf{r}) \left( \frac{\nabla^2}{2} \right) \psi_i(\mathbf{r}) d\mathbf{r} \quad \dots \text{(Eq. 1.23)}$$

The term  $E_H[\rho(\mathbf{r})]$  arises from the interaction between two charge densities,

$$E_H[\rho(\mathbf{r})] = \frac{1}{2} \iint \frac{\rho(\mathbf{r}_1)\rho(\mathbf{r}_2)}{|\mathbf{r}_1 - \mathbf{r}_2|} d\mathbf{r}_1 d\mathbf{r}_2 \quad \dots \text{(Eq. 1.24)}$$

Combining the  $T_s[\rho(\mathbf{r})]$ ,  $E_H[\rho(\mathbf{r})]$  and the electron-nuclear interaction leads to the full expression for the energy of an N-electron system within the Kohn-Sham scheme:

$$E_H[\rho(\mathbf{r})] = \sum_{i=1}^N \int \psi_i(\mathbf{r}) \left( \frac{\nabla^2}{2} \right) \psi_i(\mathbf{r}) d\mathbf{r} + \frac{1}{2} \iint \frac{\rho(\mathbf{r}_1)\rho(\mathbf{r}_2)}{|\mathbf{r}_1 - \mathbf{r}_2|} d\mathbf{r}_1 d\mathbf{r}_2 \quad \dots \text{(Eq. 1.25)}$$

$$+ E_{XC}[\rho(\mathbf{r})] - \sum_{\alpha} \frac{Z_{\alpha}}{|\mathbf{r} - \mathbf{R}_{\alpha}|} \rho(\mathbf{r}) d\mathbf{r}$$

$E_{XC}$  is simply the sum of the error made in using the non-interacting kinetic energy and the error made in treating the electron-electron interaction. When we write the functional in terms of the density built from non-interacting orbitals and applying the variational theorem, the one electron Kohn-Sham equation takes the form,

$$\left\{ -\frac{\nabla^2}{2} - \left( \sum_{\alpha=1}^M \frac{Z_{\alpha}}{r_{1\alpha}} \right) + \frac{\rho(\mathbf{r}_2)}{\mathbf{r}_{12}} + V_{XC}[\rho(\mathbf{r})] \right\} \psi_i(\mathbf{r}_1) = \varepsilon_i \psi_i(\mathbf{r}_1) \quad \dots \text{(Eq. 1.26)}$$

Here the external potential is written appropriate to the interaction with  $M$  nuclei and  $\varepsilon_i$  are the orbital energies and  $V_{XC}$  is the exchange correlation functional, which is related to exchange-correlation energy by:

$$V_{XC}[\rho(\mathbf{r})] = \left( \frac{\delta E_{XC}[\rho(\mathbf{r})]}{\delta \rho(\mathbf{r})} \right) \quad \dots \text{(Eq. 1.27)}$$

Kohn-Sham equations describe the behavior of non-interacting electrons in an effective local potential. These Kohn-Sham equations have the same structure as the Hartree-Fock equations with the non-local exchange potential replaced by the local exchange-correlation potential  $V_{XC}$ . The importance of Kohn-Sham (KS) approach is that it gives an exact correspondence between the density and ground state energy of a system consisting of non-interacting Fermions and the “real” many body system described by the Schrödinger equation.

Even the HK and KS formalisms do not lead to the exact form of exchange-correlation functional  $E_{XC}[\rho(\mathbf{r})]$ , much of it is left to a systematic search and guesswork and the utility of DFT depends on the approximation used for  $E_{XC}[\rho(\mathbf{r})]$ . The most widely used

approximation in physics is local density approximation (LDA) wherein to calculate the total energy of a system, electron density at each point in space is considered. In non-local density approximation (NLDA or GGA), the variation in density, the gradient, was taken into account. B3LYP method is one of the most common DFT methods, which is a form of hybrid between DFT and HF methods [Lee *et al.* 1988]. DFT gives better results than HF and in many cases, DFT is comparable to MP2 methods. Recently, a number of DFT methods are developed that includes standard GGA functionals, hybrid-GGA functionals, meta-GGA functionals, hybrid meta-GGA functionals, functional designed to incorporate long-range dispersion interactions, and the random phase approximation.

## 1.2.5 Molecular Dynamics and Monte Carlo Simulations

Molecular dynamics is a simulation of the time-dependent behavior of a molecular system such as vibrational motion or Brownian motion [Schlick 2002; Rapaport 2004]. Molecular dynamics calculations apply the laws of motion to molecules to calculate the energy of the system. The molecular dynamic simulations would allow us to calculate thermodynamic quantities, diffusion constants, and correlation functions also. The term Monte Carlo method (or Monte Carlo simulation) can be used to describe any technique that approximates solutions to quantitative problems through statistical sampling [Doll and Freeman 1994]. Monte Carlo simulations use probability theory to solve mathematical problems. Monte Carlo methods are generally easily parallelizable, with some techniques being ideal for use with large CPU clusters.

Unlike molecular dynamics simulations, Monte Carlo simulations are free from the restrictions of solving Newton's equations of motion. This allows for cleverness in the proposal of moves that generate trial configurations within the statistical mechanics

ensemble of choice. Since one does not solve Newton's laws of motion, no dynamical information can be obtained from a traditional Monte Carlo simulation. Difficulty of conducting large-scale moves in an explicit solvent is one of the main limitations of Monte Carlo simulations of proteins.

## 1.2.6 Hybrid Quantum Mechanics/Molecular Mechanics (QM/MM) Methods

Quantum mechanical methods (QM) can compute ground state and excited state properties of molecular systems and can model chemical reactions while it is time consuming for larger systems. Molecular mechanics (MM) is able to model very large compounds quickly. It is possible to combine quantum mechanical model and molecular mechanic methods into one calculation known as hybrid QM/MM method and this helps to attain a balance between accuracy and computational cost. Here the active site of a molecule is modeled using quantum mechanics while the rest of the molecule is modeled with the help of molecular mechanics [Warshel and Levitt 1976; Gao 1996; Mordasini and Thiel 1998].

In the case of QM/MM methodology, the total Hamiltonian of the system can be written in the form:

$$\mathbf{H} = \mathbf{H}^{QM} + \mathbf{H}^{QM/MM} + \mathbf{H}^{MM} \quad \dots \text{(Eq. 1.28)}$$

where  $\mathbf{H}^{QM}$ ,  $\mathbf{H}^{MM}$  and  $\mathbf{H}^{QM/MM}$  are the QM hamiltonian, MM hamiltonian, and the corresponding Hamiltonian for QM/MM interaction between the QM and the MM part. The energy  $E$  of the QM/MM system can be taken as the sum of the QM energy ( $E^{QM}$ ), the MM energy ( $E^{MM}$ ) and the interaction energy between the two parts  $E^{QM/MM}$ :

$$E = E^{QM} + E^{QM/MM} + E^{MM} \quad \dots \text{(Eq. 1.29)}$$

Among various hybrid methods, the ONIOM (Our N-layered Integrated molecular

Orbital + molecular Mechanics) method developed by Morokuma and coworkers is more general, that allows different levels of theory to be applied to different parts of a system and combined to produce reliable geometry and energy [Maseras and Morokuma 1995; Humbel *et al.* 1996; Dapprich *et al.* 1999].

### 1.2.7 Quantum Theory of Atoms in Molecule Analysis (QTAIM)

The quantum theory of atoms in molecules (QTAIM) theory was formulated on the fact that electron density plays a critical role in explaining and understanding the experimental observations of chemistry [Bader 1990; Matta and Boyd 2007]. The electron density  $\rho(\mathbf{r})$  is a physical quantity and this scalar field is defined over three-dimensional space. The  $\rho(\mathbf{r})$  value can be obtained both from quantum chemical calculations and on the basis of experimental measurement such as high-resolution X-ray diffraction data. The AIM theory is based on topological analysis of  $\rho(\mathbf{r})$  [Bader 1998].

A critical point (CP) in the electron density is a point in space at which the first derivatives of the density vanish,

$$\nabla\rho(\mathbf{r}) = i\frac{d\rho(\mathbf{r})}{dx} + j\frac{d\rho(\mathbf{r})}{dy} + k\frac{d\rho(\mathbf{r})}{dz} \begin{cases} = \bar{0} & (\text{at critical point and at } \infty) \\ \text{Generally } \neq \bar{0} & (\text{at all other points}) \end{cases}$$

... (Eq. 1.30)

where the zero vector signifies that each individual derivative in the gradient operator,  $\nabla\rho(\mathbf{r})$  is zero and not just their sum. The Hessian matrix is composed of nine second derivatives of the density at the critical point. The trace of Hessian is invariant to rotations of the coordinate system. This is known as the Laplacian of the density, which is given as

$$\nabla^2 \rho(\mathbf{r}) = \nabla \cdot \nabla \rho(\mathbf{r}) = i \frac{d^2 \rho(\mathbf{r})}{dx^2} + j \frac{d^2 \rho(\mathbf{r})}{dy^2} + k \frac{d^2 \rho(\mathbf{r})}{dz^2} \quad \dots \text{(Eq. 1.31)}$$

The critical points are symbolized as  $(\omega, \sigma)$ , where  $\omega$  is the rank and  $\sigma$  is the signature. The rank is the number of non-zero curvatures of  $\rho(\mathbf{r})$  at the critical point and the signature is the algebraic sum of the signs of the curvatures. There are four type of stable critical points *viz.* (3, -3) nuclear critical point (ncp), (3, -1) bond critical point (bcp), (3, +1) ring critical point (rcp) and (3, +3) cage critical point (ccp). Out of these, bcps are of particular interest since they can be used in the identification of chemical bonds between atoms and also the nature of interactions.

A bond path is the line along which the electron density is a maximum which links the nuclei of two chemically bonded atoms. A collection of bond paths linking the nuclei of bonded atoms in equilibrium geometry with the associated critical points is known as the molecular graph. Figure 1.15 shows the molecular graph of a cubane molecule.

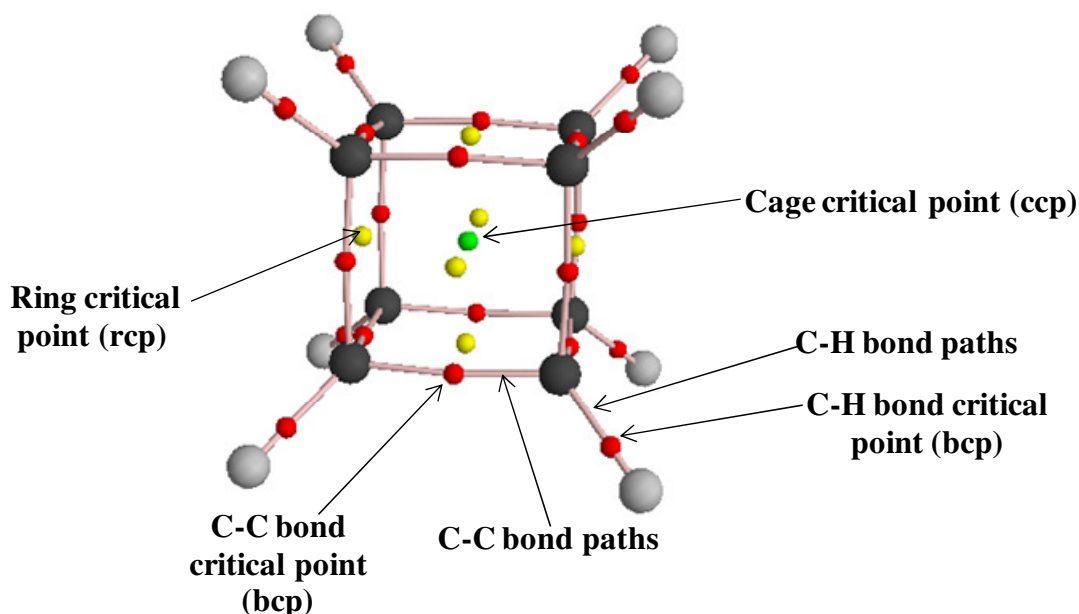


**Figure 1.15** Molecular graph of cubane (B3LYP/6-311++G(d,p)) showing the bond paths (lines) and different critical points: nuclear (colour-coded by element C = black, H = grey), red for (3, -1) or bond CP, yellow for (3, +1) or ring CP, and green for (3, +3) or cage CP.

Some criteria have been proposed to characterise chemical bonds and interactions based on AIM parameters at bond critical points [Bader 1990; Matta and Boyd 2007; Palusiak and Krygowski 2007; Bader 2009]. The following parameters of electron density functions is helpful to analyze the nature of a chemical bond *viz.* the electron density ( $\rho(\mathbf{r})$ ), the Laplacian ( $\nabla^2\rho(\mathbf{r})$ ), the density of the total energy of the electron ( $H(\mathbf{r})$ ), the kinetic electron energy density ( $G(\mathbf{r})$ ) and the potential electron energy density ( $V(\mathbf{r})$ ). In many applications,  $\rho(\mathbf{r})$  has been used as a measure of the strength of the bonding interaction, particularly the  $\sigma$ -interaction.  $\nabla^2\rho(\mathbf{r})$  indicates the regions where the  $\rho(\mathbf{r})$  is depleted or concentrated. For shared bonds,  $\nabla^2\rho(\mathbf{r})$  is negative while positive values are observed for interactions showing closed-shell character. Apart from this, valuable information about chemical bond is obtained from the  $H(\mathbf{r})$  and its two components  $G(\mathbf{r})$  and  $V(\mathbf{r})$  and the Eq. 1.32 shows the relation between these parameters.

$$H(\mathbf{r}) = G(\mathbf{r}) + V(\mathbf{r}) \quad \dots \text{(Eq. 1.32)}$$

Regions where the electrons are more localized are characterized by relatively higher  $V(\mathbf{r})$  values whereas large  $G(\mathbf{r})$  values corresponds to the regions where the electrons are move faster. In general, for covalent interactions,  $|V(\mathbf{r})| > G(\mathbf{r})$  and hence the value of  $H(\mathbf{r})$  is negative and for closed-shell interactions,  $|V(\mathbf{r})| < G(\mathbf{r})$ , thus  $H(\mathbf{r})$  shows positive value. The following Eq. 1.33 and Eq. 1.34 show the relation between  $H(\mathbf{r})$  and  $\nabla^2\rho(\mathbf{r})$ .

$$(\hbar^2/8m)\nabla^2\rho(\mathbf{r}) = H(\mathbf{r}) - (1/2)V(\mathbf{r}) \quad \dots \text{(Eq. 1.33)}$$

$$H(\mathbf{r}) = (\hbar^2/8m)\nabla^2\rho(\mathbf{r}) + (1/2)V(\mathbf{r}) \quad \dots \text{(Eq. 1.34)}$$

The combined use of both  $H(\mathbf{r})$  and  $\nabla^2\rho(\mathbf{r})$  has been practiced as an excellent descriptor for defining the nature of chemical bonds [Bushmarinov *et al.* 2008; Nakanishi *et al.* 2009]. For shared-shell interactions,  $\nabla^2\rho(\mathbf{r}) < 0$  and also by definition,  $V(\mathbf{r})$  is negative at the bcp, consequently as from Eq. 1.33,  $H(\mathbf{r})$  will be negative. For closed-shell interactions  $H(\mathbf{r})$

would be positive and this occurs when  $(\hbar^2/8m)\nabla^2\rho(\mathbf{r}) > |(1/2)V(\mathbf{r})|$ . There is another possibility that  $\nabla^2\rho(\mathbf{r}) > 0$  and  $H(\mathbf{r}) < 0$ , indicates partial ionic and partial covalent nature of the bond. Thus pure closed-shell interactions without covalency are characterized by  $H(\mathbf{r}) > 0$ , whereas  $H(\mathbf{r}) < 0$  includes two types of interactions *viz.* closed shell interactions with covalent character where  $\nabla^2\rho(\mathbf{r}) > 0$  and shared shell interactions where  $\nabla^2\rho(\mathbf{r}) < 0$ . Nakanishi *et al.* characterized the shared-shell and closed-shell interactions for a better understanding of the weak to strong interactions by plotting  $H(\mathbf{r})$  versus  $\nabla^2\rho(\mathbf{r})$  values at the bcps and found that the ratio of  $V(\mathbf{r})$  and  $G(\mathbf{r})$  (denoted as  $k(\mathbf{r})$ ;  $k(\mathbf{r}) = V(\mathbf{r})/G(\mathbf{r})$ ) is highly useful to explain these plots [<sup>a</sup>Nakanishi and Hayashi 2010; <sup>b</sup>Nakanishi and Hayashi 2010]. The higher magnitude of  $k(\mathbf{r})$  indicates the extent of dominance of  $V(\mathbf{r})$  over  $G(\mathbf{r})$  values.

## 1.2.8 Molecular Electrostatic Potential (MESP)

Coulomb's law describes the electrostatic interaction between electrically charged particles. Coulomb's law states that the electrical force between two charged objects is directly proportional to the product of the quantity of charge on the objects and inversely proportional to the square of the separation distance between the two objects. In mathematical form, Coulomb's law can be stated as,

$$F = \frac{q_1 q_2 \hat{\mathbf{r}}}{4\pi\epsilon_0 r^2} \quad \dots \text{(Eq. 1.35)}$$

where  $q_1$  and  $q_2$  are point charges separated by a distance  $r$  in vacuum;  $\hat{\mathbf{r}}$  is a  $\mathbf{r}$  unit vector joining the position vectors of  $q_1$  and  $q_2$  and  $4\pi\epsilon_0$  is the constant of proportionality. The intensity of an electric field is the force acting on a unit test charge placed at a reference point in the field. The field due to a fixed point charge  $q$  produced at a site  $\mathbf{r}$  is

$$\mathbf{E} = \frac{q\mathbf{r}}{4\pi\epsilon_0|\mathbf{r}|^3} \quad \dots \text{(Eq. 1.36)}$$

Applying the principle of superposition, for a system of two more charges  $\{q_\alpha\}$ , the electric field is the vector sum of the fields  $\mathbf{E}_\alpha$  produced by the individual charges and can be given as

$$\mathbf{E}(\mathbf{r}) = \sum_\alpha \mathbf{E}_\alpha(\mathbf{r}) = \frac{1}{4\pi\epsilon_0} \sum_\alpha \frac{q_\alpha(\mathbf{r} - \mathbf{r}_\alpha)}{|\mathbf{r} - \mathbf{r}_\alpha|^3} \quad \dots \text{(Eq. 1.37)}$$

The classical Coulombic electrostatic potential,  $V(\mathbf{r})$  at the point  $\mathbf{r}$  due to a discrete point charge  $q_\alpha$  placed at  $\mathbf{r}_\alpha$  is given by

$$V(\mathbf{r}) = \frac{1}{4\pi\epsilon_0} \frac{q_\alpha}{|\mathbf{r} - \mathbf{r}_\alpha|} \quad \dots \text{(Eq. 1.38)}$$

Since electrostatic potential (ESP) obeys the principle of superposition, the ESP at a point  $\mathbf{r}$  due to a collection of discrete charges  $\{q_\alpha\}$  located at  $\{\mathbf{r}_\alpha\}$  can be written as

$$V(\mathbf{r}) = \frac{1}{4\pi\epsilon_0} \sum_\alpha \frac{q_\alpha}{|\mathbf{r} - \mathbf{r}_\alpha|} \quad \dots \text{(Eq. 1.39)}$$

If instead of discrete charges, consider a continuous distribution of charge over space,  $\rho(\mathbf{r}')$  is the continuous charge distribution. The charge contained in an infinitesimal volume element  $d^3\mathbf{r}'$  around a point  $\mathbf{r}'$  is  $\rho(\mathbf{r}')d^3\mathbf{r}'$ . This generates a potential of  $\rho(\mathbf{r}')d^3\mathbf{r}'/|\mathbf{r} - \mathbf{r}'|$  at a reference point  $\mathbf{r}$ . Then the potential generated by the entire charge distribution is obtained by integration over the entire space, i.e.

$$V(\mathbf{r}) = \frac{1}{4\pi\epsilon_0} \int \frac{\rho(\mathbf{r}')d^3r'}{|\mathbf{r} - \mathbf{r}'|} \quad \dots \text{(Eq. 1.40)}$$

The electrostatic potential for a combination of discrete charges  $q_\alpha$  placed at  $r_\alpha$  and a smeared distribution  $\rho(\mathbf{r})$  can be written by employing superposition principle and combining eqs. 1.41 and 1.42 as

$$V(\mathbf{r}) = \frac{1}{4\pi\epsilon_0} \left\{ \sum_{\alpha} \frac{q_{\alpha}}{|\mathbf{r} - \mathbf{r}_{\alpha}|} + \int \frac{\rho(\mathbf{r}')}{|\mathbf{r} - \mathbf{r}'|} d^3\mathbf{r}' \right\} \quad \dots \text{(Eq. 1.41)}$$

In a molecular charge distribution which is a collection of positive discrete charges  $\{Z_{\alpha}\}$  and a continuous negative electron density distribution described by  $\rho(\mathbf{r})$  the molecular electrostatic potential (MESP) [Gadre and Shirsat 2000] is given as

$$V(\mathbf{r}) = \sum_{\alpha}^N \frac{Z_{\alpha}}{|\mathbf{r} - \mathbf{R}_{\alpha}|} - \int \frac{\rho(\mathbf{r}') d^3\mathbf{r}'}{|\mathbf{r} - \mathbf{r}'|} \quad \dots \text{(Eq. 1.42)}$$

where  $N$  is the total number of electrons in the molecules. The most negative valued point ( $V_{min}$ ) in electron rich regions can be obtained from MESP topology calculations. Eq. (1.42) shows that for electron dense regions, the electronic terms will dominate over the nuclear term and hence these regions are characterized by negative MESP values whereas the electron deficient regions show positive MESP values [Politzer and Murray 1996; Politzer and Murray 2002]. This is illustrated using a representative example shown in Figure 1.16. To make the electrostatic potential energy data easy to explain, a color spectrum, with red as the lowest electrostatic potential energy value and blue as the highest, is employed to convey the varying intensities of the electrostatic potential energy values.

It has been established that the MESP topography provides a succinct tool for understanding molecular reactivity, intermolecular interactions, molecular recognition and a variety of chemical phenomena [Politzer and Truhlar 1981; Luque *et al.* 1994; <sup>a</sup>Gadre *et al.* 1996; <sup>b</sup>Gadre *et al.* 1996]. MESP has been used as an alternate electronic descriptor to quantify substituent effects such as inductive effect, resonance effect, through-space effect, and ortho effect in organic and inorganic systems [Suresh and Gadre 1998; Suresh *et al.* 2000; Suresh and Koga 2002; Politzer 2004; Suresh and Gadre 2007; Suresh *et al.* 2008; Sayyed and Suresh 2009; Sayyed and Suresh 2010].

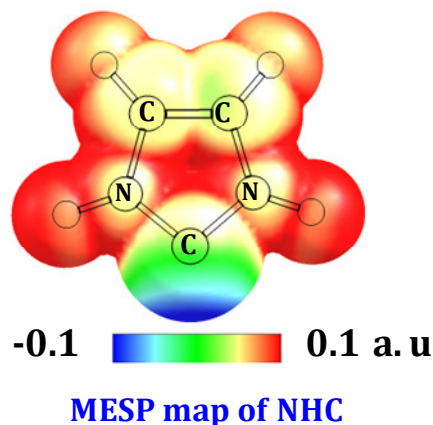


**Figure 1.16** Electrostatic potential on molecular surface of a N-heterocyclic carbenes molecule, computed at B3LYP/6-311++G(d,p) level of theory.

### 1.2.9 Quantitative Structure Activity/Property Relationships (QSAR/QSPR)

A QSAR/QSPR attempts to find consistent relationships between the variations in the values of molecular properties and the biological activity or properties for a series of compounds [Karelson and Lobanov 1995]. Thus a QSAR/QSPR is statistically derived equation which quantitatively connects between chemical structure and biological/chemical property or activity, and which takes in the form of a linear equation,

$$\text{Biological activity/property} = (k_1P_1) + (k_2P_2) + (k_3P_3) + \dots \quad \dots \text{(Eq. 1.43)}$$

where the parameters  $P_1$  through  $P_n$  are computed for each molecule in the series and the coefficients  $k_1$  through  $k_n$  are calculated by fitting variations in the parameters and the biological activity.

Quantitative structure-activity and structure-property relationship (QSAR/QSPR) studies are unquestionably of great importance in modern chemistry and biochemistry [Rogers and Hopfinger 1994]. Once such a relation is found, any number of compounds, including those not yet synthesized, can be readily screened on the computer in order to select structures with the properties desired. Numerous QSPR/QSAR models have reported based on various

known physicochemical parameters and molecular descriptors such as geometric, electronic or electrostatic, polar, steric, topological indices. The procedure for QSAR/QSPR model generation needs the experimental data, the molecular descriptors, mathematical method for the construction of QSAR/ QSPR, and the validation process [Golbraikh *et al.* 2003].

Multiple linear regression (MLR) is one of the most commonly used method for constructing QSAR/QSPR models due to its simplicity and the formation of easily interpretable mathematical expression [Vapnik 1998; Vapnik 2000]. Best multiple linear regression (BMLR), heuristic method (HM), genetic algorithm based multiple linear regression (GA-MLR) are the three most commonly used modified methodologies based on MLR. Apart from MLR, partial least squares (PLS), neural networks (NN), support vector machine (SVM) are also used as the mathematical models for the regression tools in QSAR/QSPR analysis [Wold *et al.* 1984].

The quality of mathematical models can be evaluated by correlation coefficient (r), or in terms of relative standard deviation (rsd) [Egan and Morgan 1998]. The predictive power of a QSAR model is often estimated by cross validation methodology. The original set of data is modified by taking off one (LOO- leave one out) or more (LMO-leave many out) which are used to check the predictivity of a model formed from remaining data. This is repeated with all data in the set. A cross-validated coefficient ( $Q^2$ ) was subsequently obtained and this can be used as a statistical index for predictive power.  $Q^2$  can be calculated using the following equation [Hao *et al.* 2011],

$$Q^2 = 1 - \left( \frac{\sum_{i=1}^{train} (y_i - \hat{y}_i)^2}{\sum_{i=1}^{train} (y_i - \bar{y}_{tr})^2} \right) \quad \dots \text{(Eq. 1. 44)}$$

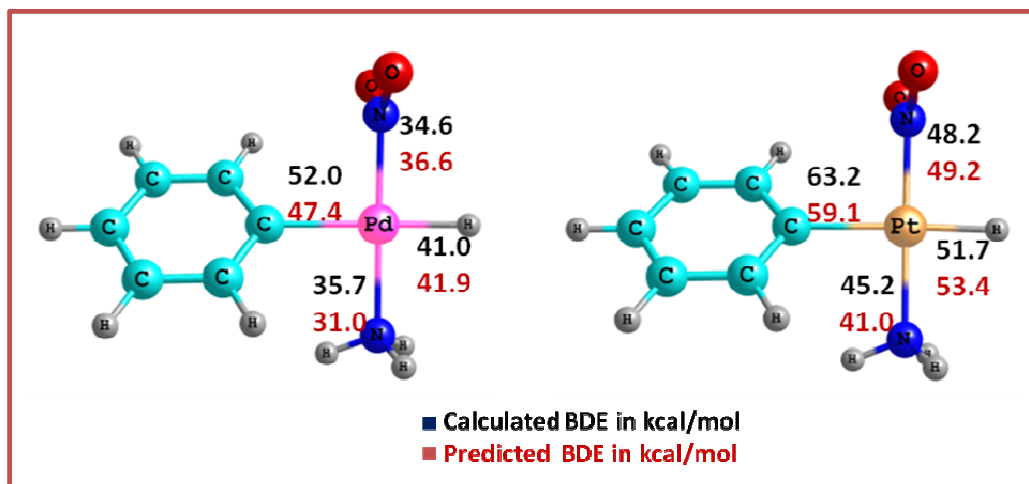
where  $y_i$ ,  $\hat{y}_i$ , and  $\bar{y}_{tr}$  are respectively for the observed, predicted, and mean values of the target property, for the training set.

## 1.3 Conclusion

The first chapter describes the evidence and significance of trans influence in transition metal complexes, main group metal complexes, and lanthanide complexes. A detailed literature survey on experimental and theoretical studies of trans influence is presented. It is clear that to establish a universal series for trans influence of various ligands is not possible in transition metal complexes because the trans influence results from the mutual effects of two trans ligand and also it shows marked dependency upon the nature of central metal atom. On the other hand, in main group elements, trans influence can be taken as a function of inductive effect of trans ligands. In most cases, the assessment of trans influence is made in terms of trans bond length parameters and an energetic parameter to measure the trans influence is still lacking. Our work is mainly concentrated on the introduction of a new energetic parameter for the assessment of mutual trans influence of various ligands.

The second part of Chapter 1 deals with the theoretical background of the computational methods which are commonly used in computational chemistry calculations. This part includes a brief account of various computational methods, *viz.* molecular mechanics, Hartree-Fock theory, the post HF methods, semi-empirical quantum chemical methods, density functional theory, molecular dynamics and Monte Carlo simulations, and hybrid QM-MM methods. The assessment of nature and strength of a chemical bond using QTAIM parameters, brief description on molecular electrostatic potential and quantitative structure activity/property relationships are also discussed.

# Quantification of the Trans Influence in Pd(II) and Pt(II) Complexes



## 2.1 Abstract

*Trans influence of a variety of 'X' ligands (X = H<sub>2</sub>O, NH<sub>3</sub>, Py, CO, SMe<sub>2</sub>, C<sub>2</sub>H<sub>4</sub>, AsH<sub>3</sub>, PH<sub>3</sub>, AsMe<sub>3</sub>, PMe<sub>3</sub>, PEt<sub>3</sub>, ONO<sup>-</sup>, F<sup>-</sup>, Cl<sup>-</sup>, Br<sup>-</sup>, N<sub>3</sub><sup>-</sup>, NO<sub>2</sub><sup>-</sup>, OH<sup>-</sup>, CN<sup>-</sup>, Ph<sup>-</sup>, H<sup>-</sup>, Me<sup>-</sup>, SiH<sub>3</sub><sup>-</sup>) has been studied using isodesmic reactions of the type  $M^{II}Cl_2X + M^{II}Cl_3 \longrightarrow M^{II}Cl_2 + M^{II}Cl_3X$  (M = Pd, Pt). All these reactions are endothermic and the energy of the isodesmic reaction ( $E_X$ ) provided a good measure of the trans influence of X as it showed good agreement with the order of trans influence measured in terms of the typically used trans bond length (the M–Cl bond trans to the ligand X) data. Further, good linear correlations are obtained between  $E_X$  and electron density at the (3, -1) bond critical point (bcp) of the trans M–Cl bond for both Pd(II) and Pt(II) complexes, which confirmed the use of  $E_X$  as a quantitative energetic measure of trans influence of X. On the basis of  $E_X$  values, different ligands can be classified into three groups, viz. strong trans influencing, moderately trans influencing, and weak trans influencing. Isodesmic reactions of the type  $M^{II}Cl_2X + M^{II}Cl_2Y \longrightarrow M^{II}Cl_2 + M^{II}Cl_2XY$  with ligands 'X' and 'Y' in the trans positions are also modeled for several random combinations to obtain the energy of the reaction  $E_{XY}$ . The  $E_{XY}$  values act as a measure of the mutual trans influence of X against a trans ligand Y.  $E_{XY}$  is the highest when two SiH<sub>3</sub><sup>-</sup> ligands are trans to each other while it is the lowest when two H<sub>2</sub>O ligands are in trans positions. Using the isodesmic reaction energies of X ( $E_X$ ) and Y ( $E_Y$ ), the empirical equation  $E_{XY} = \eta(E_X + E_Y / \sqrt{2})^2$  is derived for predicting the  $E_{XY}$  values for both Pd(II) and Pt(II) complexes, where  $\eta$  is a constant. The predicted  $E_{XY}$  showed good agreement to calculated  $E_{XY}$  as their linear correlation produced correlation coefficients higher than 0.99 in both Pd(II) and Pt(II) complexes. Further, it is possible to predict the bond dissociation energy of the ligand X ( $D_{2X}$ ) in  $[M^{II}Cl_2XY]^{n-}$  with the help of the*

equation  $D_{2X} = D_{1X} + E_X - E_{XY}$ , where  $D_{1X}$  is the bond dissociation energy of  $X$  in  $[M^{II}Cl_3X]^{n-}$ . Quantification of the contributions of  $E_X$  and  $E_{XY}$  to the bond dissociation energy of the ligand  $X$  ( $D_{3X}$ ) in complexes of the type  $[M^{II}X(Y)X'(Y')]$  ( $M = Pd, Pt$ ) is also achieved. The  $D_{3X}$  of any ligand  $X$  in these complexes can be predicted using the equations, viz.  $D_{3X(Pd)} = 1.196E_X - 0.603E_{XY} - 0.118E_{X'Y'} + 0.442D_{1X} + 15.169$  for  $Pd(II)$  complexes and  $D_{3X(Pt)} = 1.420E_X - 0.741E_{XY} - 0.125E_{X'Y'} + 0.498 D_{1X} + 13.852$  for  $Pt(II)$  complexes. These expressions suggest that the mutual trans influence from  $X$  and  $Y$  is more dominant than the mutual trans influence from  $X'$  and  $Y'$  and both factors contribute significantly to the weakening of  $M-X$  bond. We also demonstrated that using a database comprising of  $D_{1X}$  and the  $\rho(\mathbf{r})$ , the bond dissociation energy of  $X$  in complexes of the type  $[M^{II}X(Y)X'(Y')]$  can be predicted.

## 2.2 Introduction

In the present work, isodesmic reactions are employed to quantify the mutual trans influence of ligands. Here the reactions are modeled in such a way that the isodesmic reaction energies can be taken as a quantitative measure of mutual trans influence between two ligands. Since palladium and platinum forms a number of complexes with organic and inorganic ligands, and the chemistry of these metals in +2 oxidation state is one of the emerging and versatile fields of inorganic chemistry [Dedieu 2000; Negishi 2002; Tsuji 2004; Holmes 2007], we have studied the trans influence in square planar  $Pd(II)$  and  $Pt(II)$  complexes, and compared the effect of metal on the mutual trans influence of different ligands. Further, we have analyzed the bond dissociation energies of various ligands in  $[M^{II}X(Y)Cl_2]$  and  $[M^{II}X(Y)X'(Y')]$  complexes (where  $M = Pd$  and  $Pt$ ) in terms of trans influence parameters.

## 2.3 Computational Details

To get the correct trend of metal–ligand bond length, the square planar Pd(II) and Pt(II) complexes were optimized by B3LYP [Lee *et al.* 1988; Becke 1993] and MPWB1K [Zhao and Truhlar 2004] level DFT methods with Gaussian03 suite of programs [Frisch *et al.* Gaussian 03 2004]. For Pd and Pt, the basis set of Lanl2DZ [<sup>a</sup>Hay and Wadt 1985; <sup>b</sup>Hay and Wadt 1985] with extra f polarization function was chosen [Ehlers *et al.* 1993]. For all the other atoms, 6-31++G(d,p) basis set was selected and the combined basis set for all the atoms is named as BS1. It has been reported that many of the structural features of transition metal complexes are not reproduced correctly in the gas phase DFT calculations, while the correct trends are obtained by including solvent effects [Yatsenko *et al.* 2004; Hocking *et al.* 2007]. Therefore, throughout this work the solvent corrections were applied to B3LYP and MPWB1K methods using Conductor like Screening Model (COSMO) with water as solvent [Klamt and Schuurmann 1993]. The COSMO is a dielectric solvent continuum model in which the solute molecule is embedded in a molecular-shaped cavity surrounded by a dielectric medium. The solvent excluding surface was used along with an epsilon value of 78.5 for the dielectric constant of water. Water is selected as the solvent because of its higher permittivity and hence more accurate results can be achieved in COSMO method [Klamt and Schuurmann 1993].

The topological features of electron density have been analyzed for all the  $[M^{II}Cl_3X]^{n-}$  complexes using the AIM2000 program [Bader 1990; Biegler-König *et al.* 2001]. This analysis is based on the Bader's theory of atoms in molecule (AIM) approach [Bader 1990] and for the present study, the bond critical points of nature (3, -1) is located for all the M–Cl bond trans to the ligand X.

The bond length obtained from different calculations was compared to crystallographic data obtained from Cambridge Structural Database (CSD) [Allen 2002]. The trans bond lengths of ten such optimized structures were compared with crystallographic data, and the method which gives correct bond length order in various complexes is used for further calculations.

The accuracy of calculated bond dissociation energies may depend on the level of theory used. To address this issue, we tested six different DFT functionals, *viz.* standard GGA functionals BP86 [Becke 1988; Perdew 1986] PBE [Perdew *et al.* 1996], hybrid-GGA functionals B3LYP [Becke 1993; Lee *et al.* 1988] and PBE1PBE [Adamo and Barone 1999], meta GGA functional TPSS [Tao *et al.* 2003], and hybrid-meta GGA functional M05 [Zhao *et al.* 2005] for the computation of BDEs of various ligands in  $[\text{Pd}^{\text{II}}\text{X}(\text{Y})\text{X}'(\text{Y}')] ]$  complexes and this values were compared with the results obtained using MPWB1K method.

## 2.4 Results and Discussion

### 2.4.1 Analysis of trans $\text{Pd}^{\text{II}}\text{-Cl}$ and $\text{Pt}^{\text{II}}\text{-Cl}$ Bond Lengths

Trans influence affects the ground state property of the ligand, which is reflected on the strength of metal chloride bond trans to the ligand X. Hence, trans bond length is usually taken as a qualitative measure of trans influence [Appleton *et al.* 1973]. In order to find the suitable computational method, which can reproduce the correct trans influence order of different ligands, the calculations are carried out with B3LYP-COSMO/BS1 and MPWB1K-COSMO/BS1 level of theory in square planar complexes of the type  $[\text{Pd}^{\text{II}}\text{Cl}_3\text{X}]^{n-}$  and  $[\text{Pt}^{\text{II}}\text{Cl}_3\text{X}]^{n-}$  ( $n = 1$  when X is neutral and  $n = 2$  for uninegatively charged ligand X). The results are depicted in Table 2.1 along with the experimental Pd-Cl and Pt-Cl bond lengths obtained from crystallographic data.

**Table 2.1** Comparison of experimental and calculated trans M–Cl bond lengths (in Å) in complexes of the type  $[M^{II}Cl_3X]^{n-}$  (where M is Pd, Pt and X is H<sub>2</sub>O, CO, Cl<sup>-</sup>, NH<sub>3</sub>, C<sub>2</sub>H<sub>4</sub>, PEt<sub>3</sub>, NO<sub>2</sub> and PPh<sub>3</sub>). See foot notes for references.

System	Experimental	B3LYP-COSMO/BS1	MPWB1K-COSMO/BS1	Percentage Error for	
				B3LYP-COSMO/BS1	MPWB1K-COSMO/BS1
$[PdCl_3H_2O]^{-}$	2.256 <sup>a</sup>	2.331	2.290	3.3	1.5
$[PdCl_4]^{2-}$	2.306 <sup>b</sup>	2.397	2.343	4.0	1.6
$[PdCl_3NO_2]^{2-}$	2.358 <sup>c</sup>	2.414	2.363	2.4	0.2
$[PdCl_3PPh_3]^{-}$	2.363 <sup>d</sup>	2.462	2.408	4.2	1.9
$[PtCl_3H_2O]^{-}$	2.248 <sup>e</sup>	2.330	2.294	3.6	2.0
$[PtCl_3CO]^{-}$	2.289 <sup>f</sup>	2.375	2.336	3.8	2.0
$[PtCl_4]^{2-}$	2.304 <sup>g</sup>	2.388	2.338	3.6	1.5
$[PtCl_3NH_3]^{-}$	2.313 <sup>h</sup>	2.391	2.349	3.4	1.6
$[PtCl_3C_2H_4]^{-}$	2.335 <sup>i</sup>	2.410	2.364	3.2	1.3
$[PtCl_3PEt_3]^{-}$	2.380 <sup>j</sup>	2.491	2.433	4.6	2.2

<sup>a</sup>[Yang *et al.* 2006], <sup>b</sup>[Kaluderovic *et al.* 2004], <sup>c</sup>[Boganova *et al.* 2001], <sup>d</sup>[Casellato *et al.* 2006], <sup>e</sup>[Chen and Matsumoto 2006], <sup>f</sup>[Russell and Tucker 1976], <sup>g</sup>[Bisi-Castellani *et al.* 2006], <sup>h</sup>[Belskii *et al.* 2006], <sup>i</sup>[Black *et al.* 1969], <sup>j</sup>[Bushnell *et al.* 1975]

The data presented in Table 2.1 suggest that the trans bond lengths are overestimated by 2.4 to 4.6 % in the B3LYP and 0.2 to 2.2 % in the MPWB1K method. However, both B3LYP and MPWB1K method follow bond length trends very similar to the experimental trend. From the experimental trans bond length, the decreasing order of trans influence for Pt(II) complexes can be written as PEt<sub>3</sub> > C<sub>2</sub>H<sub>4</sub> > NH<sub>3</sub> > Cl<sup>-</sup> > CO > H<sub>2</sub>O and the same order is nearly preserved in the calculated bond length values using both the DFT methods. Since the better agreement to the experiment is obtained by

MPWB1K method, for further calculations, the solvent corrected MPWB1K-COSMO/BS1 method is used.

## 2.4.2 Trans Influence from Trans Bond Length

M–Cl bond length trans to X of  $[M^{II}Cl_3X]^{n-}$  complexes calculated at MPWB1K-COSMO/BS1, where M = Pd, Pt are listed in Table 2.2 for 23 ligands. The optimized structures of a representative set of  $[M^{II}Cl_3X]^{n-}$  complexes are given in Figure 2.1. According to the decreasing Pd–Cl bond lengths, different ligands can be arranged in the decreasing order of trans influence as shown in series (i),

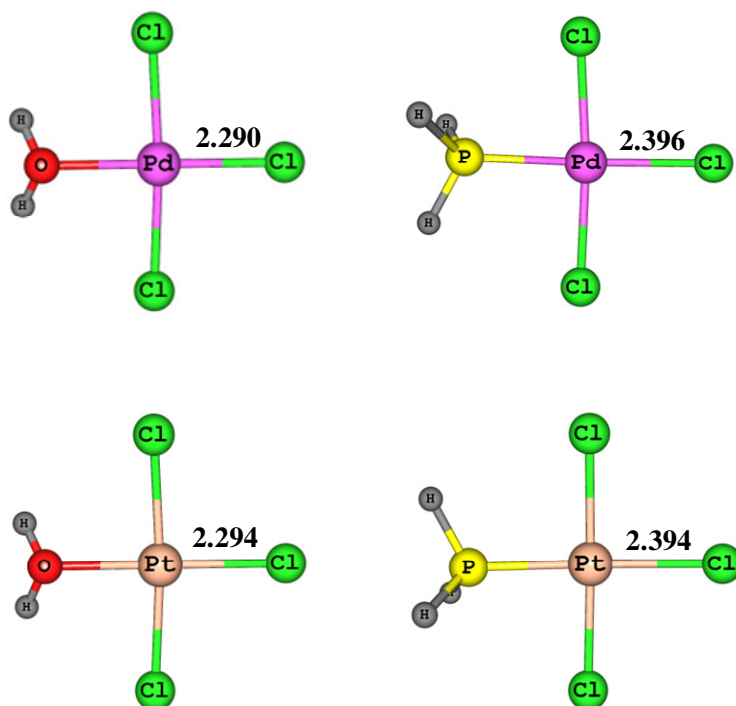
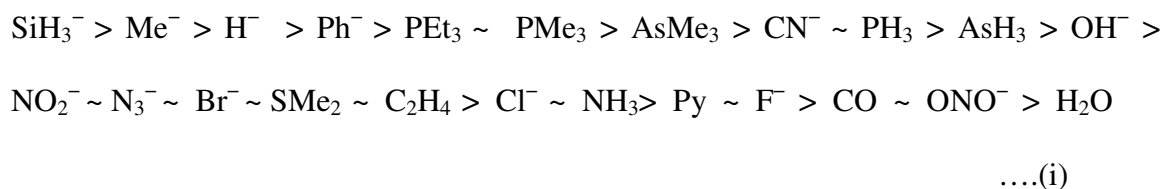


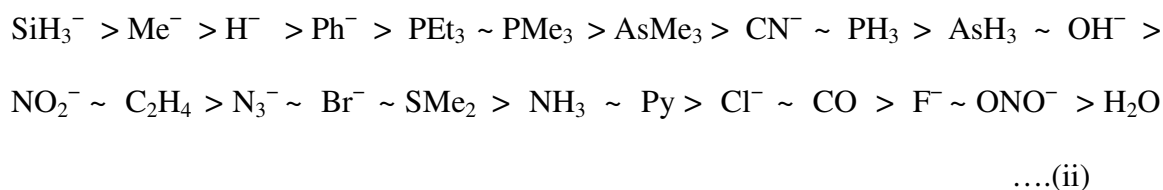
**Figure 2.1** Optimised structures of  $[M^{II}Cl_3X]^{n-}$  complexes (where M= Pd, Pt and X =  $H_2O$ ,  $PH_3$ ) at MPWB1K-COSMO/BS1 level of theory. Trans bond length in Å are also shown.

**Table 2.2** Values of the trans M–Cl (where M = Pd, Pt) bond length for the complexes of the type  $[M^II Cl_3 X]^{n-}$ .

Trans ligand X	Pd–Cl bond length in Å	Pt–Cl bond length in Å
H <sub>2</sub> O	2.290	2.294
CO	2.322	2.336
Py	2.333	2.344
NH <sub>3</sub>	2.343	2.349
SMe <sub>2</sub>	2.354	2.355
C <sub>2</sub> H <sub>4</sub>	2.355	2.364
AsH <sub>3</sub>	2.387	2.387
PH <sub>3</sub>	2.396	2.394
AsMe <sub>3</sub>	2.425	2.416
PMe <sub>3</sub>	2.432	2.430
PEt <sub>3</sub>	2.438	2.433
ONO <sup>-</sup>	2.323	2.329
F <sup>-</sup>	2.330	2.331
Cl <sup>-</sup>	2.343	2.338
Br <sup>-</sup>	2.357	2.351
N <sub>3</sub> <sup>-</sup>	2.359	2.359
NO <sub>2</sub> <sup>-</sup>	2.363	2.368
OH <sup>-</sup>	2.380	2.383
CN <sup>-</sup>	2.400	2.400
Ph <sup>-</sup>	2.534	2.511
H <sup>-</sup>	2.548	2.527
Me <sup>-</sup>	2.562	2.536
SiH <sub>3</sub> <sup>-</sup>	2.603	2.582

The highest trans influence is shown by  $\text{SiH}_3^-$  ligand whereas  $\text{H}_2\text{O}$  exhibited the lowest, accordingly the Pd–Cl bond trans to  $\text{SiH}_3^-$  is 0.313 Å longer than the Pd–Cl bond trans to  $\text{H}_2\text{O}$ . It may be noted that the trans effect values of various ligands are nearly parallel to the trans influence order given in series (i), but significant deviation exists for  $\pi$ -accepting ligands CO,  $\text{CN}^-$  and  $\text{C}_2\text{H}_4$ . These ligands are well known for their strong trans effect, which often leads to the stabilization of the transition state of square planar substitution reactions.

On the basis of the trans Pt–Cl bond lengths in square planar Pt(II) complexes, the trans influence of different ligands can be arranged in the decreasing order as displayed in series (ii)

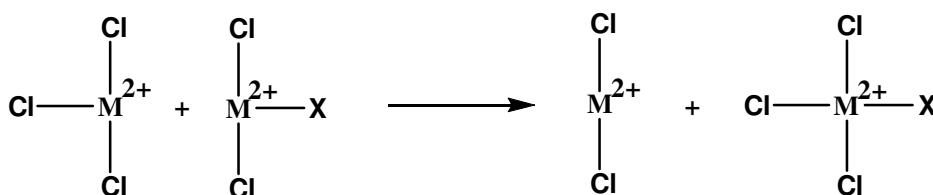


This trans influence order observed in Pt(II) complexes is almost identical to that found for Pd(II) complexes. The series (i) and (ii) show that in the case of coordinating atoms the trans influence follows the order  $\text{Si} > \text{C}(\text{sp}^3) > \text{H} > \text{P} > \text{As} > \text{Br} > \text{N} > \text{Cl} > \text{F} > \text{O}$  in both metals. It is clear that order of trans influence is not in accord with the electronegativity and atomic number of the central atom.

### 2.4.3 Trans Influence from Isodesmic Reactions

The trans influence of different ligands are investigated using isodesmic reactions of the type given in Scheme 2.1 where the metal center M is either Pd or Pt. On the reactant side there are five M–Cl bonds and one M–X bond and the same is preserved in the product side as well. When X is a uninegatively charged ligand, the total charge of the reactant side and the product side will be –2, and for neutral ligands the charge on both

sides of the reaction will be  $-1$ . Thus in addition to the type and number of bonds on reactants and product sides, the total charge is also conserved in the reaction given in Scheme 2.1. The optimised structure of  $MCl_2$  at MPWB1K-COSMO/BS1 used in the isodesmic reactions is nearly linear with a bond angle of  $175^\circ$ , while the optimised geometries of  $MCl_3$  and  $MCl_2X$  are T-shaped as shown in Scheme 2.1.



**Scheme 2.1** Isodesmic reaction in which the reactant side is free from mutual trans influence between X and  $Cl^-$ . Oxidation state +2 of the metal is also shown. The total charge of the system depends on the type of ligand X.

The energy of the isodesmic reactions ( $E_X$ ) corresponding to the 23 ligands ( $X = H_2O, NH_3, Py, CO, SMe_2, C_2H_4, AsH_3, PH_3, AsMe_3, PMe_3, PEt_3, ONO^-, F^-, Cl^-, Br^-, N_3^-, NO_2^-, OH^-, CN^-, Ph^-, H^-, Me^-, SiH_3^-$ ) is shown in the Table 2.3 for both Pd(II) and Pt(II) complexes. All the reactions are endothermic which indicates that the higher energy of the product side is due to the destabilizing mutual trans influence of X and  $Cl^-$  in  $[M^{II}Cl_3X]^{n-}$  and therefore the value of  $E_X$  can be considered as a good energetic measure of trans influence. In fact,  $E_X$  measures the mutual trans influence of X and  $Cl^-$  and in our procedure, the influence from  $Cl^-$  is assumed to be a constant as the  $E_X$  is calculated against the same trans ligand. Therefore, keeping the  $Cl^-$  as a reference ligand, the  $E_X$  value is assigned exclusively to the trans influence of X.

In Pd(II) complexes, according to the  $E_X$  values, the highest trans influence of 41.32 kcal/mol and the lowest trans influence of 5.15 kcal/mol can be assigned for the combinations ( $SiH_3^-, Cl^-$ ) and ( $H_2O, Cl^-$ ), respectively. Figure 2.2 shows the linear

correlations between  $E_X$  and the trans Pd–Cl bond lengths for both neutral and anionic ligands. The correlation coefficients ( $r$ ) of these linear plots are 0.984 for neutral and 0.988 for anionic ligands. In accordance with the  $E_X$  values, different ligands can be arranged in terms of their mutual trans influence with  $\text{Cl}^-$  as shown in series (iii)

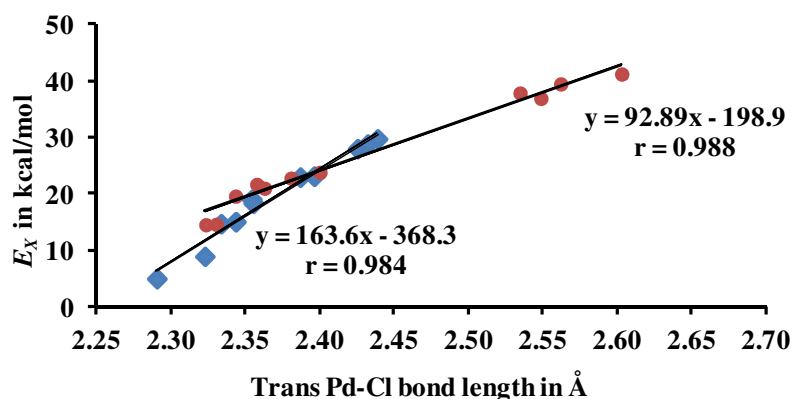
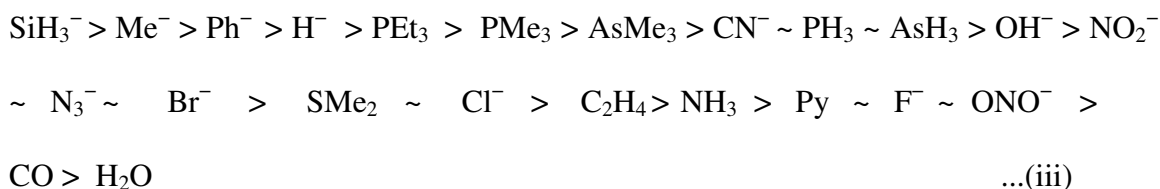


**Figure 2.2** Correlation between  $E_X$  and trans Pd–Cl bond length in complexes of the type  $[\text{Pd}^{\text{II}}\text{Cl}_3\text{X}]^{n-}$  (blue diamond is for neutral ligands and red circle is for negatively charged ligands).

The  $E_X$  based trans influence series (iii) is similar to the trans influence series (i) where the descriptor was the trans Pd–Cl bond length. However, compared to the bond length descriptor,  $E_X$  values suggest higher trans influence for the ligands  $\text{ONO}^-$ ,  $\text{Cl}^-$ , and  $\text{Ph}^-$ . Further, analysis of  $E_X$  values in Table 2.3 suggest that the ligands with modest  $\sigma$ -donating power [Appleton *et al.* 1973] have low  $E_X$  while the those with high  $\sigma$ -donating power have high  $E_X$ . Thus on the basis of  $E_X$  values, the ligands can be classified in to three, *viz.*

**Class I:** weak trans influencing: The ligands with  $E_X$  value less than 25 kcal/mol belong to this class and are characterized by weak  $\sigma$ -donating power. They are  $\text{CN}^-$ ,  $\text{PH}_3$ ,  $\text{AsH}_3$ ,  $\text{OH}^-$ ,  $\text{NO}_2^-$ ,  $\text{N}_3^-$ ,  $\text{Br}^-$ ,  $\text{SMe}_2$ ,  $\text{C}_2\text{H}_4$ ,  $\text{NH}_3$ ,  $\text{Cl}^-$ ,  $\text{Py}$ ,  $\text{F}^-$ ,  $\text{CO}$ ,  $\text{ONO}^-$ , and  $\text{H}_2\text{O}$ .

**Class II:** moderate trans influencing: Ligands in this class have  $E_X$  in between 25 and 35 kcal/mol. The ligands included in this class are  $\text{PEt}_3$ ,  $\text{PMe}_3$  and  $\text{AsMe}_3$  and are moderate  $\sigma$ -donors and also moderate  $\pi$ -acceptors.

**Class III:** strong trans influencing: Ligands showing  $E_X$  values greater than 35 kcal/mol. The alkyl, aryl, silyl, and hydride ligands are examples. They have strong  $\sigma$ -donating ability but no  $\pi$ -accepting ability.

The calculated  $E_X$  values for different ligands in Pt(II) are depicted in Table 2.3. It is seen that as in the Pd(II) complexes, the  $E_X$  values for Pt(II) complexes also showed good linear correlations with trans Pt–Cl bond length for both neutral ( $r = 0.979$ ) and anionic ( $r = 0.988$ ) ligands (Figure 2.3). According to the  $E_X$  values, the  $\text{SiH}_3^-$  is the ligand with the strongest trans influencing power (56.78 kcal/mol) while the  $\text{H}_2\text{O}$  ligand exhibits the weakest trans influence (13.06 kcal/mol).

On the basis of  $E_X$  values of Pt(II) complexes, ligands can be arranged in terms of their trans influence as shown in series (iv), which is similar to the trans influence series obtained in accordance with trans bond length (series ii). However, slight difference in the order is noticed for ligands  $\text{H}^-$ ,  $\text{ONO}^-$  and  $\text{Cl}^-$ .

$\text{SiH}_3^- > \text{Me}^- > \text{H}^- \sim \text{Ph}^- > \text{PEt}_3 > \text{PMe}_3 > \text{AsMe}_3 > \text{CN}^- \sim \text{PH}_3 \sim \text{AsH}_3 \sim \text{OH}^- >$   
 $\text{NO}_2^- \sim \text{N}_3^- \sim \text{Br}^- > \text{SMe}_2 \sim \text{Cl}^- \sim \text{C}_2\text{H}_4 > \text{NH}_3 \sim \text{Py} > \text{ONO}^- \sim \text{F}^- > \text{CO} > \text{H}_2\text{O}$

....(iv)

**Table 2.3** The isodesmic reaction energies ( $E_X$ ) in kcal/mol for the reaction  $M^{II}Cl_2X + M^{II}Cl_3 \longrightarrow M^{II}Cl_2 + M^{II}Cl_3X$ , where  $M = Pd, Pt$ .

Trans ligand X	$E_X$ in Pd(II) complexes	$E_X$ in Pt(II) complexes
H <sub>2</sub> O	5.15	13.06
CO	9.09	18.72
Py	14.86	26.42
NH <sub>3</sub>	15.22	26.34
SMe <sub>2</sub>	19.18	30.47
C <sub>2</sub> H <sub>4</sub>	18.51	30.03
AsH <sub>3</sub>	23.11	34.86
PH <sub>3</sub>	23.26	35.63
AsMe <sub>3</sub>	28.12	40.93
PMe <sub>3</sub>	28.96	41.90
PEt <sub>3</sub>	29.86	42.94
ONO <sup>-</sup>	14.69	25.75
F <sup>-</sup>	14.76	25.24
Cl <sup>-</sup>	19.74	30.15
Br <sup>-</sup>	21.83	32.84
N <sub>3</sub> <sup>-</sup>	21.46	33.21
NO <sub>2</sub> <sup>-</sup>	21.14	33.40
OH <sup>-</sup>	22.92	35.36
CN <sup>-</sup>	23.96	35.53
Ph <sup>-</sup>	37.97	51.70
H <sup>-</sup>	37.02	51.79
Me <sup>-</sup>	39.58	53.77
SiH <sub>3</sub> <sup>-</sup>	41.32	56.78

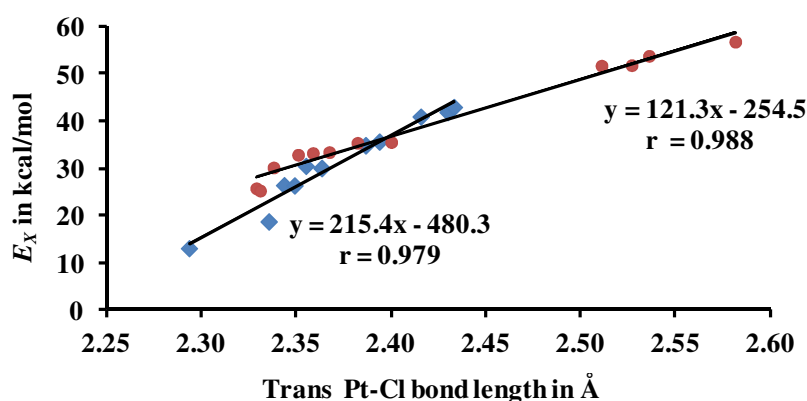


**Figure 2.3** Correlation between  $E_X$  and trans Pt–Cl bond length for  $[\text{Pt}^{\text{II}}\text{Cl}_3\text{X}]^{n-}$  complexes (blue diamonds show neutral ligands and red circles show anionic ligands).

In the case of Pt(II) complexes, the weak  $\sigma$ -donors (Class I), have  $E_X$  values less than 40 kcal/mol, while for moderate  $\sigma$ -donating (Class II), the  $E_X$  values lie between 40 and 50 kcal/mol. For strong trans influencing ligands with strong  $\sigma$ -donating ability (Class III), the  $E_X$  values are found to be greater than 50 kcal/mol.

#### 2.4.4 AIM Analysis

Bader's theory of atoms in molecules (AIM) was used to carry out the analysis of topology of electron density in both  $[\text{Pd}^{\text{II}}\text{Cl}_3\text{X}]^{n-}$  and  $[\text{Pt}^{\text{II}}\text{Cl}_3\text{X}]^{n-}$  complexes. The (3,-1) bond critical points in the AIM analysis observed for both trans Pd–Cl and trans Pt–Cl bonds are reported in Table 2.4. The  $\rho(\mathbf{r})$  of trans Pd–Cl bonds range from the highest of 0.085 a.u. for  $\text{H}_2\text{O}$  to the lowest of 0.042 au for  $\text{SiH}_3^-$ . Similarly, in the case of trans Pt–Cl bonds, the bcp values range from 0.092 to 0.050 au for  $\text{H}_2\text{O}$  to  $\text{SiH}_3^-$ . AIM topological plots of two representative examples for Pd and Pt complexes are given in the Figure 2.4. A high value of  $\rho(\mathbf{r})$  indicates the high strength of the trans bond and small trans influence of X. In both Pd(II) and Pt(II) complexes, the  $\rho(\mathbf{r})$  values show very good

linear correlations (Figures 2.5 a and b ) with the  $E_X$  values. The result strongly support that the  $E_X$  can be used as a good energetic measure of trans influence of various ligands.

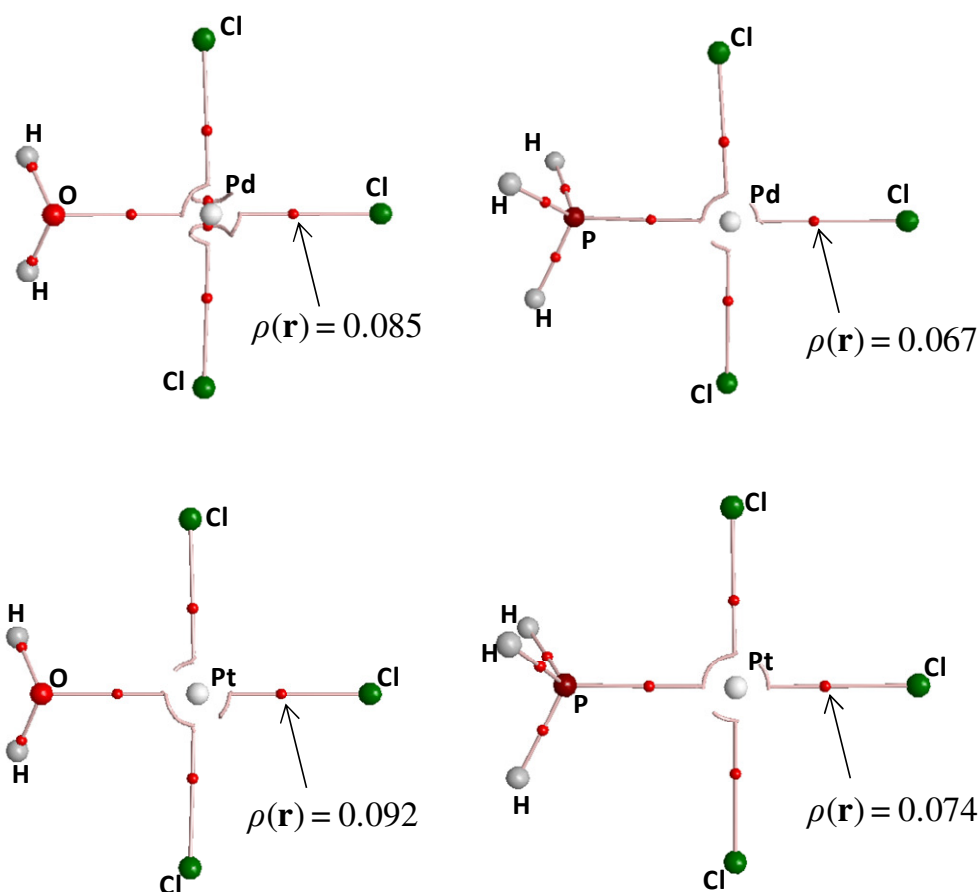
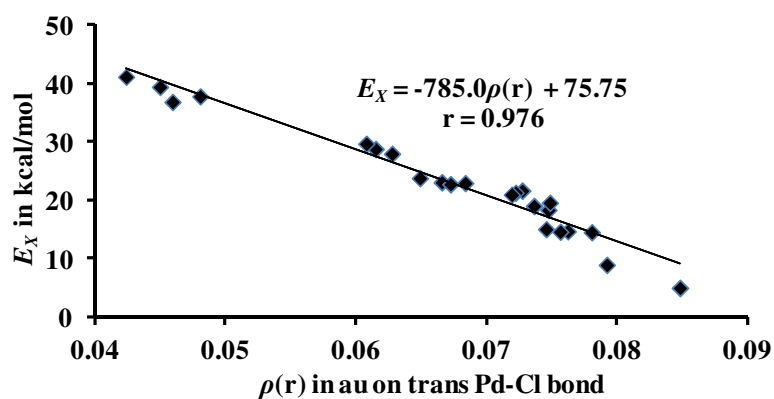
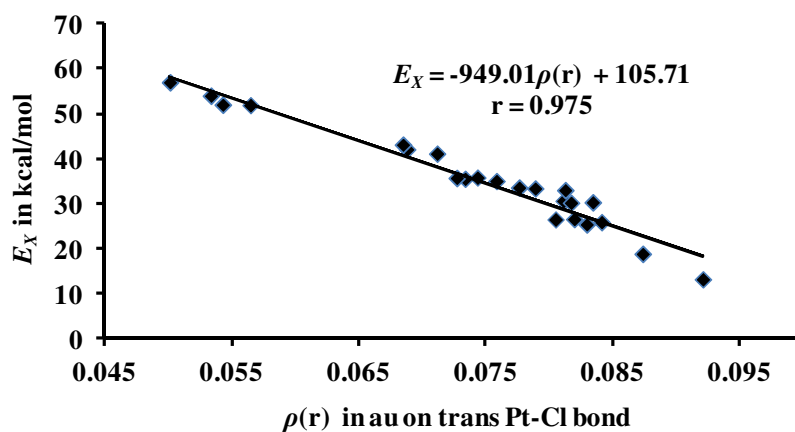


**Figure 2.4** AIM topological plot of  $[\text{Pd}^{\text{II}}\text{Cl}_3\text{X}]^{n-}$  and  $[\text{Pt}^{\text{II}}\text{Cl}_3\text{X}]^{n-}$  complexes with  $\text{X} = \text{H}_2\text{O}$  and  $\text{PH}_3$ . Big circles correspond to attractors (atomic nuclei) and small red circles indicate bond critical points. The  $\rho(\mathbf{r})$  in au at bond critical point of Pd–Cl and Pt–Cl bonds are also shown.



(a)



(b)

**Figure 2.5** Correlation between (a)  $E_X$  and  $\rho(r)$  at bond critical point of Pd-Cl trans to X for the complexes of the type  $[\text{Pd}^{\text{II}}\text{Cl}_3\text{X}]^{n-}$  and (b)  $E_X$  and  $\rho(r)$  at bond critical point of Pt-Cl trans to X for the complexes of the type  $[\text{Pt}^{\text{II}}\text{Cl}_3\text{X}]^{n-}$ .

**Table 2.4** M–Cl bond critical point trans to X for the complexes of the type  $[M^{II}Cl_3X]^{n-}$ .

Trans ligand X	$\rho(r)$ of trans Pd–Cl bond (au)	$\rho(r)$ of trans Pt–Cl bond (au)
H <sub>2</sub> O	0.085	0.092
CO	0.079	0.087
Py	0.076	0.082
NH <sub>3</sub>	0.075	0.081
SMe <sub>2</sub>	0.074	0.081
C <sub>2</sub> H <sub>4</sub>	0.075	0.082
AsH <sub>3</sub>	0.068	0.076
PH <sub>3</sub>	0.067	0.074
AsMe <sub>3</sub>	0.063	0.071
PMe <sub>3</sub>	0.062	0.069
PEt <sub>3</sub>	0.061	0.069
ONO <sup>-</sup>	0.078	0.084
F <sup>-</sup>	0.076	0.083
Cl <sup>-</sup>	0.075	0.083
Br <sup>-</sup>	0.073	0.081
N <sub>3</sub> <sup>-</sup>	0.072	0.079
NO <sub>2</sub> <sup>-</sup>	0.072	0.078
OH <sup>-</sup>	0.067	0.073
CN <sup>-</sup>	0.065	0.073
Ph <sup>-</sup>	0.048	0.057
H <sup>-</sup>	0.046	0.054
Me <sup>-</sup>	0.045	0.053
SiH <sub>3</sub> <sup>-</sup>	0.042	0.050

### 2.4.5 Comparison of Mutual Trans Influence of Different Ligands in Pd(II) and Pt(II) Complexes

In both Pd(II) and Pt(II) complexes, the order of trans influence of different ligands is comparable and, in terms of coordinating atoms, the trans influence follows the order  $\text{Si} > \text{C} (\text{sp}^3) > \text{H} > \text{P} > \text{As} > \text{Br} > \text{Cl} > \text{N} > \text{F} > \text{O}$ . Among Class III ligands, the trans influence of  $\text{H}^-$  and  $\text{Ph}^-$  is almost same in Pt(II) complexes, whereas in Pd(II) complexes,  $\text{Ph}^-$  is more trans influencing than  $\text{H}^-$ . Similarly, weak trans influencing ligands in Pt(II) complexes follow the order  $\text{Cl}^- \sim \text{C}_2\text{H}_4 > \text{NH}_3 \sim \text{Py} > \text{ONO}^- \sim \text{F}^- > \text{CO} > \text{H}_2\text{O}$  whereas in Pd(II) complexes the order is  $\text{Cl}^- > \text{C}_2\text{H}_4 > \text{NH}_3 > \text{Py} \sim \text{F}^- \sim \text{ONO}^- > \text{CO} > \text{H}_2\text{O}$ .

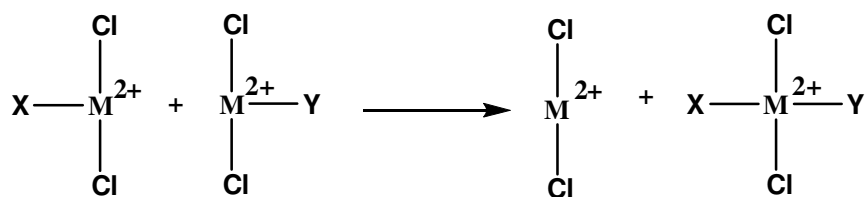
It can be seen that in Pt(II) complexes, the weakest trans influencing  $\text{H}_2\text{O}$  has  $E_X$  of 13.06 kcal/mol and the strongest trans influencing  $\text{SiH}_3^-$  has  $E_X$  of 56.78 kcal/mol, whereas these values are respectively 5.15 kcal/mol and 41.32 kcal/mol in Pd(II) complexes. Trans influence results from the competition between the trans ligands X and Y for the sharing of metal orbital [Appleton *et al.* 1973]. If Y is more  $\sigma$ -donating than X, a relative weakening of M–X bond can be observed. In recent paper, linear dependency of  $\sigma$ -donating ability of ligands and trans influence is reported [Chval *et al.* 2008]. In general, platinum forms stronger bonds with ligands than palladium [Chianese *et al.* 2007] and thus the influence of a strong  $\sigma$ -donor ligand Y on the trans ligand X will be more in Pt complexes. For  $\text{H}_2\text{O}$  ligand, the  $E_X$  value in Pt(II) complexes is 7.91 kcal/mol higher than the  $E_X$  value of the corresponding Pd(II) complexes. The difference in the  $E_X$  value between Pd(II) and Pt(II) complexes increases as the  $\sigma$ -donating power of the ligands increases. For instance, in the case of the strongest  $\sigma$ -donating  $\text{SiH}_3^-$  ligand, Pt(II) complex show an  $E_X$  value 15.46 kcal/mol higher than Pd(II) complex.

In Pt(II) complexes, the  $E_X$  values of  $\text{AsMe}_3$  and  $\text{PMe}_3$  are 40.93 and 41.90 kcal/mol, respectively, while the  $E_X$  values of unsubstituted ligands,  $\text{AsH}_3$  and  $\text{PH}_3$  are 34.86, 35.63 kcal/mol, respectively. This shows that there is a significant increase in trans influence of these ligands upon methylation. Similar observation can also be noted for Pd(II) complexes.

In a nut shell, the trans influence of a ligand X in the Pt(II) complex is approximately 8-15 kcal/mol higher than that in the Pd(II) complexes which means that the mutual trans influence of different ligands can also be influenced by the nature of the metal atom.

### 2.4.6 Mutual Trans Influence of Two Trans Ligands X and Y

In order to study the mutual trans influence of any two ligands X and Y, we have modeled the isodesmic reaction given in Scheme 2.2 which is an extension of the first isodesmic reaction given in Scheme 2.1. The combination of X and Y can be of three types (1) both anionic, (2) both neutral, and (3) one anionic and the other neutral. In all the three cases, the total charge on both reactant and the product sides are conserved in the isodesmic reaction. From the 23 ligands selected in this study (*cf.* Table 2.2), we have randomly picked 53 combinations of X and Y and studied the corresponding 53 isodesmic reactions. The isodesmic reaction energy for all the 53 reactions in accordance with Scheme 2.2 (designated here as  $E_{XY}$ ) is calculated for both Pd(II) and Pt(II) complexes. All the  $E_{XY}$  values are presented in Table 2.5.



**Scheme 2.2** Isodesmic reaction in which the reactant side is free from mutual trans influence between X and Y. Oxidation state +2 of the metal is also shown. The total charge of the system depends on the type of ligands X and Y.

**$E_{XY}$  of Pd(II) complexes:** As expected, the trans combination of two  $\text{SiH}_3^-$  ligands showed the highest  $E_{XY}$  of 99.65 kcal/mol while the lowest  $E_X$  of -3.95 kcal/mol is observed for the trans combination of two  $\text{H}_2\text{O}$  ligands. Among the combination of Class III ligands such as  $\text{Ph}^-$ ,  $\text{Me}^-$ ,  $\text{SiH}_3^-$ , and  $\text{H}^-$ , the  $E_{XY}$  is found to be in the range of 89 - 99.65 kcal/mol. This indicates that for the combination of very strong trans influencing ligands, the mutual trans influence is also very high. On the other hand, when X and Y are Class I ligands with weak trans influencing power, the  $E_{XY}$  values are below 35 kcal/mol. The  $E_{XY}$  values of all combinations of class II ligands fall in the small range 45-49 kcal/mol. For the rest of the trans (X, Y) combinations, the  $E_{XY}$  values fall in the range of 13 - 68 kcal/mol.

**$E_{XY}$  of Pt(II) complexes:** According to the  $E_{XY}$ , the lowest mutual trans influence of 0.51 kcal/mol is observed when two  $\text{H}_2\text{O}$  ligands are trans to each other. The highest mutual trans influence of 114.90 kcal/mol is observed when two  $\text{SiH}_3^-$  ligands are trans to each other. For all the trans combinations of Class I with weak trans influencing power, the  $E_{XY}$  is found in the range of 3 - 51 kcal/mol, whereas for all the trans combinations of Class III ligands the  $E_{XY}$  values are higher than 103 kcal/mol. For different combinations among Class II ligands, the  $E_{XY}$  is found to be in the small range of 61 - 67 kcal/mol. For all other (X, Y) combinations, the  $E_{XY}$  can be observed in the range of 22 - 87 kcal/mol.

**Table 2.5** The isodesmic reaction energy ( $E_{XY}$ ) for  $M^{II}Cl_2X + M^{II}Cl_2Y \longrightarrow M^{II}Cl_2 + M^{II}Cl_2XY$ . All values are in kcal/mol.

Isodesmic Reactions	Ligands in the <i>trans</i> position <sup>a</sup>		$E_{XY}$ for Pd(II) complexes	$E_{XY}$ for Pt(II) complexes
	X	Y		
1	H <sub>2</sub> O	Br <sup>-</sup>	7.26	15.70
2	NH <sub>3</sub>	Br <sup>-</sup>	18.03	29.75
3	CN <sup>-</sup>	PH <sub>3</sub>	34.13	50.73
4	NO <sub>2</sub> <sup>-</sup>	PH <sub>3</sub>	29.60	45.45
5	NH <sub>3</sub>	NO <sub>2</sub> <sup>-</sup>	18.50	31.36
6	Py	AsH <sub>3</sub>	21.52	36.00
7	ONO <sup>-</sup>	N <sub>3</sub> <sup>-</sup>	16.50	28.74
8	CO	CN <sup>-</sup>	16.68	35.01
9	OH <sup>-</sup>	PH <sub>3</sub>	29.01	41.96
10	Br <sup>-</sup>	OH <sup>-</sup>	25.87	38.54
11	OH <sup>-</sup>	CN <sup>-</sup>	29.61	42.65
12	H <sub>2</sub> O	H <sub>2</sub> O	-3.95	0.51
13	CO	Br <sup>-</sup>	11.65	23.00
14	AsH <sub>3</sub>	CN <sup>-</sup>	33.16	48.95
15	F <sup>-</sup>	PH <sub>3</sub>	18.53	29.76
16	CO	Py	8.09	21.98
17	H <sub>2</sub> O	NH <sub>3</sub>	3.56	10.05
18	NH <sub>3</sub>	SMe <sub>2</sub>	17.29	29.76
19	H <sub>2</sub> O	N <sub>3</sub> <sup>-</sup>	6.18	16.70
20	OH <sup>-</sup>	PMe <sub>3</sub>	36.49	49.99
21	CN <sup>-</sup>	PMe <sub>3</sub>	41.51	59.02
22	H <sub>2</sub> O	AsMe <sub>3</sub>	12.57	22.92
23	H <sub>2</sub> O	PMe <sub>3</sub>	12.77	24.41
24	Py	Me <sup>-</sup>	37.62	54.34
25	PH <sub>3</sub>	SiH <sub>3</sub> <sup>-</sup>	53.59	74.30
26	AsH <sub>3</sub>	SiH <sub>3</sub> <sup>-</sup>	52.12	71.35
27	CO	H <sup>-</sup>	26.75	47.48
28	NO <sub>2</sub> <sup>-</sup>	H <sup>-</sup>	45.34	62.68
29	PH <sub>3</sub>	Ph <sup>-</sup>	49.35	66.48
30	H <sub>2</sub> O	SiH <sub>3</sub> <sup>-</sup>	21.73	34.27
31	F <sup>-</sup>	SiH <sub>3</sub> <sup>-</sup>	39.87	54.09
32	SMe <sub>2</sub>	Me <sup>-</sup>	41.18	57.07
33	CO	SiH <sub>3</sub> <sup>-</sup>	39.71	56.41
34	F <sup>-</sup>	H <sup>-</sup>	34.03	48.25
35	H <sub>2</sub> O	Me <sup>-</sup>	19.07	30.47
36	NH <sub>3</sub>	Me <sup>-</sup>	39.81	55.18
37	CN <sup>-</sup>	Me <sup>-</sup>	56.25	73.90
38	OH <sup>-</sup>	H <sup>-</sup>	50.87	66.31
39	AsH <sub>3</sub>	Ph <sup>-</sup>	47.57	63.76
40	SMe <sub>2</sub>	SiH <sub>3</sub> <sup>-</sup>	44.04	62.38
41	PMe <sub>3</sub>	PMe <sub>3</sub>	48.36	66.55

**Table 2.5 (continued)**

42	AsMe <sub>3</sub>	PEt <sub>3</sub>	47.55	65.05
43	AsMe <sub>3</sub>	AsMe <sub>3</sub>	45.48	61.83
44	AsMe <sub>3</sub>	PMe <sub>3</sub>	46.89	64.23
45	AsMe <sub>3</sub>	Me <sup>-</sup>	60.84	76.91
46	PMe <sub>3</sub>	SiH <sub>3</sub> <sup>-</sup>	67.34	86.47
47	Ph <sup>-</sup>	Me <sup>-</sup>	90.17	103.95
48	Me <sup>-</sup>	Me <sup>-</sup>	94.90	108.25
49	SiH <sub>3</sub> <sup>-</sup>	SiH <sub>3</sub> <sup>-</sup>	99.65	114.90
50	H <sup>-</sup>	SiH <sub>3</sub> <sup>-</sup>	93.07	108.25
51	H <sup>-</sup>	Me <sup>-</sup>	89.27	103.88
52	Ph <sup>-</sup>	SiH <sub>3</sub> <sup>-</sup>	93.31	108.14
53	Me <sup>-</sup>	SiH <sub>3</sub> <sup>-</sup>	96.86	110.72

<sup>a</sup> The *trans* (X, Y) combinations in reactions 1 – 19 are (Class I, Class I), 20-23 are (Class I, Class II), 24 –40 are (Class I, Class III), 41 – 44 are (Class II, Class II), 45 – 46 are (Class II, Class III), and 47 – 53 are (Class III, Class III).

## 2.4.7 Prediction of $E_{XY}$ Values

A multiple linear regression (MLR) approach is presented here to predict the *trans* influence  $E_{XY}$  of any combination of X and Y in  $[M^{II}Cl_2XY]^{n-}$  using the *trans* influencing powers of X ( $E_X$ ) and Y ( $E_Y$ ) in  $[M^{II}Cl_3X]^{n-}$  and  $[M^{II}Cl_3Y]^{n-}$  complexes respectively. For this purpose, the  $E_{XY}$  values of 33 isodesmic reactions (Table 2.6) have been considered. We have defined that the ligand X is less *trans* influencing than Y i.e.  $E_X < E_Y$ . The MLR approach using the terms  $E_X$ ,  $E_Y$  and  $E_XE_Y$  as variables led to Eq. 2.1 and Eq. 2.2 for Pd(II) and Pt(II) complexes respectively.

$$E_{XY(Pd)} = -0.046 E_X + 0.227 E_Y + 0.055 E_XE_Y - 5.120 \quad \dots \text{(Eq. 2.1)}$$

$$E_{XY(Pt)} = -0.030 E_X + 0.371 E_Y + 0.030 E_XE_Y - 9.797 \quad \dots \text{(Eq. 2.2)}$$

The statistical results obtained using Eq. 2.1 and Eq. 2.2 are good with correlation coefficient of 0.985, 0.983 for Pd(II) and Pt(II) respectively. The corresponding standard deviations (s) are 3.18 kcal/mol for Pd(II) complexes and 4.51 kcal/mol for Pt(II) complexes.

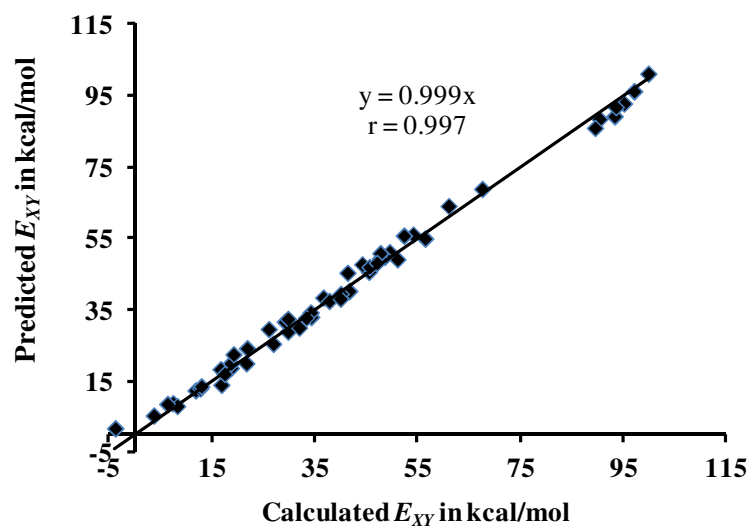
We also formulated a simple quadratic relationship using  $E_X$  and  $E_Y$  to predict the  $E_{XY}$  values,

$$E_{XY} = \eta \left( E_X + E_Y / \sqrt{2} \right)^2 \quad \dots \text{(Eq. 2.3)}$$

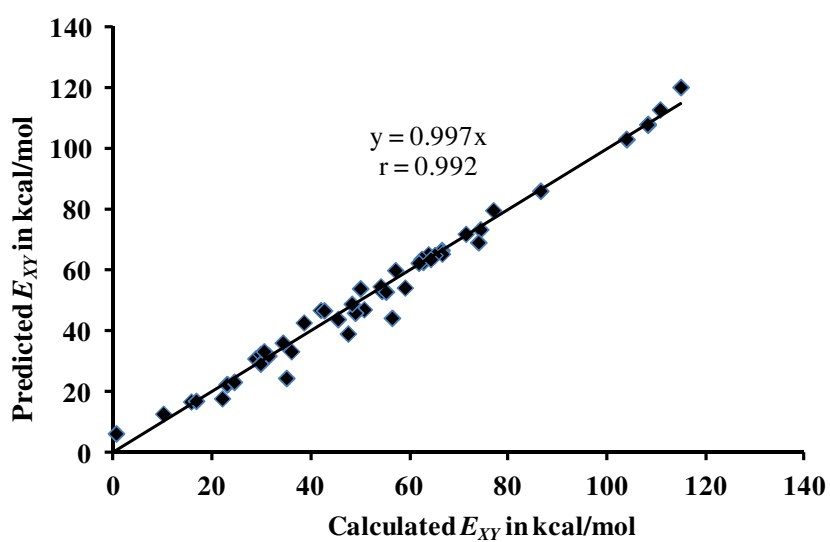
where,  $\eta$  is a constant for a particular metal atom and its value is 0.02027 and 0.01282 for Pd(II) and Pt(II) complexes. To arrive at Eq. 2.3 we have used a multiple linear regression approach using the terms  $E_X^2$ ,  $E_Y^2$  and  $E_X E_Y$ .

Table 2.6 lists the predicted  $E_{XY}$  for both Pd(II) and Pt(II) complexes. The standard deviation (s) is found 2.07 kcal/mol in Pd(II) complexes and 3.76 kcal/mol in Pt(II) complexes, showing better agreement of Eq. 2.3 compared to Eqs. 2.1 and 2.2. However, deviations exist in the predicted values of  $E_{XY}$  when a strong  $\pi$ -acceptor ligands CO, C<sub>2</sub>H<sub>4</sub> and CN<sup>-</sup> are trans to each other and also when Class III ligands are trans to a strong  $\pi$ -acceptor ligand particularly in Pt(II) complexes. Even though the trans influence of each ligand X and Y are mutual effects which depends on the bonding properties of the trans ligand [Coe and Glenwright 200], a quick and reliable prediction of  $E_{XY}$  can be made on the basis of Eq. 2.3.

The validity of Eq. 2.3 is tested with the help of another set of 20 isodesmic reactions (Table 2.7). In the prediction set of 33 reactions and in the validation set of 20 reactions, the combinations of X and Y are taken in such a way that it includes the participation of all the combinations of different classes, i.e. (Class I, Class I), (Class I, Class II), (Class I, Class III), (Class II, Class II), (Class II, Class III), and (Class III, Class III). The predicted  $E_{XY}$  for the test set using Eq. 2.3 is in very good agreement with the actual calculated values of  $E_{XY}$  (Table 2.7) and the corresponding statistical parameters are good, viz.  $r$  equal to 0.998 and 0.997 for Pd(II) and Pt(II) respectively, and  $s$  equal to 1.71 and 2.27 for Pd(II) and Pt(II) respectively. Figures 2.6 and 2.7 show the excellent agreement between calculated  $E_{XY}$  and the predicted  $E_{XY}$  for the 53 isodesmic reactions of Pd(II) and Pt(II) complexes.



**Figure 2.6** Correlation between  $E_{XY}$  and predicted  $E_{XY}$  values in Pd(II) complexes



**Figure 2.7** Correlation between  $E_{XY}$  and predicted  $E_{XY}$  values in Pt(II) complexes.

**Table 2.6** Isodesmic reactions used for the training set and predicted  $E_{XY}$  values (kcal/mol).

Ligands in the trans position		For Pd(II) complexes		For Pt(II) complexes	
X	Y	Predicted $E_{XY}$ using Eq. 2.3	Predicted $E_{XY}$ using Eq. 2.4	Predicted $E_{XY}$ using Eq. 2.3	Predicted $E_{XY}$ using Eq. 2.5
H <sub>2</sub> O	Br <sup>-</sup>	8.59	5.15	16.84	12.98
NH <sub>3</sub>	Br <sup>-</sup>	19.04	18.20	31.42	31.04
PH <sub>3</sub>	CN <sup>-</sup>	32.74	35.44	47.16	49.98
NO <sub>2</sub> <sup>-</sup>	PH <sub>3</sub>	28.62	26.45	43.91	42.89
NH <sub>3</sub>	NO <sub>2</sub> <sup>-</sup>	18.44	18.79	31.92	35.00
Py	AsH <sub>3</sub>	19.72	19.20	33.36	34.28
ONO <sup>-</sup>	N <sub>3</sub> <sup>-</sup>	18.07	14.10	31.00	27.93
CO	CN <sup>-</sup>	13.73	17.39	24.58	28.20
OH <sup>-</sup>	PH <sub>3</sub>	31.41	33.07	46.90	49.32
Br	OH <sup>-</sup>	29.32	24.86	42.80	37.78
OH <sup>-</sup>	CN <sup>-</sup>	32.20	34.57	46.79	51.61
H <sub>2</sub> O	H <sub>2</sub> O	1.57	-3.95	6.36	3.74
OH <sup>-</sup>	PMe <sub>3</sub>	38.17	37.60	54.02	55.56
CN <sup>-</sup>	PMe <sub>3</sub>	40.00	41.02	54.29	56.68
Py	Me <sup>-</sup>	37.19	35.82	53.12	55.40
PH <sub>3</sub>	SiH <sub>3</sub> <sup>-</sup>	55.80	55.73	73.44	72.65
AsH <sub>3</sub>	SiH <sub>3</sub> <sup>-</sup>	55.48	52.39	71.96	69.86
CO	H <sup>-</sup>	25.20	29.74	39.18	44.65
NO <sub>2</sub> <sup>-</sup>	H <sup>-</sup>	45.36	42.87	62.72	62.46
PH <sub>3</sub>	Ph <sup>-</sup>	50.87	50.61	66.65	66.29
H <sub>2</sub> O	SiH <sub>3</sub> <sup>-</sup>	23.93	21.57	36.21	39.50
F <sup>-</sup>	SiH <sub>3</sub> <sup>-</sup>	39.19	38.74	54.69	56.57
SMe <sub>2</sub>	Me <sup>-</sup>	45.07	40.52	60.00	56.95
CO	SiH <sub>3</sub> <sup>-</sup>	29.73	32.06	44.32	48.35
F <sup>-</sup>	H <sup>-</sup>	33.96	36.18	48.96	52.71
PMe <sub>3</sub>	PMe <sub>3</sub>	49.52	46.10	65.42	63.35
AsMe <sub>3</sub>	PEt <sub>3</sub>	49.12	44.90	64.99	59.65
AsMe <sub>3</sub>	Me <sup>-</sup>	63.79	60.34	79.72	75.26
Ph <sup>-</sup>	Me <sup>-</sup>	88.13	87.11	102.98	102.29
Me <sup>-</sup>	Me <sup>-</sup>	92.50	92.72	107.78	108.03
SiH <sub>3</sub> <sup>-</sup>	SiH <sub>3</sub> <sup>-</sup>	100.82	101.04	120.16	117.83
H <sup>-</sup>	SiH <sub>3</sub> <sup>-</sup>	88.90	94.38	108.12	110.08
H <sup>-</sup>	Me <sup>-</sup>	85.62	90.98	103.18	106.30

**Table 2.7** Isodesmic reactions used for the test set and predicted  $E_{XY}$  values (kcal/mol)

Ligands in the trans position		For Pd(II) complexes		For Pt(II) complexes	
X	Y	Predicted $E_{XY}$ using Eq. 2.3	Predicted $E_{XY}$ using Eq. 2.4	Predicted $E_{XY}$ using Eq. 2.3	Predicted $E_{XY}$ using Eq. 2.5
CO	Br <sup>-</sup>	12.19	12.28	22.50	20.56
AsH <sub>3</sub>	CN <sup>-</sup>	32.50	32.89	46.02	47.48
F <sup>-</sup>	PH <sub>3</sub>	19.74	21.27	32.53	34.05
CO	Py	7.78	10.00	17.89	19.93
H <sub>2</sub> O	NH <sub>3</sub>	5.13	4.15	12.84	13.63
NH <sub>3</sub>	SMe <sub>2</sub>	16.78	17.52	29.32	31.67
H <sub>2</sub> O	N <sub>3</sub> <sup>-</sup>	8.37	5.42	17.08	15.00
H <sub>2</sub> O	AsMe <sub>3</sub>	12.70	10.54	22.56	21.58
H <sub>2</sub> O	PMe <sub>3</sub>	13.31	11.23	23.31	23.59
H <sub>2</sub> O	Me <sup>-</sup>	22.25	20.16	33.38	36.76
NH <sub>3</sub>	Me <sup>-</sup>	37.82	38.84	52.98	58.10
CN <sup>-</sup>	Me <sup>-</sup>	54.67	56.46	69.19	72.42
OH	H <sup>-</sup>	48.85	51.43	66.28	70.26
AsH <sub>3</sub>	Ph <sup>-</sup>	50.56	47.47	65.24	63.58
SMe <sub>2</sub>	SiH <sub>3</sub> <sup>-</sup>	47.46	42.50	63.78	60.00
AsMe <sub>3</sub>	AsMe <sub>3</sub>	46.70	42.97	62.43	56.88
AsMe <sub>3</sub>	PMe <sub>3</sub>	47.86	44.21	63.66	59.32
PMe <sub>3</sub>	SiH <sub>3</sub> <sup>-</sup>	68.58	65.25	82.98	86.09
Ph <sup>-</sup>	SiH <sub>3</sub> <sup>-</sup>	91.45	90.40	107.91	106.01
Me <sup>-</sup>	SiH <sub>3</sub> <sup>-</sup>	95.90	96.17	112.83	111.83

### 2.4.8 Electron Density Values as a Measure of Trans Influence

Since  $E_X$  and  $E_Y$  values correlate with  $\rho(\mathbf{r})$  values (*cf.* Figure 2.5) at the bcp of the trans M–Cl bond, the corresponding  $\rho_X$  and  $\rho_Y$  values can also be used for the prediction of  $E_{XY}$ . Similar to Eq. 2.1, an MLR approach using the terms  $\rho_X$ ,  $\rho_Y$  and  $\rho_X\rho_Y$  of the 33 isodesmic reactions gives Eq. 2.4 to predict the  $E_{XY}$  values for Pd(II) complexes.

$$E_{XY(\text{Pd})} = -2709.906 \rho_X - 2217.285 \rho_Y + 19763.654 \rho_X\rho_Y + 274.334 \quad \dots \text{ (Eq. 2.4)}$$

$$(r = 0.996, \text{ and } s = 2.20)$$

Similarly for Pt(II) complexes,

$$E_{XY(\text{Pt})} = -2296.662\rho_X - 1641.451\rho_Y + 8568.031\rho_X\rho_Y + 293.730 \quad \dots \text{(Eq. 2.5)}$$

$$(r = 0.992, \text{ and } s = 3.64)$$

The predicted  $E_{XY}$  values using Eqs. 2.4 and 2.5 are given in Table 2.6. Eqs. 2.4 and 2.5 are validated using a test set of 20 isodesmic reaction (*cf.* Table 2.7). All the predicted  $E_{XY}$  values for both Pd(II) and Pt(II) complexes are given in Table 2.6 and 2.7. The corresponding statistical parameters are given, *viz*  $r$  equal to 0.998 and 0.995 for Eq. 2.4 and Eq. 2.5 respectively, and  $s$  equal to 1.55 and 3.06 for Pd(II) and Pt(II) respectively. The excellent agreement between predicted and calculated  $E_{XY}$  values are shown in Figures 2.8 and 2.9.

## 2.4.9 Bond Dissociation Energies in $[M^{II}X(Y)Cl_2]$ complexes

If  $D_{2X}$  represents the dissociation energy of the bond Pd–X in  $[Pd^{II}Cl_2XY]^{n-}$ , we find that the following equation relates  $D_{2X}$  with the trans influence of X and the mutual trans influence of X and Y.

$$D_{2X} = D_{IX} + E_X - E_{XY} \quad \dots \text{(Eq. 2.6)}$$

where  $D_{IX}$  is the dissociation energy of the bond M–X in  $[Pd^{II}Cl_3X]^{n-}$ . Since  $E_{XY}$  is predicted in terms of  $E_X$  and  $E_Y$  (Eq. 2.6), calculation of  $D_{2X}$  is possible if  $D_{IX}$  is known and similarly prediction of  $D_{2Y}$  can be made if  $D_{IY}$  is known.

For any trans combinations of X and Y ligands, it is thus possible to predict which ligand will dissociates first. The stability of the complex depends mainly on trans combinations because if the values of  $E_{XY}$  exceeds  $(D_{IX} + E_X)$  or  $(D_{IY} + E_Y)$ , there is no chance of forming such a complex.

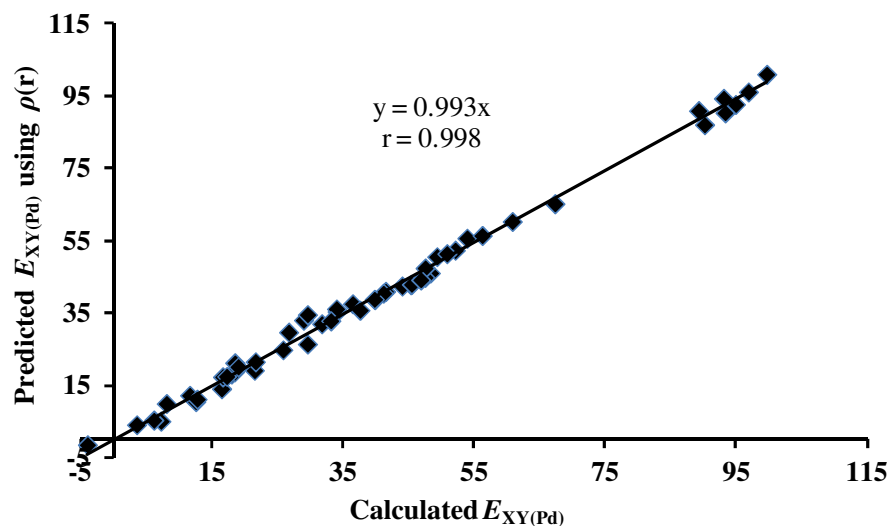


**Figure 2.8** Correlation between  $E_{XY}$  and predicted  $E_{XY}$  (using  $\rho(r)$  values) in Pd(II) complexes. All values are kcal/mol.

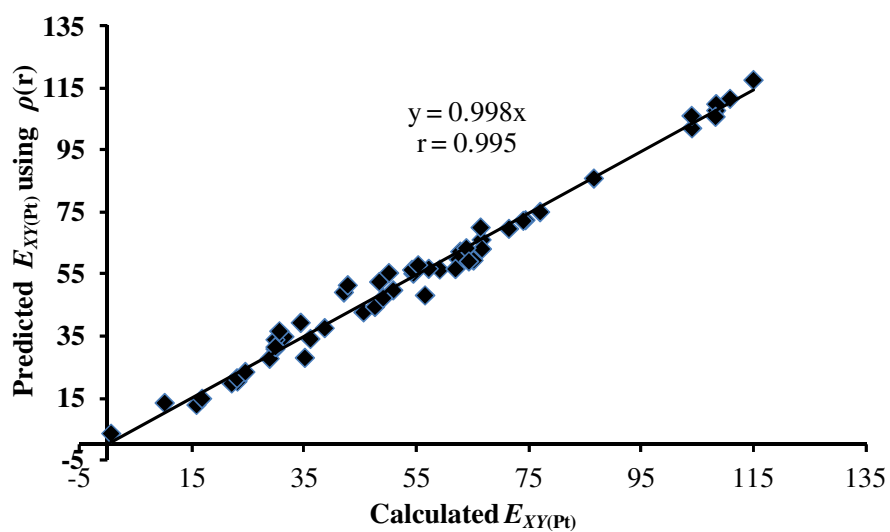


**Figure 2.9** Correlation between  $E_{XY}$  and predicted  $E_{XY}$  (using  $\rho(r)$  values) in Pt(II) complexes. All values are kcal/mol.

### 2.4.10 Bond Dissociation Energies in $[M^{II}X(Y)X'(Y')]$ Complexes

In complexes of the type  $[M^{II}X(Y)X'(Y')]$ , the X and Y as well as X' and Y' are trans to each other. Therefore, two different mutual trans influences will operate in the system at the same time. Since  $E_X$ ,  $E_Y$ ,  $E_{X'}$  and  $E_{Y'}$  are known from values in Table 2.3, the mutual trans influence of X and Y ( $E_{XY}$ ) as well as mutual trans influence of X' and Y' ( $E_{X'Y'}$ ) can be predicted using Eq. 2.3. The bond dissociation energy of X in  $[M^{II}X(Y)X'(Y')]$  (designated as  $D_{3X}$ ) is affected by mutual trans influences from X and Y as well as X' and Y'. If the value of the bond dissociation energy of X in  $[M^{II}Cl_3X]^{n-}$  is known (designated as  $D_{IX}$ , which is given in Table 2.8), using an MLR approach involving  $E_X$ ,  $E_{XY}$ ,  $E_{X'Y'}$  and  $D_{IX}$ , a very good prediction of the  $D_{3X}$  can be achieved for  $[Pd^{II}X(Y)X'(Y')]$  complexes using Eq. 2.7 and for  $[Pt^{II}X(Y)X'(Y')]$  complexes using Eq. 2.8.

$$D_{3X(Pd)} = 1.196E_X - 0.603E_{XY} - 0.118E_{X'Y'} + 0.442D_{IX} + 15.169 \quad \dots(\text{Eq. 2.7})$$

$$(r = 0.960, s = 4.01 \text{ kcal/mol})$$

$$D_{3X(Pt)} = 1.420E_X - 0.741E_{XY} - 0.125E_{X'Y'} + 0.499 D_{IX} + 13.852 \quad \dots(\text{Eq. 2.8})$$

$$(r = 0.965, s = 4.70 \text{ kcal/mol})$$

In both Eq. 2.7 and 2.8, the mutual trans influence terms are negative, indicating that they have destabilizing influence on the M–X bond strength. The contribution from  $E_{XY}$  is much higher than the contribution from  $E_{X'Y'}$ . It may be noted that if we had neglected the contribution of mutual trans influence  $E_{X'Y'}$ , a poor correlation with considerable scattering ( $r = 0.91$  for both Pd(II) and Pt(II) complexes) must have been obtained.

**Table 2.8** Dissociation energy  $D_{IX}$  for M–X bond in  $[MCl_3X]^{n-}$  complexes.

X	$D_{IX}$ in kcal/mol	
	For Pd(II) Complexes	For Pt(II) Complexes
H <sub>2</sub> O	23.31	29.17
CO	30.53	51.86
Py	38.31	49.34
NH <sub>3</sub>	41.88	51.83
SMe <sub>2</sub>	35.4	46.15
C <sub>2</sub> H <sub>4</sub>	31.65	47.29
AsH <sub>3</sub>	38.98	50.92
PH <sub>3</sub>	41.63	55.14
AsMe <sub>3</sub>	51.3	63.37
PMe <sub>3</sub>	55.37	69.16
PEt <sub>3</sub>	56.33	69.93
ONO <sup>-</sup>	29.25	36.99
F <sup>-</sup>	33.42	40.29
Cl <sup>-</sup>	26.75	33.99
Br <sup>-</sup>	28.23	35.37
N <sub>3</sub> <sup>-</sup>	35.27	44.10
NO <sub>2</sub> <sup>-</sup>	38.48	48.23
OH <sup>-</sup>	48.45	56.40
CN <sup>-</sup>	53.48	70.81
Ph <sup>-</sup>	87.65	99.93
H <sup>-</sup>	77.88	88.25
Me <sup>-</sup>	91.11	100.74
SiH <sub>3</sub> <sup>-</sup>	81.45	91.37

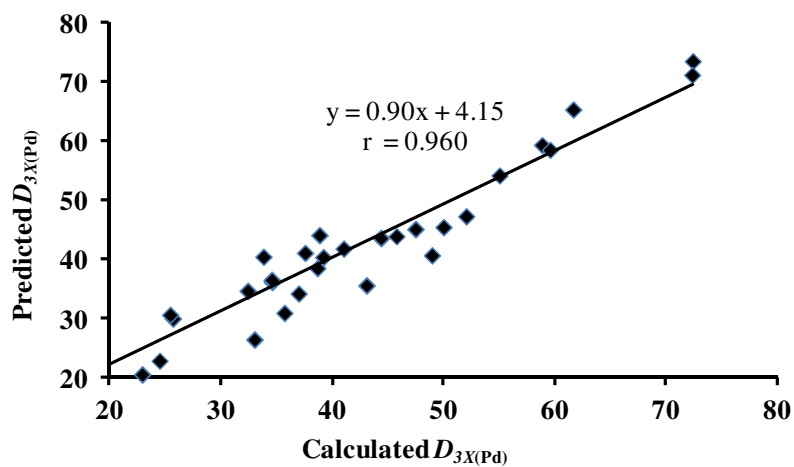


**Figure 2.10** Agreement between  $D_{3X}$  and predicted  $D_{3X}$  values in Pd(II) complexes. All values in kcal/mol.

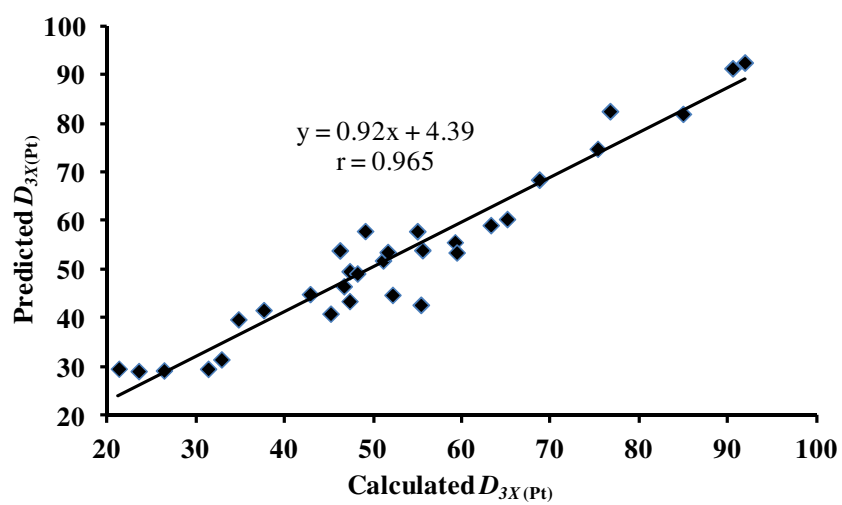


**Figure 2.11** Agreement between  $D_{3X}$  and predicted  $D_{3X}$  values in Pt(II) complexes. All values in kcal/mol.

**Table 2.9** Calculated and predicted bond dissociation energies of the ligands (using Eq. 2.7) in complexes of the type  $[\text{Pd}^{\text{II}}\text{X}(\text{Y})\text{X}'(\text{Y}')]$ . All values are in kcal/mol.

Trans Ligands		Trans Ligands		Bond dissociation energy of X ( $D_{3X}$ )		Bond dissociation energy of Y ( $D_{3Y}$ )		Bond dissociation energy of X' ( $D_{3X'}$ )		Bond dissociation energy of Y' ( $D_{3Y'}$ )	
X	Y	X'	Y'	Calculated	Predicted	Calculated	Predicted	Calculated	Predicted	Calculated	Predicted
H <sub>2</sub> O	CN <sup>-</sup>	F <sup>-</sup>	NO <sub>2</sub> <sup>-</sup>	19.63	23.57	58.85	59.41	43.08	35.67	50.00	45.53
NH <sub>3</sub>	NO <sub>2</sub> <sup>-</sup>	F <sup>-</sup>	Br <sup>-</sup>	38.67	38.60	38.85	44.18	36.99	34.30	39.20	40.46
NH <sub>3</sub>	Me <sup>-</sup>	CN <sup>-</sup>	Me <sup>-</sup>	17.32	22.64	72.40	73.56	25.69	30.06	61.67	65.40
PH <sub>3</sub>	Ph <sup>-</sup>	H <sup>-</sup>	Me <sup>-</sup>	22.93	20.64	59.58	58.59	34.59	36.28	47.49	45.20
F <sup>-</sup>	H <sup>-</sup>	ONO <sup>-</sup>	N <sub>3</sub> <sup>-</sup>	16.35	24.09	72.35	71.25	25.44	30.70	33.82	40.51
CO	Br <sup>-</sup>	AsMe <sub>3</sub>	PMe <sub>3</sub>	33.01	26.53	48.96	40.76	37.56	41.17	45.77	43.97
AsMe <sub>3</sub>	Me <sup>-</sup>	H <sup>-</sup>	Me <sup>-</sup>	24.49	22.94	55.03	54.26	32.42	34.75	44.38	43.67
H <sup>-</sup>	Ph <sup>-</sup>	NH <sub>3</sub>	NO <sub>2</sub> <sup>-</sup>	41.02	41.90	52.04	47.36	35.71	31.03	34.57	36.60

**Table 2.10** Calculated and predicted bond dissociation energies of the ligands (using Eq. 2.8) in complexes of the type  $[\text{Pt}^{\text{II}}\text{X}(\text{Y})\text{X}'(\text{Y}')]$ . All values are in kcal/mol.

Trans Ligands		Trans Ligands		Bond dissociation energy of X ( $D_{3X}$ )		Bond dissociation energy of Y ( $D_{3Y}$ )		Bond dissociation energy of X' ( $D_{3X'}$ )		Bond dissociation energy of Y' ( $D_{3Y'}$ )	
X	Y	X'	Y'	Calculated	Predicted	Calculated	Predicted	Calculated	Predicted	Calculated	Predicted
H <sub>2</sub> O	CN <sup>-</sup>	F <sup>-</sup>	NO <sub>2</sub> <sup>-</sup>	26.36	29.30	84.92	81.93	52.14	44.81	65.07	60.35
NH <sub>3</sub>	NO <sub>2</sub> <sup>-</sup>	F <sup>-</sup>	Br <sup>-</sup>	47.31	49.66	49.05	57.90	47.29	43.52	51.08	51.86
NH <sub>3</sub>	Me <sup>-</sup>	CN <sup>-</sup>	Me <sup>-</sup>	23.50	29.17	91.88	92.48	37.59	41.68	76.68	82.50
PH <sub>3</sub>	Ph <sup>-</sup>	H <sup>-</sup>	Me <sup>-</sup>	31.33	29.64	75.28	74.77	46.64	46.58	59.18	55.62

**Table 2.10 (Continued)**

F <sup>-</sup>	H <sup>-</sup>	ONO <sup>-</sup>	N <sub>3</sub> <sup>-</sup>	21.26	29.65	90.51	91.29	34.76	39.78	46.14	53.53
CO	Br <sup>-</sup>	AsMe <sub>3</sub>	PMe <sub>3</sub>	55.03	43.22	59.38	53.50	51.60	53.60	54.90	57.87
AsMe <sub>3</sub>	Me <sup>-</sup>	H <sup>-</sup>	Me <sup>-</sup>	32.84	31.57	68.70	68.43	42.84	44.95	55.51	53.98
H <sup>-</sup>	Ph <sup>-</sup>	NH <sub>3</sub>	NO <sub>2</sub> <sup>-</sup>	51.65	53.44	63.23	59.12	45.15	40.95	48.17	49.19

**Table 2.11.** The bond dissociation energies of various ligands in [M<sup>II</sup>X(Y)X'(Y')] complexes predicted using  $D_{IX}$  and  $\rho(\mathbf{r})$  values. All values in kcal/mol.

Sl. No.	Trans Ligands		Trans Ligands		Predicted $D_{3X}$		Predicted $D_{3Y}$		Predicted $D_{3X'}$		Predicted $D_{3Y'}$	
	X	Y	X'	Y'	Pd(II)	Pt(II)	Pd(II)	Pt(II)	Pd(II)	Pt(II)	Pd(II)	Pt(II)
1	H <sub>2</sub> O	CN <sup>-</sup>	F <sup>-</sup>	NO <sub>2</sub> <sup>-</sup>	27.08	34.55	60.26	82.38	37.04	46.59	43.02	58.33
2	NH <sub>3</sub>	NO <sub>2</sub> <sup>-</sup>	F <sup>-</sup>	Br <sup>-</sup>	39.65	51.19	41.35	54.34	36.33	47.50	37.69	48.23
3	NH <sub>3</sub>	Me <sup>-</sup>	CN <sup>-</sup>	Me <sup>-</sup>	23.09	27.95	73.97	91.15	29.45	38.60	65.33	81.68
4	PH <sub>3</sub>	Ph <sup>-</sup>	H <sup>-</sup>	Me <sup>-</sup>	20.89	28.81	58.28	75.47	37.29	47.81	43.18	54.35
5	F <sup>-</sup>	H <sup>-</sup>	ONO <sup>-</sup>	N <sub>3</sub> <sup>-</sup>	25.15	28.77	74.37	94.07	31.75	41.09	40.50	53.19
6	CO	Br <sup>-</sup>	AsMe <sub>3</sub>	PMe <sub>3</sub>	34.74	57.51	40.78	51.01	42.12	56.51	44.29	58.84
7	AsMe <sub>3</sub>	Me <sup>-</sup>	H <sup>-</sup>	Me <sup>-</sup>	22.80	30.22	57.10	73.82	36.19	46.76	42.09	53.29
8	H <sup>-</sup>	Ph <sup>-</sup>	NH <sub>3</sub>	NO <sub>2</sub> <sup>-</sup>	43.94	55.45	45.15	56.65	31.86	42.56	33.55	45.72

The calculated and predicted  $D_{3X}$  values for Pd(II) and Pt(II) complexes are given in Table 2.9 and 2.10 respectively. Figures 2.10 and 2.11 show the correlation between calculated and predicted  $D_{3X}$  values. No strong outliers emerge in the correlation and the predicted values are in good agreement with the calculated values. In fact some deviations are expected in the linear plot because the secondary effects such as steric and weak through space interactions from the cis ligands may operate in the system which are neglected in the present model.

Since both  $E_X$  and  $E_{XY}$  can be predicted with the help of electron density  $\rho(\mathbf{r})$  at the (3, -1) bond critical point of the trans M-Cl bond in square planar complexes of the type  $[M^{II}Cl_3X]^{n-}$ , it is also possible to predict the dissociation energies of all of the four ligands in a square planar complex  $[M^{II}X(Y)X'(Y')]$  if the  $\rho(\mathbf{r})$  values of X, Y, X' and Y' and the corresponding bond dissociation energies  $D_{IX}$  in  $[M^{II}Cl_3X]^{n-}$  complexes are known. Thus, for less trans influencing ligand X,  $D_{3X}$  can be written in terms of  $\rho(\mathbf{r})$  to obtain Eq. 2.9 and Eq. 2.10.

$$D_{3X(Pd)} = 0.364D_{IX} + 521.911\rho_X + 1337.369\rho_Y + 305.825\rho_{X'} + 250.230\rho_{Y'} \\ - 11920.572\rho_X\rho_{Y'} - 2230.416\rho_X\rho_{Y'} - 75.864 \quad \dots \text{(Eq. 2.9)}$$

$$D_{3X(Pt)} = 0.402D_{IX} + 184.510\rho_X + 1277.709\rho_Y + 269.267\rho_{X'} + 192.448\rho_{Y'} \\ - 6669.372\rho_X\rho_{Y'} - 1004.539\rho_X\rho_{Y'} - 73.223 \quad \dots \text{(Eq. 2.10)}$$

Similarly for the more trans influencing ligand Y, the  $D_{3Y}$  can be predicted using Eq. 2.11 and Eq. 2.12,

$$D_{3Y(Pd)} = 0.364D_{IY} + 1634.497\rho_X + 224.805\rho_Y + 305.825\rho_{X'} + 250.230\rho_{Y'} \\ - 11920.572\rho_X\rho_{Y'} - 2230.416\rho_X\rho_{Y'} - 75.864 \quad \dots \text{(Eq. 2.11)}$$

$$D_{3Y(Pt)} = 0.402D_{IY} + 1787.727\rho_X + 325.508\rho_Y + 269.267\rho_{X'} + 192.448\rho_{Y'} \\ - 6669.372\rho_X\rho_{Y'} - 1004.539\rho_X\rho_{Y'} - 73.223 \quad \dots \text{(Eq. 2.12)}$$

For the Pd(II) complexes, the actual and predicted values showed a standard deviation

of 4.56 kcal/mol and  $r$  value of 0.961 and in the case of Pt(II) complexes, the standard deviation and  $r$  value are 4.88 kcal/mol and 0.971, respectively. Predicted  $D_{3X}$  values using  $\rho(\mathbf{r})$  are given in Table 2.11.

### 2.4.11 Comparison of Different DFT Methods for the Calculation of BDEs

The performance of MPWB1K-COSMO/BS1 level of theory for the calculations of metal-ligand BDE is compared in the case of Pd(II) complexes with six different DFT functionals, *viz.* BP86-COSMO/BS1, PBE-COSMO/BS1, TPSS-COSMO/BS1, B3LYP-COSMO/BS1, PBE1PBE-COSMO/BS1 and M05-COSMO/BS1. The calculated values of the BDE for all these levels are presented in Table 2.12. BP86, PBE and TPSS levels showed very similar trends in the rank ordering as well as absolute values of the BDE. When compared with the MPWB1K method, BP86, PBE and TPSS methods overestimate the BDEs of the ligands CO, NO<sub>2</sub> and CN<sup>-</sup>. The hybrid methods B3LYP and PBE1PBE have nearly similar results and gives good agreement with the hybrid meta M05 and MPWB1K methods. The M05 method showed consistently lower values for BDE in almost every case. On the other hand, MPWB1K showed higher BDE values compared with other six different functionals in majority of the cases. Correlation matrix of all the seven DFT functionals and the correlations between each levels of theory are shown in Table 2.13. The BDEs at MPWB1K method showed a good correlation with BDEs calculated at all the other methods with correlation coefficients of 0.980, 0.976, 0.981, 0.997, 0.995, 0.987 for BP86, PBE, TPSS, B3LYP, PBE1PBE, and M05 methods, respectively. Thus, it can be concluded that the selection of MPWB1K or any of the methods mentioned here can be used as a reasonable choice for the study of BDEs of ligands in transition metal complexes.

**Table 2.12** BDEs of various ligands in  $[\text{Pd}^{\text{II}}\text{X}(\text{Y})\text{X}'(\text{Y}')] ]$ , calculated at different levels of theory. (X, Y) and (X', Y') are trans combinations. All values are in kcal/mol.

Sl. No.	Ligands in the complex	BP86	PBE	TPSS	B3LYP	PBE1PBE	M05
1	X = H <sub>2</sub> O	13.92	14.92	15.45	15.45	17.33	13.66
	Y = CN <sup>-</sup>	56.99	58.40	56.63	55.02	58.98	51.16
	X' = F <sup>-</sup>	37.14	37.67	39.14	37.96	40.56	32.95
	Y' = NO <sub>2</sub> <sup>-</sup>	53.28	54.78	52.55	47.65	51.89	47.08
2	X = NH <sub>3</sub>	31.55	32.27	33.06	33.22	36.02	29.58
	Y = NO <sub>2</sub> <sup>-</sup>	41.70	43.13	41.31	36.87	40.62	37.55
	X' = F <sup>-</sup>	28.10	28.97	30.02	32.09	35.06	28.70
	Y' = Br <sup>-</sup>	36.00	37.12	29.89	34.93	38.15	32.63
3	X = NH <sub>3</sub>	14.94	16.19	16.16	13.26	16.84	12.05
	Y = Me <sup>-</sup>	71.86	73.38	71.88	68.05	72.98	66.95
	X' = CN <sup>-</sup>	26.18	27.69	26.65	21.72	26.60	20.88
	Y' = Me <sup>-</sup>	58.88	60.13	59.83	56.99	61.07	55.07
4	X = PH <sub>3</sub>	20.50	22.27	21.34	17.23	22.94	17.66
	Y = Ph <sup>-</sup>	59.59	61.28	59.28	55.35	60.12	52.59
	X' = H <sup>-</sup>	34.58	36.03	33.46	30.73	35.63	28.20
	Y' = Me <sup>-</sup>	45.41	47.13	47.72	41.53	47.22	41.84
5	X = F <sup>-</sup>	14.44	15.47	16.56	14.07	16.32	13.19
	Y = H <sup>-</sup>	72.04	72.98	68.30	71.17	73.95	69.67
	X' = ONO <sup>-</sup>	25.94	26.63	24.56	23.47	25.69	21.32
	Y' = N <sub>3</sub> <sup>-</sup>	32.40	33.40	33.12	30.95	33.92	27.64
6	X = CO	40.23	42.28	39.62	32.53	38.25	30.72
	Y = Br <sup>-</sup>	44.10	46.79	45.61	41.46	46.33	39.85
	X' = AsMe <sub>3</sub>	39.42	41.60	40.59	35.64	43.38	39.46
	Y' = PMe <sub>3</sub>	43.33	45.43	43.25	40.19	46.63	38.88
7	X = AsMe <sub>3</sub>	21.76	23.89	22.35	17.94	24.27	19.90
	Y = Me <sup>-</sup>	54.67	55.85	54.92	51.48	55.43	49.09
	X' = H <sup>-</sup>	31.53	33.04	30.66	28.03	32.75	25.56
	Y' = Me <sup>-</sup>	41.74	43.62	44.33	38.33	43.79	38.06
8	X = H <sup>-</sup>	38.55	39.62	37.52	37.17	40.78	34.62
	Y = Ph <sup>-</sup>	49.23	51.06	51.17	46.71	51.56	46.24
	X' = NH <sub>3</sub>	30.54	31.42	31.87	30.64	34.18	27.26
	Y' = NO <sub>2</sub> <sup>-</sup>	35.77	37.38	36.15	31.30	35.86	29.75

**Table 2.13** Correlation matrix of 7 DFT functionals.

	MPWB1K	BP86	PBE	TPSS	B3LYP	PBE1PBE	M05
MPWB1K	1						
BP86	0.980	1					
PBE	0.976	0.999	1				
TPSS	0.981	0.993	0.993	1			
B3LYP	0.995	0.988	0.984	0.984	1		
PBE1PBE	0.994	0.994	0.992	0.991	0.997	1	
M05	0.987	0.994	0.993	0.991	0.993	0.997	1

The BDEs predicted using Eq. 2.7 shows the standard deviations of 3.71, 3.88, 4.07, 3.08, 3.24, 3.11 and 3.38 kcal/mol from the calculated BDEs obtained using BP86, PBE, TPSS, B3LYP, PBE1PBE, and M05 methods respectively. Also the predicted and the calculated BDEs obtained using different levels of theory showed a good correlation with a correlation coefficient higher than 0.965 in all the cases. Thus, it is clear that the Eq. 2.7 reproduces, to a large extent, the BDEs of various ligands irrespective of the different functionals used.

### 2.4.12 Significance of MLR Equations for Predicting BDEs

Using Eq. 2.7 and Eq. 2.8, it is possible to predict the order of metal-ligand bond dissociation energy in complexes of the type  $[M^{II}X(Y)X'(Y')]$ . For instance, in  $[PdMe(H)Ph(PH_3)]^-$ , the trans combinations are  $(Me^-$  and  $H^-)$  and  $(Ph^-$  and  $PH_3)$  and the decreasing order of Pd–X bond dissociation energy are  $Ph^-$  (59.58 kcal/mol),  $Me^-$  (47.49 kcal/mol),  $H^-$  (34.59 kcal/mol), and  $PH_3$  (22.93 kcal/mol). The predicted  $D_{3X}$  values of these ligands using Eq. 2.7 also follow nearly same magnitude and trend, *viz.* 58.59, 45.20, 36.28, and 20.64 kcal/mol for  $Ph^-$ ,  $Me^-$ ,  $H^-$ , and  $PH_3$ , respectively. Similarly, Eq. 2.8 is useful to predict the most likely dissociation pathway of a Pt(II) complex. Thus Eq. 2.7 and Eq. 2.8 are useful for predicting the most facile dissociation of a metal-ligand bond in a square planar  $[M^{II}X(Y)X'(Y')]$  complex in terms of trans influence and mutual trans influence parameters.

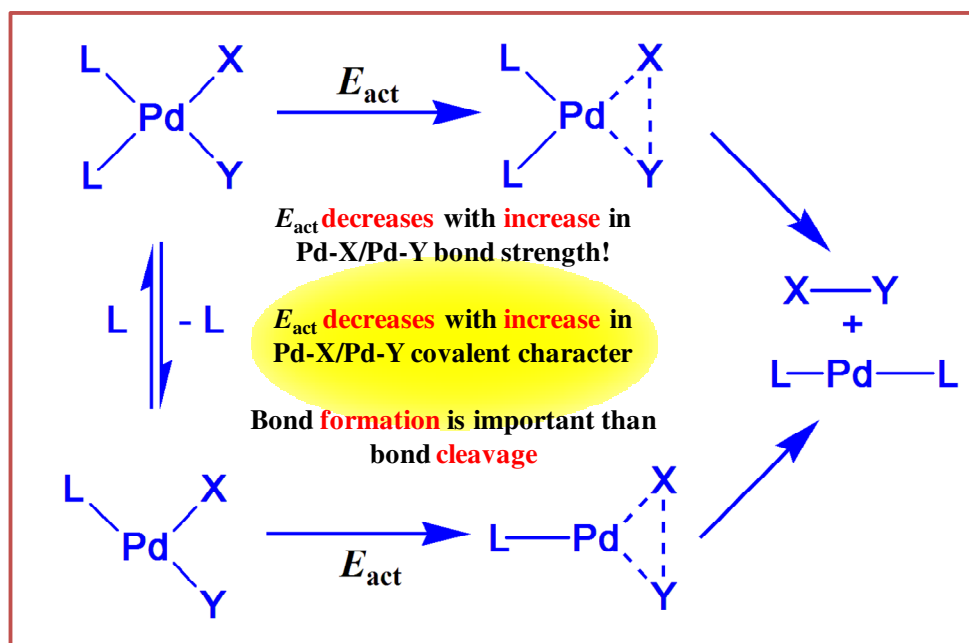
## 2.5 Conclusion

Simple isodesmic reactions of the type  $M^{II}Cl_2X + M^{II}Cl_3 \longrightarrow M^{II}Cl_2 + M^{II}Cl_3X$  (where, M = Pd, Pt), are modeled to investigate the trans influence of variety of ligands using solvent corrected DFT methods. The energy of the isodesmic reactions ( $E_X$ ) serve as an excellent energetic descriptor of the mutual trans influencing power of ligands. Using the  $E_X$  value obtained for various X ligands against  $Cl^-$  as the trans ligand, the mutual trans influence of any combination of two ligands can be predicted with the help of the equation  $E_{XY} = \eta(E_X + E_Y / \sqrt{2})^2$  for both the complexes of Pd(II) and Pt(II) where  $E_X < E_Y$ . According to the  $E_X$  values, the trans influence of a ligand X in Pt(II) complexes follow the order  $SiH_3^- > Me^- > Ph^- \sim H^- > PEt_3 > PMe_3 > AsMe_3 > CN^- \sim PH_3 \sim AsH_3 \sim OH^- > NO_2^- \sim N_3^- \sim Br^- > SMe_2 \sim Cl^- \sim C_2H_4 > NH_3 \sim Py > ONO^- \sim F^- > CO > H_2O$  whereas this order in Pd(II) complexes is  $SiH_3^- > Me^- > Ph^- > H^- > PEt_3 > PMe_3 > AsMe_3 > CN^- \sim PH_3 \sim AsH_3 > OH^- > NO_2^- \sim N_3^- \sim Br^- > SMe_2 \sim Cl^- > C_2H_4 > NH_3 > Py \sim F^- \sim ONO^- > CO > H_2O$ . In both Pd(II) and Pt(II) complexes, the order of mutual trans influence of different ligands are almost the same. However, the mutual trans influence of an X ligand in the Pt(II) complexes is approximately 8-15 kcal/mol higher than its influence in the Pd(II) complexes.

The contribution of the trans influence terms  $E_X$ ,  $E_{XY}$  and  $E_{X'Y'}$  to the bond dissociation energy of the ligands X, Y, X' and Y' has been studied in square planar complexes of the type  $[M^{II}X(Y)X'(Y')]$ . Using a multiple linear regression approach with  $E_X$ ,  $E_{XY}$ ,  $E_{X'Y'}$  and  $D_{IX}$  (the bond dissociation energy of X in  $[M^{II}Cl_3X]^{n-}$ ) as variables, the bond dissociation energy of any ligand in  $[M^{II}X(Y)X'(Y')]$  complexes is predicted. Since  $E_X$ ,  $E_{XY}$ ,  $E_{X'Y'}$  are written in terms of the electron density  $\rho(\mathbf{r})$  at the (3, -1) bond critical point of the trans M-Cl bond in  $[M^{II}Cl_3X]^{n-}$ , the bond

dissociation energy of X in  $[M^{II}X(Y)X'(Y')]$  is also predicted using the  $\rho(\mathbf{r})$ . The results presented herein clearly suggest that the bond dissociation energy of a ligand X in a square planar Pd(II) or a Pt(II) complex is highly influenced two mutual trans influences, one due to the (X, Y) trans combination, the major influence and another due to the (X', Y') trans combination. Further, the contribution of these two trans influences to the bond dissociation energy are quantified using QSPR models. The calculated  $E_X$  values may find use in the development of new trans influence-incorporated force field models for palladium complexes.

# Mechanisms of Reductive Eliminations in Square Planar Pd(II) Complexes: Nature of Eliminated Bonds and Role of Trans Influence



### 3.1 Abstract

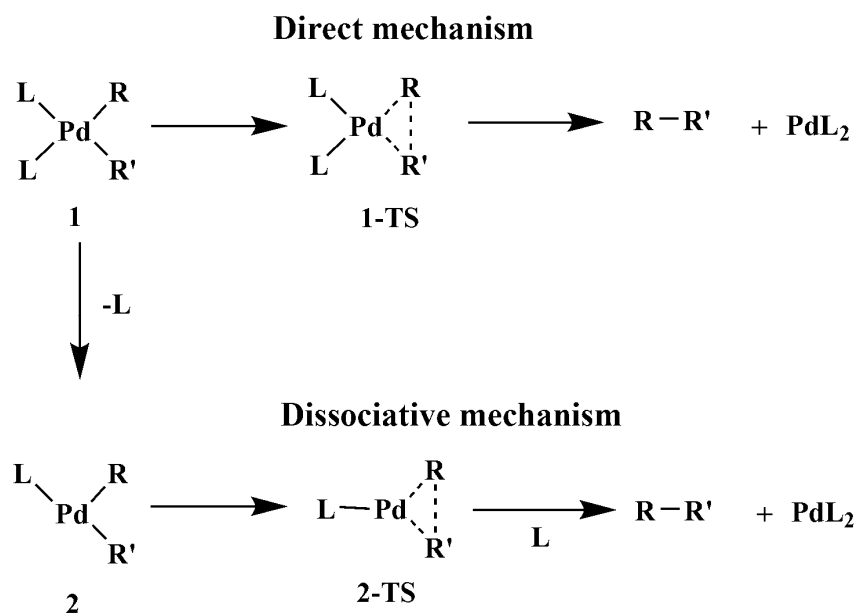
*The trans influence of various phosphine ligands (L) in direct as well as dissociative reductive elimination pathways yielding  $\text{CH}_3\text{CH}_3$  from  $\text{Pd}(\text{CH}_3)_2\text{L}_2$  and  $\text{CH}_3\text{Cl}$  from  $\text{Pd}(\text{CH}_3)(\text{Cl})\text{L}_2$  has been quantified in terms of isodesmic reaction energy,  $E_L$  using MPWB1K level of density functional theory. In the absence of large steric effect,  $E_L$  correlated linearly with the activation barrier ( $E_{act}$ ) of both direct and dissociation pathways. The minimum of molecular electrostatic potential ( $V_{min}$ ) at the lone pair region of phosphine ligands has been used to assess their electron donating power.  $E_L$  increased linearly with increase in the negative  $V_{min}$  values. Further, the nature of bonds which are eliminated during the reductive elimination have been analysed in terms of AIM parameters, viz. the electron density ( $\rho(\mathbf{r})$ ), Laplacian of the electron density ( $\nabla^2\rho(\mathbf{r})$ ), the total electron energy density ( $H(\mathbf{r})$ ), and the ratio of potential and kinetic electron energy densities ( $k(\mathbf{r})$ ).  $E_{act}$  correlated inversely with the strength of the eliminated metal-ligand bonds measured in terms of the bond length or the  $\rho(\mathbf{r})$ . Analysis of  $H(\mathbf{r})$  showed that the elimination of the C–C/C–Cl bond becomes more facile when the covalent character of the Pd–C/Pd–Cl bond increases. Thus, AIM details clearly showed that the strength of the eliminated bond is not the deciding factor for the reductive elimination but the nature of the bond, covalent or ionic. Further, a unified picture showing the relationship between the nature of the eliminated chemical bond and the tendency of reductive elimination is obtained from the  $k(\mathbf{r})$  values: the  $E_{act}$  of both direct and dissociative mechanisms for the elimination of  $\text{CH}_3\text{CH}_3$  and  $\text{CH}_3\text{Cl}$  decreased linearly when the sum of  $k(\mathbf{r})$  at the cleaved bonds showed more negative character. It means that the potential electron energy density dominates over the kinetic electron energy density when the bonds (Pd–C/Pd–Cl) become*

*more covalent and the eliminated fragments attain more radical character leading to the easy formation of C–C/C–Cl bond.*

## 3.2 Introduction

Palladium-catalysed cross coupling reactions are considered as one of the most powerful and efficient tools for carbon-carbon and carbon-heteroatom bond formation reactions in organic synthesis [Tamao *et al.* 1972; Farina *et al.* 1997; Crabtree 2001; Negishi 2002; Negishi and Anastasia 2003; Tsuji 2004; Negishi *et al.* 2010]. It has been established that the presence of appropriate phosphine as ancillary ligands in palladium complexes is highly useful for tuning the catalytic activity by controlling the steric and electronic effects of these ligands [Crabtree 2000; Negishi and Anastasia 2003; Ariafard and Lin 2006; <sup>b</sup>Ariafard and Yates 2009; Xue and Lin 2010]. Reductive elimination is a key step, often the last step in many of these cross-coupling reactions [Echavarren and Cárdenas 2004; Chass *et al.* 2010]. It is proposed that the reductive elimination reaction from square planar complexes would be proceeded through a four coordinate (direct mechanism) or a three coordinate transition state (dissociative mechanism) [Brown and Cooley 1988; Ananikov *et al.* 2002; Ananikov *et al.* 2005; Hartwig 2007]. Scheme 3.1 illustrates the reductive elimination of R–R' from a square planar complex of the type  $[L_2Pd(R)R']$ , where L indicates the ancillary phosphine ligand [Ananikov *et al.* 2007]. In general, dissociative pathway requires less activation energy than the direct pathway [Xue and Lin 2010]. However, the energy cost for the dissociation of the ancillary ligand from the four coordinate complexes often determines the feasibility of the dissociative pathway [<sup>a</sup>Ariafard and Yates 2009]. Ananikov *et al.* theoretically investigated the C–C reductive elimination reactions in Pd(II) complexes with ancillary phosphine ligands and concluded that the steric

effect of phosphine ligands has a great influence on the initial structure of square planar Pd(II) complexes, while the transition state of reductive elimination reaction is mostly affected by the electronic effect of phosphine ligands [Ananikov *et al.* 2007]. For the bulky ancillary ligands such as PCy<sub>3</sub>, the reductive elimination through dissociative pathway is more favored due to the destabilization of the initial reactant complex. Thus the preferred pathway depends on the steric nature of the ancillary phosphine ligands and the extent to which the Pd-PR<sub>3</sub> bond is destabilized [Ananikov *et al.* 2010]. Also, the reassociation of a sterically crowded ligand to a three coordinate complex is difficult compared to a sterically less crowded ligand. Recently, Ariafard and Yates have investigated various factors contributing to the energy barriers of reductive elimination reactions using energy decomposition analysis and concluded that when bulky ancillary phosphine ligands are present, steric effect destabilizes the initial reactant complex and hence decreases the energy barrier of direct reductive elimination whereas the steric effect showed only a marginal role in the reductive elimination from three coordinate complexes [<sup>a</sup>Ariafard and Yates 2009]. A computational study on the reductive elimination of organic molecules from palladium(II) complexes with chelate ancillary ligands showed that the energy barriers of reductive elimination in palladium diphosphine complexes depend largely on the electronic nature of substrates and not steric effects [Zuidema *et al.* 2005]. Very recently, Korenaga *et al.* have studied the diphosphine electronic effects in the reductive elimination of biphenyl from *cis*-[Pt(Ph)<sub>2</sub>(diphosphine)] complexes and showed good correlations between rate constant and ancillary diphosphine electronic parameters [Korenaga *et al.* 2010].



**Scheme 3.1** Formation of R–R' through direct and dissociative mechanisms, where L is ancillary phosphine ligands.

It is clear from the experimental and theoretical studies that the ancillary ligands with low electron donating nature will show an enhancement on the rate of reductive elimination reaction [Negishi *et al.* 1987]. For example, the relative reactivity in C–C bond formation in  $L_2Pd(R)(R')$  complexes with phosphine ligands as ancillary ligands follows the order:  $L = PCl_3 > PH_3 > PMe_3$  [<sup>a</sup>Ariafard and Yates 2009]. This order is inversely related with the  $\sigma$ -donating ability and the related trans influence of ancillary phosphine ligands. Even though trans influence of the ligands have a prominent effect on the rate of reductive elimination reactions, systematic studies regarding the effect of trans ligands on the rate of C–C and C–heteroatom bond formation through reductive elimination are rare [Yamashita *et al.* 2003]. In the present work, the isodesmic reaction approach will be used to quantify the trans influence of various phosphine ligands. The term  $E_L$  is used to represent the quantified values of trans influence. The main aim of this study is to elucidate the importance of  $E_L$  on the C–C and C–Cl bond formation reactions from square planar Pd(II) complexes through reductive elimination mechanism involving both direct and dissociative mechanisms.

Electronic parameter of free phosphine ligands in these reactions is discussed in terms of molecular electrostatic potential (MESP), observed in the lone pair region of a phosphine ligand [Suresh and Koga 2002; Mathew *et al.* 2007]. Further, the AIM analysis [Bader 1990] has been used to correlate the electron density features of bond critical points to the mechanistic features of the reductive elimination reactions.

### 3.3 Computational Methods

All the calculations were done at MPWB1K [Zhao and Truhlar 2004] level of DFT method with Gaussian03 suite of programs [Frisch *et al.* Gaussian 03 2004]. For Pd, the basis set Lanl2DZ [<sup>a</sup>Hay and Wadt 1985] with extra f polarization function was chosen [Ehlers *et al.* 1993]. For all the other atoms, 6-31++G(d,p) basis set was selected and the combined basis set for all the atoms is named as BS1. MPWB1K is chosen for this study because of its reliable performance in the thermo chemical kinetics, non covalent interactions and also in the determination of barrier heights [Leopoldini *et al.* 2009]. All the stationary points were confirmed by means of vibration analysis, and all the transition states were characterized by the determination of a single imaginary frequency and its relationship with nuclei motion. The MPWB1K/6-31++G(d,p) level of theory was used to calculate the molecular electrostatic potential (MESP) of free phosphine ligands [Suresh 2006; Mathew *et al.* 2007].

As in Chapter 2, the quantification of trans influence of various phosphine ligands (L = PH<sub>3</sub>, PCl<sub>3</sub>, PH<sub>2</sub>CF<sub>3</sub>, PH<sub>2</sub>Et, PH<sub>2</sub>Ph, PMeCl<sub>2</sub>, PMe<sub>3</sub>, PHEt<sub>2</sub>, PEt<sub>3</sub> and PPh<sub>3</sub>) have been done using isodesmic reactions of the type [PdCl<sub>3</sub>]<sup>-</sup> + [PdCl<sub>2</sub>L] → [PdCl<sub>3</sub>L]<sup>-</sup> + [PdCl<sub>2</sub>] at MPWB1K/BS1 level of theory and solvent corrections in water were applied through a conductor like screening model (COSMO) which is a widely used self consistent reaction field (SCRF) method [Klamt *et al.* 1993].

To calculate the topological features of electron density, atoms in molecule (AIM) analysis was done using the AIM2000 program [Bader 1990; Biegler-König *et al.* 2001]. In order to get reliable AIM parameters, the effective core potential basis set for Pd in BS1 was replaced with all electron basis set, DGDZVP [Godbout *et al.* 1992; Sosa *et al.* 1992] to generate the wavefunction at the MPWB1K method. AIM analysis is based on Bader's theory [Bader 1990] and for the present study, the bond critical points (bcp) of the nature (3, -1) is located for Pd-C<sub>methyl</sub> and Pd-Cl bonds of all the reactant complexes. At the bcp, electron density ( $\rho(\mathbf{r})$ ), the Laplacian ( $\nabla^2\rho(\mathbf{r})$ ), the density of the total energy of the electron ( $H(\mathbf{r})$ ), the kinetic electron energy density ( $G(\mathbf{r})$ ) and the potential electron energy density ( $V(\mathbf{r})$ ) were determined. For the assessment of the covalent character of Pd-C/Cl bond, we also determined  $k(\mathbf{r})$  values.

## 3.4 Results and Discussion

### 3.4.1 Reductive Elimination of CH<sub>3</sub>CH<sub>3</sub> and CH<sub>3</sub>Cl

Reductive elimination of CH<sub>3</sub>CH<sub>3</sub> from cis-[Pd(CH<sub>3</sub>)<sub>2</sub>L<sub>2</sub>] complexes as well as CH<sub>3</sub>Cl from cis-[Pd(CH<sub>3</sub>)(Cl)L<sub>2</sub>] complexes is investigated on the basis of both direct and dissociative mechanisms (Scheme 3.1). Representative examples for these reactions are depicted in Figures 3.1 and 3.2. The structures **1a-PMe<sub>3</sub>** and **1a-PMe<sub>3</sub>\_TS** are respectively the [Pd(CH<sub>3</sub>)<sub>2</sub>(PMe<sub>3</sub>)<sub>2</sub>] complex and the transition state for the direct reductive elimination of CH<sub>3</sub>CH<sub>3</sub> (Figure 3.1a). Similarly, **1b-PMe<sub>3</sub>** is the [Pd(CH<sub>3</sub>)Cl(PMe<sub>3</sub>)<sub>2</sub>] complex and **1b-PMe<sub>3</sub>\_TS** is the transition state involved in the direct reductive elimination of CH<sub>3</sub>Cl (Figure 3.1b). The dissociative elimination of CH<sub>3</sub>CH<sub>3</sub> is represented using the structures **2a-PMe<sub>3</sub>** and **2a-PMe<sub>3</sub>\_TS** (Figure 3.2c) while that of CH<sub>3</sub>Cl is described using **2b-PMe<sub>3</sub>** and **2b-PMe<sub>3</sub>\_TS** (Figure 3.2d). It may be noted that **2b-PMe<sub>3</sub>** is formed by dissociating

one of the  $\text{PMe}_3$  ligand from  $[\text{Pd}(\text{CH}_3)\text{Cl}(\text{PMe}_3)_2]$ . Because of the high trans influence of the  $-\text{CH}_3$  ligand [Chval *et al.* 2008], the  $\text{PMe}_3$  ligand trans to the  $-\text{CH}_3$  ligand is easier to dissociate than the one trans to the  $-\text{Cl}$  ligand. In all the cases, the direct mechanism passes through a four coordinate transition state to eliminate the  $\text{CH}_3\text{CH}_3$  or the  $\text{CH}_3\text{Cl}$  while in the dissociative mechanism, a three coordinate transition state is involved.

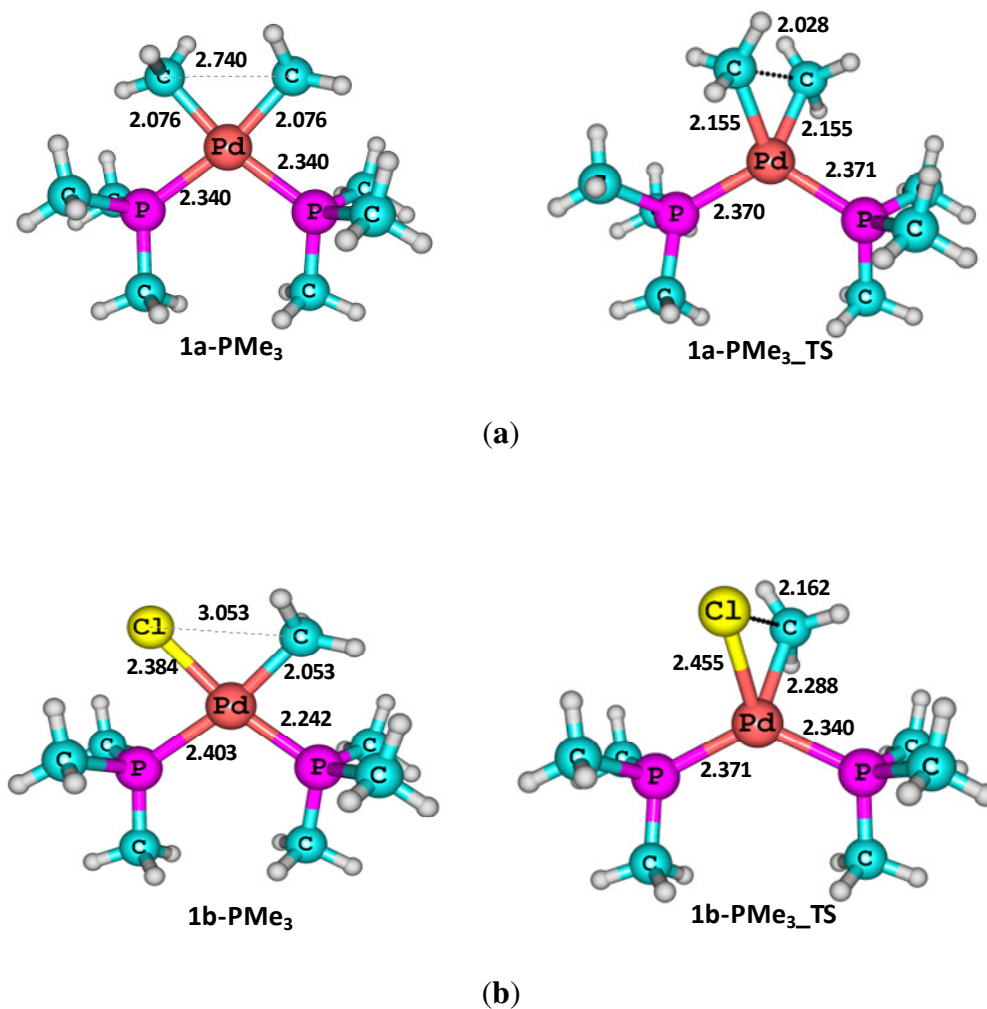
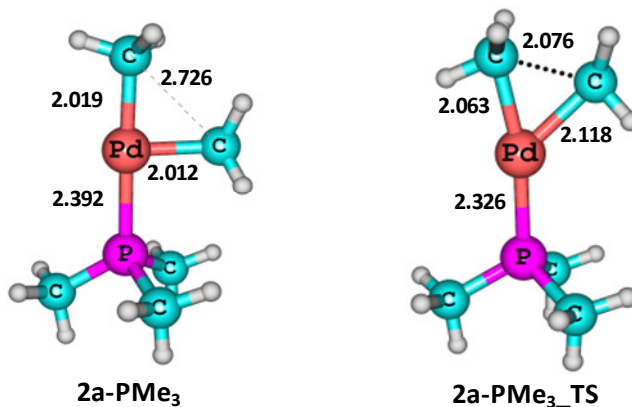
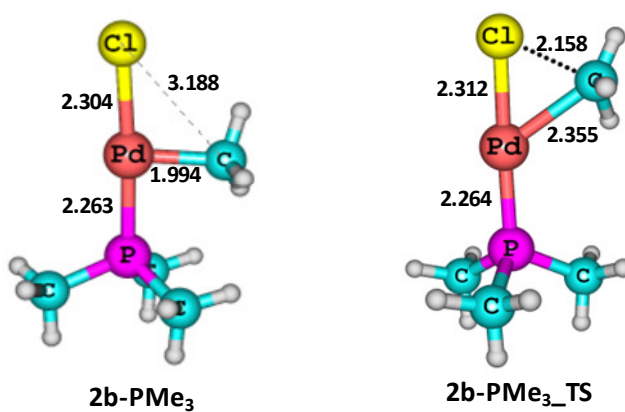


**Figure 3.1** Structures of reactants and transition states involved in the reductive elimination of  $\text{CH}_3\text{CH}_3$  and  $\text{CH}_3\text{Cl}$  through direct mechanism with  $\text{PMe}_3$  as ancillary ligands. Selected bond distances (in Å) are given.



(c)



(d)

**Figure 3.2** Structures of reactants and transition states involved in the reductive elimination of  $\text{CH}_3\text{CH}_3$  and  $\text{CH}_3\text{Cl}$  through dissociative mechanism with  $\text{PMe}_3$  as ancillary ligands. Selected bond distances (in Å) are given.

**Table 3.1**  $E_{act}$  (kcal/mol) values for the reductive elimination of  $\text{CH}_3\text{CH}_3$  and  $\text{CH}_3\text{Cl}$  via direct and dissociative mechanisms.

Ancillary Ligand (L)	$E_{act}$ for $\text{CH}_3\text{CH}_3$ reductive elimination		$E_{act}$ for $\text{CH}_3\text{Cl}$ reductive elimination	
	Direct Mechanism	Dissociative Mechanism	Direct Mechanism	Dissociative Mechanism
$\text{PH}_3$	23.91	10.25	44.02	30.28
$\text{PCl}_3$	15.12	8.57	32.18	25.78
$\text{PH}_2\text{CF}_3$	21.64	8.98	41.02	26.89
$\text{PH}_2\text{Et}$	26.64	10.67	47.99	32.34
$\text{PH}_2\text{Ph}$	26.93	10.64	47.35	32.33
$\text{PMeCl}_2$	21.13	9.97	39.97	28.33
$\text{PMe}_3$	31.35	11.72	55.68	35.85
$\text{PHEt}_2$	28.76	10.99	52.05	34.37
$\text{PEt}_3$	31.66	12.15	56.07	36.40
$\text{PPh}_3$	26.23	11.46	46.31	34.63

For all the ten ancillary ligands, the activation energy ( $E_{act}$ ) of both direct and dissociative mechanism are presented in Table 3.1. The highest  $E_{act}$  for both  $\text{CH}_3\text{CH}_3$  and  $\text{CH}_3\text{Cl}$  in the direct and dissociation pathway is observed for  $\text{PEt}_3$  whereas the lowest  $E_{act}$  is obtained for  $\text{PCl}_3$ . In the direct mechanism, the decreasing order of  $E_{act}$  values for various ancillary ligands can be written as  $\text{PEt}_3 \sim \text{PMe}_3 > \text{PHEt}_2 > \text{PH}_2\text{Et} \sim \text{PH}_2\text{Ph} \sim \text{PPh}_3 > \text{PH}_3 > \text{PMeCl}_2 \sim \text{PH}_2\text{CF}_3 > \text{PCl}_3$  while for the dissociative mechanism this order can be written as  $\text{PEt}_3 > \text{PMe}_3 > \text{PPh}_3 > \text{PHEt}_2 > \text{PH}_2\text{Et} \sim \text{PH}_2\text{Ph} > \text{PH}_3 > \text{PMeCl}_2 > \text{PH}_2\text{CF}_3 > \text{PCl}_3$ . For the  $\text{CH}_3\text{CH}_3$  elimination via direct mechanism, the  $E_{act}$  ranges from 15.12 to 31.66 kcal/mol and through dissociative mechanism the  $E_{act}$  are within a small range of 8.57 to 12.15 kcal/mol. This shows that the direct mechanism is highly influenced by the nature of the ancillary

phosphine ligands than the dissociative mechanism. For the reductive elimination of  $\text{CH}_3\text{Cl}$ , the  $E_{act}$  of the direct mechanism is in the range of 32.18 to 56.07 kcal/mol while for the dissociative mechanism it is 25.78 to 36.40 kcal/mol. Thus a comparison of the  $E_{act}$  for C–C and C–Cl reductive elimination suggests that the former is more favorable than the latter.

**Table 3.2** Calculated trans Pd–C bond length in  $\text{Pd}(\text{CH}_3)_2\text{L}_2$ ,  $\text{Pd}(\text{CH}_3)(\text{Cl})\text{L}_2$  and  $\text{Pd}(\text{CH}_3)_2\text{L}$  complexes along with Pd–Cl bond length in  $\text{Pd}(\text{CH}_3)(\text{Cl})\text{L}_2$  and  $\text{Pd}(\text{CH}_3)(\text{Cl})\text{L}$  complexes. All values are in Å.

Ancillary ligand	$\text{Pd}(\text{CH}_3)_2\text{L}_2$	$\text{Pd}(\text{CH}_3)(\text{Cl})\text{L}_2$		$\text{Pd}(\text{CH}_3)_2\text{L}$	$\text{Pd}(\text{CH}_3)(\text{Cl})\text{L}$
	trans Pd–C bond length <sup>#</sup>	trans Pd–C bond length	trans Pd–Cl bond length	trans Pd–C bond length	trans Pd–Cl bond length
$\text{PH}_3$	2.066	2.043	2.357	2.010	2.284
$\text{PCl}_3$	2.061	2.034	2.327	2.010	2.268
$\text{PH}_2\text{CF}_3$	2.076	2.041	2.357	2.008	2.276
$\text{PH}_2\text{Et}$	2.071	2.048	2.368	2.012	2.293
$\text{PH}_2\text{Ph}$	2.069	2.050	2.364	2.015	2.291
$\text{PMeCl}_2$	2.065	2.034	2.352	2.011	2.277
$\text{PMe}_3$	2.076	2.053	2.384	2.019	2.304
$\text{PHEt}_2$	2.068	2.048	2.371	2.016	2.301
$\text{PEt}_3$	2.077	2.054	2.388	2.021	2.308
$\text{PPh}_3$	2.066	2.039	2.368	2.017	2.304

<sup>#</sup>Average of the two Pd–C bonds is taken.

It is well known that the electronic nature of phosphine ligands and the related trans influence play an important role in the rate of reductive eliminations [Ananikov *et al.* 2005]. To the best of our knowledge, a relationship between the  $E_{act}$  values of reductive eliminations and trans influence parameters has not been clearly addressed yet. Trans bond length parameters have been used as a structural parameter to quantify the trans influence. In general, short trans bond length indicates the weak trans influencing ancillary ligand while the strong trans influencing ancillary ligands cause an enhancement in the trans bond length. For the cases studied herein, the trans bond length parameters are presented in Table 3.2.

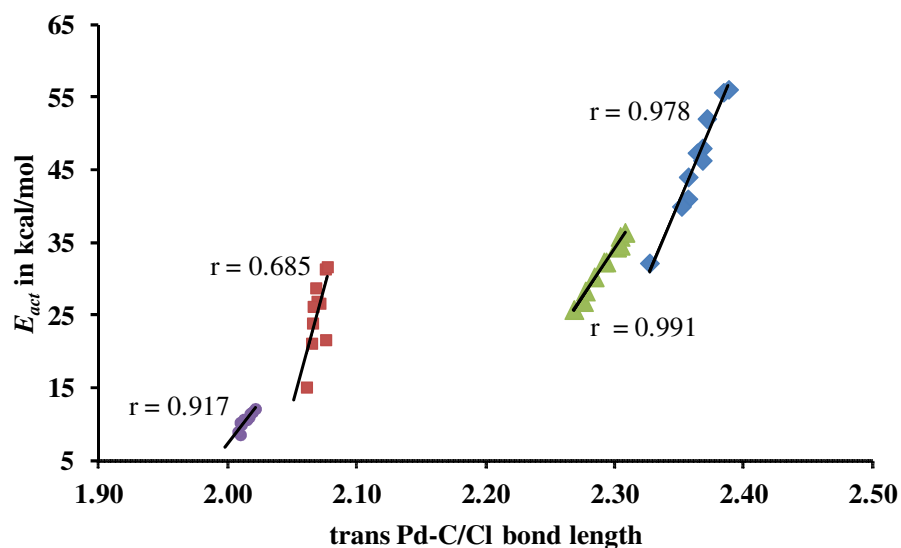


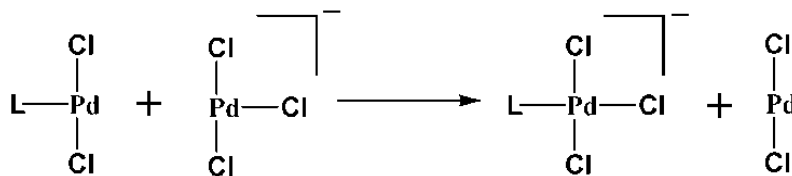
**Figure 3.3** Correlation between and trans Pd–C bond length and  $E_{act}$  for the reductive elimination of  $\text{CH}_3\text{CH}_3$  as well as correlation between trans Pd–Cl bond length and  $E_{act}$  for the reductive elimination of  $\text{CH}_3\text{Cl}$  ( $\blacklozenge$   $\text{CH}_3\text{Cl}$  direct,  $\blacksquare$   $\text{CH}_3\text{CH}_3$  direct,  $\blacktriangle$   $\text{CH}_3\text{Cl}$  dissociative,  $\bullet$   $\text{CH}_3\text{CH}_3$  dissociative mechanisms).

All the Pd–C bond lengths of both  $[\text{Pd}(\text{CH}_3)_2\text{L}_2]$  and  $[\text{Pd}(\text{CH}_3)_2\text{L}]$  complexes can be put in a small range 2.008 to 2.077 Å whereas the Pd–Cl bond length in both  $[\text{Pd}(\text{CH}_3)(\text{Cl})\text{L}_2]$  and  $[\text{Pd}(\text{CH}_3)(\text{Cl})\text{L}]$  show larger variation in the range of 2.268 to 2.388 Å. It means that

the Pd–Cl bond is very sensitive to the trans influence of the phosphine ligand than the Pd–C bond. A strong linear correlation between Pd–Cl distance and  $E_{act}$  supports this statement while the poor correlation between Pd–C distance and  $E_{act}$ , particularly observed for the direct mechanism justifies the insensitiveness of the distance parameter (Figure 3.3) to measure the trans influence. In general, all the four correlations given in Figure 3.3 suggest that the rate of reductive elimination increases when the trans influence of the ancillary ligand increases.

### 3.4.2 Trans Influence from Isodesmic Reactions

The isodesmic reaction based approach presented in Scheme 3.2 is used to quantify the trans influence of any ligand L. In this reaction, the reactant and product sides are nearly identical with respect to the type of metal to ligand bonds. The reactant and product sides differ mainly in the trans influence they experience; the product side has a trans influence from L on  $\text{Cl}^-$  while reactant side is devoid of such an influence. Therefore, the energy of this reaction (designated as  $E_L$ ) represents a good thermodynamic measure of the trans influence. The reaction is endothermic as the trans influence weakens both the Pd–L and the trans Pd–Cl bonds in the product side. The following trend in  $E_L$  values is obtained:  $\text{PEt}_3$  (29.86) >  $\text{PMe}_3$  (28.96) >  $\text{PHEt}_2$  (27.68) >  $\text{PPh}_3$  (27.07) >  $\text{PH}_2\text{Et}$  (25.39) >  $\text{PH}_2\text{Ph}$  (24.27) >  $\text{PH}_3$  (23.26) >  $\text{PMeCl}_2$  (20.37) >  $\text{PH}_2\text{CF}_3$  (19.45) >  $\text{PCl}_3$  (14.94) (values in parenthesis is  $E_L$  in kcal/mol). This order of trans influence is almost similar to the Pd–Cl bond length based order of trans influence.



**Scheme 3.2** Isodesmic reactions modeled to quantify the trans influence of the ligand L in Pd(II) complexes.

In Figure 3.4,  $E_L$  is correlated with the  $E_{act}$  values of both direct and dissociation pathways. It is gratifying that the correlation coefficient,  $r$  of all these linear plots is higher than 0.96. The slopes of the linear correlation for  $\text{CH}_3\text{Cl}$  direct mechanism,  $\text{CH}_3\text{CH}_3$  direct mechanism,  $\text{CH}_3\text{Cl}$  dissociative mechanism, and  $\text{CH}_3\text{CH}_3$  dissociative mechanism are 1.52, 1.05, 0.78, and 0.24, respectively, suggesting that  $E_{act}$  of  $\text{CH}_3\text{Cl}$  direct elimination is highly influenced by the trans influence while this influence has less impact on the  $\text{CH}_3\text{CH}_3$  dissociative elimination. The order of  $E_{act}$  corresponding to both direct and dissociative mechanism is in accordance with the  $E_L$  values of ancillary phosphine ligands. The ligand  $\text{PPh}_3$  shows some deviation from the linear plot for the direct mechanism which can be attributed to the steric effect of this ligand.

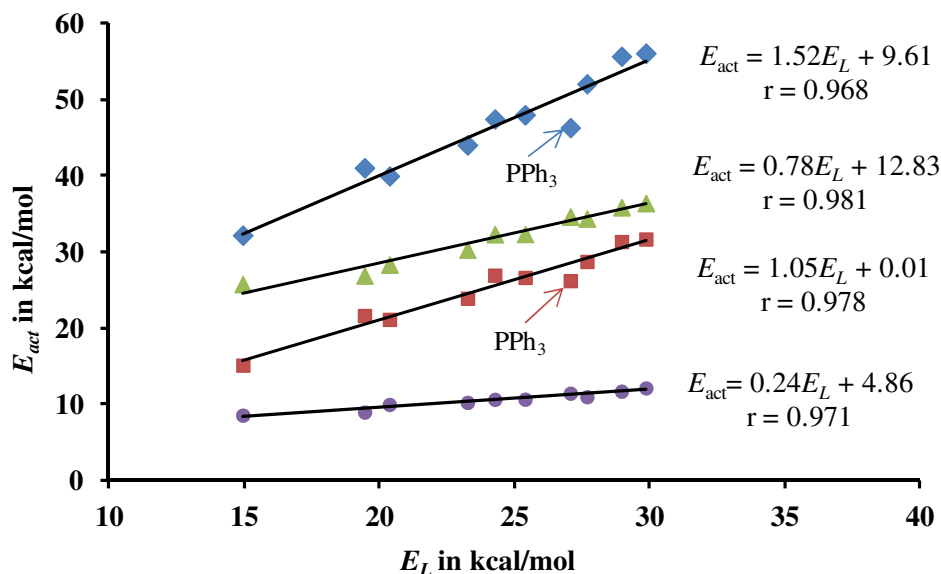


**Figure 3.4** Correlation between  $E_L$  and  $E_{act}$  values for the reductive elimination of  $\text{CH}_3\text{CH}_3$  and  $\text{CH}_3\text{Cl}$  via direct and dissociative mechanisms (◆  $\text{CH}_3\text{Cl}$  direct, ■  $\text{CH}_3\text{CH}_3$  direct, ▲  $\text{CH}_3\text{Cl}$  dissociative, ●  $\text{CH}_3\text{CH}_3$  dissociative mechanisms).

### 3.4.3 Molecular Electrostatic Potential Minimum ( $V_{min}$ ) of Free Phosphine Ligands

The trans influence originates from the competition between  $\sigma$ -donating ability of the trans ligands [Mitoraj *et al.* 2009; Anastasi and Deeth 2009]. Efforts from our laboratory have established that the use of the minimum of the molecular electrostatic potential (MESP), observed in the lone pair region of a phosphine ligand ( $V_{min}$ ) is a good parameter to assess the electronic effect of a free phosphine ligand [Suresh and Koga 2002; Suresh 2006; Mathew *et al.* 2007; Sternberg *et al.* 2010]. The MESP isosurface of value -9.0 kcal/mol and the  $V_{min}$  of all the phosphine ligands are depicted in Figure 3.5.  $\text{PEt}_3$  ligand has the most negative  $V_{min}$  (-45.11 kcal/mol) while the least negative  $V_{min}$  (-9.81 kcal/mol) is observed for  $\text{PMeCl}_2$ . For the unsubstituted  $\text{PH}_3$ , the  $V_{min}$  is -26.84 kcal/mol. The  $V_{min}$  reflects the impact of the electron donating or withdrawing effect of the P-substituent

[Suresh *et al.* 2007] and it is used as a good quantitative measure of  $\sigma$ -donating ability. A more negative  $V_{min}$  indicates higher  $\sigma$ -donating ability. In the case of  $\text{PCl}_3$ , the lone pair region of phosphorus is devoid of negative potential due to high electron withdrawing effect from the three chloro substituents. It is gratifying that the  $V_{min}$  values show almost the same order of trans influence based on either the trans Pd–Cl bond length or  $E_L$  values. Further, an excellent linear correlation is obtained between  $V_{min}$  and  $E_L$  values (Figure 3.6). It means that the trans influence of a  $\text{PR}_3$  ligand is directly related to the electron donating power of the ancillary ligand; more  $\sigma$ -donating group must show high trans influence and vice versa. Since  $E_L$  and  $E_{act}$  show a good linear correlation, the  $V_{min}$  can also be used as a good measure of the  $E_{act}$ . This also means that the reductive elimination will be inhibited substantially when the metal becomes more electron rich due to the enhancement in electron donating power of the phosphine ligand [Tatsumi *et al.* 1981].

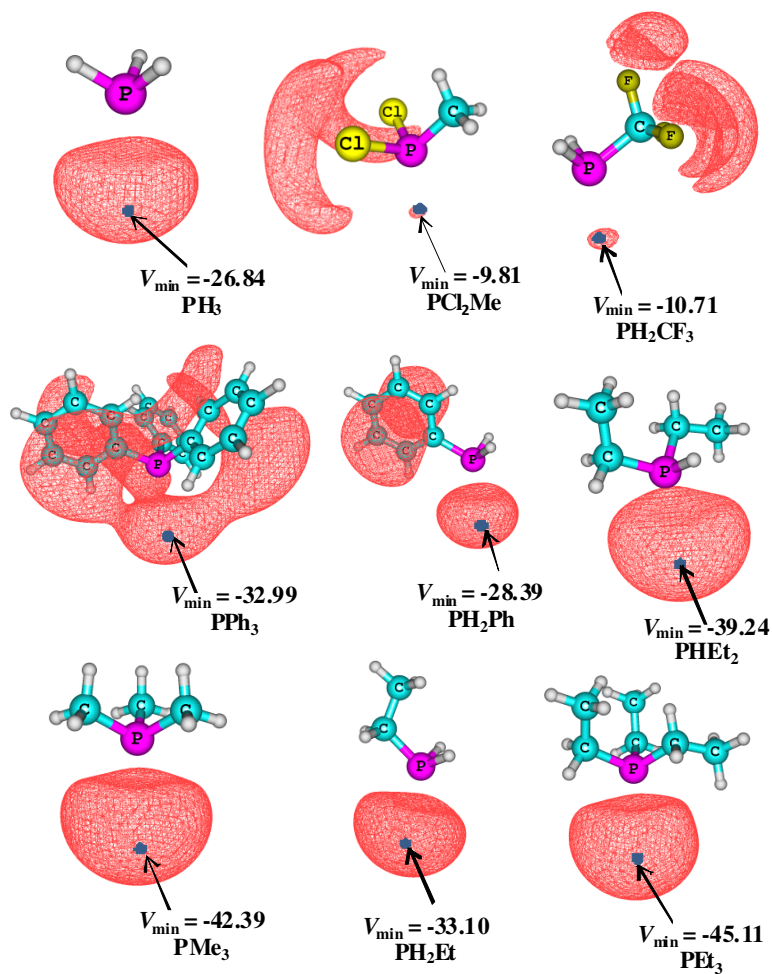


**Figure 3.5** MESP isosurface at  $-9.0$  kcal/mol for various phosphine ligands. The  $V_{\min}$  in kcal/mol is also depicted.

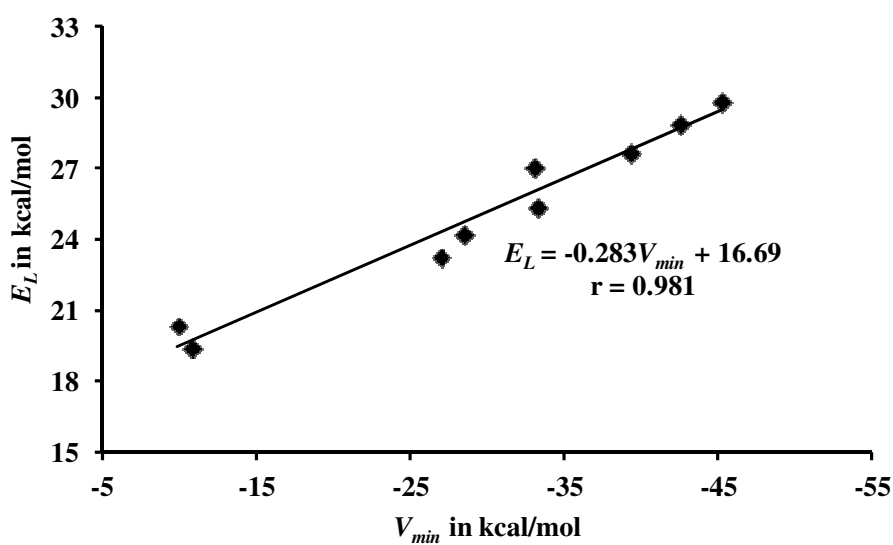
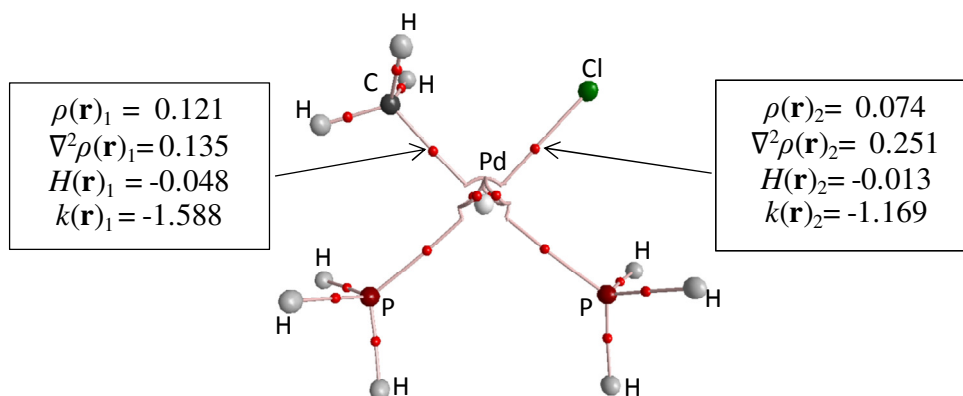


**Figure 3.6** Correlations between  $V_{\min}$  and  $E_L$  values.

### 3.4.4 AIM Analysis

The  $E_L$  or  $V_{min}$  values along with the steric effects of ancillary phosphine ligands can be used to explain the relative changes in the  $E_{act}$  values of reductive eliminations, irrespective of the direct and dissociative mechanism. However, these parameters are insufficient to explain the higher  $E_{act}$  values observed for  $\text{CH}_3\text{Cl}$  elimination than the  $\text{CH}_3\text{CH}_3$  elimination for a particular ancillary ligand. Further, these parameters alone cannot give a satisfactory explanation to why the  $E_{act}$  of the direct mechanism show higher values than the dissociative mechanism. It has been proposed that an increase in the  $\sigma$ -donating ability of the leaving groups increases the rate of reductive elimination [Tatsumi *et al.* 1981]. Therefore, knowledge about the nature of the eliminating bond is also important to assess the  $E_{act}$  and we propose to use the AIM analysis to understand this.

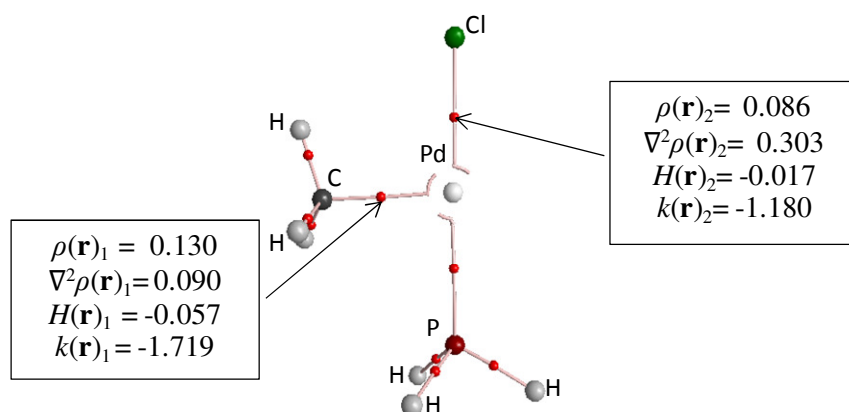
In Figure 3.7, AIM parameters,  $\rho(\mathbf{r})_1$ ,  $\nabla^2\rho(\mathbf{r})_1$ ,  $H(\mathbf{r})_1$ , and  $k(\mathbf{r})_1$  for Pd–C<sub>methyl</sub> bond and  $\rho(\mathbf{r})_2$ ,  $\nabla^2\rho(\mathbf{r})_2$ ,  $H(\mathbf{r})_2$ , and  $k(\mathbf{r})_2$  for Pd–Cl bond are depicted using the representative examples  $\text{Pd}(\text{CH}_3)(\text{Cl})(\text{PH}_3)_2$  and  $\text{Pd}(\text{CH}_3)(\text{Cl})(\text{PH}_3)$ . Since two bonds are cleaved at the same time during the reductive elimination, the total change in the AIM parameters can be assessed by taking the sum of their individual values and thus the parameters  $\rho(\mathbf{r})_s = \rho(\mathbf{r})_1 + \rho(\mathbf{r})_2$ ,  $\nabla^2\rho(\mathbf{r})_s = \nabla^2\rho(\mathbf{r})_1 + \nabla^2\rho(\mathbf{r})_2$ ,  $H(\mathbf{r})_s = H(\mathbf{r})_1 + H(\mathbf{r})_2$  and  $k(\mathbf{r})_s = k(\mathbf{r})_1 + k(\mathbf{r})_2$  are also defined. Detailed information of the AIM parameters are given in Tables 3.3, 3.4, 3.5, and 3.6.



$$\rho(\mathbf{r})_s = \rho(\mathbf{r})_1 + \rho(\mathbf{r})_2; \quad \nabla^2\rho(\mathbf{r})_s = \nabla^2\rho(\mathbf{r})_1 + \nabla^2\rho(\mathbf{r})_2$$

$$k(\mathbf{r})_s = k(\mathbf{r})_1 + k(\mathbf{r})_2; \quad H(\mathbf{r})_s = H(\mathbf{r})_1 + H(\mathbf{r})_2$$

(a)



$$\rho(\mathbf{r})_s = \rho(\mathbf{r})_1 + \rho(\mathbf{r})_2; \quad \nabla^2\rho(\mathbf{r})_s = \nabla^2\rho(\mathbf{r})_1 + \nabla^2\rho(\mathbf{r})_2$$

$$k(\mathbf{r})_s = k(\mathbf{r})_1 + k(\mathbf{r})_2; \quad H(\mathbf{r})_s = H(\mathbf{r})_1 + H(\mathbf{r})_2$$

(b)

**Figure 3.7** AIM features of representative (a)  $\text{Pd}(\text{CH}_3)(\text{Cl})\text{L}_2$  and (b)  $\text{Pd}(\text{CH}_3)(\text{Cl})\text{L}$  systems, where  $\text{L} = \text{PH}_3$ . The (3,-1) bond critical points are marked by small red circles. The  $\rho(\mathbf{r})$ ,  $\nabla^2\rho(\mathbf{r})$ ,  $H(\mathbf{r})$  (all values are in au) and  $k(\mathbf{r})$  at the bcp of the bonds that are cleaved during reductive elimination is marked along with the definitions of  $\rho(\mathbf{r})_s$ ,  $\nabla^2\rho(\mathbf{r})_s$ ,  $H(\mathbf{r})_s$  and  $k(\mathbf{r})_s$ .

**Table 3.3:** AIM parameters at the bcp of Pd–C<sub>methyl</sub> bond in Pd(CH<sub>3</sub>)<sub>2</sub>L<sub>2</sub> complexes.

Ancillary ligands	Pd–C <sup>#</sup> <sub>methyl</sub> bond					
	$\rho(\mathbf{r})$ (au)	$\nabla^2\rho(\mathbf{r})$ (au)	$H(\mathbf{r})$ (au)	$k(\mathbf{r})$	$G(\mathbf{r})$ (au)	$V(\mathbf{r})$ (au)
PH <sub>3</sub>	0.116	0.178	-0.043	-1.490	0.087	-0.130
PCl <sub>3</sub>	0.117	0.156	-0.045	-1.536	0.084	-0.129
PH <sub>2</sub> CF <sub>3</sub>	0.113	0.172	-0.042	-1.491	0.085	-0.126
PH <sub>2</sub> Et	0.114	0.183	-0.042	-1.476	0.087	-0.129
PH <sub>2</sub> Ph	0.115	0.183	-0.042	-1.479	0.088	-0.130
PMeCl <sub>2</sub>	0.116	0.166	-0.044	-1.514	0.085	-0.129
PMe <sub>3</sub>	0.113	0.192	-0.040	-1.457	0.089	-0.129
PHEt <sub>2</sub>	0.115	0.187	-0.042	-1.474	0.089	-0.131
PEt <sub>3</sub>	0.113	0.193	-0.040	-1.453	0.088	-0.129
PPh <sub>3</sub>	0.116	0.180	-0.043	-1.486	0.088	-0.130

<sup>#</sup>Average of the two Pd–C bonds is taken

**Table 3.4** AIM parameters at the bcp of trans Pd–C<sub>methyl</sub> and cis Pd–C<sub>methyl</sub> bonds in Pd(CH<sub>3</sub>)<sub>2</sub>L complexes.

Ancillary ligand	trans Pd–C <sub>methyl</sub> bond						cis Pd–C <sub>methyl</sub> bond					
	$\rho(\mathbf{r})$ (au)	$\nabla^2\rho(\mathbf{r})$ (au)	$H(\mathbf{r})$ (au)	$k(\mathbf{r})$	$G(\mathbf{r})$ (au)	$V(\mathbf{r})$ (au)	$\rho(\mathbf{r})$ (au)	$\nabla^2\rho(\mathbf{r})$ (au)	$H(\mathbf{r})$ (au)	$k(\mathbf{r})$	$G(\mathbf{r})$ (au)	$V(\mathbf{r})$ (au)
PH <sub>3</sub>	0.130	0.190	-0.052	-1.524	0.100	-0.152	0.126	0.152	-0.051	-1.575	0.089	-0.141
PCl <sub>3</sub>	0.129	0.180	-0.053	-1.540	0.098	-0.150	0.123	0.140	-0.050	-1.589	0.085	-0.135
PH <sub>2</sub> CF <sub>3</sub>	0.130	0.184	-0.053	-1.535	0.099	-0.152	0.124	0.150	-0.050	-1.574	0.088	-0.138
PH <sub>2</sub> Et	0.129	0.195	-0.052	-1.515	0.100	-0.152	0.126	0.152	-0.051	-1.575	0.090	-0.141
PH <sub>2</sub> Ph	0.128	0.193	-0.051	-1.514	0.100	-0.151	0.125	0.150	-0.051	-1.576	0.088	-0.139
PMeCl <sub>2</sub>	0.129	0.183	-0.053	-1.534	0.098	-0.151	0.123	0.150	-0.050	-1.571	0.088	-0.138
PMe <sub>3</sub>	0.127	0.200	-0.050	-1.501	0.100	-0.151	0.126	0.157	-0.051	-1.567	0.090	-0.142
PHEt <sub>2</sub>	0.128	0.199	-0.051	-1.505	0.101	-0.151	0.126	0.152	-0.052	-1.575	0.090	-0.141
PEt <sub>3</sub>	0.127	0.201	-0.050	-1.497	0.100	-0.150	0.126	0.157	-0.051	-1.567	0.091	-0.142
PPh <sub>3</sub>	0.128	0.198	-0.051	-1.506	0.100	-0.151	0.127	0.149	-0.052	-1.584	0.090	-0.142

**Table 3.5** AIM parameters at the bcp of Pd–C<sub>methyl</sub> and Pd–Cl bonds in Pd(CH<sub>3</sub>)(Cl)L<sub>2</sub> complexes.

Ancillary ligand	Pd–Cl bond						Pd–C <sub>methyl</sub> bond					
	$\rho(\mathbf{r})$ (au)	$\nabla^2\rho(\mathbf{r})$ (au)	$H(\mathbf{r})$ (au)	$k(\mathbf{r})$	$G(\mathbf{r})$ (au)	$V(\mathbf{r})$ (au)	$\rho(\mathbf{r})$ (au)	$\nabla^2\rho(\mathbf{r})$ (au)	$H(\mathbf{r})$ (au)	$k(\mathbf{r})$	$G(\mathbf{r})$ (au)	$V(\mathbf{r})$ (au)
PH <sub>3</sub>	0.074	0.251	-0.013	-1.169	0.075	-0.088	0.121	0.135	-0.048	-1.588	0.082	-0.130
PCl <sub>3</sub>	0.079	0.262	-0.015	-1.185	0.080	-0.095	0.123	0.103	-0.051	-1.665	0.077	-0.129

**Table 3.5 (Continued)**

PH <sub>2</sub> CF <sub>3</sub>	0.074	0.250	-0.013	-1.171	0.076	-0.088	0.122	0.123	-0.049	-1.616	0.080	-0.130
PH <sub>2</sub> Et	0.072	0.247	-0.012	-1.164	0.074	-0.086	0.119	0.143	-0.047	-1.568	0.082	-0.129
PH <sub>2</sub> Ph	0.072	0.251	-0.012	-1.164	0.075	-0.087	0.119	0.143	-0.047	-1.565	0.082	-0.129
PMeCl <sub>2</sub>	0.075	0.255	-0.013	-1.171	0.077	-0.090	0.123	0.112	-0.051	-1.647	0.079	-0.130
PMe <sub>3</sub>	0.069	0.243	-0.011	-1.154	0.072	-0.083	0.119	0.156	-0.045	-1.539	0.084	-0.130
PHEt <sub>2</sub>	0.070	0.248	-0.012	-1.164	0.074	-0.086	0.120	0.143	-0.047	-1.568	0.082	-0.129
PEt <sub>3</sub>	0.068	0.241	-0.011	-1.154	0.071	-0.082	0.118	0.160	-0.045	-1.529	0.085	-0.130
PPh <sub>3</sub>	0.072	0.251	-0.012	-1.162	0.075	-0.087	0.122	0.129	-0.049	-1.604	0.082	-0.131

**Table 3.6** AIM parameters at the bcp of Pd–C<sub>methyl</sub> and Pd–Cl bonds in Pd(CH<sub>3</sub>)(Cl)L complexes.

Ancillary ligand	Pd–Cl bond						Pd–C <sub>methyl</sub> bond					
	$\rho(r)$ (au)	$\nabla^2\rho(r)$ (au)	$H(r)$ (au)	$k(r)$	$G(r)$ (au)	$V(r)$ (au)	$\rho(r)$ (au)	$\nabla^2\rho(r)$ (au)	$H(r)$ (au)	$k(r)$	$G(r)$ (au)	$V(r)$ (au)
PH <sub>3</sub>	0.086	0.303	-0.017	-1.180	0.092	-0.109	0.130	0.090	-0.057	-1.719	0.080	-0.137
PCl <sub>3</sub>	0.089	0.309	-0.018	-1.191	0.095	-0.114	0.127	0.080	-0.056	-1.738	0.076	-0.133
PH <sub>2</sub> CF <sub>3</sub>	0.088	0.306	-0.017	-1.186	0.094	-0.111	0.129	0.083	-0.057	-1.732	0.078	-0.135
PH <sub>2</sub> Et	0.084	0.300	-0.016	-1.175	0.091	-0.107	0.131	0.094	-0.057	-1.709	0.081	-0.138
PH <sub>2</sub> Ph	0.084	0.301	-0.016	-1.176	0.091	-0.107	0.130	0.093	-0.057	-1.710	0.080	-0.137
PMeCl <sub>2</sub>	0.087	0.307	-0.017	-1.184	0.094	-0.111	0.128	0.082	-0.057	-1.735	0.077	-0.134
PMe <sub>3</sub>	0.082	0.296	-0.015	-1.169	0.089	-0.104	0.131	0.106	-0.057	-1.683	0.084	-0.141
PHEt <sub>2</sub>	0.082	0.297	-0.015	-1.170	0.090	-0.105	0.131	0.101	-0.057	-1.695	0.082	-0.140
PEt <sub>3</sub>	0.081	0.294	-0.015	-1.167	0.088	-0.103	0.131	0.108	-0.057	-1.678	0.084	-0.141
PPh <sub>3</sub>	0.082	0.296	-0.015	-1.170	0.089	-0.104	0.131	0.100	-0.057	-1.697	0.082	-0.140

The  $\rho(\mathbf{r})_1$  values of Pd–C<sub>methyl</sub> bond are in the range of 0.113 to 0.131 au while  $\rho(\mathbf{r})_2$  values of Pd–Cl bond are in the range of 0.068 to 0.089 au. In all the systems,  $\nabla^2\rho(\mathbf{r})$  values are positive (0.080 to 0.309 au) while the  $H(\mathbf{r})$  values are negative (-0.011 to -0.057 au). The positive  $\nabla^2\rho(\mathbf{r})$  indicates ionic nature of the bond whereas negative  $H(\mathbf{r})$  indicates the covalent nature [Bader and Matta 2001]. Thus it is clear that both Pd–C<sub>methyl</sub> and Pd–Cl bonds exhibit partial ionic and covalent characters [Bader and Matta 2001; Palusiak 2007; Palusiak and Krygowski 2009]. The  $\nabla^2\rho(\mathbf{r})$  of Pd–Cl bond (0.241 to 0.309 a.u.) is more positive than the  $\nabla^2\rho(\mathbf{r})$  of Pd–C<sub>methyl</sub> bond (0.080 to 0.201 au), indicating more ionic nature of the former. On the other hand,  $H(\mathbf{r})$  of Pd–Cl bond (-0.011 to -0.018 au) is less negative than the  $H(\mathbf{r})$  of Pd–C<sub>methyl</sub> bond (-0.040 to -0.057 au), suggesting more covalent nature to the latter. Also, the  $k(\mathbf{r})$  value of a Pd–C<sub>methyl</sub> bond is 0.37 to 0.55 au more negative than that of Pd–Cl bond which also means that the potential electron energy density is significantly higher than the kinetic electron energy density in Pd–C<sub>methyl</sub> than the Pd–Cl bond. The variation in the AIM parameters at the bcp of Pd–C<sub>methyl</sub>/Cl bond in Pd(CH<sub>3</sub>)<sub>2</sub>L<sub>2</sub>, Pd(CH<sub>3</sub>)<sub>2</sub>L, Pd(CH<sub>3</sub>)(Cl)L<sub>2</sub> and Pd(CH<sub>3</sub>)(Cl)L complexes is mainly due to the change in electron donating ability of the ancillary ligands. There is a decrease in magnitude of  $\rho(\mathbf{r})$ ,  $H(\mathbf{r})$  and  $k(\mathbf{r})$  values at the bcp of the trans Pd–C<sub>methyl</sub>/Cl bond when the  $\sigma$ -donating ability of ancillary ligand is increased while no such trend is observed in the case of  $\nabla^2\rho(\mathbf{r})$  values. In Pd(CH<sub>3</sub>)<sub>2</sub>L<sub>2</sub> complexes, for the least  $\sigma$ -donating ancillary ligand PCl<sub>3</sub>, the  $\rho(\mathbf{r})$ ,  $H(\mathbf{r})$ ,  $k(\mathbf{r})$  values at bcp of Pd–C<sub>methyl</sub> are 0.117 a.u., -0.045 au, -1.536 respectively while for the highest  $\sigma$ -donating ancillary ligand PEt<sub>3</sub>, these values are 0.113 au, -0.040 au and -1.453. Similar observations can also be noticed for other complexes, *viz.* Pd(CH<sub>3</sub>)<sub>2</sub>L, Pd(CH<sub>3</sub>)(Cl)L<sub>2</sub> and Pd(CH<sub>3</sub>)(Cl)L.

In Figure 3.8, correlation between  $\rho(\mathbf{r})_s$  and  $E_{act}$  is presented. In the case of direct and dissociative mechanisms of  $\text{CH}_3\text{Cl}$  elimination,  $E_{act}$  shows strong linear dependency to  $\rho(\mathbf{r})_s$ . However,  $E_{act}$  for  $\text{CH}_3\text{CH}_3$  elimination shows almost no correlation with  $\rho(\mathbf{r})_s$ . Interestingly, a general trend is that when  $\rho(\mathbf{r})_s$  decreases,  $E_{act}$  increases. Since higher value of  $\rho(\mathbf{r})_s$  indicates greater strength, one would expect more difficulty in breaking that bond. This observation is counter intuitive as a smaller value of  $\rho(\mathbf{r})_s$  can be associated with a weaker bond to be cleaved, indicating lowering of the activation barrier. Very similar observation is also applicable for the correlation of trans bond length versus  $E_{act}$  presented in Figure 3.3: a shorter bond is activated easily than a longer bond! It means that the metal ligand bond cleavage may not be the deciding factor for the reductive elimination but the bond formation between the dissociated ligands.

In Figure 3.9,  $H(\mathbf{r})_s$  values are plotted against the  $E_{act}$ . These plots look very similar to the  $(\rho(\mathbf{r})_s, E_{act})$  plots given in Figure 3.8. In general,  $E_{act}$  decreases with an increase in the negative character (covalent character) of the  $H(\mathbf{r})_s$ . Thus, obviously there is a fundamental difference in the interpretations that we can obtain from the  $(\rho(\mathbf{r})_s, E_{act})$  plots and  $(H(\mathbf{r})_s, E_{act})$  plots: it is not the bond strength that matters but the nature of the cleaved bonds, the more covalent they are the easier is the reductive elimination.

The correlations of  $\nabla^2\rho(\mathbf{r})_s$  versus  $E_{act}$  (Figure 3.10) nicely compliment the conclusion drawn from the plots of  $H(\mathbf{r})_s$  versus  $E_{act}$ : the more the ionic nature of the bond to be cleaved, the higher is the activation barrier for the reductive elimination. Thus, the formation of  $\text{CH}_3\text{CH}_3$  is quite easy compared to the formation of  $\text{CH}_3\text{Cl}$  due to the more ionic nature of  $\text{Pd}-\text{Cl}$  bond. Even though the  $\text{Pd}-\text{C}_{\text{methyl}}$  bond is stronger than the  $\text{Pd}-\text{Cl}$  bond, the two cleaved methyl fragments with the  $\bullet\text{CH}_3$  nature is easy to combine for the  $\text{C}-\text{C}$  bond formation.

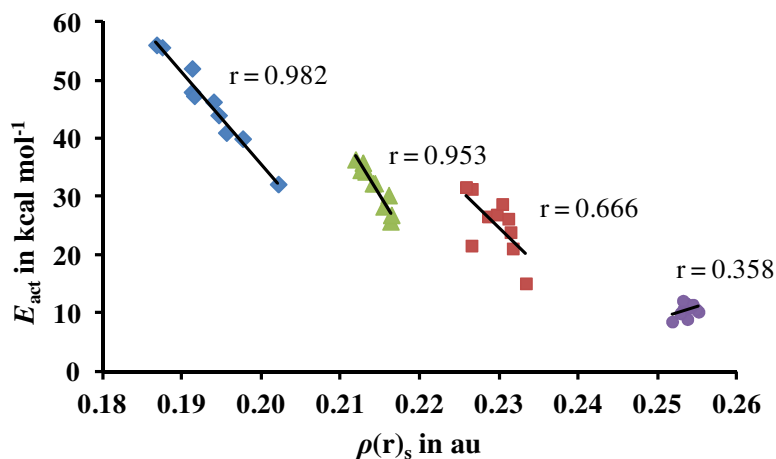


**Figure 3.8** Correlation between  $\rho(\mathbf{r})_s$  and  $E_{\text{act}}$  values ( $\blacklozenge$   $\text{CH}_3\text{Cl}$  direct,  $\blacksquare$   $\text{CH}_3\text{CH}_3$  direct,  $\blacktriangle$   $\text{CH}_3\text{Cl}$  dissociative,  $\bullet$   $\text{CH}_3\text{CH}_3$  dissociative mechanisms).

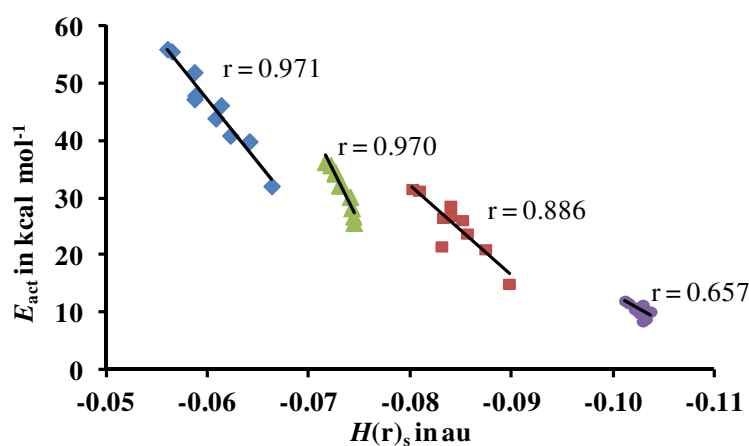


**Figure 3.9** Correlation between  $H(\mathbf{r})_s$  and  $E_{\text{act}}$  values ( $\blacklozenge$   $\text{CH}_3\text{Cl}$  direct,  $\blacksquare$   $\text{CH}_3\text{CH}_3$  direct,  $\blacktriangle$   $\text{CH}_3\text{Cl}$  dissociative,  $\bullet$   $\text{CH}_3\text{CH}_3$  dissociative mechanisms).

The plot of  $k(\mathbf{r})_s$  versus the  $E_{\text{act}}$  (Figure 3.11) shows a unified picture of the nature of chemical bond to the tendency of reductive elimination: irrespective of the type of reaction (elimination of either  $\text{CH}_3\text{CH}_3$  or  $\text{CH}_3\text{Cl}$ ) and the type of the mechanism (direct or dissociative), all the  $E_{\text{act}}$  values can be correlated with one linear equation. In other words, when the potential electron energy density dominates over the kinetic electron energy density at the bcp, reductive elimination becomes facile. This may

show that a bond with more covalent character has more potential electron energy density while a bond with more ionic character has more kinetic electron energy density and vice versa, if the covalent character of the bonds can be well estimated through  $k(\mathbf{r})_s$ . It can be assumed that the interplay between the covalent and ionic nature of the bonds which are cleaved during reaction is the controlling factor for the reductive elimination.

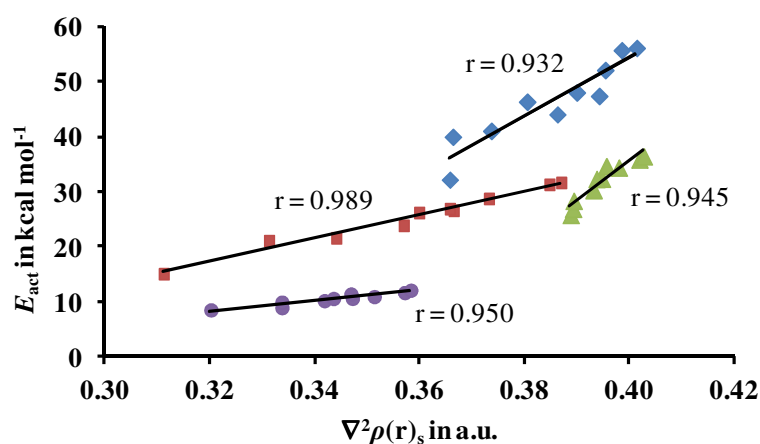


**Figure 3.10** Correlation between  $\nabla^2\rho(\mathbf{r})_s$  and  $E_{\text{act}}$  values ( $\blacklozenge$   $\text{CH}_3\text{Cl}$  direct,  $\blacksquare$   $\text{CH}_3\text{CH}_3$  direct,  $\blacktriangle$   $\text{CH}_3\text{Cl}$  dissociative,  $\bullet$   $\text{CH}_3\text{CH}_3$  dissociative mechanisms).

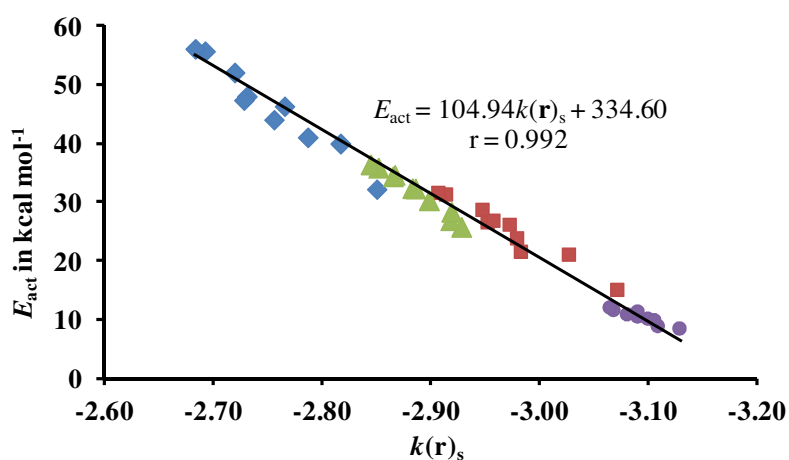


**Figure 3.11** Correlation between  $k(\mathbf{r})_s$  and  $E_{\text{act}}$  values ( $\blacklozenge$   $\text{CH}_3\text{Cl}$  direct,  $\blacksquare$   $\text{CH}_3\text{CH}_3$  direct,  $\blacktriangle$   $\text{CH}_3\text{Cl}$  dissociative,  $\bullet$   $\text{CH}_3\text{CH}_3$  dissociative mechanisms).

It may also be noted that  $\rho(\mathbf{r})_s$  values for the less electron donating phosphine ligand is higher particularly for four coordinate reactant complexes. Similar observations can also be noted for  $H(\mathbf{r})_s$  and  $k(\mathbf{r})_s$  values. Thus, when the  $\sigma$ -donating ability of the ancillary ligand decreases, an increase in the strength and covalent nature of trans bond is observed. Also,  $\nabla^2\rho(\mathbf{r})_s$  value is found to be higher for electron rich ancillary ligands and this shows more ionic character to the trans bond when such ancillary ligands are present. The nature of ancillary ligands controls the strength and covalent nature of the trans Pd–C/Cl bond and also controls the activation process for the reductive elimination.

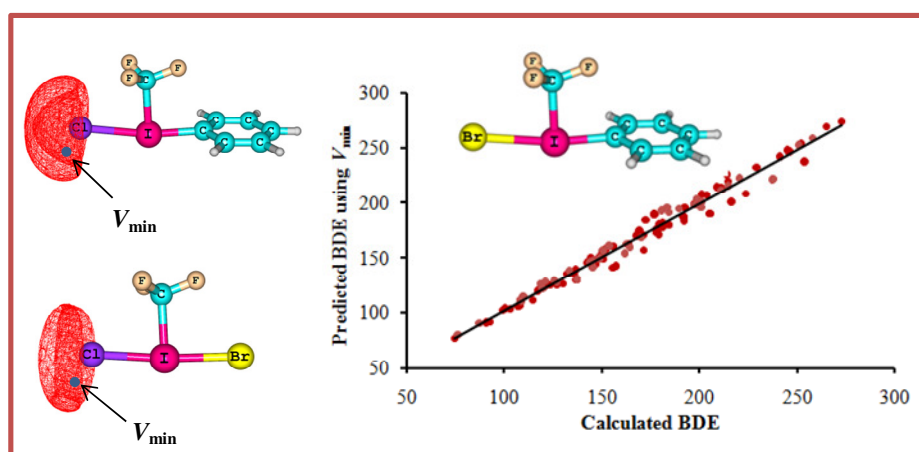
### 3.5 Conclusion

The present work has focused on the effect of ancillary phosphine ligands on C–C and C–Cl bond formation through reductive elimination mechanism in square planar complexes of the type  $\text{cis-}[\text{Pd}(\text{CH}_3)_2\text{L}_2]$  and  $\text{cis-}[\text{Pd}(\text{CH}_3)(\text{Cl})\text{L}_2]$ , where L is the ancillary phosphine ligand. The results show that the  $E_{\text{act}}$  of reductive elimination reactions are directly controlled by the  $\sigma$ -donating ability of the ancillary phosphine ligands [Hartley 1973; Lin and Hall 1991]. For bulky phosphine ligands, the steric effect was also significant. The isodesmic reaction energy based trans influence parameter  $E_L$  showed a strong linear relationship to  $V_{\text{min}}$  values of the ancillary phosphine ligands, suggesting that the trans influence is governed by the electron donating character of the phosphine ligand [MacQueen and Macgregor 1999; Anastasi and Deeth 2009; Goodman *et al.* 2010]. Both  $E_L$  and  $V_{\text{min}}$  can be used as very effective descriptors to measure the ability of the metal complex to undergo reductive elimination as both quantities showed excellent linear relationship to  $E_{\text{act}}$ . Between  $E_L$

and the  $V_{\min}$ , the latter is easy to compute as it involves the determination of the MESP of the free phosphine while the former is calculated from a reaction scheme.

AIM analysis of the reactant complexes suggests that when the covalent nature of the Pd-leaving group/atom bond increases, the energy of activation for the reductive elimination decreases and vice versa. The trans bond length analysis or the bond strength analysis using  $\rho(\mathbf{r})_s$  gives only a false impression that reductive elimination becomes easy with strong metal-ligand bonds. In fact, the correct interpretation of the reductive elimination can be obtained from the study of the ionic versus covalent nature of the bonds that are cleaved and this important conclusion is obtained by the analysis of  $\nabla^2\rho(\mathbf{r})_s$  and  $H(\mathbf{r})_s$ . Further, the  $k(\mathbf{r})_s$  in the AIM analysis showed that the relative magnitude of the potential electron energy density and kinetic electron energy density at the bcp of the bonds that are cleaved in the reductive elimination is a key factor for determining the activation energy and using this parameter, a unified view of the process can be obtained irrespective of the type of reaction and nature of the mechanism. Further, AIM analysis showed that the strength and covalent character of the Pd-CH<sub>3</sub>/Cl bond depend on the electronic nature of the ancillary ligands. In general, an electron withdrawing ancillary ligand increases the strength of the trans bond by increasing its covalent character. Since bonds with more covalent character are more susceptible for reductive elimination than bonds with more ionic character, an electron withdrawing ligand will promote reductive elimination reaction more than an electron rich ligand. It may be noted that these conclusions are based on the effect of ancillary phosphine ligands on the activation of reductive elimination reactions and no attempt has been made to generalize them for other ligands.

# Quantification of the Trans Influence in Hypervalent Iodine Complexes



## 4.1 Abstract

*The trans influence of various X ligands in hypervalent iodine (III) complexes of the type  $CF_3[I(X)Cl]$  has been quantified using trans I–Cl bond length ( $d_X$ ), electron density  $\rho(\mathbf{r})$  at the (3, -1) bond critical point of the trans I–Cl bond and topological features of molecular electrostatic potential (MESP). The MESP minimum at the Cl lone pair region ( $V_{min}$ ) is a sensitive measure of the trans influence. Trans influence of X ligands in hypervalent iodine (V) complexes is smaller than that in iodine (III) complexes while the relative ordering of this influence is same in both the complexes. In  $CF_3[I(X)Y]$  complexes, the mutual trans influence due to trans disposition of X and Y ligands is quantified using the energy,  $E_{XY}$  of the isodesmic reaction  $CF_3[I(X)Cl] + CF_3[I(Y)Cl] \rightarrow CF_3[I(Cl)Cl] + CF_3[I(X)Y]$ .  $E_{XY}$  is predicted with good accuracy using the trans influence parameters of X and Y, measured in terms of  $d_X$ ,  $\rho(\mathbf{r})$  or  $V_{min}$ . The bond dissociation energy ( $D_{2X}$ ) of X or Y in  $CF_3[I(X)Y]$  is significantly influenced by the trans influence as well as mutual trans influence. This is confirmed by deriving an empirical equation to predict BDE using one of the trans influence parameters ( $d_X$ ,  $\rho(\mathbf{r})$  or  $V_{min}$ ) and the mutual trans influence parameter,  $E_{XY}$  for a large number of complexes. The quantified values of both trans influence and mutual trans influence parameters may find use in assessing the stability of hypervalent iodine compounds as well as in the design of new stable hypervalent complexes. The knowledge about the I–X bond dissociation energies will be useful for explaining the reactivity of hypervalent iodine complexes and mechanism of their reactions.*

## 4.2 Introduction

Hypervalent iodine compounds have received considerable attention as versatile oxidizing agents in organic synthesis [Barton *et al.* 1982; Varvoglis 1992; Ochiai 1999; Ochiai 2003; Moriarty and Prakash 2008; Brand *et al.* 2011; Zhdankin 2011]. These compounds are considered as an alternative for the highly toxic heavy metal oxidants often used to achieve similar chemical transformations [Ochiai 2003; Tohma and Kita 2004; Ochiai 2007; Zhdankin and Stang 2008; Merritt and Olofsson 2011]. Hypervalent iodine complexes are environmental friendly reagents, mild and stable, low toxic, and highly selective reagents [Varvoglis 1992; Ochiai 1999; Ochiai *et al.* 2005; Yu *et al.* 2012].

The first hypervalent organic iodine complex was dichloriodobenzene Ph[ICl<sub>2</sub>], which was prepared by Willgerodt in 1886 [Willgerodt and Prakt 1886]. Though the oxidizing property of this complex was recognized in 1893 [Zhdankin and Stang 2008], hypervalent iodine complexes reached out into main stream organic synthesis only in the last 30 years [Zhao and Zhang 2007; <sup>a</sup>Cui *et al.* 2011; <sup>b</sup>Cui *et al.* 2011]. Hypervalent iodine complexes are usually designated in terms of Martin-Arduengo N-I-L designation [Perkins *et al.* 1980], where N indicates the number of valence electrons surrounding the central iodine atom and L shows the number of ligands. The compounds 8-I-2 and 10-I-3 are called  $\lambda^3$ -iodanes wherein the iodine atom is having +3 oxidation states while the complexes 10-I-4 and 12-I-5 represent the most common structural types of pentavalent iodine and are called  $\lambda^5$ -iodanes. Some of the representative examples of these types of complexes and their structures are shown in Figure 4.1.

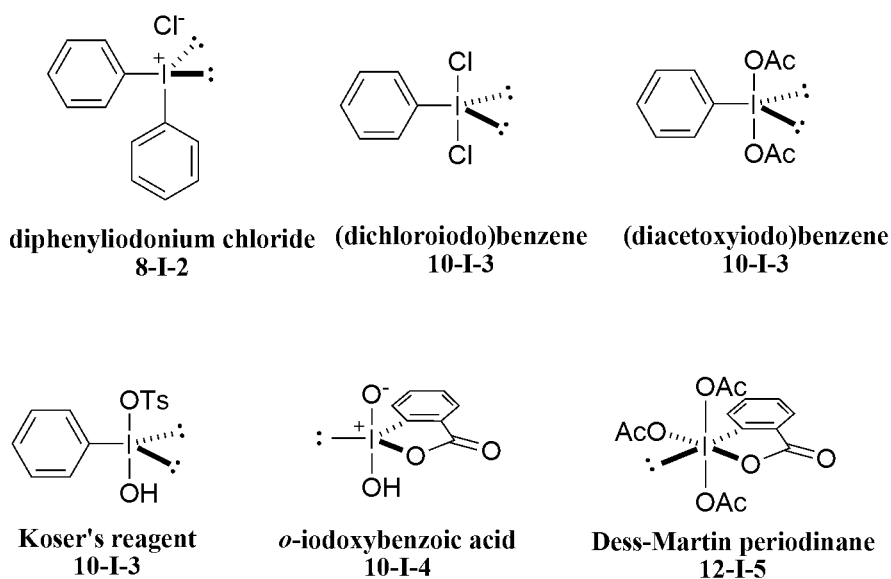


**Figure 4.1** Examples of  $\lambda^3$ -iodanes and  $\lambda^5$ -iodanes.

One of the characteristic features which distinguish hypervalent compound from others is the presence of 3-centre 4-electron (3c-4e) bond formed by the interaction of orbitals of three collinear atoms [Musher 1969]. In T-shaped iodine(III) complexes, the interaction of the filled 5p orbital of central iodine atom and the half-filled orbitals of two ligands (X and Y) trans to each other leads to the formation of three molecular orbitals, *viz.* bonding, nonbonding and antibonding (Figure 4.2) [Pimentel 1951; Musher 1969; Kutzelnigg 1984; Landrum *et al.* 1997; Su and Goddard 2005]. Because the highest occupied molecular orbital (HOMO) contains a node at the central iodine, the hypervalent bonds show highly polarised nature and hence more electronegative atoms tend to occupy the axial positions [Varvoglis 1992; Ochiai 1999; Kiprof and Zhdankin 2003; Yusubov *et al.* 2009].

The focus of the present study is to understand the phenomenon trans influence in hypervalent iodine complexes. In T-shaped iodine(III) complexes, the  $\sigma$  donating ability of ligand Y will influence the trans I–X bond through the 5p orbital of central iodine and hence the mutual trans influence caused through the 3c-4e bond is solely resulted from

the inductive effect of the trans ligands X and Y [Shustorovich and Buslaev 1976]. Ochiai *et al.* analysed various crystal structures of iodine(III) complexes and classified various ligands in the order of their trans influence and concluded that the mutual trans influence of ligands play an important role in the stability of these complexes [Ochiai *et al.* 2006]. On the basis of theoretical investigations using isodesmic reactions, Ochiai *et al.* proposed that the ligands with large and small trans influence in the axial positions are favoured over the combinations of two strong and two weak ligands in the trans positions, otherwise two moderately trans influencing ligands are favoured [Ochiai *et al.* 2006]. Thus, the phenomenon of trans influence can explain the stability of Ph[I(OH)OTs] and Ph[I(OAc)<sub>2</sub>] complexes as well as the instability of Ph[I(OH)<sub>2</sub>], Ph[I(OOtBu)<sub>2</sub>] and Ph[I(OMe)<sub>2</sub>] complexes [Zhdankin and Stang 2008].

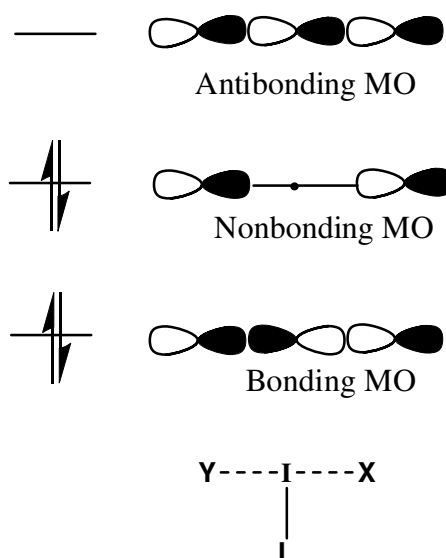


**Figure 4.2** MOs of the 3c-4e bond formed in the hypervalent iodine(III) complexes.

Trans bond length data from X-ray crystal structures are frequently used for the study of trans influence of various ligands [Hartley 1973]. Structural parameters are not very sensitive to subtle electronic variations and theoretically derived molecular properties have been used as powerful descriptors for explaining reactivity and stabilities of

hypervalent complexes [Kiprof 2004; Ochiai *et al.* 2006]. In the present study, trans influence of various ligands in hypervalent iodine complexes of the type  $\text{CF}_3[\text{I}(\text{X})\text{Cl}]$  is considered. The selected X ligands are F, Cl, Br,  $\text{CPh}_3\text{COOMe}$ ,  $\text{CPh}_3\text{COMe}$ , Et, Ph, Me, *OiPr*,  $\text{CCSiMe}_3$ ,  $\text{CH}_2\text{Cl}$ , CCH, CPh,  $\text{C}_6\text{F}_5$ ,  $\text{CF}_3$ , 2,3,5,6-tetrafluoro-4-(trifluoromethyl)benzene,  $\text{CF}_2\text{CF}_2\text{CF}_3$ ,  $\text{NH}_2$ , OMe, NHTf, *OOtBu*, OH, OAc,  $\text{NO}_2$ ,  $\text{OCOCOOMe}$ , OTs,  $\text{OSO}_2\text{Me}$ ,  $\text{OCOCCL}_3$ ,  $\text{NO}_3$ ,  $\text{OCOCF}_3$ , OTf and  $\text{BF}_4$ . Most of the selected ligands are located from the X-ray crystal structure of various hypervalent iodine complexes, retrieved from Cambridge Structural Database (CSD) [Allen 2002]. The trans influence will be analyzed using the QTAIM approach [Bader 1990]. Further, the subtle electronic variations surrounding the coordinated ligands due to 3c-4e bond will be analysed in terms of molecular electrostatic potential (MESP) [Politzer and Truhlar 1981].

### 4.3 Computational Methods

All the electronic structure calculations were performed at B3LYP [Becke 1993; Lee *et al.* 1994] level of DFT method using Gaussian 03 package of programs [Frisch *et al.* Gaussian 03 2004]. It has been proposed that all electron basis set correctly reproduce the bond length in iodine compounds [Yurieva *et al.* 2008] and hence full electron basis set DGDZVP [Sosa *et al.* 1992] was chosen to describe iodine atom and for all other atoms the basis set 6-311++G(d,p) was selected. The combined basis set is denoted as BS1. Vibrational frequency analysis at B3LYP/BS1 was performed to confirm that all the optimised geometries are minima (zero imaginary frequencies).

The B3LYP/BS1 level of theory was used for the calculation of molecular electrostatic potential (MESP). The deepest MESP minimum ( $V_{\text{min}}$ ) was obtained from the MESP topography calculations by generating cube files using Gaussian 03 [Suresh 2006; Sayyed and Suresh 2009].

For topological analysis of electron density, B3LYP/BS1 wave functions was used as input in AIM2000 program [Bader 1990; Biegler-König *et al.* 2001]. The AIM parameters such as electron density  $\rho(\mathbf{r})$ , the Laplacian of the electron density  $\nabla^2\rho(\mathbf{r})$ , the total electron energy density  $H(\mathbf{r})$  and its components potential electron energy density  $V(\mathbf{r})$  and kinetic electron energy density  $G(\mathbf{r})$  were calculated at the (3,-1) bond critical point (bcp) of the trans I–Cl bonds in  $\text{CF}_3[\text{I}(\text{X})\text{Cl}]$  complexes.

## 4.4 Results and Discussion

### 4.4.1 Trans Influence from Trans Bond Length

The T-shaped  $\text{CF}_3[\text{I}(\text{X})(\text{Y})]$  systems are the simplest stable hypervalent systems showing 3c-4e bond [Minkwitz *et al.* 2000]. The crystal structure of many such complexes with highly electronegative atoms at the axial positions have been reported [Minkwitz and Berkei 1998; Minkwitz and Berkei 1999]. The  $\text{CF}_3[\text{I}(\text{X})\text{Cl}]$  complexes are modeled in such a way that the apical positions of the T-shaped structure are occupied by the ligands Cl and X. The optimized structures of representative set of  $\text{CF}_3[\text{I}(\text{X})\text{Cl}]$  complexes are given in Figure 4.3. The trans I–Cl distance ( $d_X$ ) for 32 complexes are given in Table 4.1. Short  $d_X$  shows weak trans influencing X ligand while long  $d_X$  shows strong trans influencing X ligand which means that  $\text{BF}_4$  has the lowest trans influence ( $d_X = 2.440\text{Å}$ ) while  $\text{C}(\text{PPh}_3)\text{COMe}$  has the highest ( $d_X = 2.740\text{Å}$ ) trans influence. On the basis of  $d_X$  values, the following order of trans influence is obtained.

$\text{CPh}_3\text{COOMe} \sim \text{CPh}_3\text{COMe} > \text{Et} \sim \text{Ph} > \text{Me} > \text{CCPh} \sim \text{CCSiMe}_3 > \text{CH}_2\text{Cl} \sim \text{NH}_2 >$   
 $\text{CCH} > \text{C}_6\text{F}_5 > \text{CF}_3 \sim 2,3,5,6\text{-tetrafluoro-4-(trifluoromethyl)benzene} \sim \text{CF}_2\text{CF}_2\text{CF}_3 \sim$   
 $\text{OiPr} > \text{OMe} \sim \text{OOiBu} > \text{OH} > \text{Br} \sim \text{OAc} > \text{NO}_2 \sim \text{Cl} > \text{NHTf} > \text{OCOCOOMe} \sim \text{F} >$   
 $\text{OTs} \sim \text{OSO}_2\text{Me} > \text{OCOCCl}_3 > \text{NO}_3 \sim \text{OCOCF}_3 > \text{OTf} > \text{BF}_4 \quad \dots(\text{i})$

This order of trans influence given in series (i) is almost similar to the experimentally reported order for hypervalent iodine complexes [Ochiai *et al.* 2006]. Some minor deviations are noted because the experimental values are also affected by packing forces and interactions from the ligands in the neighboring molecules.

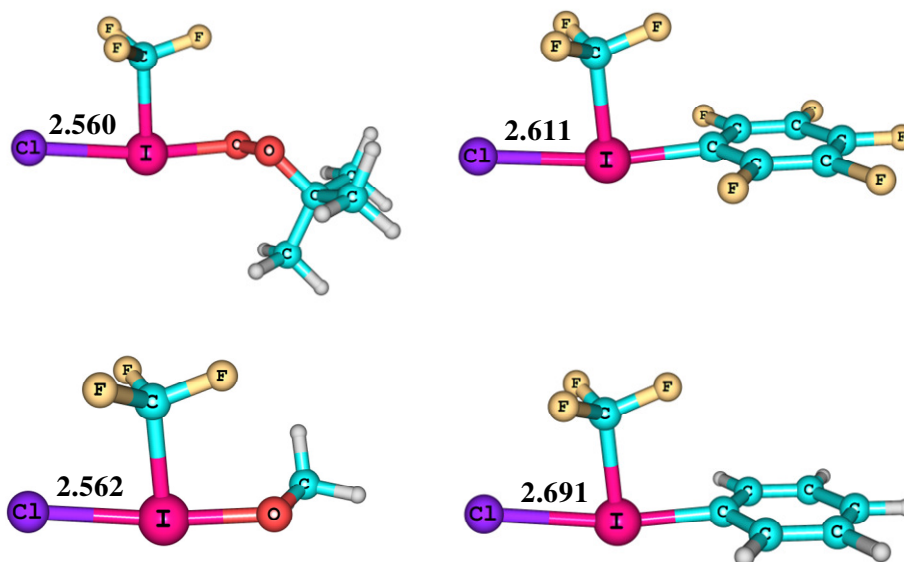


**Figure 4.3** Optimised structures of  $\text{CF}_3[\text{I}(\text{X})\text{Cl}]$  complexes ( $\text{X} = \text{OOtBu}, \text{C}_6\text{F}_5, \text{OMe}, \text{Ph}$ ). Trans bond length in  $\text{\AA}$  are also shown.

#### 4.4.2 Quantification of Trans Influence Using $\rho(\mathbf{r})$ Values

The QTAIM parameters, viz. the electron density ( $\rho(\mathbf{r})$ ), the Laplacian of electron density ( $\nabla^2\rho(\mathbf{r})$ ), total electron energy density ( $H(\mathbf{r})$ ), and ratio of potential and kinetic electron energy density ( $k(\mathbf{r})$ ) at the bond critical point (bcp) of trans I–Cl bond are reported in the Table 4.1. QTAIM topological plots of four representative examples of  $\text{CF}_3[\text{I}(\text{X})\text{Cl}]$  complexes are given in the Figure 4.4. A long trans I–Cl bond, indicative of strong trans influence of X is observed with small  $\rho(\mathbf{r})$  value while a short I–Cl bond, indicative of weak trans influence of X is seen with high  $\rho(\mathbf{r})$  value. For instance, the  $\text{CPhPh}_3\text{COMe}$  ligand showed the lowest  $\rho(\mathbf{r})$  (0.048 a.u.) while  $\text{BF}_4$  ligand exhibited the

highest  $\rho(\mathbf{r})$  (0.082 a.u.). The  $\rho(\mathbf{r})$ , often used as an indicator of the strength of a bond [Bader 1990; Szatyłowicz *et al.* 2008], shows a strong linear correlation with the trans bond length data (Figure 4.5), thus suggesting the use of this quantity as an electronic parameter to measure the trans influence.

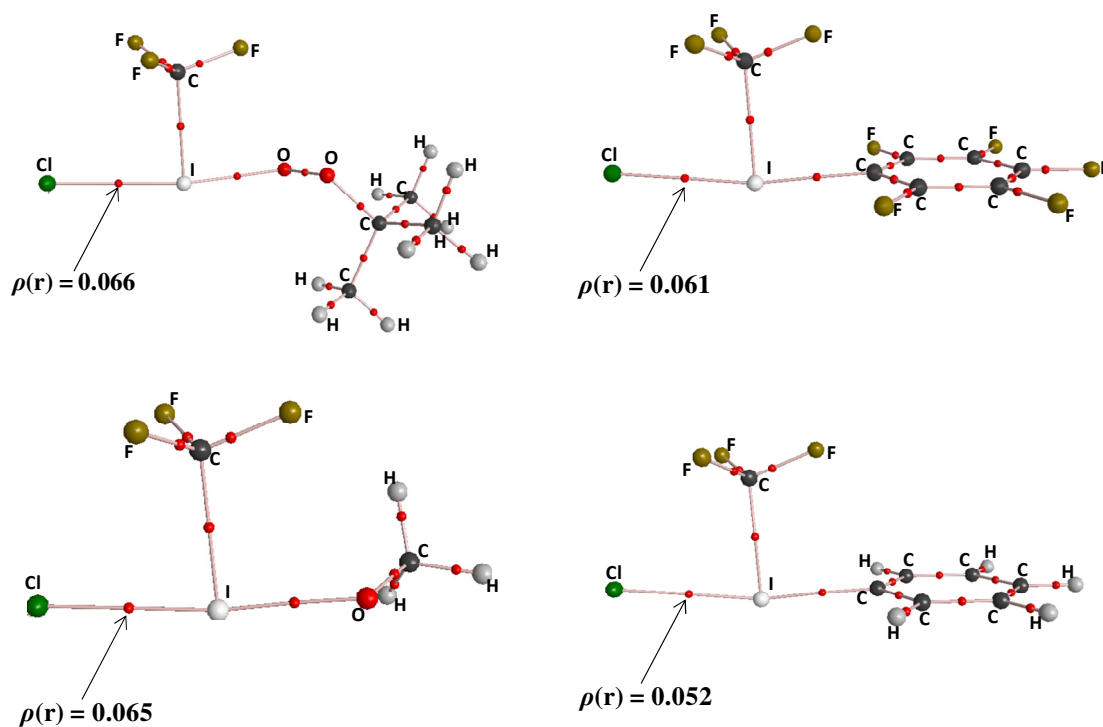


**Figure 4.4** AIM topological plot of  $\text{CF}_3[\text{I}(\text{X})\text{Cl}]$  complexes with  $\text{X} = \text{OOtBu}$ ,  $\text{C}_6\text{F}_5$ ,  $\text{OMe}$  and  $\text{Ph}$ . Big circles correspond to attractors (atomic nuclei) and small red circles indicate bond critical points. The  $\rho(\mathbf{r})$  in au at bond critical point of I-Cl bond is also shown.

**Table 4.1** QTAIM parameters at the (3,-1) bond critical points of trans I–Cl bond in  $\text{CF}_3[\text{I}(\text{X})\text{Cl}]$  complexes along with the trans I–Cl bond length.

Sl. No.	trans ligand X	trans I–Cl bond length $d_X$ (Å)	AIM parameters			
			$\rho(\mathbf{r})$ (au)	$\nabla^2\rho(\mathbf{r})$ (au)	$H(\mathbf{r})$ (au)	$k(\mathbf{r})$
1	C(PPh <sub>3</sub> )COMe	2.740	0.048	0.075	-0.007	-1.279
2	C(PPh <sub>3</sub> )COOMe	2.738	0.048	0.075	-0.007	-1.279
3	Et	2.709	0.051	0.075	-0.008	-1.304
4	Ph	2.691	0.052	0.076	-0.009	-1.323
5	Me	2.690	0.052	0.076	-0.009	-1.318
6	CH <sub>2</sub> Cl	2.647	0.057	0.077	-0.011	-1.360
7	CCPh	2.627	0.058	0.079	-0.012	-1.380
8	CCSiMe <sub>3</sub>	2.624	0.059	0.079	-0.012	-1.383
9	NH <sub>2</sub>	2.622	0.059	0.077	-0.012	-1.390
10	CF <sub>3</sub> CF <sub>2</sub> CF <sub>2</sub>	2.613	0.060	0.077	-0.013	-1.395
11	CF <sub>3</sub>	2.612	0.061	0.077	-0.013	-1.398
12	C <sub>6</sub> F <sub>5</sub>	2.611	0.061	0.077	-0.013	-1.405
13	CCH	2.609	0.060	0.079	-0.013	-1.400
14	C <sub>6</sub> F <sub>4</sub> (CF <sub>3</sub> ) <sup>#</sup>	2.602	0.062	0.077	-0.014	-1.415
15	O <i>i</i> Pr	2.571	0.065	0.077	-0.015	-1.446
16	NO <sub>2</sub>	2.568	0.066	0.074	-0.015	-1.450
17	OMe	2.562	0.065	0.077	-0.016	-1.454
18	Br	2.560	0.066	0.078	-0.015	-1.431
19	OO <i>t</i> Bu	2.560	0.066	0.076	-0.016	-1.457
20	OH	2.551	0.067	0.077	-0.017	-1.466
21	Cl	2.537	0.068	0.079	-0.016	-1.454
22	NHTf	2.525	0.071	0.076	-0.018	-1.492
23	OCOMe	2.521	0.071	0.078	-0.018	-1.483
24	OCOCOOMe	2.517	0.072	0.075	-0.019	-1.498
25	F	2.500	0.073	0.076	-0.020	-1.518
26	OTs	2.499	0.074	0.075	-0.020	-1.518
27	OCOCCl <sub>3</sub>	2.498	0.074	0.075	-0.020	-1.520
28	OSO <sub>2</sub> Me	2.497	0.074	0.075	-0.020	-1.521
29	OCOCF <sub>3</sub>	2.496	0.074	0.074	-0.020	-1.523
30	NO <sub>3</sub>	2.495	0.074	0.074	-0.021	-1.529
31	OTf	2.465	0.078	0.073	-0.023	-1.558
32	BF <sub>4</sub>	2.440	0.082	0.071	-0.025	-1.588

<sup>#</sup> 2,3,5,6- tetrafluro-4-(trifluoromethyl)benzene

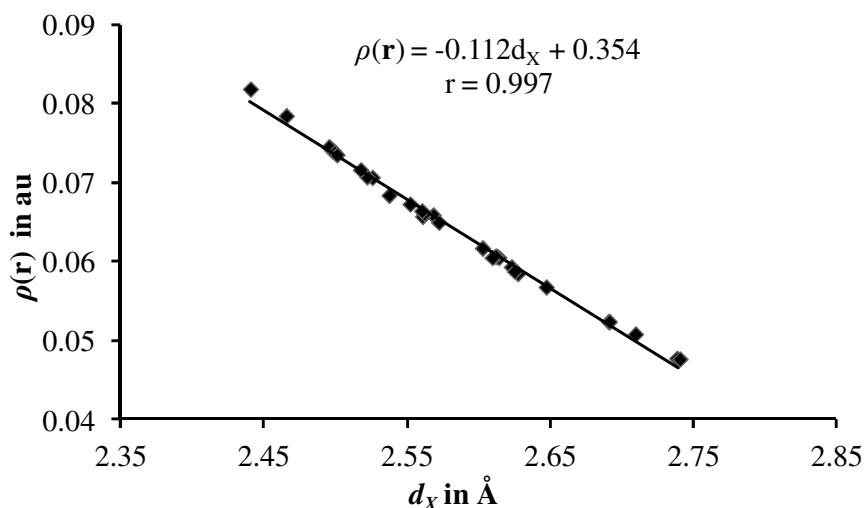


**Figure 4.5** Correlation between electron density at the bond critical point of trans I–Cl bond and trans I–Cl distance in  $\text{CF}_3[\text{I}(\text{X})\text{Cl}]$  complexes.

### 4.4.3 Trans Influence and Covalent Nature of the Hypervalent Bonds

All  $\nabla^2\rho(\mathbf{r})$  values are positive (0.071 to 0.079 au) whereas  $H(\mathbf{r})$  values are negative (-0.007 to -0.025 au). The positive  $\nabla^2\rho(\mathbf{r})$  indicates ionic nature of the I–Cl bond while the negative  $H(\mathbf{r})$  suggests covalent character. Therefore, like metal-ligand bonds [Bader and Matta 2001; Phukan and Guha 2010], the hypervalent I–Cl bonds can be considered as bonds with partial ionic and partial covalent characters.  $\nabla^2\rho(\mathbf{r})$  showed no correlation with  $d_X$  while  $H(\mathbf{r})$  correlated remarkably well with it on a second degree polynomial equation for the distance range 2.44 to 2.74 Å (Figure 4.6). It should be noted that  $d_X$  and  $H(\mathbf{r})$  show a good linear correlation with a correlation coefficient of 0.988 while the ligands with highest and lowest trans influence show a tendency to deviate from the linear plot. The  $(d_X, H(\mathbf{r}))$  correlation suggests that an increase in the trans influence of the X ligand leads to a decrease in the covalent character of the I–Cl bond.

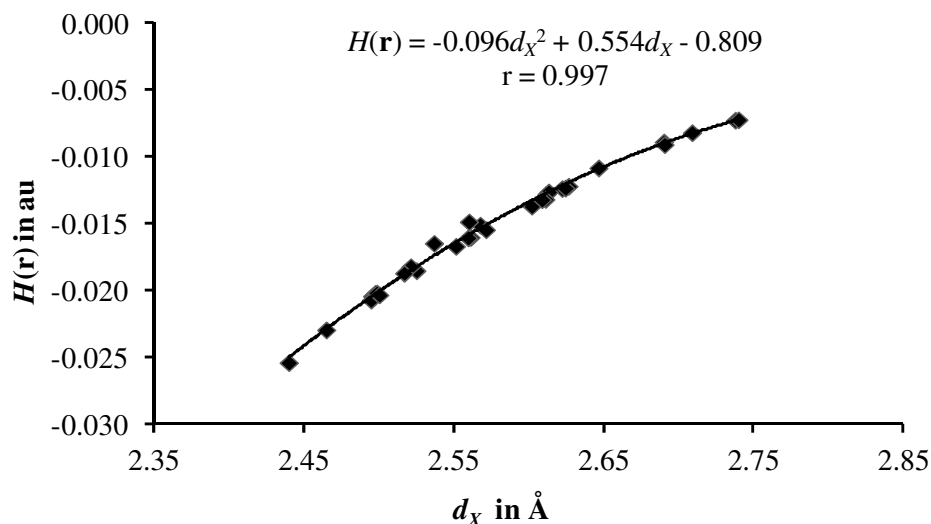


**Figure 4.6** Correlation between total electron energy density and trans I–Cl bond length in  $\text{CF}_3[\text{I}(\text{X})\text{Cl}]$  complexes.

The covalent character of I–Cl bond can also be assessed using the  $V(\mathbf{r})/G(\mathbf{r})$  ratio (denoted as  $k(\mathbf{r})$ ). In general, the value of  $|k(\mathbf{r})| < 1$  at the bcp indicates the closed shell nature of the bond while  $|k(\mathbf{r})| > 1$  shows the covalent nature. It is clear from the Table 4.1 that all the trans I–Cl bond showed  $|k(\mathbf{r})| > 1$  at the bcp with  $k(\mathbf{r})$  values ranges between -1.28 and -1.59. Figure 4.7 presents the linear relationship between  $k(\mathbf{r})$  and I–Cl distance parameter which nicely complement the conclusion obtained from the  $(d_X, H(\mathbf{r}))$  correlation.

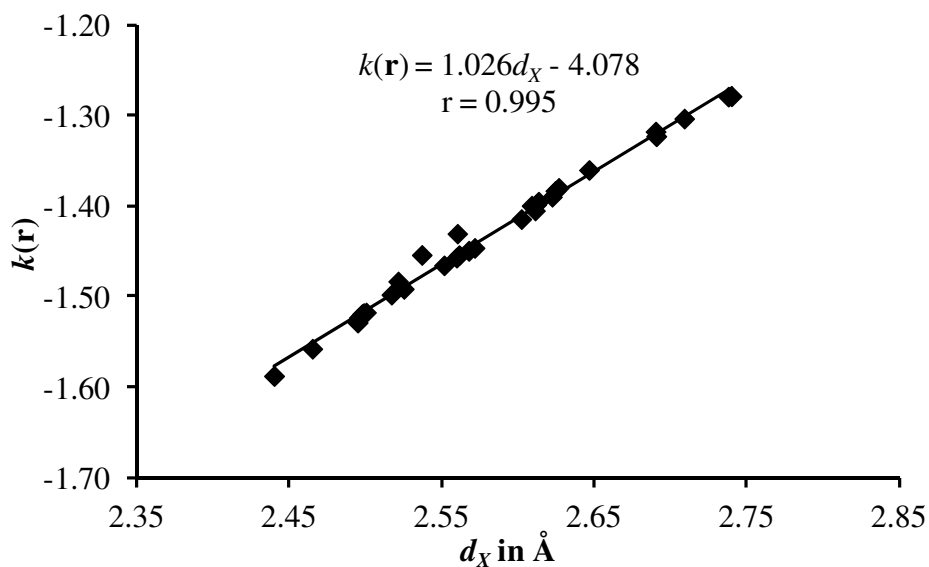


**Figure 4.7** Correlation between  $k(r)$  and trans I–Cl bond length in  $\text{CF}_3[\text{I}(\text{X})\text{Cl}]$  complexes.

#### 4.4.4 MESP Minimum as a Measure of Trans Influence

Recently we have shown that critical features of MESP can be used as good descriptors for the study of inductive effect [Suresh *et al.* 2008; Sayyed *et al.* 2009; Sayyed and Suresh 2011]. Further, the subtle variations of electronic features induced by substituents on organic molecules as well as ligands in complexed systems can be quantified by studying the topographical features of MESP [Sayyed and Suresh 2011; <sup>a</sup>Mathew and Suresh 2011; <sup>b</sup>Mathew and Suresh 2011]. For instance, minimum value of MESP in the lone pair region of phosphine [Suresh and Koga 2002] and carbene ligands [Mathew and Suresh 2010] can be used as good measure of the donating power of these ligands in coordination complexes. Hence, it is felt that MESP can provide valuable insight on the highly polarized 3c-4e bonding in hypervalent iodine complexes as this bond is largely influenced by the inductive effect of the X ligands. In MESP studies, it is convenient to select an electron rich region in the molecule for monitoring the changes in the electron density distribution. The chloro ligand in  $\text{CF}_3[\text{I}(\text{X})\text{Cl}]$  shows the most

electron rich lone pair region and therefore the MESP minimum (designated as  $V_{\min}$ ) observed for this region is used for monitoring the trans influence of X.

In Figure 4.8,  $V_{\min}$  at the Cl lone pair region is depicted along with an electrostatic representation of the molecule using an MESP isosurface of value -23 kcal/mol for a representative set of four molecules. Table 4.2 depicts the  $V_{\min}$  of all the systems. For X = CPh<sub>3</sub>COOMe, chloro ligand shows the most negative  $V_{\min}$  (-56.60 kcal/mol) while for X = BF<sub>4</sub>,  $V_{\min}$  has the highest value (2.35 kcal/mol). The chloro ligand trans to BF<sub>4</sub> is devoid of negative  $V_{\min}$  which can be attributed to the very weak trans influence of BF<sub>4</sub>, resulting to strong I-Cl bond formation. When going from electron donating to withdrawing ligands, a gradual decrease in the negative value of  $V_{\min}$  is observed. In general, a weak I-Cl bond is characterized by highly negative  $V_{\min}$ . Because the weak I-Cl bond is due to strong trans influence of X, the high negative MESP surrounding the chloro ligand can be attributed to the increased ionic character or the decreased covalent character of the I-Cl bond.

Figure 4.9 gives a good linear relation between  $V_{\min}$  and trans I-Cl distance parameter,  $d_X$ . It suggests that  $V_{\min}$  can be used as a sensitive measure of the trans influence. The *trans* bond length, a structural measure of trans influence is less sensitive than the one electron property which is immediately noted in the wide range of  $V_{\min}$  values (2 to -57 kcal/mol) observed for the 32 ligands considered in this study. Further,  $V_{\min}$  is useful as an energetic measure of trans influence because its value also represents the energy required to bring a unit test positive charge from infinity to that location [Gadre *et al.* 1996]. On the basis of  $V_{\min}$  values, ligands are classified into four groups, *viz.*

- (1) **Very strong trans influencing:**  $V_{\min}$  values more negative than -30 kcal/mol and the ligands are  $\text{CPh}_3\text{COOMe}$ ,  $\text{CPh}_3\text{COMe}$ , Et, Ph, Me,  $\text{CCPh}$ ,  $\text{CCSiMe}_3$ ,  $\text{CH}_2\text{Cl}$ , CCH, and  $\text{NH}_2$ .
- (2) **Strong trans influencing:**  $V_{\min}$  values ranges from -30 to -20 kcal/mol and the ligands are  $\text{CF}_3$ ,  $\text{C}_6\text{F}_5$ , 2,3,5,6- tetrafluoro-4-(trifluoromethyl)benzene,  $\text{CF}_2\text{CF}_2\text{CF}_3$ ,  $\text{OO}t\text{Bu}$ ,  $\text{O}i\text{Pr}$ , OMe, and OH.
- (3) **Moderate trans influencing:**  $V_{\min}$  values from -20 to -10 kcal/mol and the ligands are Br,  $\text{NO}_2$ , Cl, OAc, NHTf,  $\text{OSO}_2\text{Me}$ , OTs,  $\text{OCOCOOMe}$ , and F.
- (4) **Weak trans influencing:**  $V_{\min}$  values less negative values than -10 kcal/mol. The ligands are  $\text{OCOCCl}_3$ ,  $\text{NO}_3$ ,  $\text{OCOCF}_3$ , OTf and  $\text{BF}_4$ .

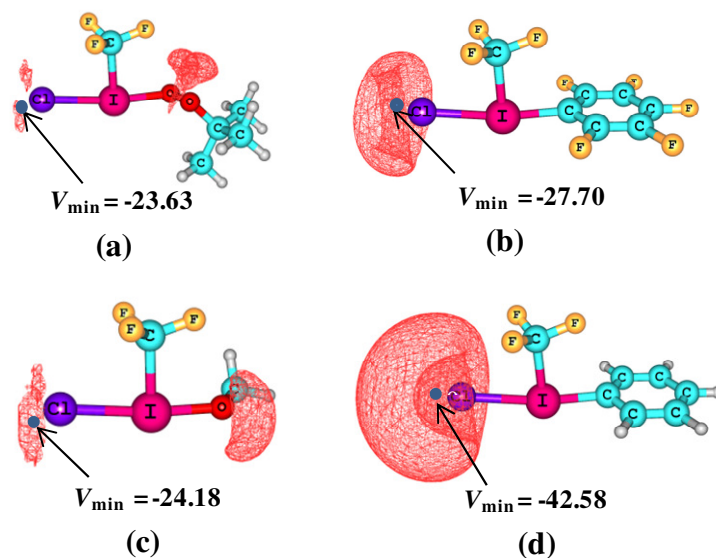


**Figure 4.8** Representation of MESP isosurface in  $\text{CF}_3[\text{I}(\text{X})\text{Cl}]$  complexes at -23 kcal/mol along with  $V_{\min}$  in kcal/mol. The ligand X are (a)  $\text{OO}t\text{Bu}$  (b)  $\text{C}_6\text{F}_5$  (c) OMe and (d) Ph.

**Table 4.2**  $V_{\min}$  values of  $\text{CF}_3[\text{I}(\text{X})\text{Cl}]$  complexes.

Sl. No.	trans ligand X	$V_{\min}$ on trans Cl in kcal/mol
1	C(PPh <sub>3</sub> )COMe	-54.32
2	C(PPh <sub>3</sub> )COOMe	-56.60
3	Et	-43.22
4	Ph	-42.58
5	Me	-40.95
6	CH <sub>2</sub> Cl	-33.36
7	CCPh	-35.39
8	CCSiMe <sub>3</sub>	-34.28
9	NH <sub>2</sub>	-33.38
10	CF <sub>3</sub> CF <sub>2</sub> CF <sub>2</sub>	-25.11
11	CF <sub>3</sub>	-25.51
12	C <sub>6</sub> F <sub>5</sub>	-27.71
13	CCH	-30.69
14	C <sub>6</sub> F <sub>4</sub> (CF <sub>3</sub> ) <sup>#</sup>	-25.14
15	O <i>i</i> Pr	-26.21
16	NO <sub>2</sub>	-14.74
17	OMe	-24.17
18	Br	-16.58
19	OO <i>t</i> Bu	-23.63
20	OH	-21.97
21	Cl	-14.38
22	NHTf	-13.94
23	OAc	-17.04
24	OCOCOOMe	-13.35
25	F	-12.13
26	OTs	-12.55
27	OCOCCl <sub>3</sub>	-8.50
28	OSO <sub>2</sub> Me	-12.43
29	OCOCF <sub>3</sub>	-7.11
30	NO <sub>3</sub>	-7.67
31	OTf	-1.32
32	BF <sub>4</sub>	2.35

<sup>#</sup> 2,3,5,6- tetrafluoro-4-(trifluoromethyl)benzene

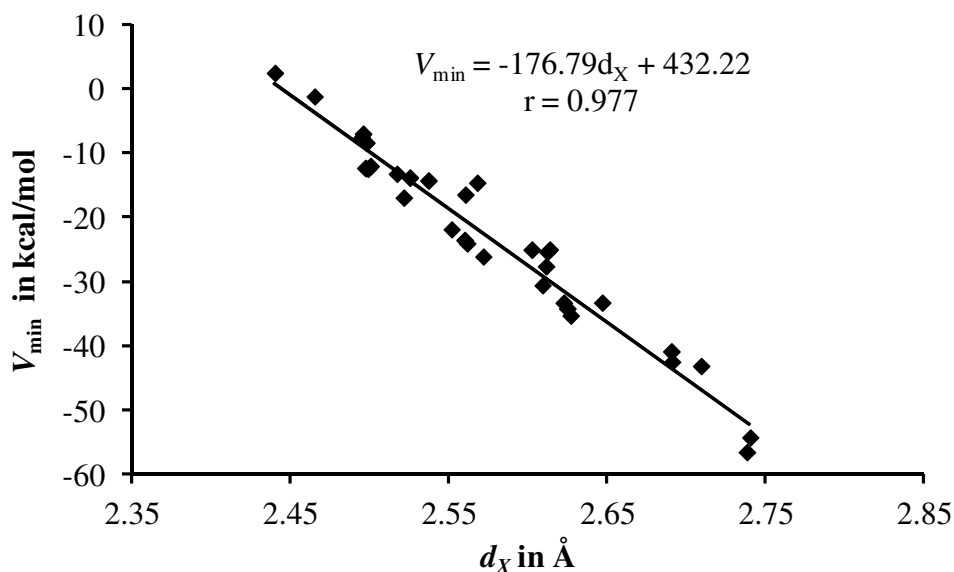


**Figure 4.9** Correlation between  $V_{\min}$  and trans I–Cl bond length in  $\text{CF}_3[\text{I}(\text{X})\text{Cl}]$  complexes.

#### 4.4.5 Trans influence in Other $\lambda^3$ -iodanes

To assess the trans influence of X in another ligand environment, various X ligands in benziodoxoles is considered for a representative set of 15 ligands. QTAIM topological plot of two representative examples are given in the Figure 4.10 along with an MESP isosurface representation of the same structures. The probe to measure  $V_{\min}$  is the lone pair region of the oxygen atom that is trans to the X ligand. The I–O bond length  $d_X$ ,  $\rho(\mathbf{r})$  value for the I–O bond, and  $V_{\min}$  are reported in Table 4.3. All the three trans influence parameters ( $d_X$ ,  $\rho(\mathbf{r})$  and  $V_{\min}$ ) correlate strongly with the corresponding values obtained for  $\text{CF}_3[\text{I}(\text{X})\text{Cl}]$  systems. Therefore, the trans influence order presented in series (i) is taken as a general order of trans influence in hypervalent iodine (III) complexes.

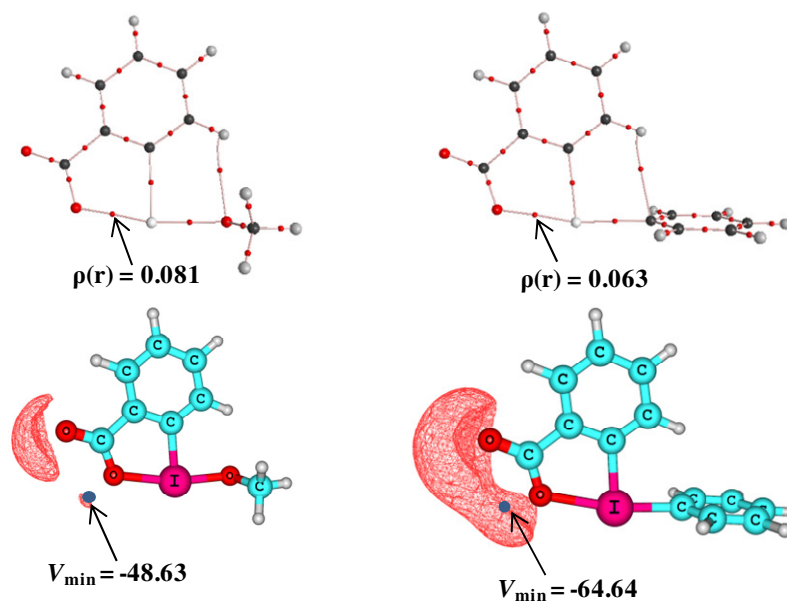


**Figure 4.10** (top) AIM topological plot of  $\lambda^3$ -aryl iodanes with X = OMe and Ph. Big circles corresponds to attractors (atomic nuclei) and small red circles indicate bond critical points. The  $\rho(r)$  in au at bond critical point of I–O bond is also shown. (bottom) The representation of MESP isosurface at -46 kcal/mol along with  $V_{\min}$  value in kcal/mol.

**Table 4.3** Trans influence parameters of  $\lambda^3$ -aryl iodanes.

Trans ligand	$d_x$ in Å	$\rho(r)$ in a.u.	$V_{\min}$ in kcal/mol
Et	2.366	0.060	-65.44
Me	2.349	0.062	-63.49
Ph	2.344	0.063	-64.64
C <sub>6</sub> F <sub>5</sub>	2.265	0.073	-51.90
CF <sub>3</sub>	2.260	0.074	-49.39
OMe	2.208	0.081	-48.63
Br	2.202	0.082	-40.85
OH	2.199	0.082	-46.94
Cl	2.181	0.085	-39.09
OAc	2.174	0.086	-42.48
F	2.147	0.090	-37.51
OTs	2.145	0.091	-38.15
OSO <sub>2</sub> Me	2.138	0.092	-35.77
NO <sub>3</sub>	2.137	0.093	-31.88
BF <sub>4</sub>	2.092	0.101	-21.72

#### 4.4.6 Trans Influence in Iodine(V) Compounds

A model of the iodine(V) complex selected for this study is shown in the Figure 4.11, which can be considered as a derivative of Dess-Martin periodane (DMP) [Dess and Martin 1983] wherein one of the OAc group trans to the O atom of aryl group is replaced by the X ligand. These  $\lambda^5$ -iodanes complexes are characterized by two orthogonal 3c-4e bonds because the central iodine atom is coordinated to four different ligands through two hypervalent bonding while the fifth ligand occupies the apical position of the square pyramidal structure through a normal covalent bond [Zhdankin and Stang 2008]. This model will help us to assess the effect of a 3c-4e bond (the AcO–I–OAc bonding) on the trans influencing power of the X ligands. The I–O bond length (trans to X ligand) is the structural parameter,  $d_X$  for the trans influence while the corresponding  $\rho(\mathbf{r})$  is the electron density based parameter. The MESP minimum on the oxygen lone pair,  $V_{\min}$  for the I–O bond (trans to X ligand) will serve as the electrostatic measure of the trans influence. In Figure 4.12, QTAIM topological plot of a representative example and the MESP isosurface of the same system along with the corresponding  $V_{\min}$  value is depicted. The trans influence parameters for the 15 ligands are reported in Table 4.4.

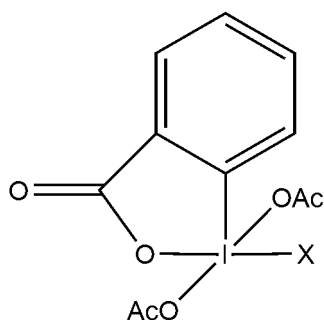


**Figure 4.11** System considered for the study of trans influence in iodine (V) compounds, where X indicates the trans ligand.

All the three trans influence parameters of  $\lambda^5$ -iodanes almost strictly follow the order of trans influence observed in the case of  $\lambda^3$ -iodanes.  $d_X$  is less sensitive as a trans influence parameter than  $\rho(\mathbf{r})$  and  $V_{\min}$  because from iodine(V) to iodine(III) complex, the former shows only 1-2% decrease whereas  $\rho(\mathbf{r})$  increase by 5-12% while  $V_{\min}$  becomes less negative by 7-23%. These data also suggest that the presence of a second 3c-4e bond decreases the trans influence of the X ligand.

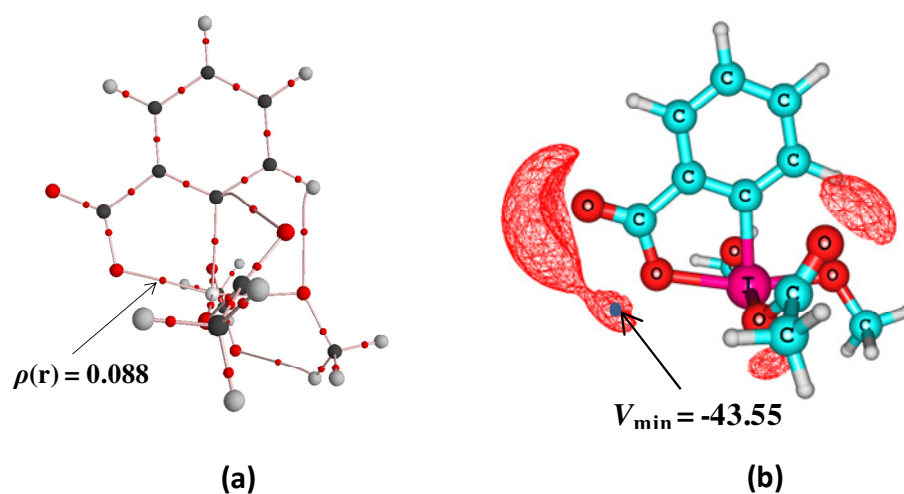


**Figure 4.12** (a) AIM topological plot of  $\lambda^5$ -aryl iodane with X = OMe. The  $\rho(\mathbf{r})$  value in au is shown. Big circles corresponds to attractors (atomic nuclei) and small red circles indicate bond critical points. The  $\rho(\mathbf{r})$  in au at bond critical point of I–O bond is shown. (b) Representation of MESP isosurface at -37 kcal/mol when X = OMe. The corresponding  $V_{\min}$  in kcal/mol is also given.

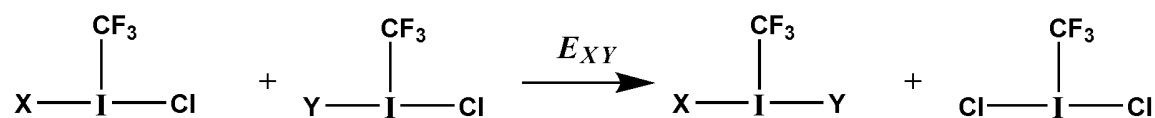
**Table 4.4** Trans influence parameters of  $\lambda^5$ -aryl iodanes.

Trans Ligand	$d_X$ in Å	$\rho(r)$ in au	$V_{\min}$ in kcal/mol
Et	2.368	0.063	-60.68
Me	2.345	0.066	-57.99
Ph	2.336	0.067	-59.50
CF <sub>3</sub>	2.253	0.078	-44.93
C <sub>6</sub> F <sub>5</sub>	2.246	0.079	-46.00
OMe	2.186	0.088	-43.55
Br	2.169	0.091	-36.29
OH	2.185	0.088	-41.42
Cl	2.147	0.095	-34.03
OAc	2.138	0.096	-34.58
F	2.113	0.100	-32.71
OTs	2.112	0.101	-34.42
OSO <sub>2</sub> Me	2.106	0.102	-31.19
NO <sub>3</sub>	2.103	0.103	-28.12
BF <sub>4</sub>	2.004	0.116	-20.10

#### 4.4.7 Isodesmic reactions to Study Mutual Trans Influence of Two Ligands X and Y

Isodesmic reactions are hypothetical reactions in which the number of bonds of the given type is conserved. Reaction depicted in Scheme 4.1 is isodesmic as the number and type of bonds in the reactant side is equal to the number and type of bonds in the product side. However, trans influence is not conserved in the reaction. Therefore, the energy of the reaction,  $E_{XY}$  will mainly account for the difference between the trans influence at the product and the reactant sides. In the reactant side, trans influence of X and Y is present while the trans influence due to (X, Y) combination as well as trans influence of Cl is present in the product side. Because the trans influence due to Cl in [CF<sub>3</sub>ICl<sub>2</sub>] is constant for all the reactions, the energy of the reaction  $E_{XY}$  can be used as a good measure of the mutual trans influence of the (X, Y) combination. In other words,

$E_{XY}$  values will indicate the stabilization/destabilization due to trans disposition of X and Y ligand around the I atom. From the 32 ligands selected in this study, we have randomly picked 63 combinations of X and Y and studied the corresponding 63 isodesmic reactions. Out of the 63 reactions, the  $E_{XY}$  of 42 reactions given in Tables 4.5 are used as a training set for statistical analysis (sample size,  $n = 42$ ) while the remaining 21 reactions in Table 4.6 are used as test set ( $n = 21$ ).



**Scheme 4.1** Isodesmic reactions used to study the mutual trans ligand influence due to X and Y.

All the  $E_{XY}$  values fall in the range of -24.96 to 33.62 kcal/mol (Tables 4.5 and 4.6). A positive  $E_{XY}$  corresponds to destabilization due to mutual trans influence while a negative  $E_{XY}$  indicates a stable trans combination. The (C(PPh<sub>3</sub>)COMe, C(PPh<sub>3</sub>)COMe) and (CPhPh<sub>3</sub>COOMe, CPhPh<sub>3</sub>COOMe) combinations show the highest  $E_{XY}$  values of 33.62 and 32.16 kcal/mol, respectively and they correspond to unstable (very strong, very strong) trans influencing pairs. Similarly,  $E_{XY}$  above 20 kcal/mol is observed for the (Me, Et) and (Et, C(PPh<sub>3</sub>)COOMe) combinations. All the very strong - very strong, very strong - strong and strong - strong trans influencing pairs are unfavourable combinations. The weak - weak combinations (BF<sub>4</sub>, BF<sub>4</sub>) and (OCOCF<sub>3</sub>, OCOCF<sub>3</sub>) are also unstable whereas the weak - weak combination, (OCOCCl<sub>3</sub>, OCOCCl<sub>3</sub>) is slightly unstable ( $E_{XY} = 0.23$  kcal/mol). As suggested by Ochiai *et al.*, moderate trans influencing combinations are stable combinations with most of the  $E_{XY}$  show negative values. The most favorable combinations are the medium-strong, weak-strong and weak-very strong trans influencing pairs [Ochiai *et al.* 2006]. For example, the lowest  $E_{XY}$  of -24.49 and -24.96

kcal/mol are shown by the (BF<sub>4</sub>, CPh<sub>3</sub>COOMe) and (BF<sub>4</sub>, CPh<sub>3</sub>COMe), respectively and they corresponds to weak - very strong trans influencing combinations.

**Table 4.5** Calculated and predicted  $E_{XY}$ . All values in kcal/mol. The  $d_X$ ,  $\rho(\mathbf{r})$  and  $V_{min}$  are expressed in Å, au and kcal/mol respectively for predicting  $E_{XY}$  values.

Isodesmic reactions	Ligands in the trans positions		Calculated $E_{XY}$	Predicted $E_{XY}$ using		
	X	Y		$d_X$	$\rho(\mathbf{r})$	$V_{min}$
1	F	Br	0.34	-1.53	-1.67	-0.11
2	F	F	-0.68	0.37	0.29	0.47
3	OCOCCL <sub>3</sub>	OH	-2.58	-1.37	-1.47	-2.09
4	OTS	Ph	-6.51	-6.44	-5.37	-3.22
5	OH	Br	0.67	1.08	1.20	0.93
6	OTs	CF <sub>3</sub>	-3.61	-3.65	-3.16	-1.12
7	Br	CCSiMe <sub>3</sub>	1.73	2.06	3.28	0.24
8	CF <sub>2</sub> CF <sub>2</sub> CF <sub>3</sub>	Me	9.23	9.93	10.90	6.34
9	OMe	O <i>i</i> Pr	2.60	1.69	1.88	3.87
10	OSO <sub>2</sub> Me	Me	-6.38	-6.12	-5.68	-3.11
11	BF <sub>4</sub>	Me	-16.22	-13.98	-15.19	-14.14
12	F	C(PPh <sub>3</sub> )COOMe	-0.67	-7.17	-6.18	-5.40
13	F	Me	-1.53	-5.66	-5.01	-3.34
14	NO <sub>3</sub>	Ph	-5.59	-6.44	-6.25	-7.03
15	F	OMe	-1.57	-1.56	-1.57	-1.12
16	BF <sub>4</sub>	C(PPh <sub>3</sub> )COOMe	-24.96	-17.41	-18.60	-20.96
17	OTs	F	-0.73	0.31	0.29	0.42
18	OO <i>t</i> Bu	Me	4.70	2.52	3.69	5.24
19	Me	Et	20.44	22.30	22.35	19.24
20	OTf	Br	-1.61	-3.34	-3.93	-2.64
21	OH	CCSiMe <sub>3</sub>	3.23	1.24	1.94	3.51
22	OTf	Et	-12.42	-11.56	-11.89	-12.22
23	NO <sub>3</sub>	Me	-5.10	-6.43	-6.25	-6.67
24	OSO <sub>2</sub> Me	Et	-6.73	-6.75	-6.13	-3.40
25	OTf	OSO <sub>2</sub> Me	0.68	0.16	0.52	-1.15
26	OH	OMe	1.04	1.09	1.16	2.75
27	Et	C(PPh <sub>3</sub> )COOMe	26.89	28.22	27.68	28.01
28	CF <sub>3</sub>	CF <sub>3</sub>	6.83	6.38	6.71	4.35
29	OCOCCL <sub>3</sub>	OSO <sub>2</sub> Me	1.74	0.42	0.43	-0.10

**Table 4.5(continued)**

30	OiPr	CCPh	5.31	3.15	3.99	6.25
31	NO <sub>2</sub>	CCPh	-0.17	2.78	3.19	-0.96
32	OCOCOOMe	OCOCOOMe	-0.27	0.21	0.05	0.52
33	OCOCCl <sub>3</sub>	OCOCCl <sub>3</sub>	0.23	0.43	0.43	0.72
34	Br	Br	0.00	1.53	1.92	0.93
35	OMe	OMe	1.76	1.60	1.68	3.62
36	NO <sub>3</sub>	OH	-1.80	-1.51	-1.65	-2.38
37	NO <sub>3</sub>	OMe	-1.38	-1.85	-2.01	-2.87
38	Br	Ph	1.55	2.60	4.54	-0.08
39	NO <sub>3</sub>	F	-0.21	0.31	0.28	-0.15
40	C(PPh <sub>3</sub> )COMe	C(PPh <sub>3</sub> )COMe	33.62	33.74	32.47	38.22
41	BF <sub>4</sub>	BF <sub>4</sub>	3.49	4.04	6.26	4.75
42	OTf	OMe	-4.45	-3.40	-3.73	-5.37

The results presented herein suggest that the presence of electronegative atoms at the apical position is not an essential criterion for explaining the stability of hypervalent iodine compounds. The electron releasing groups such as Me, Et, Ph, and CPh<sub>3</sub>COMe can also make the system stable provided that the trans position is occupied by ligands with small trans influence such as BF<sub>4</sub>, and NO<sub>3</sub>. Further, the mutual trans influence of X and Y strongly depends on the individual trans influence of X as well as Y. It is found that using the trans influence parameter of X, trans influence parameter of Y, and the product of trans influence parameters of X and Y, empirical equations 4.1, 4.2, and 4.3 can be derived for predicting the values of  $E_{XY}$  using MLR analysis.

$$E_{XY} = -1657.68d_X - 1700.66d_Y + 667.47 d_X d_Y + 4224.54 \quad \dots(\text{Eq. 4.1})$$

$$(n = 42, s = 2.05, \text{ and } r = 0.976)$$

$$E_{XY} = -4235.316\rho_X(\mathbf{r}) - 3972.016\rho_Y(\mathbf{r}) + 57427.544\rho_X(\mathbf{r})\rho_Y(\mathbf{r}) + 292.986 \quad \dots(\text{Eq. 4.2})$$

$$(n = 42, s = 1.91, \text{ and } r = 0.980)$$

$$E_{XY} = 0.115 V_{\min(X)} + 0.387 V_{\min(Y)} + 0.021 V_{\min(X)}V_{\min(Y)} + 3.460 \quad \dots(\text{Eq. 4.3})$$

$$(n = 42, s = 1.95, \text{ and } r = 0.980)$$

In these equations, the terms  $d_X$ ,  $\rho_X(\mathbf{r})$  and  $V_{\min(X)}$  indicate respectively the trans I–Cl bond distance,  $\rho(\mathbf{r})$ , and  $V_{\min}$  of the  $\text{CF}_3[\text{I}(\text{X})(\text{Cl})]$  complex while the  $d_Y$ ,  $\rho_Y(\mathbf{r})$  and  $V_{\min(Y)}$  are respectively the trans I–Cl bond distance,  $\rho(\mathbf{r})$  and  $V_{\min}$  of the  $\text{CF}_3[\text{I}(\text{Y})(\text{Cl})]$  complex. Also, trans influence of X  $\leq$  trans influence of Y.  $s$  and  $r$  are standard deviation and correlation coefficient, respectively.

**Table 4.6.** Isodesmic reactions used for the test set. Calculated and predicted  $E_{XY}$  are given. All values in kcal/mol.

Isodesmic reactions	Ligands in the trans positions		Calculated $E_{XY}$	Predicted $E_{XY}$ using		
	X	Y		Eq. 4.1	Eq. 4.2	Eq. 4.3
1	BF <sub>4</sub>	Ph	-17.52	-14.01	-15.21	-14.85
2	C(PPh) <sub>3</sub> COOMe	C(PPh) <sub>3</sub> COOMe	32.16	33.12	32.27	42.38
3	O <i>i</i> Pr	CCH	4.42	2.87	3.51	5.49
4	BF <sub>4</sub>	C(PPh) <sub>3</sub> COMe	-24.49	-17.56	-18.65	-19.97
5	NHTf	OH	-0.56	-0.13	-0.21	-0.20
6	OTs	OO <i>t</i> Bu	-2.16	-1.80	-1.62	-0.88
7	C <sub>6</sub> F <sub>5</sub> CF <sub>3</sub>	CF <sub>3</sub>	6.67	5.54	5.92	4.19
8	C <sub>6</sub> F <sub>5</sub>	CCSiMe <sub>3</sub>	9.14	6.85	7.61	6.98
9	CF <sub>2</sub> CF <sub>2</sub> CF <sub>3</sub>	Ph	9.85	9.95	10.91	6.57
10	OCOCOOMe	Br	-1.15	-0.68	-0.79	0.17
11	OCOCOOMe	CCH	-2.63	-1.69	-1.53	-1.33
12	OCOCCL <sub>3</sub>	CH <sub>2</sub> Cl	-4.11	-4.56	-4.43	-4.46
13	OCOCF <sub>3</sub>	OCOCF <sub>3</sub>	1.03	0.48	0.55	0.96
14	F	Ph	-1.84	-5.67	-5.02	-3.55
15	F	NH <sub>2</sub>	-1.60	-3.50	-3.27	-2.33
16	OCOCF <sub>3</sub>	OO <i>t</i> Bu	-2.25	-1.75	-1.87	-2.96
17	OCOMe	OH	0.16	-0.30	-0.24	0.88
18	Br	Me	1.47	2.57	4.56	-0.04
19	OMe	Ph	6.78	2.75	4.08	5.84
20	NO <sub>2</sub>	OMe	-0.03	1.65	1.77	-0.09
21	OSO <sub>2</sub> Me	CH <sub>2</sub> Cl	-2.97	-4.63	-4.44	-2.16

To test the reliability of trans influence parameters, the leave-one-out (LOO) cross validation methodology is applied. In this test, one isodesmic reaction is removed from the data set and the corresponding  $E_{XY}$  value is predicted from the rest of the data. The process is repeated for each isodesmic reaction and the cross validated correlation coefficients ( $r^2_{cv}$ ) of 0.940, 0.947, and 0.937 are obtained respectively for the trans influence parameters  $d_X$ ,  $\rho_X(\mathbf{r})$  and  $V_{\min(X)}$ . This is an indication of the high predictive power of this model. Further, Eqs. 4.1, 4.2 and 4.3 are validated using a set of 21 isodesmic reactions given in Table 4.6. The statistical parameters obtained for the test set are good, *viz.*  $s$  equal to 2.40, 2.01 and 2.85 for Eqs. 4.1, 4.2 and 4.3, respectively and  $r$  equal to 0.977, 0.987, and 0.970 for Eqs. 4.1, 4.2 and 4.3, respectively. The predicted  $E_{XY}$  values for the training set and the test set are given in Tables 4.5 and 4.6, respectively. The Figure 4.13 shows the agreement between calculated and predicted  $E_{XY}$  using  $V_{\min}$  values for all the isodesmic reactions.

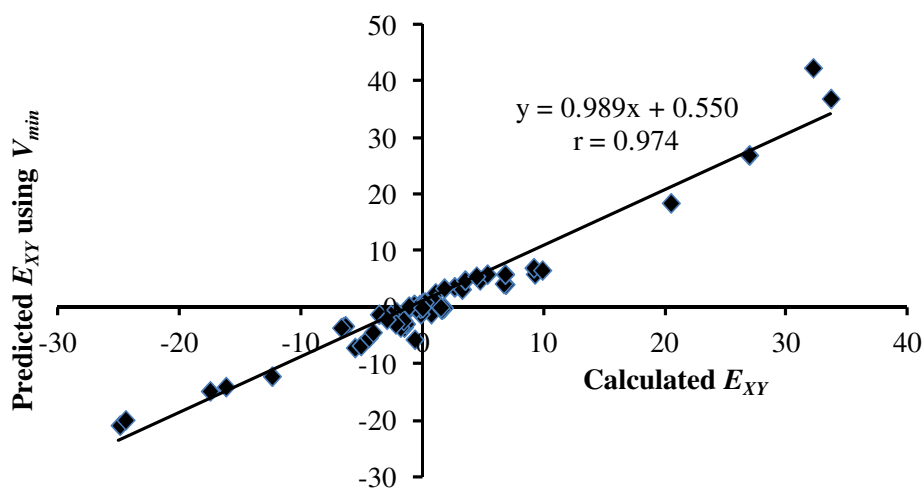


**Figure 4.13** Correlation between calculated and predicted  $E_{XY}$  values. The Eq. 4.3 is used for the prediction of  $E_{XY}$ . All values are in kcal/mol.

### 4.4.8 Bond Dissociation Energy and Trans Influence

Ligands in the axial positions of a hypervalent iodine (III) complex can be cleaved heterolytically [Stang and Zhdankin 1996; Zhdankin and Stang 2002]. This reaction can be represented as either  $\text{CF}_3[\text{I}(\text{X})(\text{Y})] \rightarrow [\text{CF}_3\text{IY}]^+ + \text{X}^-$  or  $\text{CF}_3[\text{I}(\text{X})(\text{Y})] \rightarrow [\text{CF}_3\text{IX}]^+ + \text{Y}^-$ . The dissociation of  $\text{X}^-$  or  $\text{Y}^-$  can be influenced by the trans influence of X or Y as well as the mutual trans influence of (X, Y) combination. The trans (X, Cl) combination represents the  $\text{CF}_3[\text{I}(\text{X})(\text{Cl})]$  system and used herein as the reference structure to evaluate the trans parameters  $d_X$ ,  $\rho(\mathbf{r})$  and  $V_{\min}$ . Therefore, BDE of X in the  $\text{CF}_3[\text{I}(\text{X})(\text{Cl})]$  system (designated as  $D_{IX}$  and all the values are given in Table 4.7) is used as a reference value to estimate the mutual trans influence of the (X, Y) combination on the dissociation energy of either X or Y ligand in  $\text{CF}_3[\text{I}(\text{X})(\text{Y})]$  system. The calculated BDE values for the ligands X and Y (designated as  $D_{2X}$  and  $D_{2Y}$  respectively) are given in Table 4.8. To make a reasonable prediction of the BDE of X or Y ligand in the  $\text{CF}_3[\text{I}(\text{X})(\text{Y})]$  complex, MLR analysis is done with three variables, *viz.*  $D_{IX}$ , any one of the trans influence parameter and  $E_{XY}$ . The following eqs. are obtained from the 42 compounds considered in Table 4.5.

$$D_{2X} = 0.976 D_{IX} - 258.574d_X - 0.992E_{XY} + 654.944 \quad \dots(\text{Eq. 4.4})$$

$$(n = 42, s = 6.59, r = 0.989)$$

$$D_{2X} = 0.977 D_{IX} + 2291.184\rho(\mathbf{r}) - 0.995E_{XY} - 160.084 \quad \dots(\text{Eq. 4.5})$$

$$(n = 42, s = 6.80, r = 0.988)$$

$$D_{2X} = 0.985 D_{IX} + 1.463V_{\min} - 0.993E_{XY} + 21.485 \quad \dots(\text{Eq. 4.6})$$

$$(n = 42, s = 6.44, r = 0.989)$$

**Table 4.7** The BDE of X in the CF<sub>3</sub>[I(X)(Cl)] complexes ( $D_{IX}$  in kcal/mol)

Sl. No.	Ligand (X)	$D_{IX}$
1	C(PPh <sub>3</sub> )COMe	206.09
2	C(PPh <sub>3</sub> )COOMe	206.97
3	Et	240.54
4	Ph	219.85
5	Me	236.01
6	CH <sub>2</sub> Cl	212.95
7	CCPh	187.51
8	CCSiMe <sub>3</sub>	187.95
9	NH <sub>2</sub>	219.45
10	CF <sub>3</sub> CF <sub>2</sub> CF <sub>2</sub>	175.29
11	CF <sub>3</sub>	185.87
12	C <sub>6</sub> F <sub>5</sub>	169.20
13	CCH	192.75
14	C <sub>6</sub> F <sub>4</sub> (CF <sub>3</sub> )	162.92
15	O <i>i</i> Pr	193.07
16	NO <sub>2</sub>	157.66
17	OMe	198.60
18	Br	155.83
19	OO <i>t</i> Bu	190.71
20	OH	205.20
21	Cl	159.05
22	NHTf	142.42
23	OAc	167.30
24	OCOCOOMe	150.05
25	F	188.45
26	OTs	138.82
27	OCOCCl <sub>3</sub>	139.89
28	OSO <sub>2</sub> Me	140.73
29	OCOCF <sub>3</sub>	141.72
30	NO <sub>3</sub>	141.12
31	OTf	122.74
32	BF <sub>4</sub>	115.69

**Table 4.8** Calculated bond dissociation energy values of the X and Y in  $\text{CF}_3[\text{I}(\text{X})(\text{Y})]$  complexes. All values are in kcal/mol.

Ligands in the trans positions		Calculated BDE for X ( $D_{2X}$ )	Calculated BDE for Y ( $D_{2Y}$ )
X	Y		
F	Br	181.00	171.64
F	F	205.28	205.28
OCOC $\text{Cl}_3$	OH	136.96	211.22
OTS	Ph	99.36	213.93
OH	Br	197.42	149.65
OTs	$\text{CF}_3$	119.43	177.05
Br	$\text{CCSiMe}_3$	119.58	179.12
$\text{CF}_2\text{CF}_2\text{CF}_3$	Me	127.11	201.17
OMe	OiPr	177.71	178.16
$\text{OSO}_2\text{Me}$	Me	108.16	241.04
$\text{BF}_4$	Me	92.96	272.59
F	$\text{C}(\text{PPh}_3)\text{COOMe}$	123.37	223.78
F	Me	151.03	253.69
$\text{NO}_3$	Ph	100.74	229.26
F	OMe	177.72	216.32
$\text{BF}_4$	$\text{C}(\text{PPh}_3)\text{COOMe}$	74.91	252.28
OTs	F	155.70	176.75
OO <i>t</i> Bu	Me	147.05	208.74
Me	Et	171.09	181.15
OTf	Br	117.24	169.25
OH	$\text{CCSiMe}_3$	167.45	179.22
OTf	Et	90.67	264.78
$\text{NO}_3$	Me	107.27	244.93
$\text{OSO}_2\text{Me}$	Et	102.97	245.91
OTf	$\text{OSO}_2\text{Me}$	120.70	151.86
OH	OMe	191.86	192.06
Et	$\text{C}(\text{PPh}_3)\text{COOMe}$	147.91	135.59
$\text{CF}_3$	$\text{CF}_3$	156.03	156.03
OCOC $\text{Cl}_3$	$\text{OSO}_2\text{Me}$	136.80	142.44
OiPr	CCPh	150.21	163.91
$\text{NO}_2$	CCPh	120.29	172.39
OCOCOOMe	OCOCOOMe	144.26	144.26
OCOC $\text{Cl}_3$	OCOC $\text{Cl}_3$	143.11	143.11
Br	Br	148.73	148.73
OMe	OMe	184.54	184.54
$\text{NO}_3$	OH	137.41	210.82

**Table 4.8(continued)**

NO <sub>3</sub>	OMe	130.20	203.80
Br	Ph	108.31	211.19
NO <sub>3</sub>	F	157.47	192.47
C(PPh <sub>3</sub> )COMe	C(PPh <sub>3</sub> )COMe	108.72	108.72
BF <sub>4</sub>	BF <sub>4</sub>	132.56	132.56
OTf	OMe	114.89	214.86
BF <sub>4</sub>	Ph	87.25	257.72
C(PPh <sub>3</sub> )COOMe	C(PPh <sub>3</sub> )COOMe	109.06	109.06
OiPr	CCH	162.79	170.04
BF <sub>4</sub>	C(PPh <sub>3</sub> )COMe	76.43	250.93
NHTf	OH	137.48	198.76
OTs	OO <i>t</i> Bu	118.41	180.45
C <sub>6</sub> F <sub>5</sub> CF <sub>3</sub>	CF <sub>3</sub>	133.24	153.70
C <sub>6</sub> F <sub>5</sub>	CCSiMe <sub>3</sub>	125.54	150.48
CF <sub>2</sub> CF <sub>2</sub> CF <sub>3</sub>	Ph	119.47	184.38
OCOCOOMe	Br	144.10	150.91
OCOCOOMe	CCH	126.83	189.32
OCOCCL <sub>3</sub>	CH <sub>2</sub> Cl	109.97	220.50
OCOFCF <sub>3</sub>	OCOFCF <sub>3</sub>	148.75	148.75
F	Ph	144.31	237.83
F	NH <sub>2</sub>	164.29	237.20
OCOFCF <sub>3</sub>	OO <i>t</i> Bu	121.39	201.02
OCOMe	OH	161.63	197.36
Br	Me	115.40	227.44
OMe	Ph	145.86	200.77
NO <sub>2</sub>	OMe	145.40	183.35
OSO <sub>2</sub> Me	CH <sub>2</sub> Cl	109.67	214.56

**Table 4.9** Predicted bond dissociation energy values of the X and Y for CF<sub>3</sub>[I(X)(Y)] complexes used for the training set. All values are in kcal/mol. The  $d_X$ ,  $\rho(\mathbf{r})$  and  $V_{min}$  are expressed in Å, au and kcal/mol respectively for predicting BDE values.

Ligands in the trans positions		$D_{2X}$ predicted using the trans parameter			$D_{2Y}$ predicted using the trans parameter		
X	Y	$d_X$	$\rho(\mathbf{r})$	$V_{min}$	$d_X$	$\rho(\mathbf{r})$	$V_{min}$
F	Br	176.61	174.08	182.48	160.23	160.08	156.86
F	F	193.09	192.94	190.00	193.09	192.94	190.00
OCOCCL <sub>3</sub>	OH	134.34	133.13	129.67	212.01	212.39	213.68
OTs	Ph	101.22	101.90	102.37	230.97	230.06	226.09

**Table 4.9(continued)**

OH	Br	192.63	190.10	198.64	146.68	145.46	143.02
OTs	CF <sub>3</sub>	118.70	117.95	124.46	194.92	193.99	189.75
Br	CCSiMe <sub>3</sub>	126.75	124.93	123.09	174.75	172.21	180.61
CF <sub>2</sub> CF <sub>2</sub> CF <sub>3</sub>	Me	121.34	121.90	125.04	200.48	199.77	208.03
OMe	OiPr	181.36	180.03	176.15	178.59	177.19	173.68
OSO <sub>2</sub> Me	Me	103.08	103.69	106.51	246.05	246.31	242.06
BF <sub>4</sub>	Me	88.40	89.02	91.61	270.55	273.90	273.45
F	CPPH <sub>3</sub> COOMe	131.68	133.91	124.93	211.16	211.01	208.22
F	Me	144.86	145.46	148.68	240.38	240.24	237.69
NO <sub>3</sub>	Ph	102.56	103.23	103.73	230.06	230.80	232.33
F	OMe	178.22	176.83	173.27	203.89	203.74	200.88
BF <sub>4</sub>	CPPH <sub>3</sub> COOMe	84.75	87.03	77.39	250.86	254.23	253.51
OTs	F	144.69	144.53	141.17	194.58	193.65	189.43
OO <i>t</i> Bu	Me	140.88	141.46	144.72	218.86	217.75	214.68
Me	Et	164.65	166.41	170.40	173.93	174.47	178.18
OTf	Br	114.38	111.85	119.70	171.29	173.29	174.61
OH	CCSiMe <sub>3</sub>	173.47	171.66	170.22	175.51	174.29	171.24
OTf	Et	86.65	88.48	91.46	264.73	266.77	268.77
NO <sub>3</sub>	Me	102.19	102.79	105.62	245.36	246.10	247.76
OSO <sub>2</sub> Me	Et	98.57	100.39	103.53	250.81	251.08	246.87
OTf	OSO <sub>2</sub> Me	128.44	128.66	123.49	154.27	156.27	157.47
OH	OMe	191.99	190.60	187.18	188.09	186.87	183.90
Et	CPPH <sub>3</sub> COOMe	155.21	157.38	148.88	129.89	131.63	135.39
CF <sub>3</sub>	CF <sub>3</sub>	154.28	153.51	160.43	154.28	153.51	160.43
OCOCCl <sub>3</sub>	OSO <sub>2</sub> Me	143.97	144.37	139.34	144.96	145.14	145.92
OiPr	CCPh	159.01	157.08	154.57	167.84	166.50	162.54
NO <sub>2</sub>	CCPh	129.88	127.95	125.15	174.28	174.05	184.75
OCOCOOMe	OCOCOOMe	150.91	150.69	150.00	150.91	150.69	150.00
OCOCCl <sub>3</sub>	OCOCCl <sub>3</sub>	145.47	145.82	146.58	145.47	145.82	146.58
Br	Br	145.10	142.56	150.70	145.10	142.56	150.70
OMe	OMe	184.83	183.44	179.96	184.83	183.44	179.96
NO <sub>3</sub>	OH	134.77	133.55	130.11	212.00	212.73	214.14
NO <sub>3</sub>	OMe	131.82	130.43	126.47	205.15	205.87	207.23
Br	Ph	109.83	110.49	111.12	206.06	203.53	212.20
NO <sub>3</sub>	F	146.41	146.25	142.91	194.06	194.78	196.06
CPPH <sub>3</sub> COMe	CPPH <sub>3</sub> COMe	114.36	116.87	111.61	114.36	116.87	111.61
BF <sub>4</sub>	BF <sub>4</sub>	133.52	136.80	135.39	133.52	136.80	135.39
OTf	OMe	116.92	115.53	111.42	215.87	217.88	219.55

The accuracy of the present model is assessed by LOO cross-validation procedure and excellent  $r^2_{cv}$  values of 0.976, 0.972, and 0.977 are obtained for  $d_X$ ,  $\rho(\mathbf{r})$  and  $V_{\min(X)}$  respectively, which show the high predictive nature of this model. Further, the obtained Eqs. viz. 4.4, 4.5 and 4.6 are validated using the 21 complexes given in Table 4.6. The statistical parameters of the test set respectively for Eqs. 4.4, 4.5 and 4.6 are as follows:  $s = 5.88, 6.05, \text{ and } 5.80$ ;  $r = 0.992, 0.991, \text{ and } 0.992$ . The predicted  $D_{2X}$  and  $D_{2Y}$  values using Eqs. 4.4, 4.5 and 4.6 are given in Tables 4.9 and 4.10. It can be seen that the above Eqs. can predict the BDE values (in the range 74 – 272 kcal/mol) reasonably well. Figure 4.14 illustrates the agreement between the actual and predicted BDE values as well as the predictive power of Eq. 4.6. There are 10 compounds in the training set and 4 compounds in the test set with a prediction error of more than 10 kcal/mol. If we remove these outliers and further considering the data set, the new regression equation obtained is,

$$D_{2X} = 0.988 D_{IX} + 1.394V_{\min} - 1.040E_{XY} + 18.521 \quad \dots(\text{Eq. 4.7})$$

Eq. 4.7 gives an  $s$  value of 3.56 and 3.80 for the training set and test set, respectively and shows an improved  $r$  value of more than 0.99 for both sets. The outliers are mainly the complexes with the ligand F at the axial position hence it can be assumed that the through space interactions arising from the F atom of  $\text{CF}_3$  ligand is stronger in such cases. Deviations are also expected due to steric interactions from bulky ligands. It may be noted that the constants in the above equations can vary depending on the level of theory used while these equations firmly suggest that the trans influence as well as mutual trans influence significantly affect the bond dissociation energy of ligands in hypervalent iodine complexes.

Using any of the above Eqs. it is possible to predict the BDE values of any trans combinations (X and Y) and hence to predict the most facile dissociation of a 3c-4e bond.

For example, in  $\text{CF}_3[\text{I}(\text{Br})(\text{Ph})]$  complexes, the BDE values of trans combinations Br and Ph are 108.31, and 211.19 kcal/mol, respectively. Similarly, for  $\text{CF}_3[\text{I}(\text{F})(\text{Br})]$  complexes, BDE values are 181.00 and 171.64 kcal/mol for trans combinations F and Br respectively. Thus, the I–Br bond trans to Ph ligand is 63.33 kcal/mol less stable than the I–Br bond trans to F ligand. The predicted values are also follows similar order. It is generally observed that in hypervalent iodine mediated reactions, the I–X bond which is trans to a highly trans influencing aryl ligand is cleaved regularly. Hence the understanding of BDE of I–X bonds and the influence of the trans ligand Y can be utilised for explaining the mechanistic steps involved in the cleavage of I–X bond.

**Table 4.10** The predicted bond dissociation energy values of X and Y for  $\text{CF}_3[\text{I}(\text{X})(\text{Y})]$  complexes used for the test set. All values are in kcal/mol.

Ligands in the trans positions		$D_{2X}$ predicted using the trans parameter			$D_{2Y}$ predicted using the trans parameter		
X	Y	Eq. 4.4	Eq. 4.5	Eq. 4.6	Eq. 4.4	Eq. 4.5	Eq. 4.6
$\text{BF}_4$	Ph	90.53	90.32	90.55	256.98	259.51	258.87
$\text{CPh}_3\text{COOMe}$	$\text{CPh}_3\text{COOMe}$	118.13	119.43	110.61	118.13	119.43	110.61
<i>O</i> tPr	CCH	165.41	162.66	162.38	174.77	172.59	168.62
$\text{BF}_4$	$\text{CPh}_3\text{COMe}$	84.70	86.45	80.28	250.46	253.00	252.24
$\text{NHSO}_2\text{CF}_3$	OH	135.77	133.65	130.19	203.86	202.71	203.77
OTs	<i>OO</i> tBu	131.73	129.73	125.81	199.14	197.36	193.12
$\text{C}_6\text{F}_5\text{CF}_3$	$\text{CF}_3$	132.98	131.32	138.02	157.91	156.15	161.16
$\text{C}_6\text{F}_5$	$\text{CCSiMe}_3$	133.40	130.69	128.93	155.16	153.37	157.01
$\text{CF}_2\text{CF}_2\text{CF}_3$	Ph	121.54	121.31	122.07	185.01	183.46	191.53
OCOCOOMe	Br	141.54	138.13	146.17	158.36	157.26	156.59
OCOCOOMe	CCH	130.42	127.65	127.01	195.87	194.81	194.43
OCOC $\text{Cl}_3$	$\text{CH}_2\text{Cl}$	112.23	110.65	114.54	222.02	221.57	222.88
OCOCF $_3$	OCOCF $_3$	147.94	147.70	149.65	147.94	147.70	149.65
F	Ph	145.97	145.79	146.64	225.81	224.85	222.11
F	$\text{NH}_2$	163.41	161.43	159.85	225.19	224.22	221.48
OCOCF $_3$	<i>OO</i> tBu	134.63	132.64	128.74	199.01	198.82	201.16
OAc	OH	159.33	157.24	153.97	204.11	202.17	198.52
Br	Me	110.97	110.66	113.60	222.84	219.50	228.24
OMe	Ph	147.34	147.15	148.09	201.52	199.28	195.94
$\text{NO}_2$	OMe	147.58	145.31	141.45	185.90	184.83	195.58
$\text{OSO}_2\text{Me}$	$\text{CH}_2\text{Cl}$	111.92	110.34	114.24	221.07	220.48	216.00

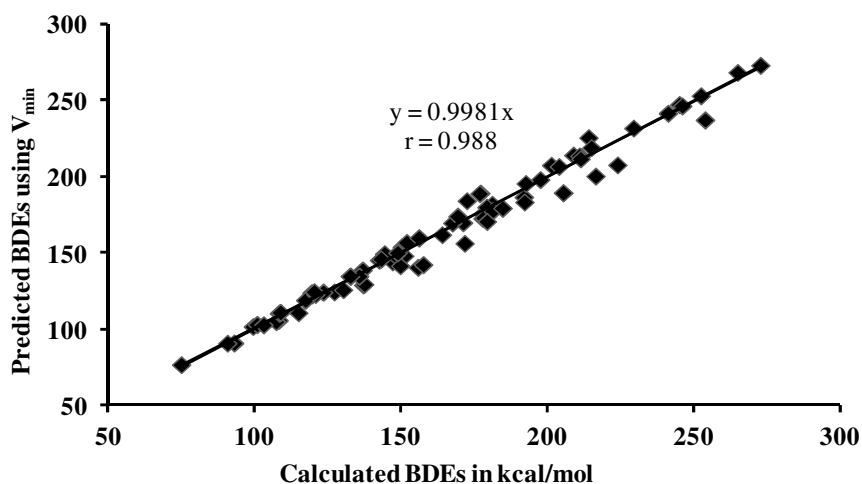


**Figure 4.14** Agreement between calculated and predicted bond dissociation energy values. All values are in kcal/mol.

## 4.5 Conclusions

The trans I–Cl bond length, electron density at the (3,-1) bond critical point at the trans I–Cl bond and the MESP minimum ( $V_{\min}$ ) at the chloro ligand in  $\text{CF}_3[\text{I}(\text{X})(\text{Cl})]$  complexes have been proposed as parameters for the quantification of trans influence of various ligands in hypervalent complexes. The  $V_{\min}$  of hypervalent iodine (III) as well as iodine(V) complexes are used as a sensitive measure of the trans influence of X. On the basis of trans influence parameters, the ligands are classified into 4 groups *viz.* very strong, strong, medium and weak trans influencing ligands. Simple isodesmic reaction of the type  $\text{CF}_3[\text{I}(\text{X})\text{Cl}] + \text{CF}_3[\text{I}(\text{Y})\text{Cl}] \rightarrow \text{CF}_3[\text{I}(\text{Cl})\text{Cl}] + \text{CF}_3[\text{I}(\text{X})\text{Y}]$  are useful for understanding the preferred trans combination of a variety of X and Y ligands. The isodesmic reaction energy,  $E_{XY}$  indicates the mutual trans influence between X and Y ligands. The medium-medium, medium-strong, weak-strong, weak- very strong *trans*

influencing combinations are found to be preferred combinations while the very strong-very strong, strong-strong, strong-very strong, weak-weak combinations are found to be unstable combinations. The mutual trans influence of a large number of (X, Y) combination is predicted with good accuracy using the trans influence parameters of X and Y ligands. Empirical equations using trans influence and mutual trans influence parameters have been derived for predicting the bond dissociation energy of either X or Y ligand in  $\text{CF}_3[\text{I}(\text{X})\text{Y}]$  complexes.

## List of Publications

### A) Articles in Journals

1. Use of molecular electrostatic potential for quantitative assessment of inductive effect : C. H. Suresh, P. Alexander, K. P. Vijayalakshmi, **P. K. Sajith** and S. R. Gadre, *Phys. Chem. Chem. Phys.* **2008**, *10*, 6492–6499.
2. Quantification of mutual trans influence of ligands in Pd(II) complexes: A combined approach using isodesmic reactions and AIM analysis : **P. K. Sajith** and C. H. Suresh, *Dalton Trans.* **2010**, *39*, 815-822.
3. Bond dissociation energies of ligands in square planar Pd(II) and Pt(II) complexes: An assessment using trans influence : **P. K. Sajith** and C. H. Suresh, *J. Organomet. Chem.* **2011**, *696*, 2086-2093.
4. Mechanisms of reductive eliminations in square planar Pd(II) complexes: Nature of eliminated bonds and role of trans influence: **P. K. Sajith** and C. H. Suresh, *Inorg. Chem.* **2011**, *50*, 8085–8093.
5. Quantification of the trans influence in hypervalent iodine complexes : **P. K. Sajith** and C. H. Suresh, *Inorg. Chem.* **2012**, *51*, 967-977.

### B) Published contributions to academic conferences

6. Presented a poster entitled “Quantification of mutual trans influence of ligands in Pd(II) complexes: A combined approach using isodesmic reactions and AIM analysis” in the National Conference on “Changing Paradigms in Theoretical and Computational Chemistry: From Atoms to Molecular Clusters” held at University of Pune, during 18-20 December 2009.
7. Presented a poster entitled “Quantification of mutual trans influence of ligands in Pd(II) complexes: An isodesmic reaction approach” in the Theoretical Chemistry Symposium 2010 held at IIT-Kanpur, India during 08–12 December 2010.
8. Presented a poster entitled “Quantification of the trans influence in hypervalent iodine complexes” in the International Conference on “Applied Theory On Molecular Systems” (ATOMS 2011) held during 2 – 5 November 2011 at CSIR-Indian Institute of Chemical Technology, Hyderabad, India.

## References

---

- Adamo, C.; Barone, V. J. "Toward reliable density functional methods without adjustable parameters: The PBE0 model" *Chem. Phys.* 110, **1999**, 6158.
- Allen, F. H. "The Cambridge Structural Database: A quarter of a million crystal structures and rising" *Acta Crystallogr.* B58, **2002**, 380.
- Allen, L. C.; Karo, A. M. "Basis Functions for Ab initio calculations" *Rev. Modern Phys.* 32, **1960**, 275.
- Al-Najjar, I. M.; Green, M.; Kerrison, S.; Sadler, P. J. "Trans effects in platinum (II) complexes: Platinum-195 nuclear magnetic resonance of nitrogen-15-labeled amine complexes" *J. Chem. Res., Syn.* 2, **1979**, 206.
- Ananikov, V. P.; Musaev, D. G.; Morokuma, K. "Vinyl-vinyl coupling on late transition metals through C–C reductive elimination mechanism. A computational study" *J. Am. Chem. Soc.* 124, **2002**, 2839.
- Ananikov, V. P.; Musaev, D. G.; Morokuma, K. "Theoretical insight into the C–C coupling reactions of the vinyl, phenyl, ethynyl, and methyl complexes of palladium and platinum" *Organometallics* 24, **2005**, 715.
- Ananikov, V. P.; Musaev, D. G.; Morokuma, K. "Critical effect of phosphane ligands on the mechanism of carbon-carbon bond formation involving palladium(II) complexes: A theoretical investigation of reductive elimination from square-planar and T-shaped species" *Eur. J. Inorg. Chem.* **2007**, 5390.
- Ananikov, V. P.; Musaev, D. G.; Morokuma, K. "Real size of ligands, reactants and catalysts: Studies of structure, reactivity and selectivity by ONIOM and other hybrid computational approaches" *J. Mol. Cat. A Chem.* 324, **2010**, 104.

- Anastasi, A. E.; Deeth, R. J. "Capturing the trans influence in low-spin  $d^8$  square-planar platinum(II) systems using molecular mechanics" *J. Chem. Theory Comput.* 5, **2009**, 2339.
- Anastasi, A. E.; Comba, P.; McGrady, J.; Lienke, A.; Rohwer, H. "Electronic structure of bispidine iron(IV) oxo complexes" *Inorg. Chem.* 46, **2007**, 6420.
- Appleton, T. G.; Clark, H. C.; Manzer, L. E. "The trans-influence: Its measurement and significant" *Coord. Chem. Rev.* 10, **1973**, 335.
- Appleton, T. G.; Bennett, M. A. "Preparation and properties of hydroxo(methyl)-1,2-bis(diphenylphosphino)ethaneplatinum(II). A trans-influence series including  $\sigma$ -carbon donor ligands based on platinum-phosphorus coupling constants" *Inorg. Chem.* 17, **1978**, 729.
- Ariafard, A.; Lin, Z. "Understanding the relative easiness of oxidative addition of aryl and alkyl halides to palladium(0)" *Organometallics* 25, **2006**, 4030.
- <sup>a</sup>Ariafard, A.; Yates, B. F. "In-depth insight into the electronic and steric effects of phosphine ligands on the mechanism of the R-R reductive elimination from  $(PR_3)_2PdR_2$ " *J. Organomet. Chem.* 694, **2009**, 2075.
- <sup>b</sup>Ariafard, A.; Yates, B. F. "Subtle balance of ligand steric effects in stille transmetalation" *J. Am. Chem. Soc.* 131, **2009**, 13981.
- Arnold, D. P.; Bennett, M. A. "Spectroscopic studies and correlation analysis of substituent effects in arylplatinum(II) complexes: cis and trans influences of aryl ligands" *Inorg. Chem.* 23, **1984**, 2117.
- Atwood, J. D. *Inorganic and Organometallic Reaction Mechanisms* Second Ed., VCH, Weinheim, **1997**.
- Bader, R. F. W. *Atoms in Molecules: A Quantum Theory*. Clarendon Press: Oxford, U. K., **1990**.

- Bader, R. F. W. "A bond path: A universal indicator of bonded interactions" *J. Phys. Chem. A* 102, **1998**, 7314.
- Bader, R. F. W.; Matta, C. F. "Bonding to titanium" *Inorg. Chem.* 40, **2001**, 5603.
- Bader, R. F. W. "Bond paths are not chemical bonds" *J. Phys. Chem. A* 113, **2009**, 10391.
- Barton, D. H. R.; Godfrey, C. R. A.; Morzycki, J. W.; Motherwell, W. B.; Stobie, A. "Observations on the chemistry of the iodoxy group" *Tetrahedron Lett.* 23, **1982**, 957.
- Basolo, F.; Pearson, R. G. "The trans effect in metal complexes" *Prog. Inorg. Chem.* 4, **1962**, 381.
- Becke, A. D. "Density-functional exchange-energy approximation with correct asymptotic behavior" *Phys. Rev. A* 38, **1988**, 3098.
- Becke, A. D. "Density-functional thermochemistry. III. The role of exact exchange" *J. Chem. Phys.* 98, **1993**, 5648.
- Belluco, U.; Graziani, M.; Rigo, P. "Influence of the entering group on the trans effect in some platinum(II) complexes" *Inorg. Chem.* 5, **1966**, 1123.
- Bel'skii, V. K.; Yu. Kukushkin, V.; Konovalov, V. E.; Moiseev, A. I.; Yakovlev, V. N. "Synthesis of QPt(Amine)XN (N = 3.5)-type platinum compounds X-ray-diffraction study of triphenylbenzylphosphonium trichloro(ammonium)-platinate(II) and triphenylbenzylphosphoniumtrichloro(pyridine) platinate(II) complexes" *Zh. Obshch. Khim.* 60, **1990**, 2180.
- Biegler-König, F.; Schönbohm, J.; Bayles, D. "AIM2000-a program to analyze and visualize atoms in molecules" *J. Comput. Chem.* 22, **2001**, 545.

- Binkley, J. S.; Pople, J.; Hehre, W. J. "Self-consistent molecular orbital methods. Small split-valence basis sets for first-row elements" *J. Am. Chem. Soc.* 102, **1980**, 939.
- Bisi-Castellani, C.; Lanfredi, A. M. M.; Tiripicchio, A.; Maresca, L.; Natile, G. "Tetrachloroplatinate(II) and hexachloroplatinate(IV) salts of N,N,N',N'-tetramethylethylenediammonium: Significant differences in the conformation of the cation, as shown by infrared and X-ray diffraction data" *Inorg. Chim. Acta* 90, **1984**, 155.
- Black, M.; Mais, R. H. B.; Owston, P. G. "The crystal and molecular structure of Zeise's salt,  $\text{KPtCl}_3 \cdot \text{C}_2\text{H}_4 \cdot \text{H}_2\text{O}$ " *Acta Cryst.* B25, **1969**, 1753.
- Boganova, L. I.; Pashchenko, D. V.; Churakov, A. V.; Minaeva, N. A.; Stromnova, T. A. "Oxidation of coordinated nitroso into nitrito group in palladium complexes: Synthesis and molecular structure of  $(\text{Pr}_4\text{P})_2[\text{Pd}_2(\text{NO}_2)_2\text{Cl}_4]$ " *Zh. Neorg. Khim.* 46, **2001**, 1481.
- Born, M.; Oppenheimer, J. R. "Zur quantentheorie der molekeln" *Ann. Phys.* 84, **1927**, 457.
- Bowen, J. P.; Allinger, N. L. "Molecular mechanics: The art and science of parameterization" *Rev. Comp. Chem.* 2, **1991**, 81.
- Boyd, D. B.; Lipkowitz, K. B. "Molecular mechanics: The method and its underlying philosophy" *J. Chem. Educ.* 59, **1982**, 269.
- <sup>a</sup>Boys, S. F. "Electronic wave functions. I. A general method of calculation for the stationary states of any molecular system" *Proc. Roy. Soc.* 200, **1950**, 542.
- <sup>b</sup>Boys, S. F. "Electronic wave functions. II. A calculation for the ground state of the beryllium atom" *Proc. Roy. Soc. (London)* 201, **1950**, 125.

- Brand, J. P.; González, D. F.; Nicolai, S.; Waser, J. "Benziodoxole-based hypervalent iodine reagents for atom-transfer reactions" *Chem. Commun.* 47, **2011**, 102.
- Braunschweig, H.; Brenner, P.; Müller, A.; Radacki, K.; Rais, D.; Uttinger, K. "Experimental studies on the trans influence of boryl ligands in square planar Platinum(II) complexes" *Chem. Eur. J.* 13, **2007**, 7171.
- Brezinski, M. M.; Schneider, J.; Radonovich, L. J.; Klabunde, K. J. " $\eta^6$ -Arene displacement by halide ions. Synthesis and structural characterization of chloro- and fluoro-bridged organonickel complexes  $[(R_2MX)_2]^{2-}$  (R = C<sub>6</sub>F<sub>5</sub>, SiCl<sub>3</sub>; X = halide)" *Inorg. Chem.* 28, **1989**, 2414.
- Brillouin, L. "Les champs self-consistents de Hartree et de Fock" *Actualities Sci. Ind.* 159, **1934**, 37.
- Brown, J. M.; Cooley, N. A. "Carbon-carbon bond formation through organometallic elimination reactions" *Chem. Rev.* 88, **1988**, 1031.
- Bulluss, G. H.; Knott, K. M.; Ma, E. S. F.; Aris, S. M.; Alvarado, E.; Farrell, N. "Trans-platinum planar amine compounds with [N<sub>2</sub>O<sub>2</sub>] ligand donor sets: Effects of carboxylate leaving groups and steric hindrance on chemical and biological properties" *Inorg. Chem.* 45, **2007**, 5733.
- Burdett, J. K.; Albright, T. A. "Trans influence and mutual influence of ligands coordinated to a central atom" *Inorg. Chem.* 18, **1979**, 2112.
- Bushmarinov, I. S.; Antipin, M. Y.; Akhmetova, V. R.; Nadyrgulova, G. R.; Lyssenko, K. A. "Stereo-electronic effects in N-C-S and N-N-C Systems: Experimental and ab initio AIM study" *J. Phys. Chem. A* 112, **2008**, 5017.
- Bushnell, G. W.; Pidcock, A.; Smith, M. A. R. "Cis- and trans-influences in platinum(II) complexes. X-ray crystal structure analysis of tetraethylammoniumtrichloro(triethylphosphine)-platinate(II)" *J. Chem. Soc., Dalton Trans.* **1975**, 572.

- Canovese, L.; Visentin, F.; Chessa, G.; Santo, C.; Dolmella, A. "Substitution reactions between bis-chelate ligands in Palladium(II) alkenyl complexes: An unusual way to form unstable trans-P complexes. A study on the isomerization mechanism" *Dalton Trans.* **2009**, 9475.
- Casellato, U.; Cavinato, G.; Graziani, R.; Toniolo, L. "Crystal structure of (cyclohexanonetriphenylphosphonium) (trichlorotriphenyl)palladate(II) - Benzene (1/1),  $[(C_6H_5)_3P(CHCH_2CO(CH_2)_3)][(C_6H_5)_3PPdCl_3] \cdot C_6H_6$ " *Z. Kristallogr. New Cryst. Struct.* **2000**, 215, 377.
- Cavallo, L. "Mechanism of ruthenium-catalyzed olefin metathesis reactions from a theoretical perspective" *J. Am. Chem. Soc.* **2002**, 124, 8965.
- Cavallo, L.; Correa, A.; Costabile, C.; Jacobsen, H. "Steric and electronic effects in the bonding of N-Heterocyclic ligands to transition metals" *J. Organomet. Chem.* **2005**, 690, 5407.
- Chass, G. A.; Kantchev, E. A. B.; Fang, D. C. "The fine balance between one cross-coupling and two  $\beta$ -hydride elimination pathways: A DFT mechanistic study of Ni( $\pi$ -allyl)<sub>2</sub>-catalyzed cross-coupling of alkyl halides and alkyl Grignard reagents" *Chem. Commun.* **2010**, 46, 2727.
- Chatt, J.; Eaborn, C.; Ibekwe, S. "Silicon, a ligand atom of exceptionally high trans-effect" *Chem. Commun.* **1966**, 700.
- Chen, W.; Matsumoto, K. "Synthesis and structural characterization of N,N'-dialkylimidazolium tetrachloroplatinate and mono aquatrachloroplatinate salts" *Bull. Chem. Soc. Jpn.* **2002**, 75, 1561.
- Chermette, H.; Rachedi, K.; Volatron, F. "Trans effect and inverse trans effect in MLX<sub>5</sub> complexes (M = Mo, U; L=O, S; X=Cl, Br): A rationalization within density functional theory study" *J. Mol. Struct. (Theochem)* **2006**, 762, 109.

- Chernyaev, I. I. "The mononitrites of bivalent platinum" *I. Ann. inst. platine (USSR)* 4, **1926**, 243.
- Chianese, A. R.; Lee, S. J.; Gagne, M. R. "Electrophilic activation of alkenes by platinum(II): So much more than a slow version of palladium(II)" *Angew. Chem., Int. Ed.* 46, **2007**, 4042.
- Chval, Z.; Sip, M.; Burda, J. V. "The trans effect in square-planar Platinum(II) complexes. A density functional study" *J. Comput. Chem.* 29, **2008**, 2370.
- Chval, Z.; Sip, M. "Pentacoordinated transition states of cisplatin hydrolysis - Ab initio study" *J. Mol. Struct. (Theochem)* 532, **2000**, 59.
- Čížek, J. "On the correlation problem in atomic and molecular systems. Calculation of wavefunction components in ursell-type expansion using quantum-field theoretical methods" *J. Chem. Phys.* 45, **1966**, 4256.
- Clementi, E. "Simple basis set for molecular wave functions containing first- and second-row atoms" *J. Chem. Phys.* 40, **1964**, 1944.
- Coe B. J.; Glenwright, S. J. "Trans-effects in octahedral transition metal complexes" *Coord. Chem. Rev.* 203, **2000**, 5.
- Cooney, K. D.; Cundari, T. R.; Hoffman, N. W.; Pittard, K. A.; Temple, M. D.; Zhao, Y. "A priori assessment of the stereoelectronic profile of phosphines and phosphites" *J. Am. Chem. Soc.* 125, **2003**, 4318.
- Correa, A.; Cavallo, L. "The elusive mechanism of olefin metathesis promoted by (NHC)Ru-based catalysts: A trade between steric, electronic, and solvent effects" *J. Am. Chem. Soc.* 128, **2006**, 13352.
- Crabtree, R. H. *The Organometallic Chemistry of the Transition Metals* John Wiley & Sons: New York, **2001**.
- Cramer, C. J. *Essentials of Computational Chemistry* John Wiley & Sons, Chichester, **2004**.

- Crumbliss, A. L.; Wilmarth, W. K. "Substitution kinetics of alkylbis (dimethylglyoximato) aquocobalt(III) in aqueous solution" *J. Am. Chem. Soc.* 92, **1970**, 2593.
- <sup>a</sup>Cui, L.-Q.; Liu, K.; Zhang, C. "Effective oxidation of benzylic and alkane C–H bonds catalyzed by sodium o-iodobenzenesulfonate with Oxone as a terminal oxidant under phase-transfer conditions" *Org. Biomol. Chem.* 9, **2011**, 2258.
- <sup>b</sup>Cui, L.-Q.; Dong, Z.-L.; Liu, K.; Zhang, C. "Design, synthesis, structure, and dehydrogenation reactivity of a water-soluble o-iodoxybenzoic acid derivative bearing a trimethylammonium group" *Org. Lett.* 13, **2011**, 6488.
- Dapprich, S.; Komaromi, I.; Byun, K. S.; Morokuma, K.; Frisch, M. J. "A new ONIOM implementation in Gaussian 98. Part I. The calculation of energies, gradients, vibrational frequencies and electric field derivatives" *J. Mol. Struct. (Theochem)* 462, **1999**, 1.
- Darensbourg, M. Y.; Ludwig, M.; Riordan, C. G. "Spectroscopic and chemical studies of Nickel( II) hydrides" *Inorg. Chem.* 28, **1989**, 1630.
- Darensbourg, D. J.; Robertson, J. B.; Larkins, D.L.; Reibenspies, J. H. "Water-soluble organometallic compounds. Further studies of 1,3,5-triaza-7-phosphaadamantane derivatives of group 10 metals, including metal carbonyls and hydrides" *Inorg. Chem.* 38, **1999**, 2473.
- Das, D.; Rao, G. K.; Singh, A. K. "Palladium(II) complexes of the first pincer (Se,N,Se) ligand, 2,6-Bis((phenylseleno)methyl)pyridine(L): Solvent-dependent formation of [PdCl(L)]Cl and Na[PdCl(L)][PdCl<sub>4</sub>] and high catalytic activity for the heck reaction" *Organometallics* 28, **2009**, 6054.
- Dedieu, A. "Theoretical studies in palladium and platinum molecular chemistry" *Chem. Rev.* 100, **2000**, 543.

- Deshmukh, M. M.; Gadre, S. R.; Tonner R.; Frenking G. "Molecular electrostatic potentials of divalent carbon(0) compounds" *Phys. Chem. Chem. Phys.* 10, **2008**, 2298.
- Dess, D. B.; Martin, J. C. "Readily accessible 12-I-5 oxidant for the conversion of primary and secondary alcohols to aldehydes and ketones" *J. Org. Chem.* 48, **1983**, 4155.
- Deubel, D. V. "Factors governing the kinetic competition of nitrogen and sulfur ligands in cisplatin binding to biological targets" *J. Am. Chem. Soc.* 126, **2004**, 5999.
- Dinur, U.; Hagler, A. T. "New approaches to empirical force fields" *Rev. Comp. Chem.* 2, **1991**, 99.
- Ditchfield, R.; Hehre, W. J.; Pople, J. "Self-consistent molecular-orbital methods. IX. An extended Gaussian-type basis for molecular-orbital studies of organic molecules" *J. Chem. Phys.* 54, **1971**, 724.
- Doll, J.; Freeman, D. L. "Monte Carlo methods in chemistry" *IEEE Comput. Sci. Eng.* 1, **1994**, 22.
- Domingos, A.; Elsegood, M. R. J.; Hillier, A. C.; Lin, G.; Liu, S. Y.; Lopes, I.; Marques, N.; Maunder, G. H.; McDonald, R.; Sella, A.; Steed, J. W.; Takats, J. "Facile pyrazolylborate ligand degradation at lanthanide Centers: X-ray crystal structures of pyrazolylborinate-bridged bimetallics" *Inorg. Chem.* 41, **2002**, 6761.
- Dreos-Garlatti, R.; Tazher, G. "Kinetic trans effect of phosphine ligands in anation reactions of aquocobaloximes" *Inorg. Chim. Acta* 142, **1988**, 263.
- Dutta, G.; Kumar, K.; Gupta, B. D. "Cobaloximes with bis(thiophenyl)glyoxime: Synthesis and structure-property relationship study" *Organometallics* 28, **2009**, 3485.

- Echavarren, A. M.; Cárdenas, D. J. *Metal-catalyzed cross-coupling reactions*, 2nd Ed.; de Meijere, A.; Diederich, F., Eds.; Wiley-VCH: Weinheim, Germany, **2004**.
- Edelmann, F. T. *Comprehensive Organometallic Chemistry*; Lappert, M. F., Ed.; Pergamon Press: Oxford, U. K., 4, **1995**.
- Egan, W. J.; Morgan, S. L. "Outlier detection in multivariate analytical chemical data" *Anal. Chem.* 70, **1998**, 2372.
- Ehlers, A. W.; Bohme, M.; Dapprich, S.; Gobbi, A.; Hollwarth, A.; Jonas, V.; Kohler, K. F.; Stegmann, R.; Veldkamp, A.; Frenking, G. "A set of f-polarization functions for pseudo-potential basis sets of the transition metals Sc...Cu, Y...Ag and La...Au" *Chem. Phys. Lett.* 208, **1993**, 111.
- Elder, R. C.; Trkula, M. "Structural trans effect in sulfur bound sulfite pentaamminecobalt(III) chloride monohydrate" *J. Am. Chem. Soc.* 96, **1974**, 2635.
- Elder, R. C.; Trkula, M. "Crystal structure of  $[(\text{NH}_3)_5\text{RuSSRu}(\text{NH}_3)_5]\text{Cl}_4 \cdot 2\text{H}_2\text{O}$ . A structural trans effect and evidence for a supersulfide  $\text{S}_2^-$  bridge" *Inorg. Chem.* 16, **1977**, 1048.
- Feller, D.; Davidson, E. R. "Basis sets for ab initio molecular orbital calculations and intermolecular interactions" *Rev. Comp. Chem.* **1990**, 1.
- Farina, V.; Krishnamurthy, V.; Scott, W. J. *The stille reaction in organic reactions*, John Wiley & Sons Inc., New York, **1997**.
- Fermi, E. "Eine statistische methode zur bestimmung einiger eigenschaften des atomes und ihre anwendung auf die theorie des periodischen systems der elemente" *Z. Phys.* 48, **1928**, 73.
- Fermi, E. "Un metodo statistice per la determinazione di alcune oroprieta dell'atomo"

*Rend. Acad. Lincei* 6, **1927**, 602.

Flemming, J. P.; Pilon M. C.; Ya Borbulevitch O.; Yu Antipin M.; Grushin, V. V. "The trans influence of F, Cl, Br and I ligands in a series of square-planar Pd(II) complexes. Relative affinities of halide anions for the metal centre in trans-[(Ph<sub>3</sub>P)<sub>2</sub>Pd(Ph)X]" *Inorg. Chim. Acta* 280, **1998**, 187.

Farrer, N, J.; Gierth, P.; Sadler, P. J. "Probing platinum azido complexes by <sup>14</sup>N and <sup>15</sup>N NMR spectroscopy" *Chem. Eur. J.* 17, **2011**, 12059.

Fock, V. "Näherungsmethode zur lösung des quantenmechanischen mehrkörper problems" *Z. Phys.* 61, **1930**, 126.

Foresman, J. B.; Head-Gordon, M.; Pople, J. A.; Frisch, M. J. "Toward a systematic molecular orbital theory for excited states" *J. Phys. Chem.* 96, **1992**, 135.

Foss, O. "Stereochemistry of tellurium(ii) complexes and related compounds" *Pure Appl. Chem.* 24, **1970**, 3.

Foss, O.; Maartmann-Moe, K. "Complexes of tellurium dichloride, dibromide and diiodide with thiourea and tetramethylselenourea, TeL<sub>2</sub>X<sub>2</sub>. X-ray crystal structures" *Acta chemica scandinavica* A41, **1987**, 121.

Freedman, D.; Melman, J. H.; Emge, T. J.; Brennan, J. G. "Cubane clusters containing lanthanide ions: (py)<sub>8</sub>Yb<sub>4</sub>Se<sub>4</sub>(SePh)<sub>4</sub> and (py)<sub>10</sub>Yb<sub>6</sub>S<sub>6</sub>(SPh)<sub>6</sub>" *Inorg. Chem.* 37, **1998**, 4162.

Gadre, S. R.; Bhadane, P. K.; Pundlik, S. S.; Pingale, S. S. *Molecular Electrostatic Potential: Concepts and Applications* Ed: J. S. Murray and K. D. Sen, Elsevier, Amsterdam, **1996**.

Gadre, S. R.; Shirsat, R. N. *Electrostatics of Atoms and Molecules*. Universities Press: Hyderabad, India, **2000**.

Gao, J. "Methods and applications of combined quantum mechanical and molecular

- mechanical potentials” *Rev. Comp. Chem.* 7, **1996**, 119.
- Gholivand, K.; Mahzouni, H. R. “Trans influence and covalent bonding in a new octahedral lanthanum(III) complex of diphenylmorpholinyl phosphinamide” *Inorg. Chim. Acta* 386, **2012**, 8.
- Giandomenico, C. M.; Abrams, M. J.; Murrer, B. A.; Vollano, J. F.; Harrap, K. R.; Goddard, P. M.; Kelland, L. R.; Morgan, S. E. *Platinum and other metal coordination compounds in cancer chemotherapy*; Howell, S. B., Ed.; Plenum Press: New York, **1991**; 93.
- Godbout, N.; Salahub, D. R.; Andzelm, J.; Wimmer, E. “Optimization of gaussian-type basis-sets for local spin-density functional calculations .1. Boron through neon, optimization technique and validation” *Can. J. Chem.* 70, **1992**, 560.
- Golbraikh, A.; Shen, M.; Xiao, Z. Y.; Xiao, Y. D.; Lee, K. H.; Tropsha, A. “Rational selection of training and test sets for the development of validated QSAR models” *J. Comput.-Aided Mol. Des.* 17, **2003**, 241.
- Goodman, J.; Grushin, V. V.; Larichev, R. B.; MacGregor, S. A.; Marshall, W. J.; Roe, D. C. “Fluxionality of  $[(\text{Ph}_3\text{P})_3\text{M}(\text{X})]$  (M = Rh, Ir). The red and orange forms of  $[(\text{Ph}_3\text{P})_3\text{Ir}(\text{Cl})]$  which phosphine dissociates faster from Wilkinson’s catalyst?” *J. Am. Chem. Soc.* 132, **2010**, 12013.
- Green, S. P.; Jones, C.; Mills, D. P.; Stasch, A. “Group 9 and 11 metal(I) allyl complexes stabilized by *N*-heterocyclic carbene coordination: First structural characterization of Ga–M (M = Cu or Ag) bonds” *Organometallics* 26, **2007**, 3424.
- Grinberg, A. A. *Izv. Inst. Izucheniya Platiny.* 10, **1932**, 58.
- Gupta, M.; Cramer, R. E.; Ho, K.; Pettersen, C.; Mishina, S.; Belli, J.; Jensen, C. M. “Trans Influence of phosphines on dimer-monomer interconversion of 2-

- pyridinethiolate complexes: structures of  $[\text{Pd}\mu\text{-}\eta^2\text{-pyS-}N,S)\text{C1(L)}]_2$  (L =  $\text{PMe}_2\text{Ph}$ ,  $\text{PMePh}_2$ ) and  $\text{Pd}(\eta^2\text{-pyS})\text{C1}(\text{PPh}_3)$ ” *Inorg. Chem.* 34, **1995**, 60.
- Gusev, D. G. “Electronic and steric parameters of 76 *N*-heterocyclic carbenes in  $\text{Ni}(\text{CO})_3(\text{NHC})$ ” *Organometallics* 28, **2009**, 6458.
- Hao, M.; Li, Y.; Wang, Y.; Yan, Y.; Zhang, S. “Combined 3D-QSAR, molecular docking, and molecular dynamics study on piperazinyl-glutamate-pyridines/pyrimidines as potent  $\text{P2Y}_{12}$  antagonists for inhibition of platelet aggregation” *J. Chem. Inf. Model.* 51, **2011**, 2560.
- Hartley, F. R. “The cis- and trans-effects of ligands” *Chem. Soc. Rev.* 2, **1973**, 163.
- Hartree, R. R. “The wave mechanics of an atom with a non-coulomb central field. Part I. theory and methods” *Proc. Cambridge Phil. Soc.* 24, **1928**, 89.
- Hartwig, J. F. “Electronic effects on reductive elimination to form carbon-carbon and carbon-heteroatom bonds from palladium(II) complexes” *Inorg. Chem.* 46, **2007**, 1936.
- Harvey, J. N.; Heslop, K. M.; Orpen, A. G.; Pringle, P. G. “Factors controlling the relative stabilities of cis- and trans- $[\text{PtX}_2\text{L}_2]$  isomers: Chatt and Wilkins-50 years on” *Chem. Commun.* **2003**, 278.
- <sup>a</sup>Hay, P. J.; Wadt, W. R. “Ab initio effective core potentials for molecular calculations. potentials for the transition metal atoms Sc to Hg” *J. Chem. Phys.* 82, **1985**, 270.
- <sup>b</sup>Hay, P. J.; Wadt, W. R. “Ab initio effective core potentials for molecular calculations. Potentials for K to Au including the outermost core orbital” *J. Chem. Phys.* 82, **1985**, 299.
- Hehre, W. J.; Ditchfield, R.; Pople, J. “Self-consistent molecular orbital methods. XII.

- Further extensions of Gaussian-type basis sets for use in molecular orbital studies of organic molecules” *J. Chem. Phys.* 56, **1972**, 2257.
- Herrmann, W. A.; Felixberger, J. K.; Anwander, R.; Herdtweck, E.; Kiprof, P.; Riede, J. “Multiple bonds between transition metals and main-group elements. 73. Synthetic routes to Rhenium(V) alkyl and Rhenium(VII) alkylidyne complexes. X-ray crystal structures of  $(\eta^5\text{-C}_5\text{Me}_5)\text{Re(=O)(CH}_3\text{)[CH}_2\text{C(CH}_3\text{)}_3\text{]}$  and  $(\eta^5\text{-C}_5\text{Me}_5)(\text{Br})_3\text{Re=CC(CH}_3\text{)}_3$ ” *Organometallics* 9, **1990**, 1434.
- Hitchcock, P. B.; Lapper, M. F.; Thomas, S. A.; Thorne, A. J.; Carty, A. J.; Taylor, N. J. “Electron-rich carbeneiron(0) trigonal bipyramidal carbonyls and their germanium(II) and tin(II) analogues  $[\text{Fe}(\text{CO})_3\text{LL}']$  (L =  $\text{CNMe}(\text{CH}_2)_2\text{NMe}$ , L' =  $\text{PEt}_3$ , 3CO's Equatorial; or L =  $\text{M}(\text{OAr})_2$  (Equatorial. M = Ge or Sn, Ar =  $\text{C}_6\text{H}_2\text{Bu}_{2-2,6}\text{-Me-4}$ ), L = CO)” *J. Organomet. Chem.* 315, **1986**, 27.
- Hocking, R. K.; Deeth, R. J.; Hambley, T. W. “DFT study of the systematic variations in metal-ligand bond lengths of coordination complexes: The crucial role of the condensed phase” *Inorg. Chem.* 46, **2007**, 8238.
- Hohenberg, P.; Kohn, W. “Inhomogeneous electron gas” *Phys. Rev.* 136, **1964**, B864.
- Hollis, L. S.; Roberts, M. M.; Lippard, S. J. “Synthesis and structures of platinum (III) complexes of  $\alpha$ -pyridone,  $[\text{X}(\text{NH}_3)_2\text{Pt}(\text{C}_5\text{H}_4\text{NO})_2\text{Pt}(\text{NH}_3)_2\text{X}](\text{NO}_3)_2 \cdot n\text{H}_2\text{O}$  ( $\text{X}^- = \text{Cl}^-, \text{NO}_2^-, \text{Br}^-$ )” *Inorg. Chem.* 22, **1983**, 3637.
- Holmes, E. *Palladium, Platinum's cheaper sister, makes a bid for love* Wall Street Journal, Eastern Ed. **2007**.
- Honeychuck, R. V.; Hersh, W. H. “Observation of a novel phosphorus-31 NMR cis-influence series: implications for the relative basicity of triphenylphosphine

- and trimethylphosphine in tungsten carbonyl complexes” *Inorg. Chem.* **26**, **1987**, 1826.
- Hope, E. G.; Levason, W.; Powell, N. A. “Coordination chemistry of higher oxidation states. Part 21. Platinum-195 NMR studies of platinum (II) and platinum (IV) complexes of bi- and multi-dentate phosphorus, arsenic and sulfur ligands” *Inorg. Chim. Acta* **115**, **1986**, 187.
- Hopmann, K. H.; Conradie, J. “Density functional theory study of substitution at the square planar acetylacetonato-dicarbonyl-rhodium(I) complex” *Organometallics* **28**, **2009**, 3710.
- Howard, J.; Woodward, P. “Crystal and molecular structure of cis-fluoro-(1,1,1,3,3,3-hexafluoroisopropyl)bis(triphenylphosphine)platinum,  $\text{PtF}[\text{CH}(\text{CF}_3)_2](\text{PPh}_3)_2$ : A square planar metal fluoro-complex” *J. Chem. Soc. Dalton Trans.* **1973**, 1840.
- Hruszkewycz, D. P.; Wu, J.; Green, J. C.; Hazari, N.; Schmeier, T. J. “Mechanistic studies of the insertion of  $\text{CO}_2$  into Palladium(I) bridging allyl dimers” *Organometallics* **31**, **2012**, 470.
- Hughes, R. P.; Meyer, M. A.; Tawa, M. D.; Ward, A. J.; Williamson, A.; Rheingold, A. L.; Zakharov, L. N. “Does  $\alpha$ -Fluorination affect the structural trans-influence and kinetic trans-effect of an alkyl ligand? Molecular structures of  $\text{Pd}(\text{TMEDA})(\text{CH}_3)(\text{R}_\text{F})$  and a kinetic study of the trans to cis isomerization of  $\text{Pt}(\text{TMEDA})(\text{CH}_3)_2\text{I}(\text{R}_\text{F})$  [ $\text{R}_\text{F} = \text{CF}_2\text{CF}_3, \text{CFHCF}_3, \text{CH}_2\text{CF}_3$ ]” *Inorg. Chem.* **43**, **2004**, 747.
- Huheey, J. E.; Keiter, E. A.; Keiter, R. L. *Inorganic chemistry: principles of structure and reactivity* Harper Collins College Publishers 4th ed.: New York, **1993**.
- Humbel, S.; Sieber, S.; Morokuma, K. “The IMOMO method: integration of different

- levels of molecular orbital approximations for geometry optimization of large systems: Test for n-butane conformation and SN2 reaction: RCl<sup>+</sup>Cl<sup>-</sup>” *J. Chem. Phys.* 105, **1996**, 1959.
- Huzinaga, S.; Andzelm, J.; Klobukowski, M.; Radzio-Andzelm, E.; Sakai, Y.; Tatewaki, H. *Gaussian basis sets for molecular calculations* Elsevier, Amsterdam, **1984**.
- Jensen, F. *Introduction to Computational Chemistry* John Wiley & Sons: Chichester, **1999**.
- Jorgensen, C. K. “Symbiotic ligands, hard and soft central atoms” *Inorg. Chem.* 3, **1964**, 1201.
- <sup>a</sup>Jones, P. G.; Williams, A. F. “Structure and bonding in gold(I) compounds. Part 1. The trans influence in linear complexes” *J. Chem. Soc., Dalton Trans.* 15, **1977**, 1430.
- <sup>b</sup>Jones, P. G.; Williams, A. F. “Structure and bonding in gold(I) compounds. Part 2. Mössbauer spectrum of linear gold(I) complexes” *J. Chem. Soc., Dalton Trans.* 15, **1977**, 1434.
- Kaluderovic, G. N.; Heinemann, F. W.; Knezevic, N. Z.; Trifunovic, S. R.; Sabo, T. J. “Crystal structure of (ethylenediammonium-N,N'-di-3-propanoic acid) tetrachloropalladate(II) complex” *J. Chem. Crystallogr.* 34, **2004**, 185.
- Karelson, M.; Lobanov, V. S.; Katritzky, A. R. “Quantum-chemical descriptors in QSAR/QSPR studies” *Chem. Rev.* 96, **1996**, 1027.
- Kapadia, R.; Pedley, J. B.; Young, G. B. “Relative metal-carbon bond enthalpies and trans influences for neopentylplatinum(II) and trimethyl silylmethyl platinum(II) complexes: An unusual case of weaker M-C binding by a β-silylmethyl ligand than its carbon analogue” *Inorg. Chim. Acta* 265, **1997**, 235.

- Kapoor, P.; Loeqvist, K.; Oskarsson, Å. "Cis/trans influences in platinum(II) complexes. X-ray crystal structures of cis-dichloro(dimethyl sulfide)(dimethyl sulfoxide)platinum(II) and cis-dichloro(dimethyl sulfide)(dimethyl phenyl phosphine)platinum(II)" *J. Mol. Struct.* 470, **1998**, 39.
- Kapoor, P. N.; Kakkar, R. "Trans and cis influence in square planar Pt(II) complexes: A density functional study of [PtClX(dms)<sub>2</sub>] and related complexes" *Theochem.* 679, **2004**, 149.
- Kasparkova, J.; Novakova, O.; Marini, V.; Najajreh, Y.; Gibson, D.; Perez, J-M.; Brabec, V. "Activation of trans geometry in bifunctional mononuclear platinum complexes by a piperidine ligand. Mechanistic studies on antitumor action" *J. Biol. Chem.* 278, **2003**, 47516.
- Kastner, M. E.; Smith, D. A.; Kuzmission, A. G.; Cooper, J. N.; Tyree, T.; Yearick, M. "Structural trans effects in some bis(ethylenediamine)cobalt(III) complexes" *Inorg. Chim. Acta* 158, **1989**, 185.
- Kelly, H. P. *Advances in chemical physics* John Wiley & Sons, New York, **1969**.
- Kiprof, P. "The nature of iodine oxygen bonds in hypervalent 10-I-3 iodine compounds" *ARKIVOC* **2004**, 19.
- Kiprof, P.; Zhdankin, V. V. "Self-assembly of hypervalent iodine through primary and secondary bonding" *ARKIVOC* **2003**, 170.
- Klamt, A.; Schuurmann, G. "COSMO: A new approach to dielectric screening in solvents with explicit expressions for the screening energy and its gradient" *J. Chem. Soc., Perkin Trans 2*, **1993**, 799.
- Knipp, M.; Karotki, A. V.; Chesnov, S.; Natile, G.; Sadler, P. J.; Brabec, V.; Vasak, M. "Reaction of Zn<sub>7</sub>metallothionein with cis- and trans-[Pt(N-donor)<sub>2</sub>Cl<sub>2</sub>]

- anticancer complexes: trans-Pt<sup>II</sup> complexes retain their N-donor ligands” *J. Med. Chem.* 50, **2007**, 4075.
- Kohn, W.; Sham, L. J. “Self-consistent equations including exchange and correlation effects” *Phys. Rev.* 140, **1965**, A1133.
- Korenaga, T.; Abe, K.; Ko, A.; Maenishi R.; Sakai, T. “Ligand electronic effect on reductive elimination of biphenyl from cis-[Pt(Ph)<sub>2</sub>(diphosphine)] complexes bearing electron-poor diphosphine: Correlation study between experimental and theoretical results” *Organometallics* 29, **2010**, 4025.
- Kornienko, A.; Emge, T.; Hall, G.; Brennan, J. G. “Chalcogen rich lanthanide clusters from halide starting materials (II): Selenido compounds” *Inorg. Chem.* 41, **2002**, 121.
- Kriegelstein, R.; Breiting, D. K.; Liehr, G. “Structural investigations of sulfite-bridged binuclear complexes of platinum(II) and palladium(II)” *Eur. J. Inorg. Chem.* **2001**, 3067.
- Krogh-Jespersen, K.; Romanelli, M. D.; Melman, J. H.; Emge, T. J.; Brennan, J. G. “Covalent bonding and the trans influence in lanthanide compounds” *Inorg. Chem.* 49, **2010**, 552.
- Kukushkin, V. Yu.; Belsky, V. K.; Konovalov, V. E.; Kirakosyan, G. A.; Konovalov, L. V.; Moiseev, A. I.; Tkachuk, V. M. “cis-influence determination of ethylene and benzyl cyanide ligands in the complexes cis-[Pt(Me<sub>2</sub>SO)(C<sub>2</sub>H<sub>4</sub>)Cl<sub>2</sub>] and cis-[Pt(Me<sub>2</sub>SO)-(PhCH<sub>2</sub>CN)Cl<sub>2</sub>] on the basis of X-ray structure data. IR and <sup>1</sup>H, <sup>13</sup>C and <sup>195</sup>Pt NMR characterization of the cis-[Pt(Me<sub>2</sub>SO)LC<sub>2</sub>] series” *Inorg. Chim. Acta* 185, **1991**, 143.
- Kümmel, H. G. *A biography of the coupled cluster method* Ed: R.F. Bishop, T. Brandes, K.A. Gernoth, N.R. Walet, Y. Xian, Recent progress in many-body theories proceedings of the 11th international conference. World Scientific

Publishing. Singapore, **2002**.

Kumar, K.; Gupta, B. D. "Synthesis, characterization and structure-property relationship studies of cobaloximes with dithienylglyoxime as the equatorial ligand" *J. Organomet. Chem.* **696**, **2011**, 3785.

Kutzelnigg, W. "Chemical bonding in higher main group elements" *Angew. Chem. Int. Ed.* **23**, **1984**, 272.

Landis, C. R.; Cleveland, T.; Firman, T. K. "Valence bond concepts applied to the molecular mechanics description of molecular shapes. 3. Applications to transition metal alkyls and hydrides" *J. Am. Chem. Soc.* **120**, **1998**, 2641.

Landrum, G. A.; Goldberg, N.; Hoffmann, R. "Bonding in the trihalides ( $X_3^-$ ), mixed trihalides ( $X_2Y^-$ ) and hydrogen bihalides ( $X_2H^-$ ). The connection between hypervalent, electron-rich three-center, donor-acceptor and strong hydrogen bonding" *J. Chem. Soc.-Dalton Trans.* **1997**, 3605.

Lang, H.; Taher, D.; Walfort, B.; Pritzkow, H. "Linear homobimetallic palladium complexes" *J. Organomet. Chem.* **691**, **2006**, 3834.

Lee, J.; Brewer, M.; Berardini, M.; Brennan, J. "Trivalent lanthanide chalcogenolates: synthesis, structure, and thermolysis chemistry" *Inorg. Chem.* **34**, **1995**, 3215.

Lee, C. T.; Yang, W. T.; Parr, R. G. "Development of the colle-salvetti correlation-energy formula into a functional of the electron density" *Phys. Rev. B* **37**, **1988**, 785.

Leopoldini, M.; Russo, N.; Toscano, M. "Determination of the catalytic pathway of a manganese arginase enzyme through density functional investigation" *Chem. -Eur. J.* **15**, **2009**, 8026.

Lewinski, J.; Gos, P.; Kopec, T.; Lipkowski, J.; Luboradzki, R. "Evidence for the trans-influence of axial substituents as a significant factor determining the

- structure and stability of five-coordinate complexes: molecular structure of the first simple five-coordinate dialkyl aluminum O,O'-chelate complex” *Inorg. Chem. Commun.* 2, **1999**, 374.
- Lin, Z.; Hall, M. B. “Theoretical studies of inorganic and organometallic reaction mechanisms. 2. The trans effect in square-planar platinum(II) and rhodium(I) substitution reactions” *Inorg. Chem.* 30, **1991**, 646.
- Lupin, M. S.; Shaw, B. L. “Electronic effects in some ruthenium(II)-carbonyl and -tertiary phosphine or -tertiary arsine complexes” *J. Chem. Soc. A* **1968**, 741.
- Luque, F. J.; Orozco, M.; Bhadane, P. K.; Gadre, S. R. “Effect of solvation on the shapes, sizes and anisotropies of polyatomic anions via molecular electrostatic potential topology: an ab initio self consistent reaction field approach” *J. Chem. Phys.* 100, **1994**, 6718.
- MacQueen, D.; Macgregor, S. A. “Theoretical study of the electronic structure of group 6  $[M(CO)_5X]$ - Species (X = NH<sub>2</sub>, OH, Halide, H, CH<sub>3</sub>) and a reinvestigation of the role of  $\pi$ -Donation in CO lability” *Inorg. Chem.* 38, **1999**, 4868.
- Madhuri, J. V.; Satyanarayana, S. “A trans influence study in propyl (aquo)cobaloxime by imidazoles and amino acids” *J. Chem. Sci.* 117, **2005**, 305.
- Malito, J.; Alyea, E. C. “A correlation of pyridine ligand cis- and trans-influences in  $[Pt(Pmes_2C_6H_2Me_2CH_2)Cl(NC_5H_4X)]$ ” *Transition Met. Chem.* 17, **1992**, 481.
- Manalastas Jr, W. W.; Dy, E. S.; Quevada1, N. P.; Kasai, H. “Trans-influence of nitrogen- and sulfur-containing ligands in trans-platinum complexes: a density functional theory study” *J. Phys.: Condens. Matter* 21, **2009**, 64210.
- Manojlovic-Muir, L.; Muir, K. W.; Solomun, T. “Cis- and trans-influence of ligands in platinum(II) complexes. The crystal and molecular structure of cis- $[PtCl_2(PEt_3)(CO)]$ ” *J. Organomet. Chem.* 142, **1977**, 265.

- Marchant, J. A.; Matsubara, T.; Ford, P. C. "Syntheses and properties of the ruthenium(III) complexes cis- and trans-Ru(NH<sub>3</sub>)<sub>4</sub>(L)X<sup>2+</sup>. Application of cyclic voltammetry to study cis and trans effects on substitution reactions of the ruthenium(II) analogues" *Inorg. Chem.* 16, **1977**, 2160.
- Maseras, F.; Morokuma, K. "IMOMM: A new integrated ab initio + molecular mechanics geometry optimization scheme of equilibrium structures and transition states" *J. Comput. Chem.* 16, **1995**, 1170.
- Mason, R.; Towl, A. D. C. "Crystal structure and stereochemistry of the solvated complex dichlorodipyridine-[o-(di-o-tolylphosphino)benzyl]rhodium(III)-0·61 chloroform: The trans-influence of ligands in octahedral complexes" *J. Chem Soc. A.* **1970**, 1601.
- Mathew, J.; Thomas, T.; Suresh, C. H. "Quantitative assessment of the stereoelectronic profile of phosphine ligands" *Inorg. Chem.* 46, **2007**, 10800.
- Mathew, J.; Koga, N.; Suresh, C. H. "C–H bond activation through  $\sigma$ -bond metathesis and agostic interactions: Deactivation pathway of a grubbs second-generation catalyst" *Organometallics* 27, **2008**, 4666.
- <sup>a</sup>Mathew, J.; Suresh, C. H. "Assessment of stereoelectronic effects in Grubbs first-generation olefin metathesis catalysis using molecular electrostatic potential" *Organometallics* 30, **2011**, 1438.
- <sup>b</sup>Mathew, J.; Suresh, C. H. "Assessment of steric and electronic effects of N-heterocyclic carbenes in grubbs olefin metathesis using molecular electrostatic potential" *Organometallics* 30, **2011**, 3106.
- Matta, C. F.; Boyd, R. J. *The quantum theory of atoms in molecules from solid state to DNA and drug design*, Wiley-VCH; **2007**.

- McQuarrie, D. A.; Simon, J. A. *Physical Chemistry, A Molecular Approach*; University Science Books: Sausalito, **1997**. Lowe, J.P. *Quantum Chemistry*, Academic Press Inc.: New York, **1978**.
- McWeeny, R.; Mason, R.; Towl, A. D. C. "The geometries of and bonding in certain transition metal complexes" *Faraday Discuss.* 47, **1969**, 20.
- Melnik, M.; Holloway, C. E. "Stereochemistry of platinum coordination compounds" *Coord Chem. Rev.* 250, **2006**, 226.
- Merritt, E. A.; Olofsson, B. "∞-functionalization of carbonyl compounds using hypervalent iodine reagents" *Synthesis* **2011**, 517.
- Milani, B.; Marson, A.; Zangrando, E.; Mestroni, G.; Ernsting, J. M.; Elsevier, C. J. "New monocationic methylpalladium(II) compounds with several bidentate nitrogen-donor ligands: Synthesis, characterisation and reactivity with CO" *Inorg. Chem. Acta.* 327, **2002**, 188.
- Michelin, R. A.; Ros, R. "Synthesis of hydridotrifluoromethyl complexes of platinum(II). A spectroscopic investigation of the trans and cis influence of ligands in hydridoplatinum(II) compounds" *J. Chem. Soc., Dalton Trans.* **1989**, 1149.
- Minkwitz, R.; Berkei, M. "A new preparation and crystal structure of trifluoromethyl iodine difluoride CF<sub>3</sub>IF<sub>2</sub>" *Inorg. Chem.* 37, **1998**, 5247.
- Minkwitz, R.; Berkei, M. "A new method for preparation and crystal structure of (trifluoromethyl)iodine dichloride" *Inorg. Chem.* 38, **1999**, 5041.
- Minkwitz, R.; Berkei, M.; Ludwig, R. "Synthesis and characterization of novel iodine(III) compounds; Crystal structures of toxy(trifluoromethyl)iodine(III) chloride [CF<sub>3</sub>I(Cl)OCH<sub>3</sub>] and

- dimethoxy(trifluoromethyl)iodine(III) [CF<sub>3</sub>I(OCH<sub>3</sub>)<sub>2</sub>]" *Eur. J. Inorg. Chem.* **2000**, 2387.
- Mitoraj, M. P.; Zhu, H.; Michalak, A.; Ziegler, T. "On the origin of the trans-influence in square planar d<sup>8</sup>- complexes: A theoretical study" *Int. J. Quantum Chem.* **109**, **2009**, 3379.
- Moigno, D.; Kiefer, W.; Callejas-Gaspar, B.; Gil-Rubiob, J.; Werner H. "Meta-carbon vibrational modes as a probe of the trans influence in vinylidene and carbonyl rhodium(I) complexes" *New J. Chem.* **25**, **2001**, 1389.
- Mordasini, T. Z.; Thiel, W. "Combined quantum mechanical and molecular mechanical approaches" *Chimia* **52**, **1998**, 288.
- Moriarty, R. M.; Prakash, O. *Hypervalent iodine in organic chemistry: Chemical transformations*; Wiley-Interscience, **2008**.
- Muenzenberg, R.; Rademacher, P.; Boese, R. "Chiral platinum(II) complexes with phosphorus derivatives of the amino acid l-proline. NMR spectroscopic and X-ray structure investigations of the cis influence of tertiary phosphorus ligands" *J. Mol. Struct.* **444**, **1998**, 77.
- Musher, J. I. "The chemistry of hypervalent molecules" *Angew. Chem. Int. Ed.* **8**, **1969**, 54.
- Nakajima, K.; Kojima, M.; Fujita, J.; Ishii, T.; Ohba, S.; Ito, M.; Saito, Y. "Preparation and characterization of [M<sup>III</sup>(SeCH<sub>2</sub>CH<sub>2</sub>NH<sub>2</sub>){N(CH<sub>2</sub>CH<sub>2</sub>NH<sub>2</sub>)<sub>3</sub>}]<sup>2+</sup> (M<sup>III</sup> = Co, Rh) and molecular structure of the perchlorate of the rhodium(III) complex" *Inorg. Chim. Acta.* **99**, **1985**, 143.
- Nakanishi, W.; Hayashi, S.; Narahara, K. "Polar coordinate representation of H<sub>b</sub>(**r**<sub>c</sub>) versus (ħ<sup>2</sup>/8m)∇<sup>2</sup>ρ<sub>b</sub>(**r**<sub>c</sub>) at bcp in AIM analysis: Classification and evaluation of weak to strong interactions" *J. Phys. Chem. A* **113**, **2009**, 10050.

- <sup>a</sup>Nakanishi, W.; Hayashi, S. "Atoms-in-molecules dual functional analysis of weak to strong interactions" *Curent. Org. Chem.* 14, **2010**, 181.
- <sup>b</sup>Nakanishi, W.; Hayashi, S. "Dynamic behaviors of interactions: application of normal coordinates of internal vibrations to AIM dual functional analysis" *J. Phys. Chem. A* 114, **2010**, 7423.
- Negishi, E.; Anastasia, L. "Palladium-catalyzed alkynylation" *Chem. Rev.* 103, **2003**, 1979.
- Negishi, E.; Takahashi, T.; Akiyoshi, K. "Palladium-catalyzed or promoted reductive carbon-carbon coupling. Effects of phosphines and carbon ligands" *J. Organomet. Chem.* 334, **1987**, 181.
- Negishi, E. *Handbook of Organopalladium Chemistry for Organic Synthesis*, Wiley Interscience, New York, **2002**.
- Negishi, E.; Wang, G. W.; Rao, H. H.; Xu, Z. Q. "Alkyne elementometalation-pd-catalyzed cross-coupling. toward synthesis of all conceivable types of acyclic alkenes in high yields, efficiently, selectively, economically, and safely: 'green' way" *J. Org. Chem.* 75, **2010**, 3151.
- Nekrasov, B.V. *J. Gen. Chem. USSR*, 7, **1937**, 1594.
- Netland, K. A.; Krivokapic, A.; Tilset, M. "Pt(II) complexes with diimine and chelating 5-ring iminocarbene ligands: synthesis, characterization, and structural and spectroscopic trends" *J. Coord. Chem.* 63, **2010**, 2909.
- Norton, K.; Kumar, G. A.; Dilks, J. L.; Emge, T. J.; Riman, R. E.; Brik, M. G.; Brennan, J. G. "Lanthanide compounds with fluorinated aryloxy ligands: Near-infrared emission from Nd, Tm, and Er" *Inorg. Chem.* 48, **2009**, 3573.
- Ochiai, M. *Chemistry of Hypervalent Compounds*; Wiley-VCH, New York, **1999**.
- Ochiai, M. "Hypervalent Iodine Chemistry" *Top. Curr. Chem.* 224, **2003**, 5.

- Ochiai, M.; Takeuchi, Y.; Katayama, T.; Sueda, T.; Miyamoto, K. "Iodobenzene-catalyzed  $\alpha$ -acetoxylation of ketones. In situ generation of hypervalent (diacyloxyiodo)benzenes using m-chloroperbenzoic acid" *J. Am. Chem. Soc.* 127, **2005**, 12244.
- Ochiai, M.; Sueda, T.; Miyamoto, K.; Kiprof, P.; Zhdankin, V. V. "Trans influences on hypervalent bonding of aryl  $\lambda^3$ -iodanes: their stabilities and isodesmic reactions of benziodoxolones and benziodazolone" *Angew. Chem. Int. Ed.* 45, **2006**, 8203.
- Ochiai, M. "Stoichiometric and catalytic oxidations with hypervalent organo-  $\lambda^3$ -iodanes" *Chem. Rec.* 7, **2007**, 12.
- Ochiai, M.; Miyamoto, K.; Hayashi, S.; Nakanishi, W. "Hypervalent N-sulfonylimino-  $\lambda^3$ -bromane: Active nitrenoid species at ambient temperature under metal-free conditions" *Chem. Commun.* 46, **2010**, 511.
- Ohnishi, Y.; Matsunaga, T.; Nakao, Y.; Sato, H.; Sakaki, S. "Ruthenium(II)-catalysed hydrogenation of carbon dioxide to formic acid. Theoretical study of real catalyst, ligand effects and solvation effects" *J. Am. Chem. Soc.* 127, **2005**, 4021.
- Okazaki, M.; Ohshitanai, S.; Iwata, M.; Tobita, H.; Ogino, H. "Synthesis and reactivity of (phosphinoalkyl)silyl complexes" *Coord. Chem. Rev.* 226, **2002**, 167.
- Otto, S.; Johansson, M. H. "Quantifying the trans influence of triphenylarsine. Crystal and molecular structures of cis-[PtCl<sub>2</sub>(SMe<sub>2</sub>)(AsPh<sub>3</sub>)] and cis-[PtCl<sub>2</sub>(AsPh<sub>3</sub>)<sub>2</sub>] $\cdot$ CHCl<sub>3</sub>" *Inorg. Chim. Acta* 329, **2002**, 135.
- Owen, J. S.; Labinger, J. A.; Bercaw, J. E. "Pyridinium-derived N-heterocyclic carbene complexes of platinum: Synthesis, structure and ligand substitution kinetics" *J. Am. Chem. Soc.* 126, **2004**, 8247.

- Palusiak, M. "Substituent effect in para substituted Cr(CO)<sub>5</sub>-pyridine complexes" *J. Organomet. Chem.* 692, **2007**, 3866.
- Palusiak, M.; Krygowski, T. M. "Application of AIM parameters at ring critical points for estimation of p-electron delocalization in six-membered aromatic and quasi-aromatic rings" *Chem. -Eur. J.* 13, **2007**, 7996.
- Palusiak, M.; Fonseca, G.; Bickelhaupt, F. M. "π-Electronic communication through mono and multinuclear Gold(I) complexes" *Int. J. Quantum Chem.* 109, **2009**, 2507.
- Palusiak, M.; Krygowski, T. M. "Unusual electron density topology and intramolecular steric π-π interaction in 1,3,5,7-cyclooctatetraene" *Chem. Phys. Lett.* 481, **2009**, 34.
- Parish, R. V.; Howe, B. P.; Wright, J. P.; Mack, J.; Pritchard R. G.; Buckley, R. G.; Elsome, A. M.; Fricker, S. P. "Chemical and biological studies of dichloro(2-((dimethylamino)methyl)phenyl)gold(III)" *Inorg. Chem.* 35, **1996**, 1659.
- Pfeiffer, J.; Schubert, U. "Transition metal silyl complexes. Enhanced reactivity of a platinum dimethyl complex toward trimethoxysilane due to a P,N-chelating co ligand" *Organometallics* 18, **1999**, 3245.
- Phukan, A. K.; Guha, A. K. "Nature of transannular intramolecular interactions in group 4 and 6 metallatranes: A combined density functional theory and atoms in molecules theory study" *Inorg. Chem.* 49, **2010**, 9884.
- Pearson, R. G. "Antisymbiosis and the trans effect" *Inorg. Chem.* 12, **1973**, 712.
- Perdew, J. P. "Density-functional approximation for the correlation energy of the inhomogeneous electron gas" *Phys. Rev. B* 33, **1986**, 8822.

- Perdew, J. P.; Burke, K.; Ernzerhof, M. "Generalized gradient approximation made simple" *Phys. Rev. Lett.* 77, **1996**, 3865.
- Perkins, C. W.; Martin, J. C.; Arduengo, A. J.; Law, W.; Alegria, A.; Kochi, J. K. "An electrically neutral s-sulfuranyl radical from the homolysis of a perester with neighboring sulfenyl sulfur: 9-S-3 species" *J. Am. Chem. Soc.* 102, **1980**, 7753.
- Pidcock, A.; Richards, R. E.; Venanzi, L. M. "<sup>195</sup>Pt-<sup>31</sup>P nuclear spin coupling constants and the nature of the trans-effect in platinum complexes" *J. Chem. Soc. (A)* **1966**, 1707.
- Pimentel, G. C. "The bonding of trihalide and bifluoride ions by the molecular orbital method" *J. Chem. Phys.* 19, **1951**, 446.
- Politzer, P.; Truhlar, D. G. *Chemical Applications of Atomic and Molecular Electrostatic Potentials*. Plenum Press: New York, **1981**.
- Politzer, P.; Murray, J. S. "Relationships between Dissociation Energies and Electrostatic Potentials of C-NO<sub>2</sub> Bonds: Applications to Impact Sensitivities" *J. Mol. Struct.* 376, **1996**, 419.
- Politzer, P.; Murray, J. S. "The Fundamental Nature and Role of the Electrostatic Potential in Atoms and Molecules" *Theor. Chem. Acc.* 108, **2002**, 134.
- Politzer, P. "Atomic and molecular energies as functionals of the electrostatic potential" *Theor. Chem. Acc.* 111, **2004**, 395.
- Pople, J. A.; Beveridge, D. L. *Approximate Molecular Orbital Theory*, McGraw-Hill, New York, **1970**.
- Pople, J. A.; Binkley, J. S.; Seeger, R. "Theoretical Models Incorporating Electron Correlation" *Int. J. Quantum Chem. Symp.* 10, **1976**, 1.

- Prenzler, P. D.; Hockless, D. C. R.; Heath, G. A. "Steric and electronic effects in the first homoleptic imino ether complex: Synthesis and X-ray crystallographic determination of  $[\text{Pt}(\text{NHC}(\text{OEt})\text{Et})_4](\text{CF}_3\text{SO}_3)_2$ " *Inorg. Chem.* **36**, **1997**, 5845.
- Randaccio, L.; Furlan, M.; Geremia, S.; Šlouf, M.; Srnova, I.; Toffoli, D. "Similarities and differences between cobalamins and cobaloximes. Accurate structural determination of methylcobalamin and of LiCl- and KCl-containing cyanocobalamins by synchrotron radiation" *Inorg. Chem.* **39**, **2000**, 3403.
- Rapaport, D. C. *The Art of Molecular Dynamics Simulation*, Cambridge University Press, Cambridge, **2004**.
- Raymond, K. N.; Eigenbrot, C. W. "Structural criteria for the mode of bonding of organoactinides and lanthanides and related compounds" *Acc. Chem. Res.* **13**, **1980**, 276.
- Rigamonti, L.; Manassero, C.; Rusconi, M.; Manassero, M.; Pasini, A. "Cis Influence in trans-Pt(PPh<sub>3</sub>)<sub>2</sub> complexes" *Dalton Trans.* **2009**, 1206.
- <sup>a</sup>Rigamonti, L.; Rusconi, M.; Manassero, C.; Manassero, M.; Pasini, A. "Quantification of cis and trans influences in  $[\text{PtX}(\text{PPh}_3)_3]^+$  complexes. A <sup>31</sup>P NMR study" *Inorg. Chim. Acta.* **363**, **2010**, 3498.
- <sup>b</sup>Rigamonti, L.; Forni, A.; Manassero, M.; Manassero, C.; Pasini, A. "Cooperation between cis and trans influences in cis-Pt II(PPh<sub>3</sub>)<sub>2</sub> complexes: Structural, spectroscopic, and computational studies" *Inorg. Chem.* **49**, **2010**, 123.
- Rigamonti, L.; Rusconi, M.; Forni, A.; Pasini, A. "The role of the atomic charges on the ligands and platinum(ii) in affecting the cis and trans influences in  $[\text{PtXL}(\text{PPh}_3)_2]^+$  complexes (X = NO<sub>3</sub>, Cl, Br, I; L = 4-substituted pyridines, amines, PPh<sub>3</sub>). A <sup>31</sup>P NMR and DFT investigation" *Dalt. Trans.* **40**, **2011**, 10162.

- Rocha, W. R.; deAlmeida, W. B. "Theoretical study of the olefin insertion reaction in the heterobimetallic  $\text{Pt}(\text{H})(\text{PH}_3)_2(\text{SnCl}_3)(\text{C}_2\text{H}_4)$  compound" *Organometallics* 17, **1998**, 1961.
- Roecker, L.; Dickman, M. H.; Nosco, D. L.; Doedens, R. J.; Deutsch, E. "Syntheses and characterization of bis(ethylenediamine)cobalt(III) complexes containing chelated thioether and selenoether ligands. Single-crystal structure analysis of [(1-ethyl-2,5-dioxo-3-pyrrolidiny] 2-aminoethyl thioether)-N,S]bis(ethylenediamine)cobalt(III) perchlorate" *Inorg. Chem.* 22, **1983**, 2022.
- Rogers, D.; Hopfinger, A. J. "Application of genetic function approximation to quantitative structure-activity relationships and quantitative structure-property relationships" *J. Chem. Inf. Comput. Sci.* 34, **1994**, 854.
- Roodt, A.; Otto, S.; Steyl, G. "Structure and solution behaviour of rhodium(I) Vaska-type complexes for correlation of steric and electronic properties of tertiary phosphine ligands" *Coord. Chem. Rev.* 245, **2003**, 121.
- Rosenberg, B.; Van Camp, L.; Trosko, J. E.; Mansour, V. H. "Platinum compounds: a new class of potent antitumour agents" *Nature* 222, **1969**, 385.
- Rudd, M. D.; Lindeman, S. V.; Husebye, S. "Three-centre, four-electron bonding and structural characteristics of two-coordinate iodine(I) complexes with halogen and chalcogen ligands. Synthesis, spectroscopic characterization and X-ray structural studies of (triiodo)-[tris(dimethylamino)phosphane selenide] iodine(I) and Bis{triiodo}[tri(N-morpholy] phosphane selenide] iodide(I)/Diiodine molecular complex" *Acta. Chemica. Scandinavica.* 51, **1997**, 689.
- Russell, D. R.; Tucker, P. A.; Wilson, S. "The crystal structure of tetrabutylammonium trichlorocarbonylplatinate(II)" *J. Organomet. Chem.* 104, **1976**, 387.

- Sakaki, S.; Masahiro, O.; Musashi, Y.; Ami, T. "C<sub>2</sub>H<sub>4</sub> Insertion into Pt<sup>II</sup>-SiH<sub>3</sub> and Pt<sup>II</sup>-H Bonds. An ab Initio MO/MP4 Study" *J. Am. Chem. Soc.* 116, **1994**, 7258.
- Salcedo, R.; Sharma, P.; Cabrera, A.; Fomine, S.; "Triphenylstybine complexes of Pt(II), theoretical description and trans influence study" *Theochem* 579, **2002**, 151.
- Sargent, A. L.; Hall, M. B. "Theoretical studies of inorganic and organometallic reaction mechanisms. 4. oxidative addition of dihydrogen to d<sup>8</sup> square-planar iridium complexes with trans phosphines" *Inorg. Chem.* 31, **1992**, 317.
- Sayyed, F. B.; Suresh, C. H. "An electrostatic scale of substituent resonance effect" *Tetrahedron Lett.* 50, **2009**, 7351.
- Sayyed, F. B.; Suresh, C. H.; Gadre, S. R. "Appraisal of through-bond and through-space substituent effects via molecular electrostatic potential topography" *J. Phys. Chem. A* 114, **2010**, 12330.
- Sayyed, F. B.; Suresh, C. H. "Substituent effects in cation-π interactions: A unified view from inductive, resonance, and through-space effects" *J. Phys. Chem. A* 115, **2011**, 5660.
- Schlegel, H. B. "An efficient algorithm for calculating ab initio energy gradients using s, p cartesian gaussians" *J. Chem. Phys.* 77, **1982**, 3676.
- Schlick, T. *Molecular Modeling and Simulation*, Springer-Verlag, New York, **2002**.
- Schrödinger, E. "Quantisierung als eigenwertproblem" *Ann. Phys.* 79, **1926**, 361.
- Shustorovich, E. M. "Perturbation theory, 3-orbital-4-electron and 4-orbital-4-electron bonding, and the inductive effect in tetrahedral compounds" *J. Am. Chem. Soc.* 100, **1978**, 7513.

- Shavitt, I. *Methods in computational physics* Academic Press, New York, **1963**.
- Shustorovich, E. M.; Buslaev, Y. A. "Mutual influence of ligands in main group element coordination compounds" *Inorg. Chem.* 15, **1976**, 1142.
- Slater, J. C. "Note on Hartree's Method" *Phys. Rev.* 35, **1930**, 210.
- Sokolov, A. Yu.; Sizova, O. V. "Quantum-chemical study of trans influence in gold(I) linear complexes" *Russ. J. Gen. Chem.* 80, **2010**, 1223.
- Sosa, C.; Andzelm, J.; Elkin, B. C.; Wimmer, E.; Dobbs, K. D.; Dixon, D. A. "A local density functional study of the structure and vibrational frequencies of molecular transition-metal compounds" *J Phys. Chem.* 96, **1992**, 6630.
- Stang, P. J.; Zhdankin, V. V. "Organic polyvalent iodine compounds" *Chem. Rev.* 96, **1996**, 1123.
- Stein, C. A.; Ellis, P. E. Jr.; Elder, R. C.; Deutsch, E. "Synthesis and characterization of cobalt(III) complexes containing a coordinated selenol. A structural trans effect in (2-selenolatoethylamine-N,Se)bis(ethylenediamine)cobalt(III) nitrate" *Inorg. Chem.* 15, **1976**, 1618.
- Sternberg, M.; Suresh, C. H.; Mohr, F. "2-Thia-1,3,5-triaza-7-phosphaadamantane-2,2-dioxide Revisited: Computational and experimental studies of a neglected phosphine" *Organometallics* 29, **2010**, 3922.
- Stewart, J. J. P. "Semiempirical molecular orbital methods" *Rev. Comp. Chem.* 1, 1990, 45.
- Strömberg, S.; Svensson, M.; Zetterberg, K. "Binding of ethylene to anionic, neutral, and cationic nickel(ii), palladium(ii), and platinum(ii) cis/trans chloride ammonia complexes. A theoretical study" *Organometallics* 16, **1997**, 3165.
- Stranks, D. R.; Yandell, J. K. "Dissociative mechanisms for substitution of sulfite complexes" *Inorg. Chem.* 9, **1970**, 751.

- Sturmayr, D.; Schubert, U. "Ab-initio calculations of T-shaped phosphine-platinum(II) complexes" *Monatshefte fur Chemie* 134, **2003**, 791.
- Su, J. T.; Goddard, W. A. "Enhancing 2-iodoxybenzoic acid reactivity by exploiting a hypervalent twist" *J. Am. Chem. Soc.* 127, **2005**, 14146.
- Sugimoto, M.; Yamasaki, I.; Mizoe, N.; Anzai, M.; Sakaki, S. "Acetylene-insertion reactions into Pt(II)-H and Pt(II)-SiH<sub>3</sub> bonds. An abinitio MO study and analysis based on the vibronic coupling model" *Theor. Chem. Acc.* 102, **1999**, 377.
- Suresh, C. H.; Gadre, S. R. "A novel electrostatic approach to substituent constants: doubly substituted benzenes" *J. Am. Chem. Soc.* 120, **1998**, 7049.
- Suresh, C. H.; Koga, N.; Gadre, S. R. "Molecular electrostatic potential and electron density topography: Structure and reactivity of (substituted arene) Cr(CO)<sub>3</sub> Complexes" *Organometallics* 19, **2000**, 3008.
- Suresh, C. H.; Koga, N. "Quantifying the electronic effect of substituted phosphine ligands via molecular electrostatic potential" *Inorg. Chem.* 41, **2002**, 1573.
- Suresh, C. H.; Baik, M. H. "α, β-(C-C-C) agostic bonds in transition metal based olefin metathesis catalyses" *Dalton Trans.* **2005**, 2982.
- <sup>a</sup>Suresh, C. H. "Molecular electrostatic potential approach to determining the steric effect of phosphine ligands in organometallic chemistry" *Inorg. Chem.* 45, **2006**, 4982.
- <sup>b</sup>Suresh, C. H. "Nature of α, β-CCC agostic bonding in metallacyclobutanes" *J. Organomet. Chem.* 691, **2006**, 5366.
- Suresh, C. H.; Gadre, S. R. "Electrostatic potential minimum of the aromatic ring as a measure of substituent constant" *J. Phys. Chem. A.* 111, **2007**, 710.

- Suresh, C. H.; Alexander, P.; Vijayalakshmi, K. P.; Sajith, P. K.; Gadre, S. R. "Use of molecular electrostatic potential for quantitative assessment of inductive effect" *Phys. Chem. Chem. Phys.* 10, **2008**, 6492.
- Suresh, C. H.; Gadre, S. R. "Electrostatic potential minimum of the aromatic ring as a measure of substituent constant" *J. Phys. Chem. A.* 111, **2007**, 710.
- Suzuki, K.; Yamamoto, H. "Synthesis and characterization of  $MCl(CH_2COY)(PPh_3)_2$  ( $M = Pd, Pt$ ;  $Y = C_6H_5, CH_3, CH_2Cl$ )" *Inorg. Chim. Acta* 208, **1993**, 225.
- Syrkin, Y.K. *Izv. Akad. Nauk SSSR Otd. Khim. Nauk* **1948**, 69.
- Szabo, A.; Ostlung, N. A. *Modern quantum chemistry: Introduction to advanced electronic structure theory*, McGraw-Hill: New York, **1989**.
- Szatyłowicz, H.; Krygowski, T. M.; Panek, J. J.; Jezierska, A. "H-bonded complexes of aniline with HF/F<sup>-</sup> and anilide with HF in terms of symmetry-adapted perturbation, atoms in molecules, and natural bond orbitals theories" *J. Phys. Chem. A.* 112, **2008**, 9895.
- Tamao, K.; Sumitani, K.; Kumada, M. "Selective carbon-carbon bond formation by cross-coupling of Grignard reagents with organic halides. Catalysis by nickel-phosphine complexes" *J. Am. Chem. Soc.* 94, **1972**, 4374.
- Tao, J.; Perdew, J. P.; Staroverov, V. N.; Scuseria, G. E. "Climbing the density functional ladder: Nonempirical meta-generalized gradient approximation designed for molecules and solids" *Phys. Rev. Lett.* 91, **2003**, 146401.
- Tatsumi, K.; Hoffmann, R.; Yamamoto, A.; Stille, J. K. "Reductive elimination of d<sup>8</sup>-organotransition metal complexes" *Bull. Chem.Soc. Jpn.* 54, **1981**, 1857.
- Tau, K. D.; Meek, D. W. "Platinum(II) complexes of the chelating triphosphine bis(3-(diphenylphosphino)propyl)phenylphosphine. Phosphorus-31 NMR studies of the cis and trans influence on these model compounds" *Inorg. Chem.* 18, **1979**, 3574.

- Tessier, C.; Rochon F. D. "Multinuclear NMR study and crystal structures of complexes of the types cis- and trans-Pt(YPy)<sub>2</sub>X<sub>2</sub>, where Ypy = pyridine derivative and X = Cl and I" *Inorg. Chim. Acta* 95, **1999**, 25.
- Tfouni, E.; Ford, P. C. "Thermal and photochemical properties of some trans-disubstituted tetraammineruthenium(II) complexes of aromatic nitrogen heterocycles, trans-Ru(NH<sub>3</sub>)<sub>4</sub>LL<sup>n+</sup>" *Inorg. Chem.* 19, **1980**, 72.
- Thomas, L. H. "The calculation of atomic fields" *Proc. Cambridge Phil. Soc.* 23, **1927**, 542.
- Thomson, L. M.; Hall, M. B. "A theoretical study of the primary oxo transfer reaction of a dioxo molybdenum(VI) compound with imine thiolate chelating ligands: A molybdenum oxotransferase analogue" *J. Am. Chem. Soc.* 123, **2001**, 3995.
- Tilley, T. D.; Patai, S.; Rappoport, Z. *The chemistry of organic silicon compounds* Wiley, New York, **1989**, 1415.
- Tohma, H.; Kita, Y. "Hypervalent iodine reagents for the oxidation of alcohols and their application to complex molecule synthesis" *Adv. Synth. Catal.* 346, **2004**, 111.
- Tolman, C. A. "Electron donor-acceptor properties of phosphorus ligands. Substituent additivity" *J. Am. Chem. Soc.* 92, **1970**, 2953.
- Tolman, C. A. "Steric effects of phosphorus ligands in organometallic chemistry and homogeneous catalysis" *Chem. Rev.* 77, **1977**, 313.
- Tsipis, A. C.; Orpen, A. G.; Harvey, J. N. "Substituent Effects and the mechanism of alkene metathesis catalyzed by ruthenium dichloride catalysts" *Dalton Trans.* **2005**, 2849.
- Tsuiji, J. *Palladium Reagents and Catalysts: New Perspectives for the 21st Century*; Wiley, Chichester: **2004**.

- Tsuji, H.; Inoue, T.; Kaneta, Y.; Sase, S.; Kawachi, A.; Tamao, K. "Synthesis, structure, and properties of 9-phospha-10-silatriptycenes and their derivatives" *Organometallics* 25, **2006**, 6142.
- Tubert-Brohman, I.; Schmid, M.; Meuwly, M. "Molecular mechanics force field for octahedral organometallic compounds with inclusion of the trans influence" *J. Chem. Theory Comput.* 5, **2009**, 530.
- Varvoglis, A. *The Organic Chemistry of Polycoordinated Iodine*; VCH, New York, **1992**.
- Venanzi, L. M. "Phosphine complexes.  $\sigma$  vs  $\pi$  bonds and the nature of the trans effect" *Chem. Brit.* 4, **1968**, 162.
- Vapnik, V. N. *Statistical learning theory* Wiley, New York, **1998**, 736.
- Vapnik, V. N. *The Nature of statistical learning theory* Springer, New York, **2000**.
- von Schenck, H.; Akermark, B.; Svensson, M. "Electronic control of the regiochemistry in the Heck Reaction" *J. Am. Chem. Soc.* 125, **2003**, 3503.
- Warshel, A.; Levitt, M. "Theoretical studies of enzymatic reactions: Dielectric, electrostatic and steric stabilization of the carbonium ion in the reaction of lysozyme" *J. Mol. Biol.* 103, **1976**, 227.
- Watt, G. W.; Cude, W. A. "Secondary trans effect in platinum(II) complexes" *J. Am. Chem. Soc.* 90, **1968**, 6382.
- Weiner, P. K.; Kollman, P. A. "AMBER: Assisted model building with energy refinement. A general program for modeling molecules and their interactions" *J. Comput. Chem.* 2, **1981**, 287.
- Wendt, O. F.; Ake Oskarsson; Leipoldt, J. G.; Elding L. I. "Synthesis, structure, and reactivity of arylchlorobis(dialkyl sulfide)platinum(II) complexes" *Inorg. Chem.* 36, **1997**, 4514.

- Wendt, O. F.; Elding, L. I. "Trans Effect and trans influence of triphenyl-stibine and phosphine in platinum(II) complexes. A comparative mechanistic and structural study" *J. Chem. Soc., Dalton Trans.* **1997**, 4725.
- Werner, A. "Beitrg zur konstitution anorganischer" *Verndungen Zeitschrift für anorganische Chemie* **3**, **1893**, 267.
- Willgerodt, C. "Ueber einige aromatische Jodid Chloride" *J. Prakt. Chem.* **33**, **1886**, 154.
- Wilkins, R. G. *Kinetics and Mechanism of Reactions of Transition Metal Complexes* Wiley-VCH Verlag; 2nd, **1991**.
- Wold, S.; Ruhe, A.; Wold, H.; Dunn, W. III "The collinearity problem in linear regression. The partial least squares (PLS) approach to generalized inverses" *SIAM J. Sci. Stat. Comput.* **5**, **1984**, 735.
- Wysokinski, R.; Michalska, D. "The performance of different density functional methods in the calculation of molecular structures and vibrational spectra of platinum(II) antitumor drugs: cisplatin and carboplatin" *J. Comp. Chem.* **22**, **2001**, 901.
- Xue, L.; Lin, Z. "Theoretical aspects of palladium-catalysed carbon-carbon cross-coupling reactions" *Chem. Soc. Rev.* **39**, **2010**, 1692.
- Yamanaka, M.; Mikami, K. "Theoretical study on the Tropos nature of the BIPHEP-Pd(II)/DABN and DPEN complexes: PIO analysis of phosphine-Pd(II) interaction and trans influence" *Organometallics* **24**, **2005**, 4579.
- Yamashita, H.; Hayashi, T.; Kobayashi, T.; Tanaka, M.; Goto, M. "Oxidative addition of halosilanes to zero-valent platinum complexes [3]" *J. Chem. Soc.* **1988**, 110.
- Yamashita, M.; Vicario, J. V. C.; Hartwig, J. F. "Trans influence on the rate of reductive elimination. reductive elimination of amines from isomeric arylpalladium

- amides with unsymmetrical coordination spheres” *J. Am. Chem. Soc.* **125**, **2003**, 16347.
- Yang, Z.; Ebihara M.; Kawamura, T. “One-dimensional chain structures constructed from tetra(acetamidato)dirhodium(II,III) complexes and square planar platinum and palladium complexes” *Inorg. Chim. Acta* **359**, **2006**, 2465.
- Yang, H. C.; Huang, Y. C.; Lan, Yi. K.; Luh, T. Y.; Zhao, Y.; Truhlar, D. G. “Carbene rotamer switching explains the reverse trans effect in forming the Grubbs second generation olefine metathesis catalyst” *Organometallics* **30**, **2011**, 4196.
- Yatsenko, A. V.; Kudryavtsev, I. K.; Zakharov, M. A.; Aslanov, L. A. “Static influence of ligands: Comparison of DFT calculations with experimental data” *Russ. J. Coord. Chem.* **30**, **2004**, 1.
- Yu, J.; Liu, S.-S.; Cui, J.; Hou, X.-S.; Zhang, C. “A Mild and Efficient Direct  $\alpha$ -Amination of  $\beta$ -Dicarbonyl Compounds Using Iodosobenzene and p-Toluenesulfonamide Catalyzed by Perchlorate Zinc Hexahydrate” *Org. Lett.* **14**, **2012**, 832.
- Yurieva, A. G.; Poleshchuk, O. Kh.; Filimonov, V. D. “Comparative analysis of a full-electron basis set and pseudopotential for the iodine atom in DFT quantum-chemical calculations of iodine-containing compounds” *J. Struct. Chem.* **49**, **2008**, 548.
- Yusubov, M. S.; Yusubova, R.Y.; Funk, T.V.; Chi, K.-W.; Zhdankin, V. V. “Oligomeric iodosylbenzene sulfate: A convenient hypervalent iodine reagent for oxidation of organic sulfides and alkenes” *Synthesis*, **2009**, 2505.
- Zakovska A.; Novakova, O.; Balcarova Z.; Bierbach U.; Farrell, N.; Brabec, V. “DNA interactions of antitumor trans-[PtCl<sub>2</sub>(NH<sub>3</sub>)(quinoline)] ” *Eur. J. Biochem.* **254**, **1998**, 547.

- Zeng, G.; Sakaki, S. "Theoretical study on the transition-metal oxoboryl complex: M-BO bonding nature, mechanism of the formation reaction, and prediction of a new oxoboryl complex" *Inorg. Chem.* 51, **2012**, 4597.
- Zhao, X. -F.; Zhang, C. "Iodobenzene dichloride as a stoichiometric oxidant for the conversion of alcohols into carbonyl compounds; two facile methods for its preparation" *Synthesis* **2007**, 551.
- Zhao, Y.; Truhlar, D. G. "Hybrid meta density functional theory methods for thermochemistry, thermochemical kinetics, and noncovalent interactions: The MPW1B95 and MPWB1K models and comparative assessments for hydrogen bonding and van der waals interactions" *J. Phys Chem. A.* 108, **2004**, 6908.
- Zhao, Y.; Schultz, N. E.; Truhlar, D. G. "Exchange-correlation functional with broad accuracy for metallic and nonmetallic compounds, kinetics, and noncovalent interactions" *J. Chem. Phys.* 123, **2005**, 161103.
- Zhdankin, V. V.; Stang, P. J. "Recent developments in the chemistry of polyvalent iodine compounds" *J. Chem. Rev.* 102, **2002**, 2523.
- Zhdankin, V. V.; Stang, P. J. "Chemistry of polyvalent iodine" *Chem. Rev.* 108, **2008**, 5299.
- Zhdankin, V. V. "Organoiodine(V) reagents in organic synthesis" *J. Org. Chem.* 76, **2011**, 1185.
- Zhu, H.; Ziegler, T. "A theoretical study of the original Shilov reaction involving methane activation by platinum tetrachloride in an acidic aqueous solution" *J. Organomet. Chem.* 691, **2006**, 4486.
- Zhu, H.; Ziegler, T. "Influence of cis and trans ligands in platinum(II) complexes on the ability of the platinum center to activate C-H bonds. A density functional theory study" *Organometallics* 127, **2008**, 1743.

- Zhu, H.; Ziegler, T. "Probing the influence of trans and leaving ligands on the ability of square-planar platinum(II) complexes to activate methane. A theoretical study" *Organometallics* 28, **2009**, 2773.
- Zhu, J.; Lin, Z.; Marder, T. B. "Trans influence of boryl ligands and comparison with C, Si, and Sn ligands" *Inorg. Chem.* 44, **2005**, 9384.
- Zobi, F. "Parametrization of the contribution of mono- and bidentate ligands on the symmetric C=O stretching frequency of *fac*-[Re(CO)<sub>3</sub>]<sup>+</sup> complexes" *Inorg. Chem.* 48, **2009**, 10845.
- Zuidema, E.; van Leeuwen, P. W. N. M.; Bo, C. "Reductive elimination of organic molecules from palladium-diphosphine complexes" *Organometallics* 24, **2005**, 3703.
- Zumdahl, S. S.; Drago, R. S. "A molecular orbital study of the trans influence and kinetic trans effect in square-planar platinum (II) complexes" *J. Am. Chem. Soc.* 90, **1968**, 6669.